Characterization of the Chikungunya virus entry process and the development of novel antiviral strategies

vom Fachbereich Biochemie, Chemie und Pharmazie (14) der

Johann Wolfgang Goethe–Universität als Dissertation angenommen.

Dekan: _____

Gutachter:_____

Datum der Disputation:_____

Eidesstattliche Erklärung

Hiermit erkläre ich, dass ich die vorliegende Arbeit: „Characterization of the Chikungunya virus entry process and the development of novel antiviral strategies" selbständig verfasst habe und keine anderen als die angegebenen Quellen und Hilfsmittel verwendet wurden.

Frankfurt am Main, 17.10.2014

_____

Christopher Weber

Teile dieser Arbeit sind bereits in internationalen Fachzeitschriften veröffentlicht worden, bei anderen ist die Veröffentlichung geplant.

"Die gefährlichste Weltanschauung ist die Weltanschauung derer, die die Welt nie angeschaut haben."

Meiner Familie und meinen Freunden

Table of contents

1. Zusammenfassung

Das Chikungunya Virus (CHIKV) ist ein durch Moskitos (Gattung: *Aedes*) übertragenes Alphavirus, es ist umhüllt und hat ein (+) Einzelstrang-RNA-Genom von etwa 12 Kilobasen Länge. Das Virus verursacht in Menschen hohes Fieber, Hautausschlag, und Arthritis. Alle Symptome außer die Gelenkschmerzen legen sich für gewöhnlich innerhalb einer Woche wieder, jedoch können sie in ca. 30% der Fälle über Monate oder Jahre andauern und betroffene Personen für diese Zeit arbeitsunfähig machen. Die Mortalitätsrate ist sehr gering (0,1%) und schwere Fälle, die Enzephalitiden oder Hepatitiden auslösen können, sind auf Neugeborene, Ältere und Patienten mit anderen Grunderkrankungen beschränkt. Asymptomatische Fälle sind mit ca. 15% eher selten. Nach einem Moskitostich vermehrt sich das CHIKV zunächst in Fibroblasten der Haut, von wo es mit dem Blutstrom zu Leber, zu den Gelenken, Muskeln und Lymphorganen gelangt und sich dort vermehrt. Bei schweren Verläufen wird, wie oben erwähnt, auch das Gehirn infiziert. Es werden mehr oder weniger alle Epithel- und Endothelzellen und in geringem Umfang auch Makrophagen befallen, hämatopoetische Zellen allerdings nicht. Durch das angeborene und das erworbene Immunsystem wird das Virus eliminiert, ob jedoch den über lange Zeiträume anhaltenden Gelenkschmerzen eine persistierende CHIKV-Replikation ausschließlich in den Gelenken oder auch eine Autoimmunkomponente zugrunde liegt, konnte bisher noch nicht geklärt werden.

Das Virus ist endemisch in Sub-Sahara-Afrika, einigen Inseln im Indischen Ozean, Indien und Südostasien. Es wird angenommen, dass die ursprüngliche Heimat des Virus Afrika ist. Hier gibt es zwei Virusstämme, die „east-central-south-African"-Linie (ECSA), und die „west-African"-Linie, die genetisch nur entfernt miteinander verwandt sind. In Afrika zirkuliert das Virus in einem enzootischen Kreislauf, der verschiedene waldbewohnende Moskitos der Gattung *Aedes* und kleine Affen sowie andere Säugetiere, möglicherweise auch Vögel, mit einschließt. Von hier wird das Virus gelegentlich auf Menschen übertragen, die in kleinen waldnahen Siedlungen wohnen (ländlicher Kreislauf). Durch Reisen akut CHIKV-infizierter Dorfbewohner in Ballungszentren kann es in diesen wiederum zu großen Epidemien kommen. Von hier hat sich ein Virus des ECSA-Stammes in den 1950er Jahren bis nach Indien und Südostasien ausgebreitet, wo es seitdem endemisch ist. Dieses wird nun als „Asian lineage" bezeichnet. Es wird angenommen, dass das CHIKV hier in einem urbanen Kreislauf zirkuliert, der ausschließlich Menschen und anthropophile Moskitos (*Aedes aegypti* und *A. albopictus*) einschließt.

Das CHIKV war in den letzten Jahren für schwere Ausbrüche mit Millionen von Infizierten verantwortlich. Die Hauptprobleme bei CHIKV-Ausbrüchen sind, in Kombination mit den andauernden Gelenkschmerzen, die hohen Prävalenzzahlen (teilweise über 30%) und die seltenen asymptomatischen Fälle (ca. 15%). CHIKV-Epidemien überfordern folglich die lokalen Gesundheitsbehörden und führen zu hohen ökonomischen Kosten. Dies war zum Beispiel 2005/06 der Fall, als eine CHIKV-Epidemie, die 2004 an der Küste Kenias begann, auf einige Inseln im Indischen Ozean (unter anderem nach La Réunion, ein französisches Übersee-Département) und nach Indien überschwappte. Von hier aus breitete sie sich weiter bis nach Südostasien aus. Auf La Réunion wurde dabei mehr als jeder dritte Einwohner der Insel infiziert. Während dieser Epidemie im gesamten Bereich des Indischen Ozeans, bei der insgesamt mehrere Millionen Menschen erkrankten, trat mindestens 4 Mal unabhängig voneinander eine Mutation in einem Hüllprotein des CHIKV auf (E1 A226V), durch die das Virus deutlich besser durch *A. albopictus* übertragen wird. Dies trug wesentlich zur explosionsartigen Ausbreitung des Epidemie-Virus bei. Diese Variante hat sich seitdem in den genannten Gebieten durchgesetzt, in denen sie nun endemisch ist. Sie wird nun „Indian Ocean Lineage" (IOL) genannt. Die „Asian lineage" des CHIKV konnte in mehreren Jahrzehnten Zirkulation im gleichen Gebiet nicht diese effektive *A. albopticus*-Anpassung vollziehen, da sie an zwei weiteren Stellen in den CHIKV-Hüllproteinen nicht den Aminosäurephänotyp aufweist, der Voraussetzung für den positiven Effekt der E1 A226V Mutation ist. Einige ECSA-Varianten hingegen hatten die erforderlichen Aminosäurephänotypen und so die genetischen Voraussetzungen, um zur IOL zu werden. *A. albopictus* tritt, im Gegensatz zum ursprünglichen Vektor *A. aegypti*, auch in gemäßigten Klimazonen auf (Südeuropa, Osten der USA), wohin es sich in den letzten Jahrzehnten aus seinem Ursprungsgebiet in Südostasien ausgebreitet hat. Dementsprechend schaffte es das Virus während der IOL-Epidemie, mit einem Reisenden von Indien nach Italien zu gelangen und hier 2007 eine Epidemie mit 205 Betroffenen zu verursachen. Außerdem wurde das CHIKV (ein Vertreter der „Asian lineage") Ende 2013 in die Karibik eingeführt und sorgt seitdem dort und in angrenzenden Regionen für eine Epidemie, die immer noch andauert und bisher (Stand: Anfang September 2014) für geschätzte 660.000 Fälle verantwortlich ist. Wegen Klimaerwärmung, Globalisierung und Vektorwechsel ist zu erwarten, dass das Virus sich in den nächsten Jahren und Jahrzehnten weiter ausbreiten und für neue Ausbrüche sorgen wird, auch in Weltgegenden mit gemäßigtem Klima, wie Europa und die USA. Im Unterschied zu diesen Gefahren gibt es aber bisher keine zugelassene spezifische Behandlung oder einen Impfstoff gegen das CHIKV.

Der Zelleintrittsprozess des CHIKV ist zudem auch noch nicht im Detail verstanden und wurde in dieser Arbeit deshalb näher untersucht. Die Hüllproteine des Virus heißen E1 und

E2, besitzen beide Transmembrandomänen und sind als Trimere aus E2-E1 Heterodimeren auf der Virusoberfläche angeordnet. Dabei sind auf einem Viruspartikel exakt 240 Heterodimere und dementsprechend 80 Trimere vorhanden. E2 bedeckt E1 und ist verantwortlich für Zellbindung und –eintritt. Es besteht aus der Domäne C, die sich nahe der viralen Membran befindet, der Domäne A in der Mitte des Proteins und Domäne B am distalen Ende, exponiert auf der Virusoberfläche. Der β-Schleifen-Verbinder verbindet Domäne B mit den Domänen A und C. Ein Trimer aus E2-E1 Heterodimeren hat eine Propeller-ähnliche Form, wobei die E2 Domäne B dabei die exponierten Enden der „Rotorblätter" bildet. E1 enthält die Fusionsschleife an seiner Spitze und ist folglich verantwortlich für die Fusion der viralen und der endosomalen Membran. Nach Bindung an den noch nicht identifizierten zellulären Rezeptor durch E2 wird das Virus über Rezeptor-vermittelte Endozytose aufgenommen. Infolge der Ansäuerung des Endosoms dissoziiert das E2-E1 Heterodimer. Hierdurch wird die E1 Fusionsschleife exponiert, in die endosomale Membran inseriert und nach einer Serie von Konformationsänderungen in und von E2 und E1 verschmelzen die virale und die endosomale Membran. Im Folgenden wird das virale Nukleokapsid durch die Fusionspore in das Zytoplasma der Zelle entlassen und die intrazelluläre Replikation startet.

In dieser Arbeit wurde, wie oben erwähnt, der Zelleintrittsprozess des CHIKV näher untersucht. Um ein geeignetes Werkzeug an der Hand zu haben, mit dem man diesen Prozess genauer untersuchen kann, wurden lentivirale Vektorpartikel (VP) hergestellt, die mit den CHIKV-Hüllproteinen pseudotypisiert waren. Sie übernahmen somit alle Zelleintritts-Eigenschaften des CHIKV. Als Reportergen enthielten sie, je nach Experiment, ein für Luziferase oder für GFP kodierendes Gen. Der Vorteil von pseudotypisierten Vektorpartikeln ist, dass man mit diesen im Falle des CHIKV unter einer niedrigeren Sicherheitsstufe als mit dem Originalvirus arbeiten kann (S2 statt S3) und dass man rein die Zelleintrittseigenschaften des Virus untersuchen kann. Nach dem Zelleintritt ist außerdem keine weitere Replikation der Partikel mehr möglich, da die entsprechenden Gene nicht mit in die Vektorpartikel verpackt werden. Die hergestellten CHIKV-VP mussten zunächst jedoch umfassend charakterisiert werden, um als CHIKV-Zelleintritts-Modell dienen zu können. Es konnte festgestellt werden, dass das CHIKV-Hüllprotein von den VP-produzierenden Zellen exprimiert und auch im Überstand derselben vorhanden war. Aus dem Überstand konnte es durch Ultrazentrifugation zusammen mit dem wichtigen VP-Strukturprotein p24 sedimentiert werden, was für einen effektiven Einbau des CHIKV-Hüllproteins in die VP spricht. Zudem konnte durch Chloroquin-Behandlung die Transduktion von Zielzellen mit CHIKV-VP konzentrationsabhängig gehemmt werden, was für einen pH-abhängigen Zelleintritt der VP spricht, der auch beim Wildtyp-CHIKV vorliegt. Weiterhin entsprach die Bandbreite der

transduzierbaren Zellen (Endo- und Epithelzellen verschiedener Säugerarten einschließlich des Menschen, keine hämatopoetischen Zellen) denen der durch das Wildtyp-CHIKV infizierbaren Zelltypen. Die CHIKV-Hüllprotein pseudotypisierten VP spiegelten somit die wesentlichen Zelleintrittseigenschaften des Wildtyp-CHIKV wider und konnten im Folgenden als Grundlage zur Untersuchung des CHIKV-Zelleintrittsprozesses genutzt werden.

Bisher ist, wie bereits oben erwähnt, kein Impfstoff gegen CHIKV zugelassen. Darum war es unter anderem das Ziel dieser Arbeit, verschiedene neue Impfstoffansätze zu testen. Im Tierversuch wurden bereits einige wirksame CHIKV-Vakzine getestet. Dabei kamen unter anderem DNA-, Protein-, oder auf abgeschwächten Viren basierende Ansätze zum Einsatz. Dabei war in vielen Impfstoffen das E2-Hüllprotein ein wesentlicher Bestandteil, jedoch nie nur einzelne Bereiche aus E2. Es wurde aber interessanterweise publiziert, dass die Mehrheit früher neutralisierender Antikörper in CHIKV-infizierten Patienten gegen ein einzelnes lineares Epitop des CHIKV-E2-Hüllproteins gerichtet ist. Dieses befindet sich exponiert auf der Virusoberfläche am N-Terminus der Domäne A. Um nun herauszufinden, welche Bereiche von E2 wirklich für eine effektive Anti-CHIKV-Immunantwort notwendig sind, wurden 7 künstliche, E2-abgeleitete Proteine kreiert, in *E.coli* exprimiert und erfolgreich aufgereinigt. Sie bestanden aus 5 durch Glycin-Serin-Linker verbundenen Einheiten des erwähnten linearen Epitops (L), den wiederum durch Glycin-Serin-Linker verknüpften oberflächenexponierten Bereichen von Domäne A (sA), der gesamten Domäne B plus einem Teil des β-Schleifen-Verbinders (B^+), oder einer Kombination dieser 3 Module. Anschließend wurden Mäuse mit diesen Proteinen geimpft und die Seren auf CHIKV-neutralisierende Antikörper untersucht. Dies geschah mit Hilfe eines eigens entwickelten Hochdurchsatz-CHIKV-Neutralisations-Assay, der für das 384-Loch-Format optimiert wurde und auf der Verwendung CHIKV E2-E1 pseudotypisierter VP mit Luziferase-Reportergen basierte. Die Analyse der Mausseren ergab, dass B^+ notwendig und ausreichend war, um eine neutralisierende Immunantwort gegen das CHIKV zu erzeugen. Die Impfung mit den Proteinen sA oder L alleine führte dagegen nicht zur Bildung neutralisierender Antikörper, obwohl via SDS-PAGE/Western Blot nachgewiesen werden konnte, dass grundsätzlich Antikörper gebildet worden waren, die das entsprechende geimpfte Konstrukt binden konnten. Lineare Epitope, wie sie in sA und L ausschließlich vorkamen, genügen also offensichtlich nicht als Basis für einen wirksamen CHIKV-Impfstoff. Die höchstwahrscheinlich vorhandenen Strukturepitope in B^+ hingegen wären hierfür ein Kandidat. Dabei ist es möglich, dass die neutralisierenden gegen B^+ gebildeten Antikörper sowohl die Zellbindung als auch die Dissoziation des E2-E1 Heterodimers während des CHIKV-Zelleintrittsprozesses verhindern. Das Protein sAB^+ induzierte nach Impfung am effektivsten neutralisierende Antikörper, möglicherweise hatte hier der sA-Anteil eine stabilisierende

Wirkung hinsichtlich Halbwertszeit oder 3D-Struktur von B$^+$ auf das Gesamtprotein. Eine sAB$^+$-Impfung von Mäusen konnte dann auch bei anschließender Infektion mit Wildtyp-CHIKV die viralen Titer im Mausserum signifikant gegenüber der Kontrollgruppe senken. Ein eigens generierter Impfstoff basierend auf einem rekombinanten „Modified Vaccinia virus Ankara" (MVA; MVA-CHIKV-sAB$^+$), einem abgeschwächten, für humane Impfungen bewährten Pockenvirusstamm, der ein für sAB$^+$ kodierendes Gen in sein Genom eingebaut hatte und dieses in infizierten Zellen exprimierte, konnte dagegen die viralen Titer nach Infektion nicht signifikant absenken. Der Grund hierfür war möglicherweise eine verstärkte zelluläre gegenüber einer eher schwächeren humoralen Immunantwort, die weniger effektiv gegen die gewählte intranasale Infektionsroute sein könnte. Dies wurde jedoch nicht im Detail untersucht. Nichtsdestotrotz zeigen diese Experimente, dass ein rational designtes, kleines, CHIKV E2-abgeleitetes Protein nach weiteren Optimierungen hinsichtlich einiger Vakzinierungsparamameter (wie beispielsweise die Verwendung eines geeigneten Adjuvants) eine gute Basis für einen sicheren, einfach zu produzierenden und dementsprechend billigen CHIKV-Impfstoff sein könnte. Diese Parameter sind vor allem für die vielen Entwicklungsländer, in denen das CHIKV endemisch ist, von großer Relevanz.

Bei der genaueren Analyse des CHIKV-Zelleintrittsprozesses konnte in dieser Arbeit aufgeklärt werden, dass Zelloberflächen-Glykosaminoglykane (GAGs) hierbei eine wichtige Rolle spielen. GAGs werden aus zu langen Ketten verknüpften und stark sulfatisierten Disaccharid-Einheiten gebildet und können kovalent mit Membran-assoziierten Proteinen verbunden sein. Sie sind ubiquitär auf allen tierischen Zellen vorhanden. GAGs sind essentiell an einigen zellulären Signalwegen beteiligt und wurden auch schon als Zellbindungsfaktoren für einige Pathogene beschrieben. Im Zusammenhang mit dem CHIKV wurde aber bisher nur von Zellkultur-adaptierten Stämmen berichtet, die aufgrund einer erhöhten Anpassung an GAG-Bindung (basierend auf Mutationen in E2 Domäne A) *in vivo* wiederum attenuiert waren. In dieser Arbeit jedoch konnte unter Benutzung von CHIKV oder CHIKV-pseudotypisierten VP, deren E2-Hüllproteinsequenz nicht Zellkultur-adaptiert war, gezeigt werden, dass Zelloberflächen-GAGs den CHIKV-Zelleintritt unterstützen. Wenn eine bestimmte Zelllinie, die Oberflächen-GAG-defizient ist (pgsA-745), mit CHIKV VP und Wildtyp-CHIKV transduziert bzw. infiziert wurde, so zeigten sich verminderte Transduktions- bzw. Replikationsraten im Vergleich zur parentalen Zelllinie, die Zelloberflächen-GAGs besitzt (CHO-K1). Des Weiteren wurde in Gegenwart von löslichen GAGs der Zelleintritt (Wildtyp-CHIKV) bzw. die Transduktionsrate (CHIKV-VP) bei GAG-haltiger Zellen konzentrationsabhängig verringert. Ein gegenteiliges Bild zeigte sich bei pgsA-745-Zellen, hier wurden die Transduktionraten mit CHIKV-VP bei Zugabe löslicher GAGs sogar erhöht. Bindungsexperimente mit rekombinanten CHIKV E2 Domänen A, B, und C deuten darauf

hin, dass Domäne B für die Bindungen an Zelloberflächen-GAGs zuständig ist, während A an andere zelluläre Strukturen, möglicherweise den zellulären Rezeptor, bindet. Domäne C hingegen scheint nicht an der Zellbindung des CHIKV E2-Proteins beteiligt zu sein. Diese Erkenntnisse lassen sich mit der bekannten Anordnung der CHIKV-Hüllproteine auf der Virusoberfläche in Einklang bringen, die zeigen, dass die Domäne A und besonders die Domäne B sehr exponiert sind. Alle in dieser Arbeit gewonnenen Erkenntnisse führen zu einem Modell, in dem das CHIKV-Partikel bzw. dessen Hüllproteine zunächst durch Bindung an GAGs auf der Zelloberfläche (durch Domäne B) aktiviert werden (basierend auf der Verstärkung der Transduktion durch Zugabe von löslichen GAGs auf pgsA-745-Zellen). Dem liegt möglicherweise eine Konformationsänderung bereits außerhalb der Zelle zugrunde, wie sie auch bei einem verwandten Alphavirus beobachtet wurde. Durch diese Aktivierung, die möglicherweise eine Dislokation der Domäne B beinhaltet, wäre dann die Bindung an einen zellulären Rezeptor durch Domäne A möglich. Alternativ müsste es aber noch mindestens einen weiteren Eintrittsweg des CHIKV in die Zelle geben, da pgsA-745-Zellen immer noch infizierbar/transduzierbar sind und die Zugabe löslicher GAGs dieselben Vorgänge zwar vermindern, jedoch nicht vollständig hemmen kann. Dieser Weg(e) bzw. die Bindungsstellen auf CHIKV E2, die darin involviert sind, werden aber offensichtlich nicht durch GAGs gehemmt, da auf pgsA-745-Zellen nur eine reine Verstärkung der Transduktion durch GAG-Zugabe zu beobachten ist. Es müssen also andere molekulare Strukturen in E2 beteiligt sein als beim GAG-abhängigen Zelleintritt, beispielsweise eine direkte Bindung von Domäne A, ohne vorher Domäne B zu involvieren. Das Bild eines CHIKV, das die ubiquitär auf Tierzellen vorhandenen GAGs für seinen Zelleintritt unterstützend rekrutiert, daneben aber noch alternative Wege findet, in die Zielzelle zu gelangen, erscheint naheliegend und sinnvoll bei einem Virus, das evolutionär weit entfernte Spezies wie Mensch und Moskito produktiv infizieren kann und auch innerhalb eines Organismus verschiedene Organe, Gewebe sowie Zelltypen befällt.

Ein Hauptbestandteil von Grüntee ist Epigallocatechingallat (EGCG). Es gehört zu den Catechinen und ihm wird eine Reihe von positiven Wirkungen auf die Gesundheit, zum Beispiel bei Krebserkrankungen, nachgesagt. Unter Benutzung des bereits erwähnten Hochdurchsatz-CHIKV-Neutralisations-Assay und mit Hilfe weiterer Bestätigungsexperimente mit Wildtyp-CHIKV wurde es als ein Hemmer des CHIKV-Zelleintritts identifiziert. Das ebenfalls im grünen Tee vorkommende Epicatechin (EC) wirkte dabei deutlich schlechter, was höchstwahrscheinlich auf das Fehlen einer Galloyl-Seitenkette im Vergleich zu EGCG zurückzuführen ist. Es wurde kürzlich publiziert, dass EGCG den Zelleintritt mehrerer verschiedener Viren hemmt, indem es deren Bindung an Zelloberflächen-GAGs verhindert. Im Licht der in dieser Arbeit herausgefundenen

unterstützenden Wirkung von GAGs beim CHIKV-Zelleintritt wäre dies ein naheliegender Wirkmechanismus. EGCG könnte für eine Entwicklung eines „small molecule" zur Behandlung der CHIKV-Infektion als Leitsubstanz dienen oder auch direkt in Form einer Salbe bei Moskitostichen als Postexpositionsprophylaxe angewandt werden. Dieses Beispiel zeigt zudem, wie nützlich der entwickelte Hochdurchsatz-CHIKV-Neutralisationsassay zur Testung von potentiellen CHIKV-Zelleintrittsinhibitoren aus unterschiedlichen Quellen sein kann.

2. Introduction

2.1 Chikungunya virus (CHIKV) biology

2.1.1 Infection and course of disease

The Chikungunya virus (CHIKV) belongs to the family *Togaviridae* and therein to the genus *Alphavirus* (Strauss and Strauss, 1994). It is transmitted to and between vertebrates by mosquitoes, for transmission among humans *Aedes aegypti* (*A. aegypti*; the yellow fever mosquito) and *Aedes albopictus* (*A. albopictus*; the Asian tiger mosquito; Figure 1) are especially relevant. "Chikungunya" means "that which bends up" in the language of the Makonde living in south-east Tanzania and refers to the main symptom of the disease (see below).

Figure 1: Picture of *Aedes albopictus*.

A female *A. albopictus* mosquito suckling blood from a human.

http://de.wikipedia.org/wiki/Asiatische_Tigerm%C3%BCcke#mediaviewer/File:

Aedes-albopictus.jpg

Upon a mosquito bite, the virus initially replicates in skin fibroblasts. Subsequently, it disseminates via the blood stream to the liver, the muscles, lymph nodes, spleen, and, especially during severe clinical causes, to the brain (Schwartz and Albert, 2010) (Figure 2). In these organs, epithelial and endothelial cells are infected. Macrophages seem to be additionally infected, however the *in vivo* relevance of this infection is not yet clear. In contrast, lymphocytes are not a target of the virus (Sourisseau et al., 2007).
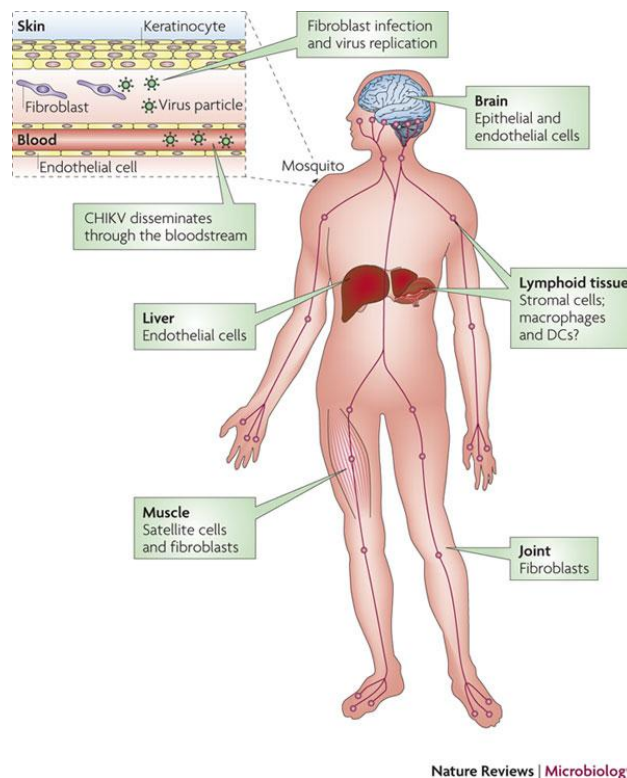
Figure 2: CHIKV spread within the human body following infection.
Upon a mosquito bite, the virus first replicates in fibroblasts and is then disseminated by the blood stream to the liver, the muscles, the lymphoid tissue, and to the joints. In severe cases, CHIKV also replicates in the brain. (Schwartz and Albert, 2010)

The disease caused by CHIKV infection is called Chikungunya fever (CHIKF) and includes acute onset of high fever, muscle pain, and a petechial or maculopapular rash. The symptom that distinguishes CHIKF from another arbovirus-caused fever with very similar symptoms, the Dengue fever, is the swelling of the joints and an accompanied severe joint pain, which can be recurrent and last for months or even years in about 30% of infected individuals (Schwartz and Albert, 2010). The estimated proportion of asymptomatic infections is 15% (Gallian et al., 2014). Symptoms occur usually 2-4 days after the mosquito bite and last typically not longer than 1 week (except the recurrent joint pain) (Figure 3). The viral load in plasma ranges from 10^5 to 10^8 RNA copies/ml during the acute phase (Schwartz and Albert, 2010). Severe clinical symptoms and complications are rare but can manifest themselves in neonates, elderly, or otherwise immunocompromised patients. They include lymphopenia, hepatitis, or encephalitis. Neonates of acutely infected pregnant women can be infected before or during delivery and this infection often leads to abortion or neonatal encephalopathy (Sourisseau et al., 2007), which can result in neurocognitive disorders later in childhood (Gérardin et al., 2014). Transmission via blood donation can also occur (Gallian et al., 2014). The mortality rate is 0.1% (Pialoux et al., 2007).
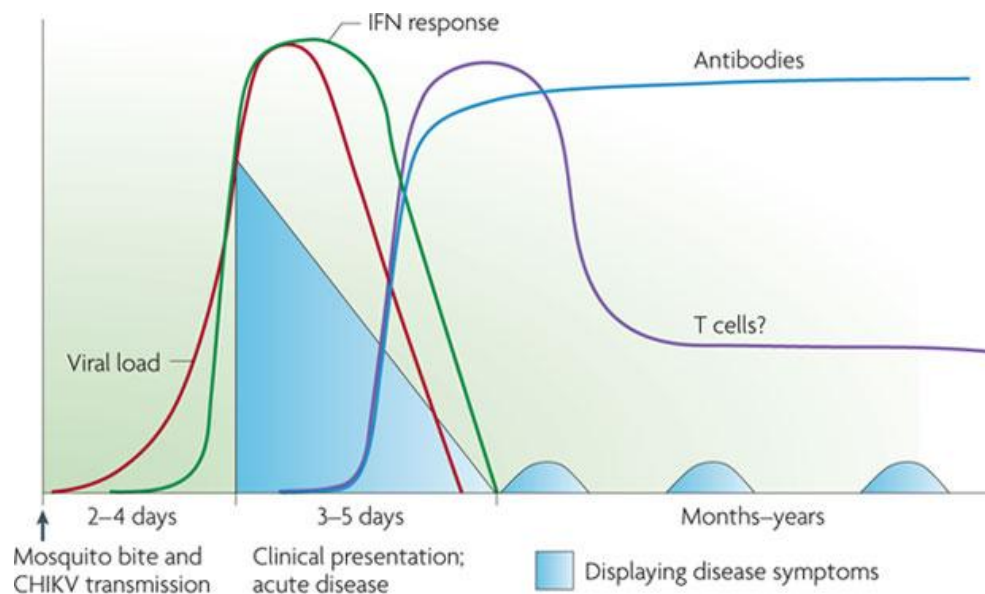
Figure 3: Course of disease and immune response during CHIKF.
Shortly (2-4 days) after infection, there is a sudden onset of disease symptoms. The innate immune response is essential to control the virus (interferon (IFN) response) and neutralizing antibodies are developed following induction of the adaptive immune response. T cells might play a role in viral clearance but are also thought to be responsible for the recurrent joint pain months or years after the acute phase. The other symptoms of the acute phase, like fever or rash, are usually improved after one week.
(Schwartz and Albert, 2010)

Reasons for the syndrome's hallmark, the potentially recurrent joint pain, are not yet understood. Infectious virus could not be detected in patients with chronic arthritis (Schwartz and Albert, 2010), thus a chronic infection seems to be excluded. However, a chronic infection of macrophages in the tissues of macaques was observed after remission of the acute phase (Labadie et al., 2010). Furthermore, CD4+ T cells were blamed to be the cause of autoimmune arthritis without affecting viral replication in the joints of mice (Teo et al., 2013). In contrast to this finding, other studies in mice show that chronic joint disease can only be controlled by the adaptive immune system (Hawman et al., 2013), or that macrophages are essential to avoid prolonged inflammation in the synovial tissue (Poo et al., 2014). The former is underpinned by the fact that aged macaques cannot escape chronic CHIKV infection because of the lack of a robust antiviral adaptive immunity (Messaoudi et al., 2013). Furthermore, there was no difference in the anti-CHIKV T cell responses of recovered CHIKV infected patients or people with chronic arthritic symptoms (Hoarau et al., 2013). Additionally, the risk of chronic joint pain in humans increases with advancing age (Thiberville et al., 2013). A recent publication proposed that a possible infection of osteoblasts by an alphavirus may also promote chronic arthritis. However, these findings

were ascertained using not CHIKV itself but a close relative, the Ross River virus (RRV) (Chen et al., 2014).

2.1.2   Epidemiology

2.1.2.1   Situation before 2004

It is believed that the origin of CHIKV lies in Sub-Saharan Africa. There, it circulates endemically in an enzootic cycle in which nonhuman primates are probably the main host. Other small mammals or birds could also play a role as a potential vertebrate host. In these areas, the virus is transmitted between vertebrates by different arboreal *Aedes* mosquitoes (Powers et al., 2000). Occasionally, there are spillovers from nonhuman primates to humans living in rural areas. Travelling of these infected humans from rural to urban regions is then the cause for the introduction of CHIKV into urban areas. This introduction then results in a solely human-mosquito cycle. In those cycles, the virus is mainly or exclusively transmitted by the peridomestic *A. aegypti*. These urban cycles can lead to explosive epidemics, which sometimes spread beyond Africa (Weaver, 2014). This spread has happened several times in the past. It is, for example, suggested that, as early as the 18th century, the virus was introduced to Indonesia, possibly alongside the primary human vector *A. aegypti* (Carey, 1971). The first outbreak in modern times was detected in Tanzania in 1952, and during this outbreak the first clinical isolate (S27-African prototype) was also characterized. Several epidemics in and outside of Africa were observed since then, for example in Thailand (1958 and 1962), Nigeria (1969), Malaysia (1998), or the Democratic Republic of the Congo (2000) (Weaver, 2014).

There are three main genetic lineages of CHIKV, which have a common ancestor that existed within the last 500 years (Volk et al., 2010): The east-central-south African (ECSA) lineage, the west African genotype, and the Asian lineage. Both African genotypes are more distantly related, whereas the Asian lineage is a descendent of the ECSA clade introduced in Southeast Asia in the 1950s. In this region, the virus is transmitted in an urban cycle, where *A. aegypti* is the only vector and humans are the only vertebrate hosts (Chen et al., 2013).

2.1.2.2   The Indian Ocean epidemic

In 2004, an epidemic (ECSA strain) occurred in coastal Kenya and subsequently spread to some islands in the Indian Ocean (including La Réunion),to India and then to Southeast Asia (Pialoux et al., 2007) (Figure 4). When the virus is introduced into immunologically naïve populations, it causes explosive outbreaks with very high infection rates. This was especially

the case on La Réunion (which belongs to France) and had never been observed to this magnitude before. An estimated 300,000 cases (population: 775,000) were observed during the CHIKV epidemic in 2005-06. In India, between 1.4 and 6.5 million people were infected during the period 2005-08 (Weaver, 2014).
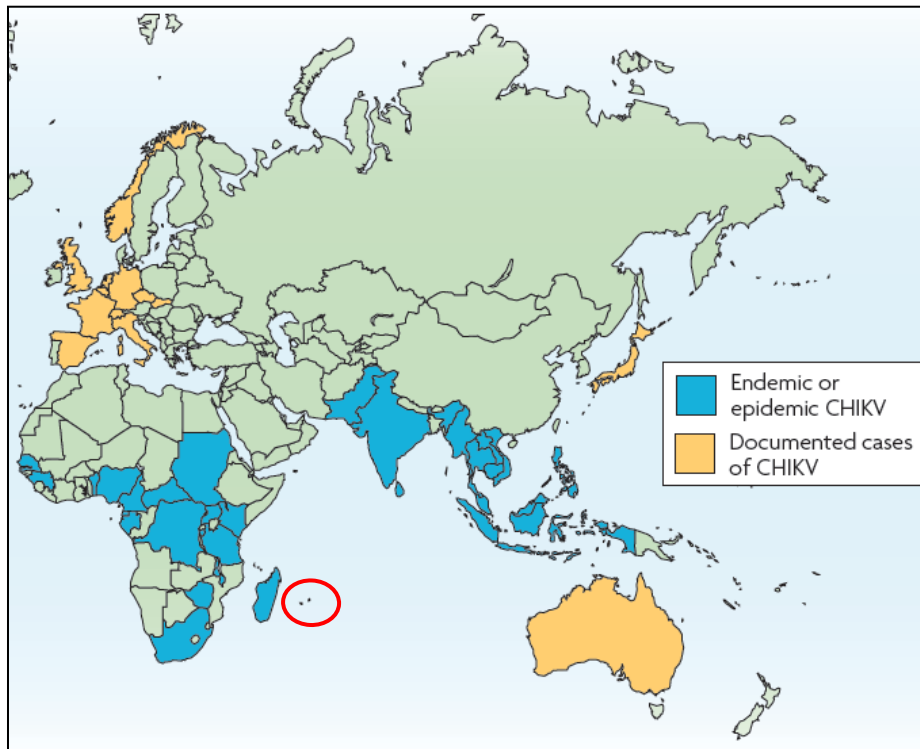
Figure 4: Regions of the world endemic for CHIKV before December 2013.

The location of La Réunion is labeled with a red circle (the left island within the circle).

Note that the small epidemics in Italy and France are not considered in this map.

Adapted from (Schwartz and Albert, 2010)

During the epidemic, a mutation in the viral envelope protein E1 occurred (A226V; see 2.1.5.3) at least four times independently of one another and allowed a much more efficient transmission by *A. albopictus* without affecting the transmission by *A. aegypti* (Schuffenecker et al., 2006; Tsetsarkin et al., 2007, Vazeille et al., 2007; Tsetsarkin et al., 2014). The reason for this efficient transmission is the enhanced entry into and replication in midgut cells, which is followed by subsequent spread into the mosquito's haemocoel (Arias-Goeta et al., 2013). Indeed, *A. albopictus* was identified as the likely primary CHIKV vector in La Réunion (Pialoux et al., 2007). *A. aegypti* is found only in tropical and subtropical regions around the world (Figure 5 A). *A. albopictus,* however, spread from its origin in Southeast Asia to the more temperate regions of southern Europe and the eastern US during the last decades (Figure 5 B). With ongoing climate change and globalization, this spread is expected to continue (Caminade et al., 2012). This spread increases the danger of a permanent

introduction of CHIKV into Europe or the USA by this vector. The first cases of this introduction have occurred: In Italy, the virus was introduced by a traveler returning from an epidemic area in India in 2007 and caused a small outbreak, with autochthonous transmission and 205 identified detected cases (Rezza et al., 2007). Another two autochthonous transmissions (again, the source was a traveler returning from India) were observed in France in 2010 (Grandadam et al., 2011). The ECSA derived strain with the E1 A226V mutation is now endemic in the Indian Ocean and Southeast Asian regions and is now called the Indian Ocean lineage (IOL). It might replace the old Asian genotype, which has been circulating in Southeast Asia for decades, due to its more efficient transmission by *A. albopictus*. The Asian genotype has not been able to efficiently adapt to *A. albopictus* during its entire existence due to the epistatic amino acid variants in the CHIKV E2 envelope protein prolonging the distance to a potential fitness peak in *A. albopictus* (Tsetsarkin et al., 2011; see 2.1.5.3).

A)
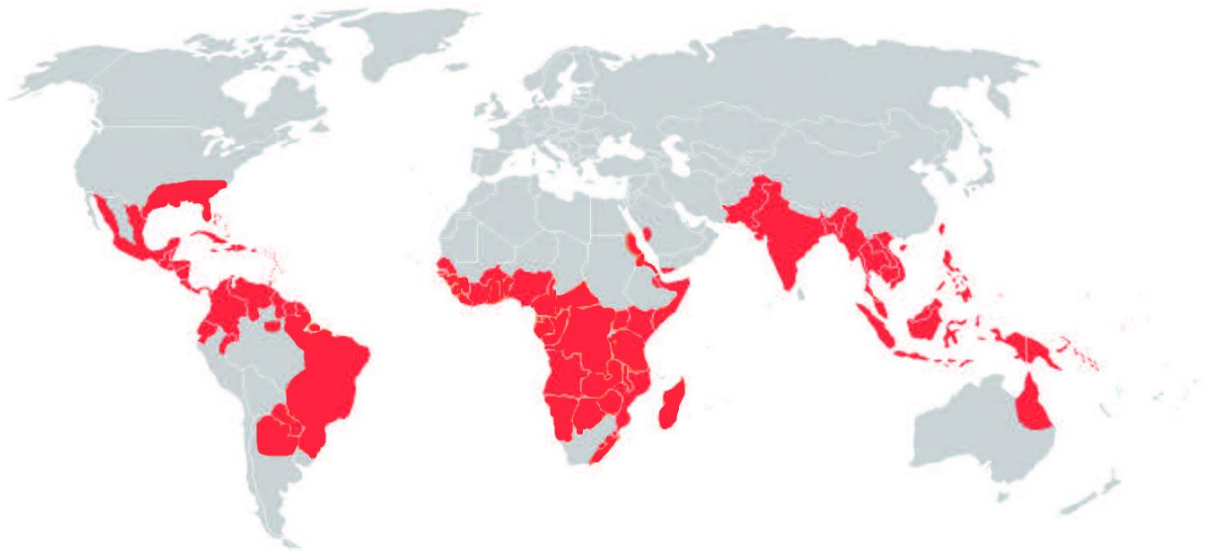
B)
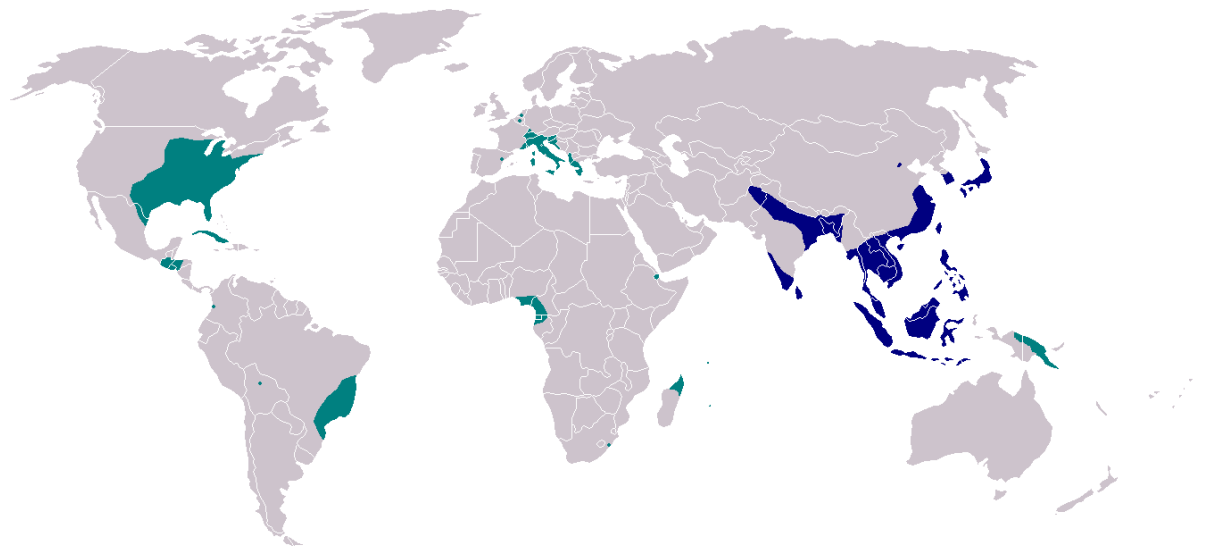
Figure 5: Worldwide distributions of *A. aegypti* and *A. albopicuts*.

A) The red labeled regions represent the distribution areas of *A. aegypti*. B) The blue labeled areas are the original distribution areas of *A. albopictus*, and the green colored regions represent the spread of the mosquito within the last 30 years.

http://www.bluesci.org/?p=9924

http://de.academic.ru/pictures/dewiki/65/Albopictus_distribution_2007.png

2.1.2.3   The Caribbean epidemic

Despite the fact that an optimal adaption of the Asian CHIKV lineage to *A. albopictus*, similar to the ECSA genotype, is rather unlikely, this genotype has been introduced into the Caribbean, with the first laboratory confirmed cases occurring in December 2013 (Leparc-Goffart et al., 2014). Thus, these cases were the first local transmission (main vector: *A. aegypti*) of CHIKV in the Western Hemisphere reported in modern times. As of end of September 2014, about 730,000 suspected, and around 10,000 laboratory confirmed cases have been reported in 36 countries or territories (PAHO and WHO, 2014). The epidemic started in Saint Martin and also swashed to continental North, South, and Central America in February 2014 (Cauchemez et al., 2014). It is still ongoing (Figure 6). An overview of selected epidemics of CHIKV during the last few decades is given in Figure 7.
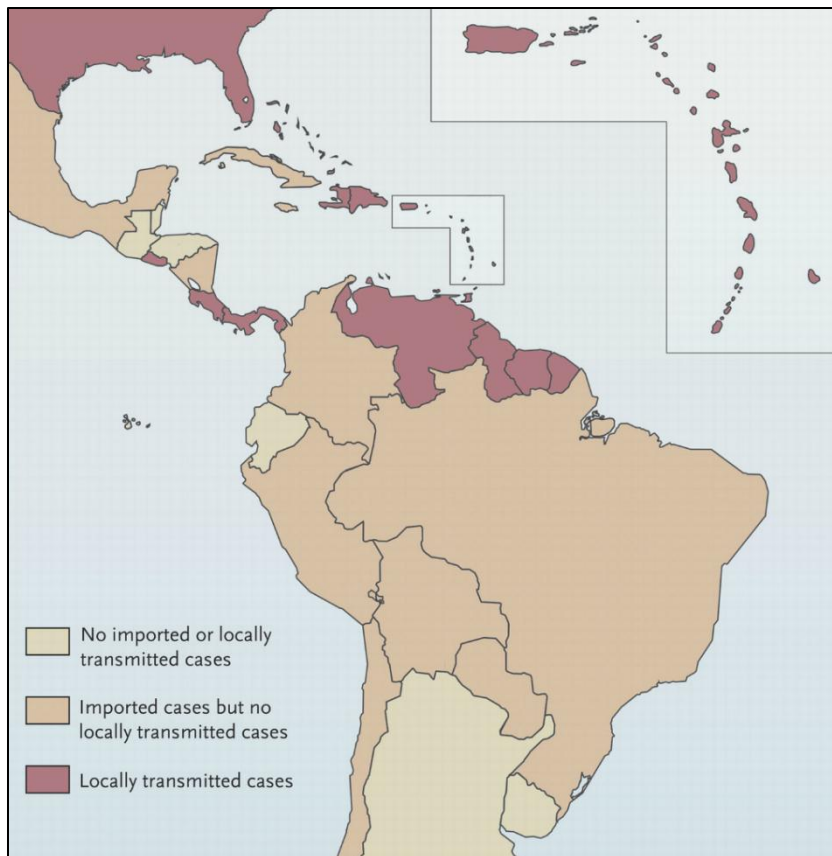
Figure 6: Map of the Caribbean CHIKV epidemic 2013-present.
The origin of the epidemic, the Caribbean islands (including Saint Martin),
are highlighted. The map visualizes the available data as of August 1, 2014.
(Fischer and Staples, 2014)
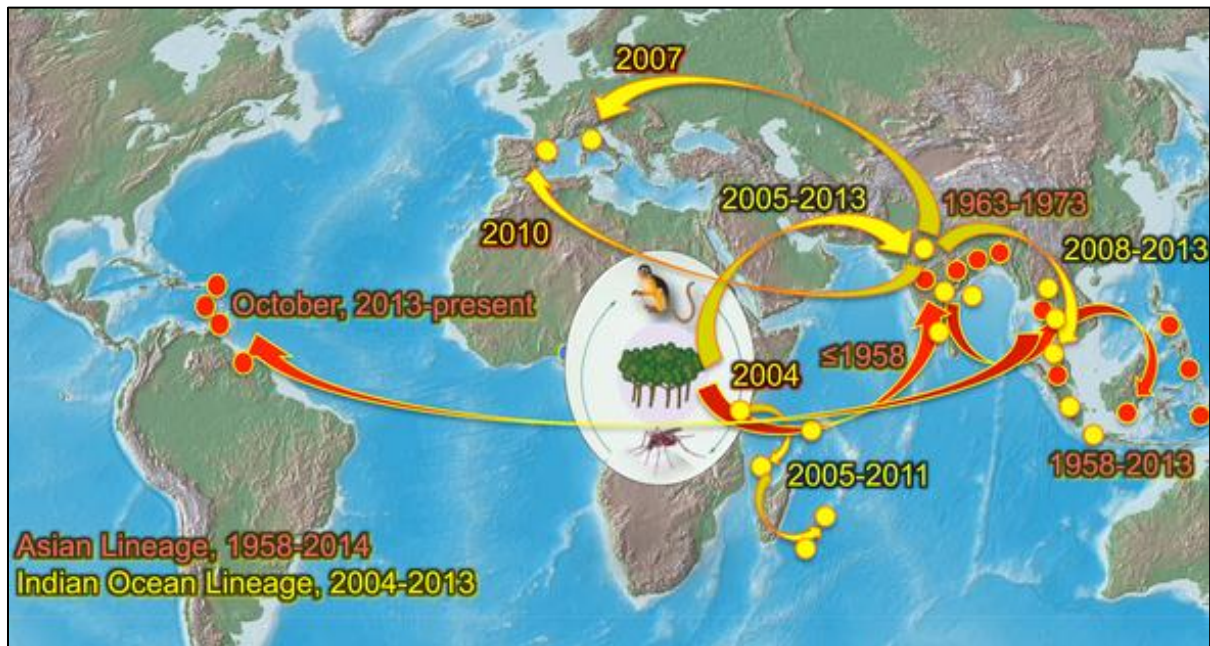
Figure 7: Overview of selected CHIKV epidemics since the 1950s.

In Sub-Saharan Africa, the ECSA lineage of CHIKV is endemic in a sylvatic cycle including monkeys and different forest-dwelling *Aedes* species. Around the 1950s, the ECSA genotype spread to India and Southeast Asia (red arrows) and has since then caused several epidemics there (red circles). The introduced virus resulted in the Asian CHIKV lineage and is today still endemic in these areas. In late 2013, this lineage from Southeast Asia was introduced into the Caribbean, and caused an epidemic in the whole area (red circles), including the American mainland, which is still ongoing. In 2004, a CHIKV epidemic of the ECSA lineage occurred in coastal Kenya and subsequently has spread to and has caused epidemics on the Indian Ocean islands and in India (yellow arrows and dots, respectively). From there, it further spread to Southeast Asia and to Italy and France. During the epidemic, the virus gained a mutation in the viral envelope protein that has rendered it to be much more transmissible by *A. albopictus* (usually *A. aegypti* is the main vector). This epidemic resulted in the IOL and this genotype is endemic today in all formerly epidemic regions (except Europe). In India and Southeast Asia, it thus circulates beside the "ancient" Asian genotype.

(Weaver, 2014)

2.1.3   Genomic organization, viral proteins, and virus morphology

2.1.3.1   Genomic organization

The CHIKV particle contains a (+) single stranded (ss) RNA genome of about 11.8 kb. As a regular mRNA, it exhibits a 5' cap and a 3' poly(A) tail (Figure 8). For the S27 strain, the 5'-non-translatable region (NTR) is 76 nucleotides (nt) long, and the 3'-NTR is made of 526 nt and contains repeated sequences believed to regulate RNA synthesis. About 2/3 of the genome (7424 nt) encode the non-structural polyprotein (nsP1-4), and the other 1/3 of the genome (3732 nt) encodes the structural polyprotein (C-E3-E2-6K-E1). Additionally, there is an opal stop codon at the end of nsP3. Between the non-structural and the structural protein genes, there is a non-translatable junction region of 68 nt in length. It contains an internal promoter for synthesis of the 26S subgenomic mRNA (enconding only the structural polyprotein), its respective start site and the 5'-non-translatable leader sequence (Solignat et al., 2009).
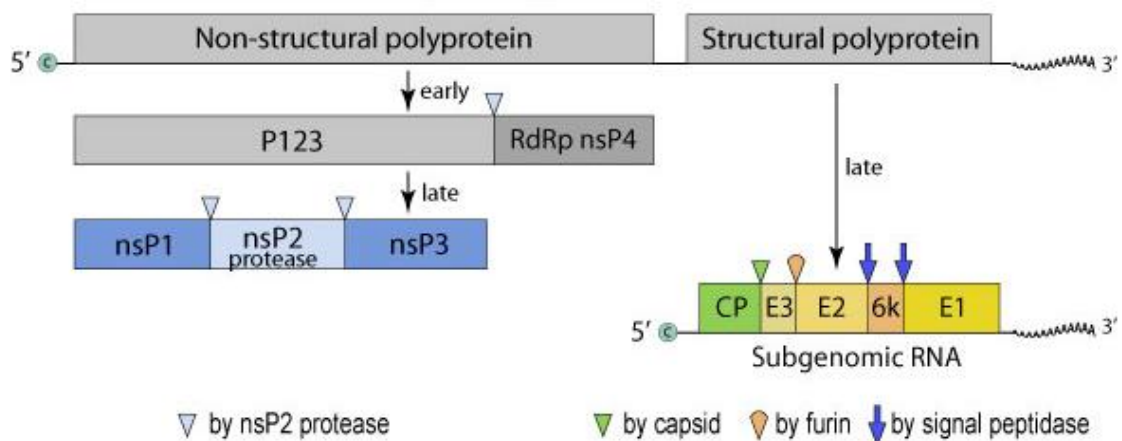
Figure 8: Organization of the CHIKV genome.
CHIKV exhibits a (+) ssRNA genome, including a 5' cap and a 3' poly(A) tail, and has 2 ORFs coding for the non-structural and for the structural polyprotein, respectively. Upon release of the viral genome into the cytoplasm of the cell, first the non-structural protein is translated. Initially, nsP4 is cleaved from the polyprotein. Later, the nsP2 protease is also cleaved at the nsP1/2 and the nsP2/3 linker regions, resulting in the mature replication complex. The structural polyprotein is translated later in infection from a subgenomic RNA using its own subgenomic promoter. Viral and cellular proteases cleave the immature polyprotein as indicated to obtain the immature structural proteins.
http://viralzone.expasy.org/all_by_protein/3.html

2.1.3.2   Viral proteins

nsP1 exhibits a methyltransferase and a guanyltransferase activity, and is thus responsible for capping of the viral mRNA (Rana et al., 2014). Furthermore, its association with the plasma membrane localizes the whole replication complex to the plasma membrane. nsP2 is additionally needed for RNA capping (NTPase and RNA triphosphatase activities), and acts as a helicase for the double stranded (ds) RNA intermediates. It is also needed for maturation of the nsP1-4 polyprotein (protease activity) and is responsible for the recruitment of and interaction with many host cell proteins, thereby promoting viral replication (Bouraï et al., 2012). The highly phosphorylated nsP3 also recruits and is associated with many cellular proteins required for the replication complex, and can bind to RNA. nsP4 is the RNA-dependent RNA polymerase (RdRp) (Rana et al., 2014).

The capsid protein (C) contains a protease domain for maturation of the structural polyprotein, and forms the regular structure of the virus by interaction with the viral genome and the E2 envelope protein cytoplasmic tail (Solignat et al., 2009). Envelope protein 3 (E3) contains the signal sequence required for guidance of E3-E2-6K-E1 into the secretory pathway of the host cell, and is vital for proper folding and pH protection of the E2-E1 heterodimer (Voss et al., 2010; Uchime et al., 2013). Envelope protein 2 (E2) contains the receptor binding site and covers the fusion loop of envelope protein 1 (E1), which is necessary for fusion of viral and host endosomal membranes. The membrane spanning 6K contains a signal sequence for translocation of the E1 protein (Voss et al., 2010).

2.1.3.3   Particle morphology

CHIKV is an enveloped virus of about 70 nm in diameter (Figure 9). A CHIKV particle is a highly organized structure with no space remaining for incorporated host cell proteins. The nucleocapsid contains exactly 240 copies of the C protein associated with one copy of the viral genome. C forms dimers and these dimers again interact to form oligomers. The interactions of the C protein make up an icosahedral lattice (T=4 triangulation number). This lattice coats the inner surface of the viral membrane. One C protein interacts additionally with the cytoplasmic tail of one E2 protein (Solignat et al., 2009). The majority of the E2 protein nonetheless is located on the other side of the viral membrane, thus on the particle surface. It is linked with its cytoplasmic part via a transmembrane domain. E2 interacts with and covers the E1 protein (which also contains a transmembrane domain and a short cytoplasmic tail) to form heterodimers with it. Three E2-E1 heterodimers (240 per virion) again form a trimer of heterodimers. These trimers are also called spikes (80 per virion) and cover the whole viral surface (Voss et al., 2010), again revealing an icosahedral lattice. Thus, the interaction of the icosahedral capsid protein lattice with the E2 envelope protein establishes

and stabilizes the shell of the viral particle, and ensures the strongly symmetric nature of the CHIKV virion.

Recently, a new alphaviral protein was identified, the transframe (TF) protein (Firth et al., 2008; Snyder et al., 2013). It is the result of a frameshift during translation of the 6K gene, which leads to a C-terminal extension of 6K. TF was found to be incorporated in submolar quantities into the viral particle and promotes virion assembly.
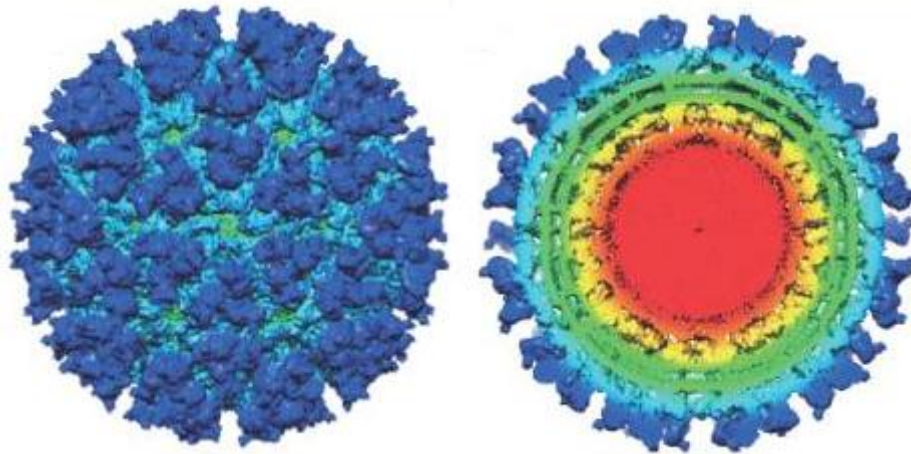
Figure 9: Morphology of a CHIKV particle.
On the **left side**, the particle (about 70 nm in diameter) is shown with the spikes (dark blue; mainly E2) and the skirt region (light blue, mainly E1) on the surface. The small areas of non-covered membrane are shown in green. On the **right side**, a cross-section of a viral particle is visualized. The spikes (again dark blue; mainly E2) surround the whole particle and the skirt region (again light blue, mainly E1) lies underneath. Both envelope proteins cross the viral membrane (green) and each E2 molecule interacts with one capsid molecule (yellow). The capsid proteins also interact with the genomic RNA. The blending region of capsid proteins and viral RNA is shown in orange, whereas the center of the particle is solely occupied with RNA (red).
Adapted from (Jose et al., 2009)

2.1.4   Viral replication

To start a new replication cycle (Figure 10), the virus first binds via E2 to its unknown cellular receptor. Subsequently, it is taken up by receptor mediated endocytosis. Upon acidification of the early endosome (Bernard et al., 2010), the E2-E1 heterodimer dissociates. This enables E1 to interact and fuse with the endosomal membrane after a series of protein interactions and conformational changes (Kielian et al., 2010). The nucleocapsid is then released into the cytoplasm of the cell. It disassembles by binding of C to the large ribosomal subunit, which liberates the viral genome. The host cell translational machinery translates the non-structural polyprotein nsP1234 (and partly nsP123 due to the opal stop codon 3' of the

nsP3 gene) from the mRNA like viral genome (Solignat et al., 2009). The product is directly cleaved by the protease function of nsP2 into nsP123 and nsP4 in *cis* or *trans.* nsP123 and nsP4 form a complex to initiate and conduct the synthesis of the (-) strand of the viral genome. After cleavage of the nsP1/2 junction by nsP2 (in *cis* only), the resulting nsP1-nsP23-nsP4 complex still preferentially produces (-) strand viral RNA. Only after cleavage into the mature non-structural polyproteins do the nsP1-nsP2-nsP3-nsP4 replication proteins switch to the production of (+) strand genomic (49S) and subgenomic (26S) RNA using the (-) viral RNA as a template (Shin et al., 2012). The subgenomic RNA is synthesized from the subgenomic (internal) promoter in the junction region of the genome between the open reading frames (ORFs) for the non-structural and the structural viral proteins (see 2.1.3.1). The 26S RNA acts as an mRNA for the host cell mediated translation of the structural polyprotein C-E3-E2-6K-E1. The capsid protein C cleaves itself in *cis* from the nascent polypeptide chain. Following this cleavage, the signal peptide of E3 ensures translation of the remaining polypeptide sequence into the lumen of the endoplasmatic reticulum (ER). Due to the transmembrane domain of E2, the polypeptide chain behind this domain is again located outside of the ER, in the cytoplasma of the cell. The 6K peptide (located after the cytoplasmic tail of E2), with its transmembrane domains, again acts to translocate the upcoming E1 into the lumen of the ER (similar to E2) (Solignat et al., 2009). Subsequently, cellular signal peptidases cleave the polyprotein at the E2-6K and 6K-E1 junctions, resulting in p62 (E3-E2), 6K, and E1. p62 and E1 then form heterodimers, and these again form trimers. These oligomerization processes are required for proper folding of the involved proteins (Andersson et al., 1997). The ER membranes fuse with membranes of the Golgi apparatus, and thus guide their protein cargo to the plasma membrane for secretion. E3 supports correct folding of the p62-E1 heterodimer and acts as a brace to avoid premature pH induced conformational changes in the slightly acidic environment of the Golgi apparatus. Before secretion of the envelope proteins, the cellular protease furin cleaves p62 into E3 and E2, resulting in the final E2-E1 heterodimer (Voss et al., 2010). It is, by this final cleavage, in a metastable conformation (Snyder and Mukhopadhyay, 2012) and thus primed for dissociation upon exposure to acidic pH at the beginning of the next viral life cycle. After secretion, the heterodimers accumulate at the plasma membrane of the host cell. The E2 cytoplasmic tail interacts with the lattice of 240 capsid proteins (which itself interact with the genomic RNA and encapsidate it). Only after association of E2 with C, does E2 aggregate in certain regions of the plasma membrane, which no longer contain host proteins (Martinez et al., 2014). The E2-C interaction furthermore enables budding of new mature virions (Solignat et al., 2009; Jose et al., 2012). E3 is only loosely associated with the free virion and diffuses away, and 6K is present in submolar quantities in the viral particle (Strauss and Strauss, 1994).
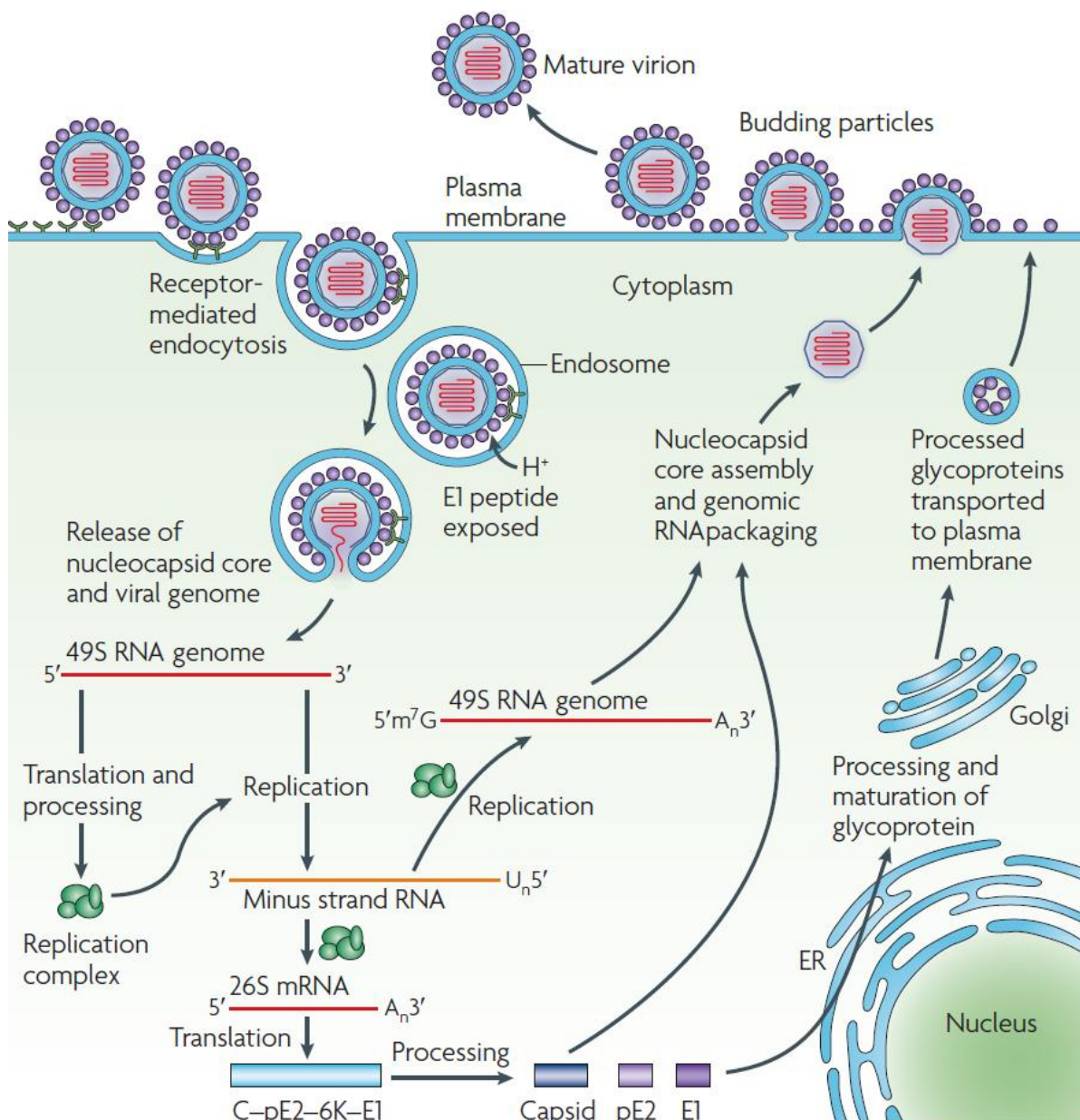
Figure 10: Replication cycle of CHIKV.

CHIKV binds to the host cell via its unknown cellular receptor and is taken up by receptor mediated endocytosis. Acidification of the early endosome leads to a conformational change of the viral envelope proteins. This conformational change results in the exposure of the E1 fusion loop and the subsequent fusion of the viral and the endosomal membrane. The viral nucleocapsid containing the viral genomic (49S) RNA genome is released into the cytoplasm of the cell. The viral non-structural proteins are translated and form a replication complex that first synthesizes (-) strand genomic RNA from the (+) strand template. After complete cleavage and thus maturation of the non-structural proteins, does the complex switch to produce (+) genomic and subgenomic (26S) RNA from the (-) strand template. The structural polyprotein is subsequently translated from the (26S) RNA via a subgenomic promoter. It is cleaved by viral and cellular proteases into mature structural proteins. These interact with each other and with the viral genomic RNA to enable budding and formation of new virions.
(Schwartz and Albert, 2010)

2.1.5   The CHIKV envelope proteins and the entry process

2.1.5.1   The envelope proteins

The structure of the CHIKV envelope proteins has been solved by X-ray crystallography in 2010 (Voss et al., 2010) (Figure 12). The E3 protein encompasses the first 64 amino acids of the envelope polyprotein and has one glycosylation site (N12) (Figure 11, upper panel). It is exposed prominently on the surface of the immature viral particle and consists of an N-terminal β-hairpin followed by three α-helices. The overall structure is similar to a horseshoe. E3 makes several contacts with E2 (especially with the E2 β-ribbon connector, see below) and thereby ensures, as mentioned in 2.1.4, correct folding of the E2-E1 heterodimer, as well as prevention of premature E2-E1 dissociation (Lobigs et al., 1990; Snyder and Mukhopadhyay, 2012; Uchime et al., 2013). However, after cleavage at the furin cleavage site between E3 and E2 in the secretory pathway, E3 is no longer covalently linked to E2 (precursor is called p62; see 2.1.4) and diffuses away from the viral surface.
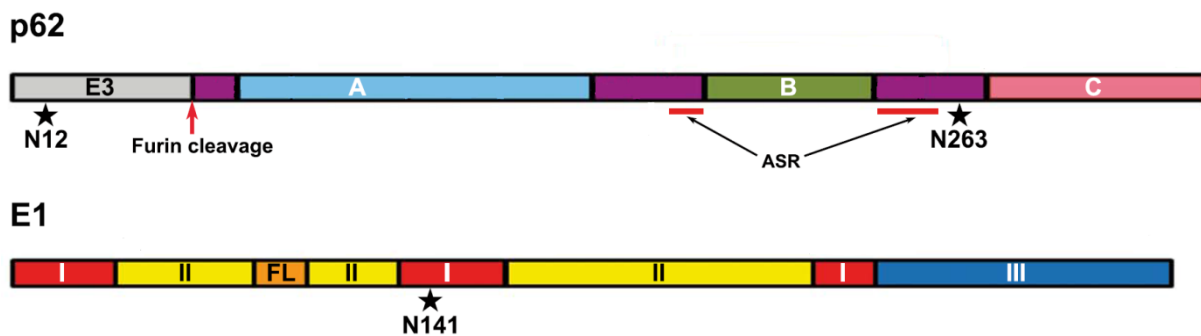
Figure 11: Schematic overview of the structure of the CHIKV envelope proteins (extracellular parts; without stem regions).

The precursor protein p62 (**upper panel**) is composed of E3 (grey) and E2 (different colors). The furin cleavage site which separates E3 from E2 is indicated by a red arrow. E2 domains A (light blue), B (green), and C (rose) are shown. The β-ribbon connector parts are labeled in violet (note that the N-terminal part of E2 does not belong to the connector) and the acid sensitive region (ASR) within the connector is labeled by bolded red lines. The glycosylation sites are indicated by asterisks. The extracellular part of the E1 protein (**lower panel**) is composed of the domains I (red), II (yellow), and III (dark blue). The fusion loop (FL) within domain II is highlighted in orange. The glycosylation site is indicated by an asterisk.

Adapted from (Voss et al., 2010)

E2 consists of the 432 amino acids in the C-terminal direction from E3 (Figure 11, upper panel), and exhibits two N-linked glycosylation sites (at N263 and N345, the latter one within the stem region). This composition results in a molecular weight of 56 kDa with and 47.0 kDa without glycosylations. E2 has three extracellular domains called A, B, and C (from N- to C-terminus). All of them are immunoglobulin (Ig)-like (Figure 12), and thus solely form β-sheets (expect a short α-helix at the N-terminus of E2, which strictly speaking does not belong to

domain A). Domain B is located at the tip of the protein protruding from the viral surface and is linked to domain A (in the middle) via a long β-ribbon connector (containing an acid sensitive region (ASR)). Domain C is found close to the viral membrane and is followed by the stem region, which is a linker to the transmembrane region composed of hydrophobic amino acids. The short cytoplasmic tail (32 amino acids) interacts with the capsid protein to maintain the regular structure of the virion (Solignat et al., 2009). The function of 6K (between E2 and E1) was described in 2.1.3.2.

The E1 protein is covered by E2 (Figure 12) and is composed of 439 amino acids (Figure 11, lower panel). It contains, similar to E2, three extracellular domains (I, II, and III), and one glycosylation site (N141; molecular mass with glycosylation 52 kDa, without 47.5 kDa). Domain II plays a key role, as this domain solely makes the majority of contacts with E2 in the E2-E1 heterodimer. Additionally, it is the largest domain of E1 and contains the hydrophobic fusion loop, indispensable for fusion of viral and endosomal membranes, at its' distal end. A few histidine residues within E2 stabilize the fusion loop conformation, which is buried between the domains A and B of E2. E1 is, similar to E2, an all β-sheet protein, with domain II forming its tip. Domain I lies at the center and is, via a linker region, connected to the Ig-like domain III that is located close to the viral membrane, thus it also plays an important role in facilitating the conformational change upon pH lowering (see below) (Sánchez-San Martín et al., 2008). A stem region links DIII and the transmembrane segment of E1. The transmembrane segments of E2 and E1 within one heterodimer interact with each other (Tang et al., 2011; Aggarwal et al., 2012). At the C-terminus of E1, there is a very short cytoplasmic tail (3 amino acids). E1 belongs to the class II viral fusion proteins (Kielian et al., 2010).
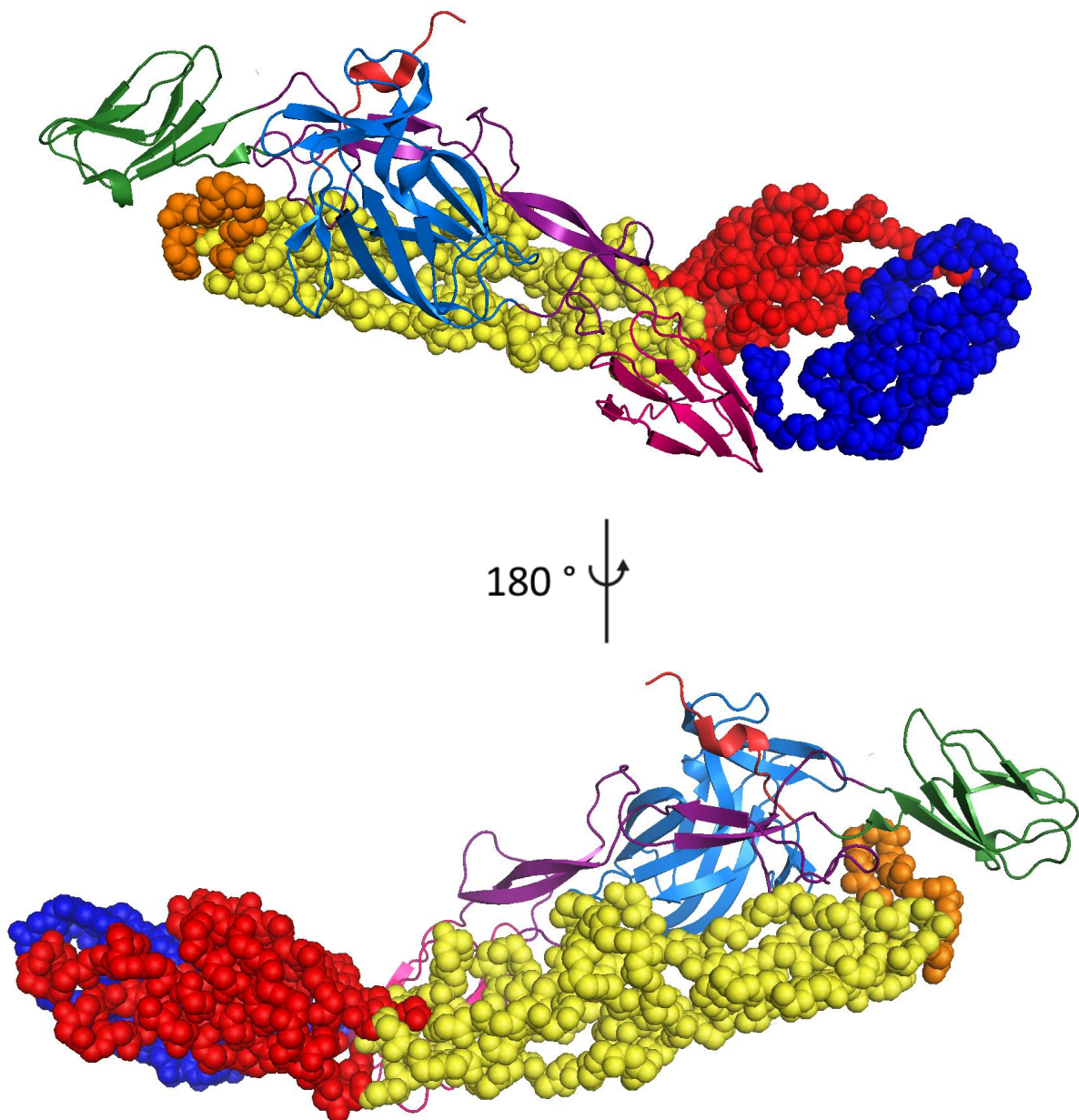
Figure 12: Structure of the CHIKV envelope proteins (E2-E1 heterodimer; extracellular parts; without stem regions).

E2 is shown in ribbon style. E2 domains A (light blue), B (green), and C (pink) are shown. The β-ribbon connector parts are labeled in violet. Note that the N-terminal part of E2 does not belong to the connector, for clarity it is not colored in violet (as in Figure 11), but in light red. The extracellular part of the E1 protein is shown in spheres style. The protein is composed of the domains I (red), II (yellow), and III (dark blue). The fusion loop (FL) within domain II is highlighted in orange.

Adapted from (Voss et al., 2010)

As mentioned in 2.1.3.3, 240 E2-E1 heterodimers form 80 trimers on the viral surface (Voss et al., 2010). A trimer (or spike; Figure 13) has a propeller-like shape with E2 domain B sitting at the tip of each of the three blades. All inter-spike contacts are created by amino acid side chains of E1. Contrary to this connection, there are no E1-E1 contacts within one spike. Additionally, E1 interacts with E2 (but not E1) of adjacent E2-E1 heterodimers from the same spike. Opposing these contacts, E2 residues form intra-spike chemical bonds across heterodimers to other E2 and E1 proteins, but no contacts to adjacent spikes (inter-spike contacts).

A)

B)

C)

D)
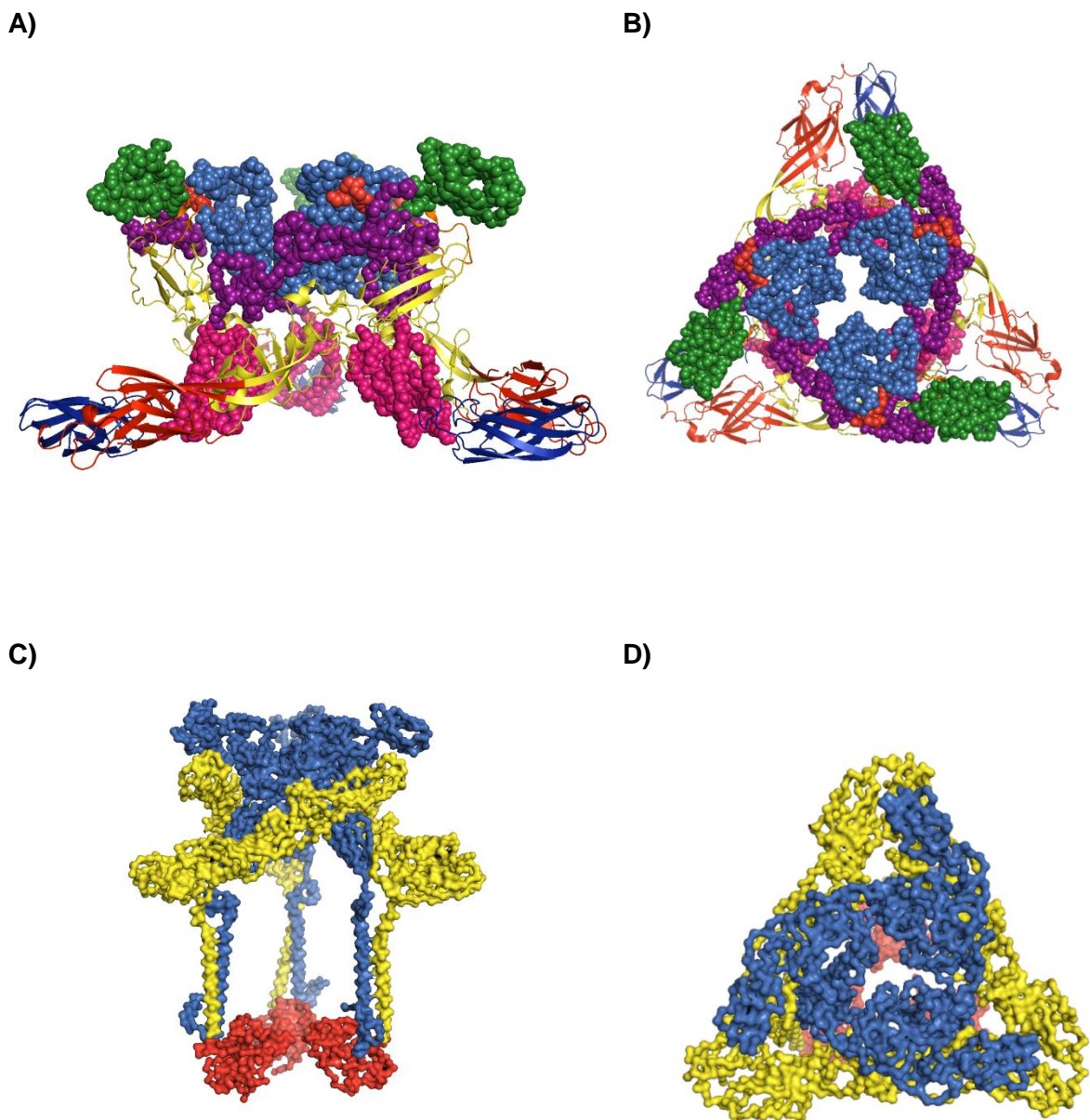
Figure 13: Structure of a CHIKV envelope protein spike.

One CHIKV spike (trimer of E2-E1 heterodimers; only the extracellular parts; without stem regions) is shown in side view (A), and rotated by 90° in top view (B). E2 is shown in spheres style. E2 domains A (light blue), B (green), and C (pink) are visualized. The β-ribbon connector parts are labeled in violet. Note that the N-terminal part of E2 does not belong to the connector, for clarity it is not colored in violet (as in Figure 11), but in light red (as in Figure 12). The extracellular part of the E1 protein is shown in ribbon style. The protein is composed of the domains I (red), II (yellow), and III (dark blue). The fusion loop (FL) within domain II (below E2 domains A-B junction) is highlighted in orange. In (C) (side view) and (D) (rotated by 90°, top view) a spike (all proteins in spheres style) is shown including the transmembrane parts of E1 (yellow) and E2 (blue) (which interact with each other), and the capsid proteins (red), each associated with one E2 protein. Note that the figures (C) and (D) are derived from the spike structure of SINV, another alphavirus.

Adapted from (Voss et al., 2010; Tang et al., 2011)

2.1.5.2   The entry process

The entry process of CHIKV begins with the attachment of the particle to the cell surface. Binding (and release) of viral particles occurs at the apical domain of polarized cells (Lim and Chu, Justin Jang Hann, 2014). The cellular receptor of CHIKV is not yet identified. It was published that Prohibitin plays a role in CHIKV entry into microglial cells (Wintachai et al., 2012). The ATP synthase β subunit might be involved in CHIKV entry into insect cells (Fongsaran et al., 2014). Several other proteins have been proposed as attachment/promotion factors for alphavirus entry, such as DC-SIGN/L-SIGN or heparan sulfate for example (Kielian et al., 2010). However, their *in vivo* relevance remains unknown. In general, the success in searching for alphaviral cellular receptors is so far limited, given that all alphaviruses exhibit a very broad, yet unique for each virus, cellular and host range. For this reason, several receptors might be engaged by each alphavirus (Kielian et al., 2010). Nonetheless, the cellular receptor on insect and mammalian cells for one alphavirus, the Sindbis virus (SINV), has recently been identified as natural resistance-associated macrophage protein (NRAMP) (Rose et al., 2011). The exact receptor binding site on the CHIKV E2 protein has mainly been speculated to lie within domain A (Li et al., 2010; Porta et al., 2014). However, residues identified as important for cell attachment or for binding of neutralizing antibodies are located in the alphaviral E2 domains A and B (Li et al., 2010; Voss et al., 2010).

The receptor mediated endocytosis after receptor binding is clathrin-independent (Bernard et al., 2010). Upon acidification of the early endosome (Bernard et al., 2010), the E2-E1 heterodimer begins to dissociate at a pH threshold of about 6.0. The first part of E2 that becomes disordered is domain B and the adjacent parts of the β-ribbon connector, the ASR (Figure 14). A crystal structure of SINV E2 with the disordered domain B was solved at pH 5.6 (Li et al., 2010). Many histidine side chains form contacts between E2 and E1 in the heterodimer at neutral pH, especially around the fusion loop. Histidine is the only amino acid of which the side chain's pK_s (around 6.0) lies within the changed pH range of the endosome. Thus, these residues are protonated upon a pH lower than 6.0. This changes the overall charge at the E2-E1 interface, bonds are disrupted, and the E2-E1 dissociation can take place. Lowering of the pH to under 5.6 finally leads to a total dissociation. The E1 fusion loop within domain II is now exposed and inserted into the host cell membrane. Subsequently, E1 proteins form homotrimers. For this assembly, the E2 proteins have to move out of the center of the spike and E1 proteins have to rotate by 180°. Once the homotrimer is formed, E1 domain III moves 30-40 Å towards the fusion loop and packs against the groove between two E1 monomers, thereby bringing the viral (near E1 domain III) and endosomal membrane (fusion loop inserted) in close proximity to each other. The transition from the metastable

heterodimeric/monomeric E1 to the stable trimeric E1 conformation, with the inserted fusion loop and the folded-back domain III, releases enough energy to let viral and endosomal membranes fuse (Kielian and Rey, 2006; Chernomordik and Kozlov, 2008). By the cooperation and interaction of many homotrimers, a fusion pore is created through which the viral nucleocapsid is released into the cytoplasm of the cell.
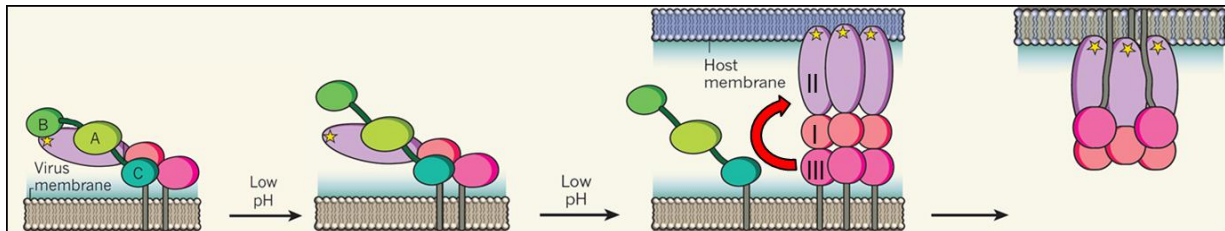
Figure 14: Schematic representations of the structural changes of the CHIKV envelope proteins during the membrane fusion process.

At neutral pH, E2 (greenish colors; domains A, B, and C) covers nearly the whole E1 protein (reddish colors) and especially the fusion loop at the tip of domain II (labeled by an asterisk). Upon acidification in the endosome, first the E2 domain B is disordered, and then a continued decline of the pH leads to full dissociation of the E2-E1 heterodimer. The fusion loop is then exposed and inserted into the endosomal membrane. Subsequently, E1 forms homotrimers. Following this assembly, E1 domain III moves 30-40 Å towards the fusion loop and folds back into a groove between E1 domains I and II. Finally, the E1 stem region (between domain III and the transmembrane domain) and the fusion loop are on the same side of the molecule. This orientation and the transition from a metastable to a stable conformation of E1 enables fusion of the viral and the endosomal membranes.

Adapted from (Kielian, 2010)

2.1.5.3   The E1 A226V mutation and its consequences

The E1 A226V mutation that appeared during the La Réunion epidemic in 2006 had a big impact on vector dependency of CHIKV, and enhanced replication and transmission by *A. albopictus* by several times (Schuffenecker et al., 2006; Vazeille et al., 2007).The residue 226 in E1 lies in close proximity to the fusion loop and thus probably influences its flexibility (Voss et al., 2010) (Figure 15). The mutation enhanced cholesterol dependency in the target membrane during fusion in the endosome (Tsetsarkin et al., 2007). This change could be hinting towards the changes in lipid composition in endosomes of *A. aegypti* and *A. albopictus*. The mutation enhances entry and replication in the midgut cells of the mosquito (Arias-Goeta et al., 2013). Prerequisites for the observed enhanced transmission owing to the E1 A226V mutation are a threonine at position 211 in E2, and an alanine at position 98 in E1 (Tsetsarkin et al., 2009; Tsetsarkin et al., 2011) (Figure 15). Both phenotypes are fulfilled for some ECSA isolates (and of course especially for the IOL strain). In contrast to this

fulfillment, the Asian strain isolates have an isoleucine at position 211 in E2, and a threonine at position 98 in E1. This amino acid phenotype is likely due to a founder effect of the Asian lineage. It prevented the Asian lineage, despite its circulating within Southeast Asia for decades, from more efficient adaption to transmission by *A. albopictus*. Another constraint to gaining and fixing the necessary mutations is the, relative to other RNA viruses, slower evolution rate of arboviruses, due to their continual switch between the very different environments of an arthropod and a vertebrate host (Greene et al., 2005). Since the emergence of the initial E1 A226V mutation, second-step mutations in some IOL sub-lineages occurred and have further enhanced the transmission by *A. albopictus* (Tsetsarkin et al., *2014).* These mutations include, for example, E2 R198Q, L210Q, K252Q, and E3 S18F. The exact molecular roles of the prerequisite phenotypes E2 211T and E1 98A, the key mutation E1 A226V, and of the mentioned second-step mutations are not yet clear. They are all located near the fusion loop (for the E1 mutations; Figure 15), in the ASR, or in domain B (for the E2 mutations), possibly altering fusogenic properties and/or receptor binding (Tsetsarkin et al., 2014). These recent developments highlight that the radiation within the IOL following a key mutation is still ongoing. Additionally, some other possible mutations also enhancing *A. albopicus* transmission were so far only created and detected in the laboratory, but might also occur in nature in the near future (Stapleford et al., 2014).
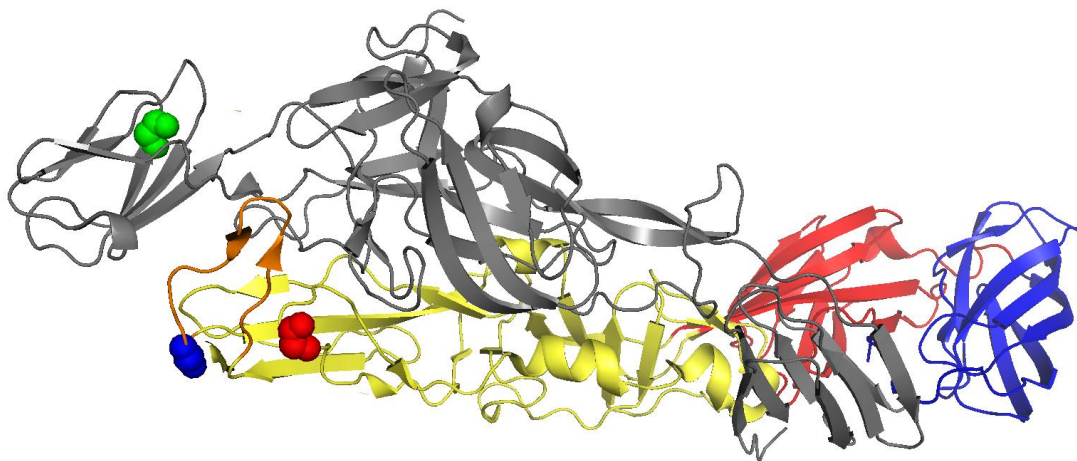
Figure 15: Location of the A226V and other key mutations/phenotypes within the CHIKV envelope E2-E1 heterodimer (extracellular parts; without stem regions) for more efficient transmission by *A. albopictus.*
E2 (grey) and E1 (colored) are shown in ribbon style. The E1 domain I is shown in red, domain II is shown in yellow, and domain III is shown in dark blue. The fusion loop (FL) within domain II is highlighted in orange. The locations of the key mutations/phenotypes for a more efficient transmission by *A. albopictus*, 98A (blue), A226V (red), and E2 211T (green), are emphasized by spheres. Note that the positions E1 98 and 226 are located at the base of and directly adjacent to the fusion loop, respectively.
Adapted from (Voss et al., 2010)

2.1.5.4   Glycosaminoglycans (GAGs) as attachment factors for viruses

GAGs are ubiquitously present on cell surfaces of all animal cells and are an essential part of the extracellular matrix (ECM) (Bishop et al., 2007; Gandhi and Mancera, 2008; Kamhi et al., 2013). They consist of linear chains of sulfated disaccharide units (30-60 per chain), exhibit molecular masses of 15-30 kDa, and are negatively charged. The disaccharide units are composed of an uronic acid (glucuronic or iduronic acid), and of an amino sugar (galactosamine or glucosamine) (Figure 16 B). Depending on the specific combination of uronic acid and amino sugar, one can distinguish between heparin (HP), heparan sulfate (HS), chondroitin sulfate (CS), and dermatan sulfate (DS) (Figure 16 A). There are also other subclasses of GAGs, which are not mentioned here (Kamhi et al., 2013).

The molecule consisting of several HS, CS, or DS chains covalently linked to serine residues of a so-called core protein (which is usually membrane-associated) is called a proteoglycan (PG) (Figure 16 A). In PGs, the carbohydrate part of the molecule exhibits a much higher mass than the protein part, in contrast to glycoproteins. Nonetheless, HS, CS, or DS can also occur in free form in the ECM without linkage to a core protein.

Hyaluronic acid and HP are never covalently linked to a core protein. Additionally, hyaluronic acid is the only example of a GAG that is not sulfated at all. Furthermore, it can form unusually long chains of up to 2600 disaccharides in length (up to 1,000 kDa molecular mass) and is an important component of the ECM of connective tissues. All GAGs are, as mentioned above, negatively charged partly due to their organic acid residue of the uronic acid. Additionally, the number of sulfate groups can vary between different GAGs (usually about one per disaccharide unit; Figure 16 B), which has a big impact on the overall charge of the molecule. HP plays a role in the inhibition of blood coagulation, is only produced in mast cells, and is the GAG with the most sulfate groups (2.7 per disaccharide unit), thus having the highest overall charge. The higher degree of sulfation and the fact that it is never linked to a core protein are the only molecular features that distinguish HP from HS.

Nonetheless, the disaccharide unit sulfation degree of every GAG is not a fixed feature but can vary spatially (position and number of C atoms sulfated, position and number of disaccharide units sulfated), temporally, between tissues, and among cell types. GAGs are never completely sulfated, which leads to clusters of sulfation along a chain and a number of different isomers of the same GAG subunits. These specific patterns are called the "sulfation code" and are believed to play a role in protein recognition and cellular regulation of signal pathways (Kamhi et al., 2013)

A)
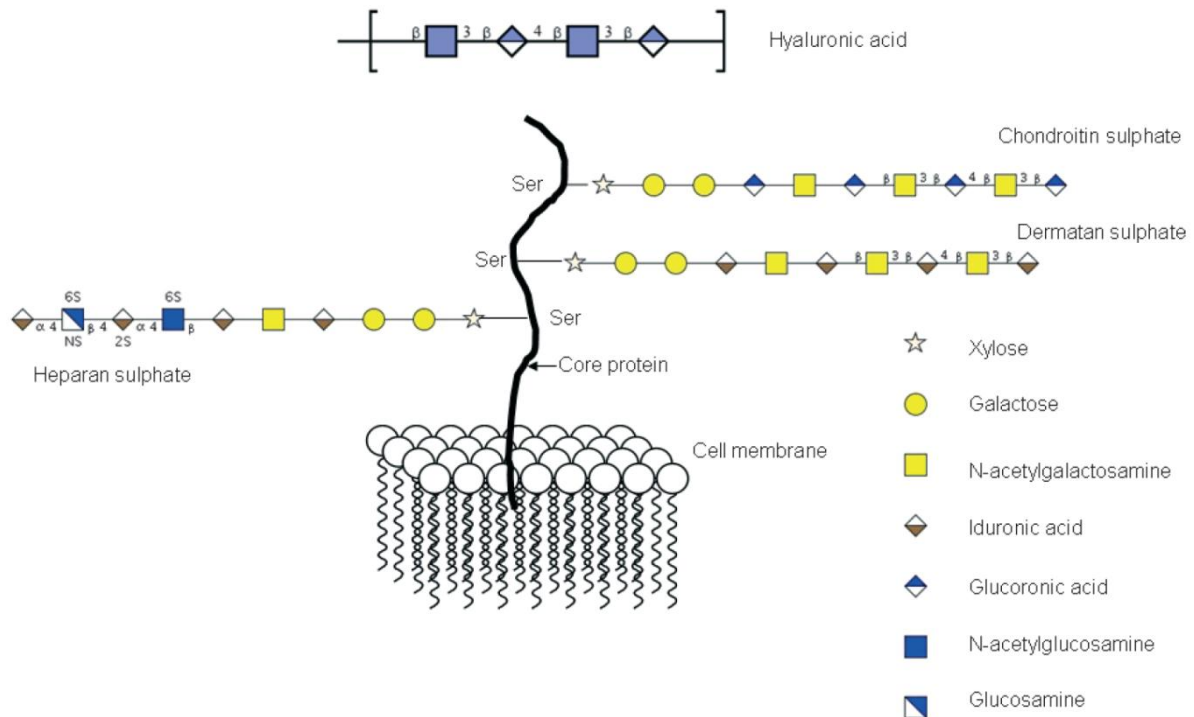
B)
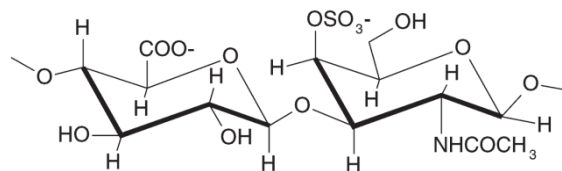
Figure 16: Structure of GAG and PGs.

A) GAGs form 30-60 units long negatively charged chains of disaccharides. The disaccharides are always composed of an uronic acid and an amino sugar. Depending on the specific composition of the disaccharide, one can distinguish the main GAGs heparan sulfate (HS), chondroitin sulfate (CS), dermatan sulfate (DS), and hyaluronic acid. The latter one is an exception to the rule due to its chain length (up to 2,600 disaccharide units), the fact that it is not sulfated, and that it is never linked to a membrane-associated core protein and thus always is located in the ECM. The other GAGs can be covalently linked to a core protein (via serine side chains of the protein and an always identical linker region (composed of one xylose and two galactose molecules)) and are sulfated (in average about one sulfation per disaccharide). Together with the protein, they are called PG. Heparin (HP), a molecule involved in the inhibition of blood clotting, exhibits no qualitative, only quantitative, differences to HS. It is much more heavily sulfated (about 2.7 times per disaccharide unit) and also is never linked to a core protein. B) Detailed molecular structure of a chondroitin sulfate disaccharide unit. Note the organic acid residue and the sulfate group.

Adapted from (Gandhi and Mancera, 2008)

PGs have a variety of biological functions in the body and are not just passive components of the cell surface or the ECM (Raman et al., 2005; Bishop et al., 2007). For example, they act as co-receptors for growth factors, transport and present chemokines at the cell surface, facilitate cell adhesion to the extracellular matrix, and are associated with the cytoskeleton. PGs can also function as classical endocytotic receptors, because binding of ligands to them can induce their uptake.

Since PGs are ubiquitously present on the cell surface, many pathogens exploit them to hurdle the cell membrane barrier and use them for initial cell attachment or as entry receptors. These pathogens include several bacteria, parasites, and viruses (Liu and Thorp, 2002; Kamhi et al., 2013). Cell surface HS, the most extensively studied GAG, promotes attachment and entry of the herpes simplex virus type 1 (HSV-1), the human immunodeficiency virus (HIV), the hepatitis C virus (HCV), the vaccinia virus, the dengue virus (DENV), and the adeno-associated virus isolate 2 (AAV-2) into cells. In some cases, there seems to be specific binding sites for the virus within the HS molecule (for example, for HCV or HSV-1). However, whether HSPG serves in these cases only as an attachment factor, as a co-receptor, or as a primary receptor is currently under debate. Binding of an alphavirus, the eastern equine encephalitis virus (EEEV), to cell surface HS, thereby enhancing its neurovirulence, has also been reported (Gardner et al., 2011).

2.2 Treatment and vaccine development

2.2.1 Treatment

2.2.1.1 Treatment of CHIKV

As of today, there is no specific treatment or vaccination available against CHIKF. In the case of disease, a symptomatic treatment is performed using corticosteroids or non-steroidal anti-inflammatory drugs against the myalgia and the arthralgia (Kaur and Chu, Justin Jang Hann, 2013).

There are some small molecule candidates, which inhibit different life cycle steps of the virus, that appear promising for further development, but they are all still far from market approval (Bourjot et al., 2012; Kaur and Chu, Justin Jang Hann, 2013; Rashad and Keller, 2013; Rashad et al., 2014). Furthermore, noncytotoxic doses of a 5'triphosphorylated RNA (5'pppRNA) before or after CHIKV challenge stimulated the innate immune system dsRNA sensor RIG-I and protected cells *in vitro* from CHIKV infection (Olagnier et al., 2014). Additionally, several other approaches have been tried in animal experiments. For example, siRNAs against E2 and nsP1 have been tested successfully in mice (Parashar et al., 2013).

Most approaches used different neutralizing monoclonal antibodies derived from infected human patients or vaccinated mice, and these were solely directed against the E1 or more frequently E2 envelope protein. These treatments were administered prophylactically and/or therapeutically and conferred protection against CHIKV in mouse models (Fric et al., 2013; Goh, Lucas Y H et al., 2013; Pal et al., 2013; Selvarajah et al., 2013). However, 5'pppRNA and siRNA are rather expensive and they are also temperature sensitive molecules. Monoclonal antibodies are even more expensive to produce (as compared to small molecules). These are not optimal features for the treatment of millions of people mainly in subtropical/tropical and/or poor countries, where CHIKV is currently epidemic or endemic. Therefore, a prophylactic vaccination would be the most efficient and cheapest solution to prevent the further spread of CHIKV and to avoid future outbreaks.

2.2.1.2 Novel antiviral molecules: Epigallocatechin-3-gallate (EGCG) and epicatechin (EC)

EGCG belongs to the catechins, whose structure is composed of a flavan-3-ol (Figure 17 A). It is the major catechin of green tea in regards to influence on human diseases, because it is thought to have anti-cancer and anti-diabetes properties. The source of green tea is the unfermented leaves of *Camellia sinensis*. In black tea extract, those leaves are fully fermented, and thus all catechins are inactivated. Besides EGCG, there are also other catechins in green tea extracts, for example epigallocatechin (EGC), epicatechin gallate (ECG), and epicatechin (EC). EC does, opposing EGCG, not contain a galloyl side chain (Figure 17 B). This side chain likely promotes the biological activities of EGCG (Nagle et al., 2006).

EGCG has also been published to have antiviral activities against several viruses. It inhibits the transcription of the hepatitis B virus (HBV), adenoviruses, and herpesviruses (Steinmann et al., 2013). In contrast to this activity, EGCG inhibits the viral entry process of influenza virus (Kim et al., 2013), HIV (Fassina et al., 2002; Yamaguchi et al., 2002; Williamson et al., 2006), and HCV (Ciesek et al., 2011; Calland et al., 2012; Chen et al., 2012; Colpitts and Schang, 2014). The steps inhibited in the viral life cycle are, as described above, usually known, but there is in general a lack of understanding of EGCG's in-depth mechanisms of action.

A)

B)
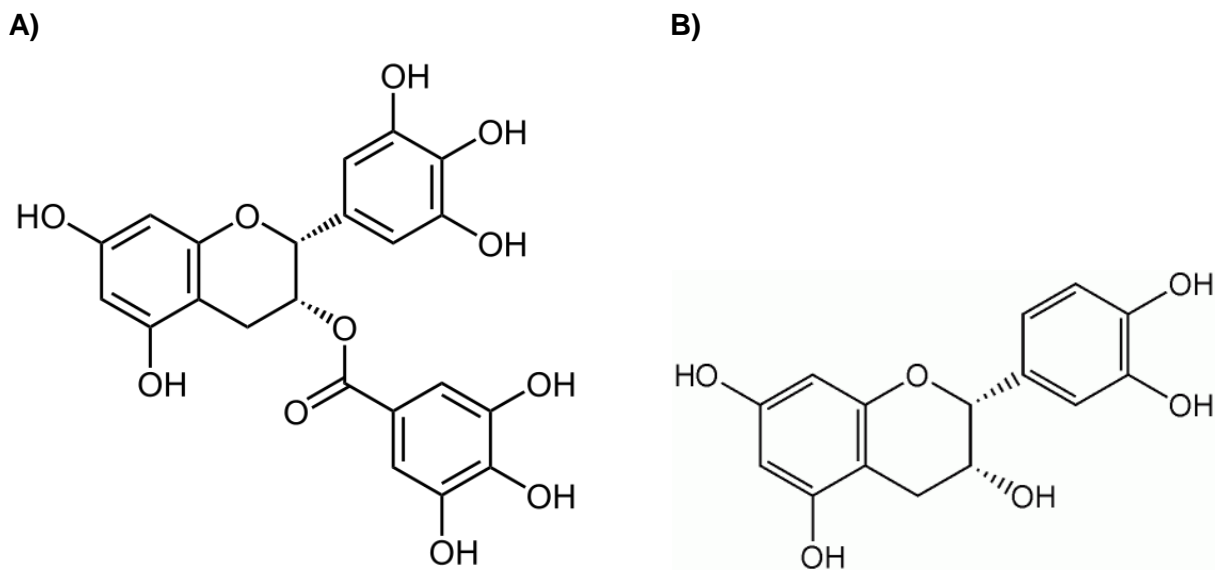
Figure 17: Structures of EGCG and EC.

Displayed are the chemical structures of EGCG (A) and EC (B). Note the missing galloyl side chain (down, right) of EC in comparison to EGCG.

http://en.wikipedia.org/wiki/Epigallocatechin_gallate

http://en.wikipedia.org/wiki/Catechin

2.2.2 Vaccine development

2.2.2.1 CHIKV vaccine development

The innate immune system and an adaptive anti-CHIKV antibody response are essential to control CHIKV infections (Tang, 2012; Lum et al., 2013). This essentialism implies that vaccination might also prevent disease. However, vaccine safety has to be assured. The appearance of unwanted side effects similar to a CHIKV infection has to be excluded.

The first CHIKV vaccine to reach clinical trials (phase 2) was a CHIKV strain attenuated by 18 passages on MRC5 cells (Edelman et al., 2000). Some study subjects experienced mild to moderate joint pain and phase 3 trials thus did not take place (Schwartz and Albert, 2010). Several vaccination approaches have been tried since then in animal experiments (Weaver et al., 2012). Recombinant E2 protein, inactivated virus (Kumar et al., 2012), live attenuated vaccines with an artificial IRES (Plante et al., 2011; Chu et al., 2013; Roy et al., 2014), or a large deletion in the viral genome (Hallengärd et al., 2014), and chimeric viruses (Wang et al., 2011b) have successfully been tested in mice or nonhuman primates. In other promising animal experiments, DNA (Muthumani et al., 2008; Tretyakova et al., 2014), adenovirus (Wang et al., 2011a), measles (Brandler et al., 2013), and Modified Vaccinia virus Ankara

(MVA) (García-Arriaza et al., 2014; van den Doel et al., 2014; Weger-Lucarelli et al., 2014) based CHIKV vaccinations were tested. Recently, a successful clinical phase 1 trial was performed using a virus-like particle previously tested in nonhuman primates as the vaccine basis, and no serious side effects and a good toleration were reported (Akahata et al., 2010; Chang et al., 2014).

Safety of CHIKV vaccines might be accomplished by using small CHIKV epitopes able to induce neutralizing antibodies. A promising feature for this type of vaccine development is that the majority of early neutralizing antibodies in CHIKV-infected mice (Lum et al., 2013), nonhuman primates (Kam et al., 2014), and humans (Kam et al., 2012a; Kam et al., 2012b; Kam et al., 2012c) were found to be directed against one single linear epitope of the E2 protein, which comprises its 12 N-terminal amino acids.

2.2.2.2   Modified Vaccinia virus Ankara (MVA) as a vector for vaccine development

MVA is derived from the Chorioallatois Vaccinia virus Ankara (CVA) and is a highly attenuated vaccinia virus strain (Sutter and Moss, 1992). Despite severe adverse effects, CVA was used as a vaccine against smallpox in Turkey. Due to the adverse effects, efforts were made to create a safer CVA based vaccine (Fenner, 1988). This safer vaccine was achieved by passaging CVA 516 times serially on chicken embryo fibroblasts, which attenuated the virus markedly. The resulting vaccinia virus was called MVA and used for vaccination against smallpox in Germany, vaccinating more than 120,000 people without any adverse effects (Stickl, 1974; Hochstein-Mintzel et al., 1975). An in-depth analysis of the viral genome revealed that, besides some small deletions, six large parts of the MVA genome had been deleted (Meyer et al., 1991; Antoine et al., 1998). These deletions led to major constraints in the host range due to the loss of virulence and host range genes. Accordingly, MVA is only able to infect and produce viral proteins in human cells, and not able to produce new infectious particles. Furthermore, foreign transgenes can be inserted into the large deletions within the MVA genome and are then together with the viral proteins expressed in infected cells. For the creation of recombinant MVA, the transgene is inserted into the MVA genome together with a host-range gene for extended host tropism (for selection of positive clones) by homologous recombination (Sutter et al., 1994; Staib et al., 2004). Therefore, MVA is a suitable vector for any vaccination of choice (Sutter and Moss, 1992; Volz and Sutter, 2013). Several clinical trials with recombinant MVA have been performed so far (Sutter and Staib, 2003).

3. Aim of this work

The Chikungunya virus (CHIKV) causes high fever and severe recurrent arthritis in humans, which can last for months or years. It is transmitted by mosquitoes and endemic in Sub-Saharan Africa, the Indian Ocean islands, India, and Southeast Asia. In the last few years, it was responsible for several large outbreaks with millions of infected people and infection rates of over 30%. One small epidemic also occurred in Italy in 2007, and recently (in late 2013) the virus has spread to the Caribbean and neighboring regions. The epidemic in the Caribbean is currently still ongoing and has caused the infection of an estimated 660,000 people as of the beginning of September. Due to climate change, globalization, and vector switching, the virus is expected to continue its spread in the next years and decades, including world regions with temperate climate. Despite these facts, there is little known about the viral life cycle. For example, the cellular receptor for virus attachment and entry is not yet identified. Furthermore, there is so far no approved specific treatment or vaccination against a virus infection.

Henceforth, the aim of this work was to analyze the entry process of CHIKV in detail. To have a tool at hand for studying this part of the viral life cycle, CHIKV envelope (Env) pseudotyped lentiviral vector particles (VPs) carrying a gene encoding luciferase or GFP was produced and analyzed to determine if their entry properties are comparable to the wild-type virus. The domains and parts of CHIKV Env necessary for cell attachment was to be determined. In addition, the structures and molecules on the cell surface that are involved in viral entry was to be identified. By these analyses, the end goal was to come closer to the identification of the cellular receptor(s) of the virus.

Furthermore, inhibitors of viral entry derived from different sources were to be identified and characterized in order to discover candidates for a potential specific CHIKV treatment. Different vaccine approaches were to be tested, and a recombinant Modified Vaccinia virus Ankara (MVA) with a gene coding for a CHIKV antigen was to be generated and evaluated for its potential as a future CHIKV vaccine.

In general, working with wild-type CHIKV and a CHIKV animal model was to be established in the laboratory to verify the relevance of the data obtained from VP and *in vitro* experiments.

4. Material and Methods

4.1 Material

4.1.1 Cell lines and microorganisms

4.1.1.1 Bacteria

The microorganisms listed below are all derivatives of *E.coli* K12.

Strain	genotype	Reference
Top 10	F- *mcr*A Δ(*mrr-hsd*RMS-*mcr*BC) φ80*lac*ZΔM15 Δ*lac*X74 *rec*A1 *ara*D139 Δ(*araleu*)7697 *gal*U *gal*K *rps*L (StrR) *end*A1 *nup*G	Invitrogen (Karlsruhe)
DH5α	F⁻ endA1 glnV44 thi-1 recA1 relA1 gyrA96 deoR nupG Φ80d*lac*ZΔM15 Δ(*lacZYA-argF*)U169, hsdR17(r$_K^-$ m$_K^+$), λ⁻	NEB, (Frankfurt/Main)
BL21-CodonPlus (DE3)-RIPL	F– ompT hsdS(rB– mB–) dcm+ Tetr gal λ(DE3) endA Hte [argU proL Camr] [argU ileY leuW Strep/Specr]	Agilent Technologies, Böblingen

4.1.1.2   Cell lines

cell line	description	medium	reference
A549	Human alveolar adenocarcinoma cell line	DMEM; 10% FCS; 2mM glutamine	ATCC: CCL-185
BHK-21	Baby hamster kidney cells	DMEM; 10% FCS; 2mM glutamine	ATCC: CCL-10
BJAB	Human pre B-lymphocyte	RPMI; 10% FCS; 2mM glutamine	TC collection Barbara Schnierle
BSC-1	African green monkey kidney epithelial	DMEM; 10% FCS; 2mM glutamine	ATCC: CCL-26
CHO-K1	Chinese hamster ovary epithelial cells	F-12; 10% FCS, 2mM glutamine	Mhairi Ferguson, Pirbright Institute, UK
DF-1	Chicken fibroblast spontaneously transformed	DMEM; 10% FCS; 2mM glutamine	ATCC: CRL-12203
HaCaT	Human keratinocyte cell line	RPMI; 10% FCS; 2mM glutamine	(Broukamp et al., 1988)
HEK 293T	Human embryonic kidney cells, stably transfected with pcDNA3.1	DMEM; 10% FCS; 2mM glutamine	ATCC: CRL-1573
HeLa	Human cervical cancer	DMEM; 10% FCS; 2mM glutamine	ATCC: CCL-2
HepG2	Human liver carcinoma cell line	DMEM; 10% FCS; 2mM glutamine	ATCC: HB-8065
HT 1080	Human fibrosarcoma cell line	DMEM; 10% FCS; 2mM glutamine	ATCC: CCL-121
Huh7	Human hepatocellular carcinoma	DMEM; 10% FCS; 2mM glutamine	TC collection Barbara Schnierle
HuT 78	Human cutaneous CD4$^+$ T-lymphocytes	RPMI; 10% FCS; 2mM glutamine	ATCC: TIB-161
Jurkat	Human CD4$^+$ T-lymphocytes	RPMI; 10% FCS; 2mM glutamine	ATCC: TIB-152
MCF7	Human breast adenocarcinoma	RPMI; 10% FCS; 2mM glutamine	ATCC: HTB-22
MRC5	Human lung fibroblast cell line	EMEM; 10% FCS; 2mM glutamine	ATCC: CCL-171
NIH 3T3	Murine embryonic fibroblasts	DMEM; 10% FCS; 2mM glutamine	ATCC: CCL-92

pgsA-745	Chinese hamster ovary epithelial cells; CHO-K1 derived; xylosyltransferase I deficient → no proteoglycan synthesis	F-12; 10% FCS, 2mM glutamine	Mhairi Ferguson, Pirbright Institute, UK
PM-1	Human CD4$^+$ T lymphocytes	RPMI; 10% FCS; 2mM glutamine	TC collection Barbara Schnierle
Renca	Murine renal carcinoma	RPMI; 10% FCS; 2mM glutamine	ATCC: CRL-2947
RK-13	Rabbit kidney cells	EMEM; 10% FCS; 2mM glutamine	ATCC: CCL-37
Vero	African green monkey kidney epithelial cells	DMEM; 10% FCS; 2mM glutamine	Matthias Niedrig, Robert-Koch-Institut (Berlin)

4.1.2   Media and supplements for cell culture

100x Penicillin Streptomycin	Lonza AG (Cologne)
Dulbecco's Modified Eagle's Medium (DMEM)	Biochrom AG (Berlin)
Eagle's Minimal Essential Medium (EMEM)	Biochrom AG (Berlin)
Fetal calf serum (FCS)	Biowest (Renningen)
Ham's F-12 Nutrient Mix	Gibco (Invitrogen, Karslruhe)
L-glutamine, 200mM	Lonza AG (Cologne)
Phosphate-buffered salt solution (PBS-Dulbecco)	Section 3/3 (Paul-Ehrlich-Institut)
RPMI 1640	Biochrom AG (Berlin)
Trypsin/EDTA	Lonza AG (Cologne)
10 mM TRIS, pH 9.0	Section 3/3 (Paul-Ehrlich-Institut)
HEPES buffer, pH 7.4	Section 3/3 (Paul-Ehrlich-Institut)
Opti-MEM® I Reduced Serum Media	Gibco; via Invitrogen (Karlsruhe)
Fusion buffer	10mM HEPES, 10mM 2-(N-morpholino)ethanesulfonic acid (MES) in PBS; pH 5.2

4.1.3   Chemicals, enzymes and reagents

2-(N-morpholino)ethanesulfonic acid (MES)	Carl Roth GmbH & Co. KG (Karlsruhe)
3-(4,5-dimethylthiazol-2-yl)-2,5-diphenyltetrazolium bromide (MTT)	Sigma-Aldrich Chemie GmbH (Taufkirchen)
Acetic acid	Carl Roth GmbH & Co. KG (Karlsruhe)
Agarose (SeaKem® ME)	Lonza AG (Cologne)
Alhydrogel 2%	InvivoGen (Toulouse, France)
Ammonium persulfate (APS)	Sigma-Aldrich Chemie GmbH (Taufkirchen)
Ampicillin sodium salt	Carl Roth GmbH & Co. KG (Karlsruhe)
β-Mercaptoethanol	Sigma-Aldrich Chemie GmbH (Taufkirchen)
Boracic acid	Merck KGaA (Darmstadt)
Bovine serum albumin (BSA, 10mg/ml)	New England Biolabs (Frankfurt/Main)
Bovine serum albumin (solid)	AppliChem (Darmstadt)
Britelite	Perkin Elmer (Rodgau)
Bromophenol blue	Merck KGaA (Darmstadt)
Chloroquine	Sigma-Aldrich Chemie GmbH (Taufkirchen)
Chondroitin sulfate	Sigma-Aldrich Chemie GmbH (Taufkirchen)
Coomassie Brilliant Blue G-250	Bio-Rad Laboratories GmbH (Munich)
Crystal violet	Sigma-Aldrich Chemie GmbH (Taufkirchen)
Dermatan sulfate	Sigma-Aldrich Chemie GmbH (Taufkirchen)
Deoxyribonucleotides (dNTPs)	Qiagen (Hilden)
Dextran sulfate	Sigma-Aldrich Chemie GmbH (Taufkirchen)
Dimethyl sulfoxide (DMSO)	Sigma-Aldrich Chemie GmbH (Taufkirchen)
Di sodium hydrogen phosphate dihydrate	Merck KGaA (Darmstadt)
DNA loading buffer	Fermentas (Schwerte)
Epicatechin (EC)	Sigma-Aldrich Chemie GmbH (Taufkirchen)
Epigallocatechin gallate (EGCG)	Sigma-Aldrich Chemie GmbH (Taufkirchen)
Ethanol	Materiallager (Paul-Ehrlich-Institute)
EZ Vision	MoBiTec (Göttingen); AMRESCO
Formaldehyde	Sigma-Aldrich Chemie GmbH (Taufkirchen)
FuGENE	Promega (Mannheim)
Gelred	VWR (Darmstadt; Biotium)
Gene Ruler 1 kb Plus DNA Ladder	Thermo Scientific (Dreieich)
Glutaraldehyde	Merck KGA (Darmstadt)
Glycerol	Carl Roth GmbH & Co. KG (Karlsruhe)
Guanidine hydrochloride	Carl Roth GmbH & Co. KG (Karlsruhe)
Heparan sulfate	Sigma-Aldrich Chemie GmbH (Taufkirchen)
Heparin	Biochrom AG (Berlin)
$H_2O_{bidest.}$ ("Reinstwasser")	Section 3/3 (Paul-Ehrlich-Institut)
Imidazole	Merck KGaA (Darmstadt)
Isofluran	Baxter (Unterschleißheim)
Isopropanol	Materiallager (Paul-Ehrlich-Institute)
Isopropyl-β-D-thiogalactopyranosid (IPTG)	Fermentas GmbH (St. Leon-Rot)
Kanamycin	Carl Roth GmbH & Co. KG (Karlsruhe)
Lipofectamine 2000	Invitrogen (Karlsruhe)
Lumi-Light Western Blot Substrate	Roche (Mannheim)
Methanol	Materiallager (Paul-Ehrlich-Institute)
Nonidet P-40	Sigma-Aldrich Chemie GmbH (Taufkirchen)
Paraformaldehyde (PFA)	Merck (Darmstadt)
Penicillin/Streptomycin	Gibco; via Invitrogen (Karlsruhe)
Phusion High-Fidelity DNA Polymerase	Thermo Scientific (Dreieich); Finnzymes
Polyethylenimine (PEI; M_W ~25000kDa)	Sigma-Aldrich Chemie GmbH (Taufkirchen)
Roti®-Block	Carl Roth GmbH & Co. KG (Karlsruhe)
Rotiphorese® Gel 30	Carl Roth GmbH & Co. KG (Karlsruhe)

Silver nitrate   Sigma-Aldrich Chemie GmbH (Taufkirchen)
Sodium acetate   Carl Roth GmbH & Co. KG (Karlsruhe)
Sodium carbonate   Sigma-Aldrich Chemie GmbH (Taufkirchen)
Sodium chloride   Merck KGaA (Darmstadt)
Sodium di hydrogen phosphate monohydrate   Merck KGaA (Darmstadt)
Sodium dodecyl sulfate (SDS)   Sigma-Aldrich Chemie GmbH (Taufkirchen)
Sodium hydroxide (NaOH)   Merck (Darmstadt)
Sodium thiosulfate pentahydrate   Merck (Darmstadt)
T4 DNA Ligase   NEB (Frankfurt/Main)
T4 DNA Polymerase   NEB (Frankfurt/Main)
Taq polymerase   Qiagen (Hilden)
Tetramethylendiamine (UltraPure™ TEMED)   Invitrogen (Karlsruhe)
TRIS   Carl Roth GmbH & Co. KG (Karlsruhe)
TRIS-Base   Merck KGA (Darmstadt)
TRIS-HCl   Carl Roth GmbH & Co. KG (Karlsruhe)
TrueBlue   KPL (Gaithersburg, USA)
Trypan blue   Sigma-Aldrich Chemie GmbH (Taufkirchen)
Urea   Carl Roth GmbH & Co. KG (Karlsruhe)
X-Gal   Carl Roth GmbH & Co. KG (Karlsruhe)

All other chemicals used that are not listed above were purchased from Carl Roth GmbH & Co. KG (Karlsruhe), Merck (Darmstadt), or Sigma-Aldrich Chemie GmbH (Taufkirchen).

4.1.4   Kits

Pierce® BCA Protein Assay Kit   Fisher Scientific GmbH (Schwerte)

QIAamp Viral RNA Mini Kit   Qiagen (Hilden)

RealStar® Chikungunya RT-PCR Kit 1.0   altona Diagnostics GmbH (Hamburg)

Amersham ECL Plus™ Western Blotting Detection   GE Healthcare (Munich)
Reagents

GeneJET™ Plasmid Miniprep Kit   Fermentas GmbH (St. Leon-Rot)

NucleoBond® Xtra Maxi Plus   Macherey-Nagel GmbH & Co. KG
                                                       (Düren)
NucleoSpin® Extract II Kit   Macherey-Nagel GmbH & Co. KG
                                                       (Düren)
DNeasy Blood & Tissue Kit   Qiagen (Hilden)

T7 Quick High Yield RNA Synthesis Kit   NEB (Frankfurt/Main)

4.1.5 Antibodies

4.1.5.1 Primary antibodies

Specificity	species	dilution	source
α-CHIKV E2 serum 1250 GP (large bleed)	rabbit	WB: 1:1000	Eurogentec GmbH (Cologne)
α-CHIKV E2 serum 1250 PPI (naive)	rabbit	WB: 1:1000	Eurogentec GmbH (Cologne)
α-His-tag	mouse	WB: 1:100 FACS: 1:20	
α-c-Myc	mouse	WB: 1:125	BD-Bioscience (Heidelberg)
α-ß-Actin	mouse	WB: 1:10.000	Sigma-Aldrich Chemie GmbH (Taufkirchen)
α-vaccinia virus (lister strain)	rabbit	immuno stain 1:2000	Acris (Hiddenhausen)

4.1.5.2 Secondary antibodies

Specificity	species	dilution	source
α-mouse-FITC	donkey	FACS: 1:200	DIANOVA GmbH (Hamburg)
α-mouse-HRP	goat	WB: 1:10000	DIANOVA GmbH (Hamburg)
α-rabbit-HRP	donkey	WB: 1:10000 immuno stain: 1:2000	DIANOVA GmbH (Hamburg)
α-human-HRP	goat	immuno stain: 1:2000	DIANOVA GmbH (Hamburg)

4.1.6 Plasmids

Designation	description	reference
GeneArt CHIKV E2 main epitope_enhancer (in this thesis called L)	Plasmid containing synthesized gene L	GeneArt (Regensburg)
GeneArt CHIKV E2 D AB (in this thesis called sAB⁺)	Plasmid containing synthesized gene sAB⁺	GeneArt (Regensburg)
pET-15b	Ampicillin; T7 promoter; N-term. His-tag; lac-operon	Novagen
pET-15b - CHIKV E2 main epitope_D AB (in this thesis called LsAB⁺)	Ampicillin; T7 promoter; N-term. His-tag; lac-operon; LsAB⁺	this work
pET-15b - CHIKV E2 main epitope_D A (in this thesis called LsA)	Ampicillin; T7 promoter; N-term. His-tag; lac-operon; LsA	this work
pET-15b - CHIKV E2 main epitope_D B (in this thesis called LB⁺)	Ampicillin; T7 promoter; N-term. His-tag; lac-operon; LB⁺	this work
pET-15b - CHIKV E2 D AB (in this thesis called sAB⁺)	Ampicillin; T7 promoter; N-term. His-tag; lac-operon; sAB⁺	this work
pET-15b - CHIKV E2 D A (in this thesis called sA)	Ampicillin; T7 promoter; N-term. His-tag; lac-operon; sA	this work
pET-15b - CHIKV E2 D B (in this thesis called B⁺)	Ampicillin; T7 promoter; N-term. His-tag; lac-operon; B⁺	this work
pET-15b - CHIKV E2 main epitope (in this thesis called L)	Ampicillin; T7 promoter; N-term. His-tag; lac-operon; L	this work
pET-15b - CHIKV E2 domain A (including β-ribbon connector)	Ampicillin; T7 promoter; N-term. His-tag; lac-operon; CHIKV E2 domain A	this work
pET-15b - CHIKV E2 domain B* (in this thesis called B)	Ampicillin; T7 promoter; N-term. His-tag; lac-operon; CHIKV E2 domain B	this work
pET-15b - CHIKV E2 domain C	Ampicillin; T7 promoter; N-term. His-tag; lac-operon; CHIKV E2 domain C	this work
pET-15b - CHIKV E2 ecto	Ampicillin; T7 promoter; N-term. His-tag; lac-operon; CHIKV E2 ecto (dom. A, B, this work C)	this work

pET-22b-HERV-K UTPase	Ampicillin; T7 promoter; C-term. His-tag; lac-operon; human endogenous retrovirus K UTPase	Benjamin Kraus (Paul-Ehrlich-Institut, 2/2)
pSecTag2 B	Ampicillin; CMV promoter; encoding secretion signal peptide,C-term. c-myc- and His-tag	Invitrogen (Karlsruhe)
pSecTag2 B-CHIKV-E2 D AB (in this thesis called sAB[+])	Ampicillin; CMV promoter; encoding secretion signal peptide, C-term. c-myc- and His-tag; sAB[+]	this work
pIII-lacZ2_A	Ampicillin; MVA rec. plasmid; del III flanks; pmH5 promoter; K1L	Plasmid collection Barbara Schnierle (Paul-Ehrlich-Institut, 2/2)
pIII-lacZ2_A SecTag-CHIKV E2 D AB (in this thesis called sAB[+])	Ampicillin; MVA rec. plasmid; del III flanks; pmH5 promoter; K1L; sAB[+] (plus signal peptide sequ.)	this work
pMDLg/pRRE	Ampicillin; HIV-1 *gag-pol*; rev responsive element	(Dull et al., 1998)
pRSVrev	Ampicillin; HIV-1 rev	(Dull et al., 1998)
pRRLsinCMV-GFPpre	Ampicillin; CMV promoter; HIV pack. signal Ψ	(Dull et al., 1998)
pCSII-EF-luciferase	Ampicillin; firefly luciferase; HIV pack. signal Ψ	Renate König (NG3, Paul-Ehrlich-Institut) (Agarwal et al., 2006)
pIRES2-EGFP-CHIKV E3-E1	Kanamycin; CMV promoter; CHIKV envelope protein (E3-E1)	diploma thesis Christian Donnerhak (Paul-Ehrlich-Institut, 2/2), S27 strain-based
pHITG	Ampicillin; VSV-G	(Soneoka et al., 1995)
LCMV Env	Ampicillin; LCMV Env	Plasmid collection Barbara Schnierle (Paul-Ehrlich-Institut, 2/2)
GaLV Env delta R	Ampicillin; GaLV Env delta R	Christian Buchholz (Paul-Ehrlich-Institut, Pr1) (Merten et al., 2005)
pCHIKV-mCherry-490	Whole CHIKV genome containing an *mCherry* gene within the CHIKV *nsP3* gene	Beate Kümmerer (Universität Bonn) (Kümmerer et al., 2012)

4.1.7   Viruses and vector particles

Chikunguna virus   Matthias Niedrig, Robert-Koch-
                                                        Institut (Berlin), (Panning et al.,
                                                        2009) (the isolate from La Réunion)

AAV-2 luciferase vector particles   Christian Buchholz, Robert Münch
                                                        (Paul-Ehrlich-Institut, Pr1) (Münch et
                                                        al., 2013)

4.1.8 Oligonucleotides

All Oligonucleotides (primers) were purchased from Eurofins MWG Operon (Ebersberg).

__Name__	__Purpose__	__sequence 5`-3`__
C7L for	MVA charact.	ATGGGTATACAGCACGAATTC
C7L rev	MVA charact.	CATGGACTCATAATCTCTATAC
Del III for	MVA charact.	GTACCGGCATCTCTAGCAGT
Del III rev	MVA charact.	TGACGAGCTTCCGAGTTCC
K1L int-1	MVA charact.	TGATGACAAGGGAAACACCGC
K1L int-2	MVA charact.	GTCGACGTCATATAGTCGAGC
ChW35 (transgene *sAB*$^+$) int rev	MVA charact.	TGGCCTCCTCCTCCGCTG
M_AB fw	MVA charact.	AAAAGTCGACAGCACCAAGGACAACTTCAAC
M_AB rev	MVA charact.	AAAAGGATCCTCAGTGGATCTTGCCCTTCCGG
M_A rev	LsA, sA	AAAAGGATCCTCAGGTGGTGGCGGCGGTGC
M_B fw	LB$^+$	AAAAGTCGACCCCCCCGACACCCCCG
AB fw	sAB$^+$, sA	AAAACATATGAGCACCAAGGACAACTTCAAC
B fw	B$^+$	AAAACATATGCCCCCCGACACCCCCG
Dom AI fw	E2 A, whole extracell. E2	AAAACATATGAGCACCAAGGACAACTTCAAC
Dom AI rev	E2 A	AAAACCCGGGGCCGCCGCCGCCGGGCATGTGCACCTCGATC
Dom AII fw	E2 A	AAAACCCGGGGGCGGCGGCGGCAACCACAAGAAGTGGCAGTAC
Dom AII rev	E2 A	AAAAGGATCCTCACTTGGGCACCATGCAGGTC
Dom B fw	E2 B	AAAACATATGCCCGACACCCCCGATAGAA
Dom B rev	E2 B	AAAAGGATCCTCAGGTCACGGCGGCGTGGC
Dom C fw	E2 C	AAAACATATGGCCCGGAACCCTACCGTG
Dom C rev	E2 C, whole extracell. E2	AAAAGGATCCTCACTGGGGCCAGTACTTGTAGG

4.1.9   DNA sequences ordered at GeneArt (Regensburg)

Sequences of the constructs synthesized by GeneArt (5' -> 3', including restriction sites, amino acid sequences derived from CHIKV strain LR2006) are given below. The genes were sent already cloned into the required plasmids (see 4.1.6).

Construct *L* (to obtain the construct L used for the experiments, the part between the *Sal*I and *Bam*HI restriction sites was removed by cutting with *Sal*I and *Bam*HI and replaced by the base pairing oligonucleotides 5'GATCCTCAG 3' and 5'TCGACTGAG 3' containing appropriate overhangs for the mentioned restriction sites and a stop codon).
CATATGAGCACCAAGGACAACTTCAACGTGTACAAGGCCACCGGCGGCGGCGGCAGC
GGCGGCGGCGGCAGCACCAAGGACAACTTCAACGTGTACAAGGCCACCGGCGGCGGC
GGCAGCGGCGGCGGCGGCAGCACCAAGGACAACTTCAACGTGTACAAGGCCACCGGC
GGCGGCGGCAGCGGCGGCGGCGGCAGCACCAAGGACAACTTCAACGTGTACAAGGCC
ACCGGCGGCGGCGGCAGCGGCGGCGGCGGCAGCACCAAGGACAACTTCAACGTGTA
CAAGGCCACCGGCGGCGGCGGCAGCGGCGGCGGCGTCGACGGCCAGTACATCAAGG
CCAACAGCAAGTTCATCGGCATCACCGAGCTGTGAGGATCC

Construct *sAB*⁺
GGCCCAGCCGGCCAGCACCAAGGACAACTTCAACGTGTACAAGGCCACCGGCGGAGG
CAGCGGAGGCGGCATCAAGACCGACGACAGCCACGACTGGACCAAGCTGCGGTACAT
GGACAACCACATGCCCGCCGACGCCGAGAGAGCCGGAGGCGGAGGAGGCGGCAGCG
GCACCGGCACCATGGGCCACGGCAGCGGCGGCGGCGGAGGAGGCTTCACCGACAGC
CGGAAGATCAGCCACGGCGGCAGCGGAGGAGGAGGCCAGAGCACCGCCGCCACCAC
CGGAGGCGGCGGAAGCGGCTTCGAAGGCCCCCCCGACACCCCCGATAGAACCCTGAT
GAGCCAGCAGAGCGGCAACGTGAAGATCACCGTGAACGGCCAGACCGTGCGGTACAA
GTGCAACTGCGGCGGCAGCAACGAGGGCCAGACCACCACCGACAAAGTGATCAACAA
CTGCAAGGTGGACCAGTGCCACGCCGCCGTGACCAACCACAAGAAGTGGCAGTACAAC
AGCCCCCTGGTGCCCCGGAATGCCGAGCTGGGCGACCGGAAGGGCAAGATCCACGGG
CCC

These sequences thus contain the following amino acid sequences derived from CHIKV LR2006:

L: five repeats S1- T12; linked by G-S linkers (G_4SG_4)

sA: S1-T12, I56-G82, T94-H99, G114-H12, Q158-T164: linked by G-S linkers (G_6S; the relative position of S is variable to avoid recombination between G-S linkers in recombinant MVA).

B^+: P172-H256

For detailed amino acid sequences, see 10.2.

4.1.10 Microbial media

Name	**source**
LB (lysogeny broth) medium	Section 3/3 (Paul-Ehrlich-Institut)
LB agar plates + ampicillin	Section 3/3 (Paul-Ehrlich-Institut)
LB agar plates + kanamycin	Section 3/3 (Paul-Ehrlich-Institut)
SOC medium	Section 3/3 (Paul-Ehrlich-Institut)

4.1.10.1.1   SDS-Polyacrylamide gel electrophoresis (SDS-PAGE)

Name	**source/receipt**
SDS-running buffer (10x)	Section 3/3 (Paul-Ehrlich-Institut)
Stacking gel buffer	500mM TRIS-HCl, 0.4% SDS, pH6.8
Running gel buffer	1.5M Tris, 0.4% SDS, pH8.8
SDS sample buffer (4x)	200mM TRIS-HCl (pH6.8), 8% SDS, 40% Glycerol, 0.2% bromophenol blue, 4% β-mercaptoethanol (added freshly)
Stacking gel (5%)	0.9 ml stacking gel buffer, 2.2 ml H_2O, 0.6 ml Rotiphorese® Gel 30, 20 µl APS (10%), 5 µl TEMED
Running gel (12.5%)	2.3 ml stacking gel buffer, 3.1 ml H_2O, 3.9 ml Rotiphorese® Gel 30, 95 µl APS (10%), 5 µl TEMED
Running gel (15.0%)	2.3 ml stacking gel buffer, 2.4 ml H_2O, 4.7 ml Rotiphorese® Gel 30, 95 µl APS (10%), 5 µl TEMED
Lysate buffer	1% Nonidet P-40, 50mM TRIS-HCl pH 7.5 , 5mM EGTA, 150mM NaCl, 40 µl/ml Complete Protease Inhibitor Cocktail (Roche, Mannheim)
Coomassie staining solution	0.125% Coomassie Brillant Blue G250, 50% methanol, 10% acetic acid
Coomassie destaining solution I	50% methanol, 10 % acetic acid
Coomassie destaining solution II	5 % methanol, 7.5% acetic acid
Fixation solution (silver staining)	30% ethanol, 10% acetic acid, 60% H_2O
Conditioner solution (silver staining, freshly prepared)	20% 2M sodium acetate, 30% ethanol, 0.1% sodium thiosulfate pentahydrate, 2 % glutaraldehyde, add. H_2O
Staining solution (silver staining, freshly prepared)	0.5% of 20% silver nitrate stock (protect from light), 25 µl/100 ml solution formaldehyde, add. H_2O
Developing solution (silver staining, freshly prepared)	2.5% sodium carbonate, 80 µl/100 ml solution formaldehyde, add. H_2O; stop reaction with acetic acid (10 ml/50 ml developing solution)

4.1.11 Western blot

Name	source/receipt
Blotting buffer	6g TRIS-Base, 3.1g boracic acid, 10ml 10% SDS, add. 900ml H_2O + 100ml methanol
TBS-T (*Tris-buffered saline Tween 20*)	Section 3/3 (Paul-Ehrlich-Institut)
ReBlot Plus Mild Antibody Stripping Solution (10x)	Millipore (Bedford, USA)

4.1.12 DNA agarose gel buffers

TAE buffer	Section 3/3 (Paul-Ehrlich-Institut)

4.1.13 ÄKTA HPLC buffers

Name	source/receipt
Sample buffer (native, Ni-NTA)	1 mM imidazole, add. PBS, pH 7.4
Elution buffer (native, Ni-NTA)	300 mM imidazole, add. PBS, pH 7.4
Sample buffer (denaturing, Ni-NTA)	6 M guanidine hydrochloride, 10 mM TRIS, 5 mM β-mercaptoethanol, 100 mM di sodium hydrogen phosphate dihydrate, pH 8.0
Equilibration buffer (denaturing, Ni-NTA)	6 M urea, 10 mM TRIS, 100 mM sodium di hydrogen phosphate monohydrate, pH 8.0
Washing buffer (denaturing, Ni-NTA)	6 M urea, 10 mM TRIS, 100 mM sodium di hydrogen phosphate monohydrate, pH 6.3
Elution buffer (denaturing, Ni-NTA)	6 M urea, 10 mM TRIS, 100 mM sodium di hydrogen phosphate monohydrate, 250 mM imidazole, pH 6.3
Sample buffer (for A, E2; ion-exchange)	6 M urea, 20 mM sodium di hydrogen phosphate monohydrate, 2% ethanol. 20 mM NaCl, 5 mM β-mercaptoethanol, pH 6.0
Elution buffer (for A, E2; ion-exchange)	6 M urea, 20 mM sodium di hydrogen phosphate monohydrate, 2% ethanol, 1 M NaCl, 5 mM β-Mercaptoethanol, pH 6.0

4.1.14 Laboratory equipment

Consumable	type	company
Agarose gel apparatus	Mini Horizontal Submarine Unit	Hoefer (Holliston, USA)
Autoclave	Varioklav	H+P (Oberschleissheim)
Cell counter	Z1 Coulter Particle Counter	Beckman Coulter (Brea, USA)
Cell seeding device 384-well plates	MultiFlo Microplate Dispenser	(BioTek, Bad Friedrichshall)
Centrifuges	RC 26 Plus (Rotor SLA-1500)	Heraeus Sorvall (Hanau)
	Eppendorf 5810R (Rotor A-4-62)	Eppendorf (Hamburg)
	Biofuge fresco (Rotor 3325B)	Heraeus Sorvall (Hanau)
	Eppendorf 5415C (Rotor F-45-18-11)	Eppendorf (Hamburg)
	Galaxy MiniStar	VWR (Darmstadt)
	Biofuge primo R (Rotor 7590)	Heraeus Sorvall (Hanau)
	Megafuge 1.0 R	Heraeus Sorvall (Hanau)
	Eppendorf Concentrator 5301	Eppendorf (Hamburg)
Chemiluminescence detection system	Fusion FX-7	Vilber (Eberhardzell)
Clean Bench	Sterilgard III Advanced	The Baker Company (Sanford, USA)
Counting chamber	Neubauer	Brand (Wertheim)
Coverplate	Shandon	Thermo Shandon Limited (Astmoor, Runcorn Cheshire, USA)
Detector luciferase signal	PHERAstar	BMG LABTECH (Ortenberg)
DNA concentration measurement device	NanoDrop 2000c	Thermo Fisher (Schwerte)
Ear puncher	DF 401	Aesculap (Tuttlingen)
Flow cytometer	BD LSR II SORP	BD (Heidelberg)
Gel scanner	GS-800 calibrated densitometer	BioRAD (Munich)

Ice machine	AF80	Scotsman (Vernon Hills, USA)
Incubator (cell culture)	BBD 6220	Hereaus Sorvall (Hanau)
Incubator (bacteria)	Innova 4200 incubator shaker	New Brunswick scientific (Eppendorf, Hamburg)
HPLC	ÄKTA Purifier 10	GE Healthcare (Munich)
Matrix pipette for 384-well plates	Matrix Multichannel Equalizer Electronic Pipette 125 µl	Thermo Scientific (Dreieich)
Microplate reader	GENios Microplate Reader	(Tecan)
Microscope	Axiovert 25	Carl Zeiss AG (Göttingen)
Microwave	-	Bosch (Gerlingen-Schillerhöhe)
N_2 storage tank	Chronos/Apollo	Messer Group (Sulzbach)
Optical densitometer	Biophotometer	Eppendorf (Hamburg)
Pipet Boy	pipetus®	Integra Biosciences (Fernwald)
Power Supply SDS-PAGE chamber	Power-Pac 3000	BioRad (Munich)
Refrigerator	4°C/-20°C	Liebherr (Biberach)
Freezer	-80°C	Heraeus Sorvall (Hanau)
Roller Mixer	RollerMixer SRT6	Stuart (Asbach)
RT-PCR device	Lightcycler® 480 instrument II	Roche (Mannheim)
Scales	LA1200S	Sartorius (Göttingen)
	TE214S-OCE	Sartorius (Göttingen)
SDS-PAGE chamber	Mini PROTEAN 3/tetra system	BioRad (Munich)
Semi-dry Western blot apparatus	Trans-Blot SD semi-dry transfer cell	BioRad (Munich)
Shaker apparatus	Unimax 1010	Heidolph Instruments (Schwambach)
Sonification device	Bandelin Sonoplus	Bandelin electronic (Berlin)
Thermocycler	Professional Thermocycler	Biometra (Göttingen)
Thermomixer	Compact or comfort	Eppendorf (Hamburg)
UV detection apparatus	Gel iX Imager	Intas (Göttingen)
Vacuum aspiration	Vacuboy	Integra Biosciences

		(Fernwald)
Veterinary inhalational anesthesia apparatus	Matrix	Midmark (Versailles, USA)
Vortexer	Vibrofix VF1 electronic	IKA (Staufen)
Water bath	System 1068	GFL (Burgwedel)

4.1.15 Consumables

Consumable	type	company
10 cm dishes	-	Sarstedt,(Nümbrecht)
384-well filter tips	Matrix Filterspitzen,125 µl	VWR (Darmstadt)
384-well plates	CELLSTAR 384-well microtiterplate	Greiner Bio-One (Frickenhausen)
Bacterial culture tubes	-	Sarstedt (Nümbrecht)
Blood collection tubes	Serum (gold)	BD (Heidelberg)
Cell culture flask	T25, T75, T175	Greiner (Kremsmünster, Austria)
Cell culture plates	6- 12-, 24-, 96-wells	Sarstedt (Nümbrecht)
Cell scraper Centrifugal filter units	Cell scraper 39 cm Amicon Ultra-15 Centrifugal Filter Units, 3K cutoff Amicon Ultra-4-Centrifugal Filter units, 3K cutoff	VWR (Darmstadt) Millipore (Bedford, USA)
Cover slip	24 x 50 mm	Menzel (Braunschweig)
Cuvettes	-	Sarstedt (Nümbrecht)
Cryovials	1.8 ml	Greiner (Kremsmünster, Austria)
Dialysis chambers	Slide-A-Lyzer Dialysis Cassettes; 3.5, 10.0, 20.0 kDa	Thermo Scientific (Dreieich)
Dissecting set	diverse	VWR (Darmstadt)
ELISA cover plate	25 µm, PE, adhesive	Roth (Karlsruhe)
ELISA plates	96-well, high binding capacity	BD (Heidelberg)
FACS tubes	5ml	BD (Heidelberg)
Glass Pasteur pipettes	150 mm, #612-1701	VWR (Darmstadt)
Glass slide	Superfrost Ultra Plus	Menzel (Braunschweig)
Gloves	Latex	Braun (Sempach, Switzerland)
Ion-exchange chrom. columns	Mono Q 5/50 GL Mono S 5/50 GL	GE Healthcare (Munich)

Microliter pipets	10 µl, 200 µl, 1000 µl	Eppendorf (Hamburg)
Microwell plate 96 U	TC microwell 96U	Thermo Scientific (Dreieich
Needle (cannula)	25G, 26G	Braun (Sempach, Switzerland)
Ni-NTA columns	HisTrap FF Crude 1 ml	GE Healthcare (Munich)
Petri Dish	35 mm, Nunc™ Cell Culture	Thermo Fisher (Schwerte)
Pipet tips	1 ml, 200 µl, 20 µl	Eppendorf (Hamburg)
Pipets with filter	1 ml, 200 µl, 100 µl, 10 µl	Nerbe Plus (Winsen/Luhe)
Plastic pipets	50 ml, 10 ml, 5 ml	Greiner (Kremsmünster, Austria)
Polyvinylidene fluoride (PVDF)membrane	Immobilon®-P	Millipore (Bedford, USA)
Reaction tubes	1.5 ml, 2.0 ml	Eppendorf (Hamburg)
Reagent tubes	15 ml and 50 ml PP tubes	Greiner (Kremsmünster, Austria)
Scalpels	-	Braun (Sempach, Switzerland)
Skin disinfection	Desderman	Schülke & Mayr (Norderstedt)
Solution basin (sterile)	55 ml PS sterile solution basin	Roth (Karlsruhe)
Sterile filter, 0.2 µm (for syringes)	-	Sartorius (Göttingen)
Sterile filter, 0.45 µm (for syringes)	-	Sartorius (Göttingen)
Sterile filter, 0.45 µm (for bottles)	-	Amsterdam (Netherlands)
Surface disinfection	Terralin	Schülke & Mayr (Norderstedt)
Surgical mask	Coldex	Attends (Schwalbach)
Syringes	1 ml, 5 ml, 10 ml, 20 ml	Braun (Sempach, Switzerland)
Whatman paper	-	Hartenstein (Würzburg)

4.1.16 Software

Flow cytometry analysis	BD FACSDiva™ Software Version 6.1.3; FCS Express V4.0
Picture analysis	Adobe Photoshop CS3
Plasmid maps	VectorNTI Suite 9
Protein 3D analysis	PyMOL 1.5.0.4
Statistical analysis	Microsoft Office Professional Plus 2010; GraphPad Prism 5.04; CombiStats 5.0
WB analysis	Fusion FX-7

4.1.17 Internet tools

Alignments of DNA and protein sequences
http://multalin.toulouse.inra.fr/multalin/

Reverse complement DNA sequences
http://www.bioinformatics.org/sms/rev_comp.html

Translation from DNA to protein sequences
http://web.expasy.org/translate/

Virtual digestion of DNA sequences
http://tools.neb.com/NEBcutter2/

Appropriate conditions for digestion with two restriction enzymes from NEB simultaneously
https://www.neb.com/tools-and-resources/interactive-tools/double-digest-finder

Calculation of the molecular mass of proteins
http://pir.georgetown.edu/pirwww/search/comp_mw.shtml

Calculation of DNA amounts necessary for ligation
http://www.insilico.uni-duesseldorf.de/Lig_Input.html

Calculation of the isoelectric point of a protein
http://web.expasy.org/compute_pi/

Codon usage optimization
http://www.encorbio.com/protocols/Codon.htm

4.2 Methods

4.2.1 Microbiological methods

Microbiological work was performed to clone plasmids and to amplify them. Additionally, bacteria were used to express recombinant proteins. Bacteria were grown at 30°C for the purpose of amplifying a plasmid with homologous sequences (e.g., the plasmid pIII-lacZ2_A), otherwise all bacteria were cultivated at 37°C. Cultivation was always completed for at least 16 hours and with continuous shaking (220 rounds/minute (rpm)) if the bacteria were grown in flasks or tubes.

4.2.1.1 Bacterial growth for plasmid amplification

To obtain large amounts of plasmid DNA, the growth of 500 ml *E. coli* (DH5α or TOP10) cultures was performed in Erlenmeyer flasks containing LB medium at 30 or 37°C with continuous shaking at 220 rpm. For selection of plasmid containing cells, the antibiotic with the respective resistance gene encoded by the plasmid was added to the medium (ampicillin: 100 µg/ml; kanamycin: 50 µg/ml). To obtain single colonies after a transformation, bacterial suspensions were plated on LB agar plates containing ampicillin or kanamycin with a Drigalski spatula. Subsequently, the plates were incubated at 30 or 37°C for at least 16 hours. For confirmation of successful cloning, 5 ml of medium (in 15 ml tubes) was inoculated with a sterile pipette tip, which had been used to pick a single colony from the required LB agar plate. The growth conditions of these tubes were the same as mentioned above.

4.2.1.2 Preparation of bacterial glycerol stocks

Glycerol stocks were only created to store the bacteria used for protein expression. For the preparation of bacterial glycerol stocks, 100 ml of LB medium was inoculated with a single colony from an LB agar plate of *E.coli* BL21-CodonPlus (DE3)-RIPL transformed with an expression plasmid for the required protein. The inoculated medium was subsequently incubated overnight at 37°C, 220 rpm. After 16 hours, 1 ml of the culture was mixed with 100 µl glycerol in cryovials and directly frozen and stored at -80°C.

4.2.1.3   Bacterial growth for protein expression

For expression of high amounts of recombinant protein, first a starter culture (100 ml LB medium + ampicillin) was prepared. The medium was inoculated with *E.coli* BL21 from a frozen glycerol stock (always kept on ice) containing the required expression plasmid. After overnight incubation (37°C, 220 rpm), the main cultures containing 2 L of LB medium (+ ampicillin) were inoculated with the starter cultures. The optical density at 600 nm (OD_{600}) was measured regularly and at an OD_{600} of 0.5 to 0.7, protein expression was induced via addition of 1 mM isopropyl β-D-1-thiogalactopyranoside (IPTG). The cultures were then cultivated for another 3 hours. Afterwards, the cultures were pelleted and frozen at -20°C for subsequent protein purification.

4.2.1.4   Transformation of bacteria via heat shock

To transform competent *E.coli* DH5α, TOP10, or BL21-CodonPlus (DE3)-RIPL via heat shock, 100 µl of bacterial glycerol stock were thawed slowly on ice. Then, 10 µl of the respective ligation or 100 ng of a plasmid solution (for a retransformation; 80 ng for the BL21 strain) were added. After an incubation period of 20 minutes on ice, the heat shock was performed for 90 seconds (50 seconds for the BL21 strain) at 42°C. Another 2.5 minutes incubation period on ice was then completed. Next, 300 µl of SOC medium was added, and the bacteria were subsequently grown at 30 or 37°C for 40 minutes (300 rpm). 200 µl of the bacterial suspension was then plated on antibiotic containing agar plates and incubated overnight at 30 or 37°C.

4.2.1.5   Plasmid preparation from bacteria

The isolation and purification of small amounts of plasmid DNA from *E.coli* DH5α or TOP10 (up to 10 µg) was performed utilizing the GeneJET™ Plasmid Miniprep Kit (Fermentas) for screening of successful cloning events. To obtain higher amounts of plasmid DNA (up to 500 µg), the NucleoBond® Xtra Maxi Plus Kit (Macherey-Nagel) was used. Preparations were performed according to the manufacturer's instructions.

4.2.2   Molecular biology methods

4.2.2.1   Restriction endonuclease digestions of DNA

The digestion of DNA was completed with restriction endonucleases from the company NEB (Frankfurt/Main) and performed according to the manufacturer's instructions.

4.2.2.2   Removal and overhang fill-in to form blunt ends

The digestion of DNA with restriction endonucleases will result in the occurrence of blunt (no overhangs) or sticky (3' or 5' overhangs) ends. To blunt sticky ends, T4 DNA polymerase (NEB) was used. This enzyme exhibits a 3'-5' exonuclease as well as a 5'-3' polymerase activity. Thus, it removes 3' overhangs and fills-in 5' overhangs. It was used according to the manufacturer's protocol and heat inactivated for 10 minutes at 70 °C after the sufficient incubation time.

4.2.2.3   Dephosphorylation of linearized plasmids

To avoid self-ligation of plasmids with complementary ends, the plasmids were dephosphorylated via treatment with Antarctic phosphatase. After digestion of the plasmid vectors, 1 µl of phosphatase and the Antarctic phosphatase buffer were added to the tube and incubated at 37°C for 1 hour according to the manufacturer's instructions.

4.2.2.4   Sequencing of DNA

Sequencing was done by Eurofins MWG (Ebersberg). 1 to 3 µg of DNA were vacuum-dried with the vacuum centrifuge and sent to Eurofins MWG. The analysis of the sequencing results was completed via Vector NTI and use of several online tools (see 4.1.16, 4.1.17).

4.2.2.5   Ligation of DNA

To ligate DNA fragments, a variable insert-vector molar ratio between 1:1 and 10:1 was used. The ligation was completed with T4 DNA ligase and its appropriate buffer in a final volume of 20 µl. 100 ng of vector DNA were used in every ligation approach. An incubation was then performed at room temperature (RT) for 1 hour, or overnight at 16°C. For the self-ligation control, the digested plasmid was incubated in the presence of T4 DNA ligase without the insert.

4.2.2.6   Agarose gel electrophoresis

The electrophoretic separation of DNA fragments was completed with 0.8 to 2.5% agarose gels using a voltage of 5 to 8 V/cm and 1x TAE as the running buffer. The Gene Ruler 1 kb Plus DNA Ladder was used for size determination. EZ Vision (Amresco; for fragments larger than 1 kbp) or Gelred (Biotium; for fragments smaller than 1 kbp) were utilized to stain the DNA. Visualization, analysis, and documentation was done by excitation of the respective dye via UV light (λ=312 nm) using the UV detection apparatus Gel iX Imager (Intas).

4.2.2.7   DNA isolation from agarose gels

The DNA fragments were cut from the agarose gels using a scalpel and UV light for visualization. Subsequently, the DNA was isolated from the gel using the NucleoSpin ® Extract II Kit (Macherey-Nagel) according to the manufacturer's protocol.

4.2.2.8   DNA concentration determination

Determination of DNA concentrations was completed utilizing the NanoDrop 2000 (Thermo Scientific) according to the manufacturer's instructions. 1 µl of DNA solution was used for every measurement.

4.2.2.9   Polymerase chain reaction (PCR)

The template for the PCR was always either purified plasmid or purified genomic DNA. The PCR method was used to amplify a specific part of a DNA sequence. Via repeated cycles of DNA double helix denaturation, binding of the respective complementary oligonucleotides (primers), and elongation by the DNA polymerase, the PCR product is amplified (Mullis et al., 1992). After the denaturation step, the DNA exists in the single stranded state. Primers bind specifically at the ends of the DNA part that is intended to be amplified. The elongation starts at the free 3' OH ends of the primers. Elongation is performed by thermo-stable DNA polymerases, which also exhibit a 3'-5' exonuclease activity and thereby reduce the error rate during synthesis of the new DNA strand. The DNA amplification rate is (at least under optimal conditions) exponential. If higher accuracy was necessary, the Phusion polymerase (Finnzymes; with the appropriate buffer) was used. Otherwise, the PCR experiments were performed with Taq polymerase (Qiagen; with the appropriate buffer).

For every PCR experiment, 10 or 5 µl of the respective buffer (10 µl 5x GC buffer for Phusion, 5 µl 10x buffer for Taq polymerase), 100 ng of DNA template, 1 µl of dNTPs (10

mM), 1 µl of each primer (10 pmol/µl), and 1 µl of DNA polymerase were used. DdH$_2$O was added to a final volume of 50 µl. The initial denaturing process was performed at 98°C for 2 minutes, followed by 35 cycles of denaturing (30 seconds, 98°C), primer base pairing (30 seconds, 55°C to 59°C, depending on the melting temperature of the used primer), and an elongation period (72°C, duration dependent on the size of the PCR product and on the DNA polymerase used according to the manufacturer's instructions). A final elongation step of 7 minutes completed the reaction. Afterwards, the products were cooled to 4°C and directly analyzed via an agarose gel or first stored at -20 or 4°C.

4.2.3   Cell culture methods

All cell culture methods were performed under sterile conditions using a laminar flow cabinet. Cells were incubated at 37°C, 5% CO_2, and 90% humidity.

4.2.3.1   Culturing of cells

All cell lines were cultivated in appropriate tissue culture flasks, dishes, or plates. They were split 1:10 at a confluence of 90%, usually twice a week. All culture media contained 10% FCS and 2 mM L-glutamine. If necessary, penicillin/streptomycin was added. To split adherent cells, the culture medium was discarded and cells were washed with PBS. Then, an addition of trypsin-EDTA leads to proteolytic cleavage of the extracellular adherence proteins, allowing the cells to be removed from the plastic surface. Subsequently, fresh medium was added to the cells and they were seeded in the necessary dilution. Suspension cells were generally cultivated at a minimal density of $1*10^6$ cells/ml. To split them, the required volume of medium containing cells was replaced by fresh medium.

4.2.3.2   Storage of eukaryotic cell lines

Adherent cell lines were washed with PBS, treated with trypsin/EDTA, and resuspended in fresh medium. Then, they were centrifuged (3 min, 300*g (1500 rpm)) and the supernatant was discarded. Cells were resuspended in 1 ml FCS containing 10 % DMSO (per ½ T175 flask) and transferred to cryovials. The cryovials were directly stored at -80°C, and after 24 hours they were transferred into liquid nitrogen. When required, the cells were thawed by hand and 10 ml of fresh culture medium was added directly after thawing. A centrifugation step (3 min, 1500 rpm), with subsequent discarding of the supernatant, was performed to remove DMSO from the cells. Afterwards, the pelleted cells were resuspended in fresh medium and cultivated as described above.

4.2.3.3   Determination of the cell number

To determine the exact number of cells, the cells were scraped from the plastic surface using a cell scraper or removed by the addition of Trypsin/EDTA and subsequently resuspended in fresh medium. The cells were then diluted 1:100 in 9.9 ml ISOTON® II Diluent (Beckman Coulter) and the cell number/ml was measured using the Z1 Coulter® Particle Counter (Beckman Coulter) according to the manufacturer's protocol. Alternatively, cells were

counted with a Neubauer counting chamber (hemocytometer). Prior to that, dead cells were stained by trypan blue.

4.2.3.4   Transfection of cells with polyethylenimine (PEI)

Polyethylenimine (PEI) is a polymer of aziridine, a cyclic secondary imine. PEI is a strongly basic molecule that forms a polycation after the addition of water. Therefore it can interact with the strongly negatively charged DNA. PEI solution that was ready to use for transfections was provided by the workgroup.

Prior to the transfection of cells, the cells were seeded to reveal approximately 75% confluency at the time point of transfection. For transfection, DNA and PEI were diluted in medium without supplements separately (each in either 700 µl for 10 cm dishes, or 500 µl for one well of a 6-well plate). The respective amounts of DNA (in total 11.0 or 12.0 µg DNA for a 10 cm dish, 2.0 µg for one well of a 6-well plate) and PEI (44 µl for 10 cm dishes, 6 µl for one well of a 6-well plate) were added, then the two solutions were vortexed for 10 seconds and subsequently mixed. After an additional vortexing step, the mixture was incubated for 30 minutes at room temperature. During this time, the cell medium was replaced by fresh medium (5 ml for 10 cm dishes, 1 ml for one well of a 6-well plate). Afterwards, the DNA-PEI mixture was added to the cells and the plate/dish was gently shaken to allow homogenous blending of the solutions. Medium was replaced by fresh cell culture medium again after 24 hours if necessary.

4.2.3.5   Transfection of cells with FuGENE

FuGENE transfection is a lipofection. It was always performed in 6-well plates. Cells were seeded to have a confluency of about 75% at the time point of transfection. 6 µl of FuGENE and 96 µl of serum supplement free medium were mixed and incubated for 5 minutes at room temperature. After adding 1 µg of DNA and vortexing, the mixture was incubated for another 15 minutes. Subsequently, the mixture was added to the cells in small drops. Medium was replaced by fresh cell culture medium after 24 hours if necessary.

4.2.3.6   Transfection of cells with Lipofectamine 2000

Lipofectamine transfection is also based on the lipofection method. Cells were seeded to have a confluency of about 75% at the time point of transfection. For 10 cm dishes, 25 µl of Lipofectamine were diluted in 500 µl Opti-MEM, and 22 to 24 µg of DNA (double of the amount used in PEI transfection) were diluted in the same volume of Opti-MEM separately. For one well of a 6-well plate, 5 µl of Lipofectamine and 5 µg of DNA were each diluted in a volume of 250 µl Opti-MEM. After vortexing, both solutions were mixed, vortexed, and incubated for 30 minutes at room temperature. During this time, the cell culture medium was replaced by 5 ml (for 10 cm dishes) or 1 ml (for one well of a 6-well plate) Opti-MEM. After this 30 minute period, the DNA-Lipofectamine mixture was added to the cells dropwise. Opti-MEM was replaced by fresh cell culture medium after another 24 hours.

4.2.3.7   Production of lentiviral vector particles (VPs)

Lentiviral vector particles (VPs) were produced by transfection of HEK 293T cells. The cells were seeded in 10 cm dishes, cultured overnight and then transfected using Lipofectamine or PEI as described above (see 4.2.3.4, 4.2.3.6). When PEI was used as the transfection reagent, the cells were transfected with 2.4 µg pMDLg/pRRE (encoding HIV-1 gag-pol, containing a rev responsive element), 1.2 µg pRSVrev (encoding HIV-1 rev), 5.5 µg pRRLsinCMV-GFPpre (encoding GFP and containing the HIV-1 packaging signal Ψ), and a varying fourth plasmid coding for a viral envelope protein: pIRES2-EGFP-CHIKV E3-E1 (Chikungunya virus envelope protein), LCMV Env (Lymphocytic Choriomeningitis Virus), GaLV Env delta R TM (Gibbon ape leukemia virus transmembrane protein), or pHITG (encoding VSV-G, Vesicular stomatitis virus glycoprotein). For the latter plasmid, 1.9 µg of DNA were used, and for the other three, 3.0 µg were used, per 10 cm dish. If Lipofectamine was used for transfection, double the amount of each DNA was used for transfection. The VPs used for the luciferase assay (see 4.2.3.9) were always produced with Lipofectamine. Additionally, the pRRLsinCMV-GFPpre construct was replaced by 11 µg of pCSII-EF-luciferase (encoding luciferase and also containing Ψ). 24 hours after transfection, the medium was replaced by 5 ml fresh DMEM. Another 24 hours later the VPs containing supernatant were harvested, sterile filtered with 0.45 µm filters, and freshly used or frozen and stored at -80°C. In the case of Lipofectamine transfection, a second harvest was performed 24 hours after the first one, again using 5 ml of DMEM.

4.2.3.8   Transduction of cells with pseudotyped lentiviral VPs

To transduce cells, the cells were counted and seeded in plates the day prior to transfection. Usually, $1.25*10^5$ cells were seeded per well in 1 ml medium in 24-well plates. The next day, the cell culture medium was replaced with medium containing pseudotyped VPs (CHIKV Env, GaLV Env delta R, VSV-G; containing a transfer vector encoding GFP; volume depending on the specific VP titer). Cells were incubated for 6 hours at 37°C with the VPs. Then, the VP medium was replaced by 1 ml fresh cell culture medium. Cells were incubated for another 48 to 72 hours. Subsequently, GFP expression was analyzed by flow cytometry (see 4.2.3.10).

4.2.3.9   384-well luciferase assay

For the luciferase assay, HEK 293T cells (counted with the Neubauer counting chamber) were seeded in white 384-well plates (Greiner) with a MultiFlo Microplate Dispenser (BioTek) adding 6000 cells in 20 µl DMEM (plus Pen/Strep) to every well. When CHO-K1 or pgsA-745 cells were seeded, only 3000 cells per well were used. 16 to 24 hours later, pseudotyped VPs (CHIKV Env, LCMV Env, or VSV-G; containing a gene encoding luciferase) mixed with the respective potential CHIKV entry inhibitor were added to the cells. Prior to the addition, a dilution of the VPs (60 µl) was mixed 1:1 with the inhibitor (concentration in final 120 µl approach 1000 µg/ml for soluble glycosaminoglycans (GAGs), 1:30 for mouse sera, 50 µg/ml EC/EGCG). The mixture was then serially diluted 1:3 in 80 µl of a 1:1 DMEM-VP mixture 4 times in 96 U-well plates, transferring 40 µl of the previous dilution to the next well each time. This inhibitor-VP mixture was then incubated for 30 to 60 minutes at 4°C. Subsequently, 60 µl of every well of the 96 U-well plate were transferred to the 384-well plate with the cells via a Matrix Multichannel Equalizer Electronic Pipette (Thermo Scientific). The total 60 µl were separated into 3 times 20 µl aliquots. Thus, 20 µl were added into every well of the 384-well plate and the experiment was thus performed in triplicates. The potential inhibitors were again diluted 1:2 by adding the mixtures to the cells (20 µl VPs/inhibitor to 20 µl cell supernatant), thus the final concentrations were 500 µg/ml for the GAGs, 1:60 for the mouse sera, and 25 µg/ml EC/EGCG. LCMV Env and VSV-G pseudotyped VPs or AAV-2 VPs, were also used in the assay, respectively. After another incubation period of 16 to 24 hours, 20 µl of Britelite substrate (Perkin Elmer) were added to the cells. 5 minutes later, the luciferase signal was detected using the PHERAstar FS (BMG LABTECH).

The strength of the luciferase signal of the differentially pseudotyped VPs was measured in advance for every new stock, and the VP dilutions in the experiments were then adjusted to have a luciferase signal in the same range for all different VPs (about 100,000 relative light units per well).

4.2.3.10   Flow cytometry

The flow cytometer (FACS is a special part of the flow cytometry, the Fluorescence Activated Cell Sorting) enables the analysis of certain features of cells or cell populations by means of the antigen-antibody binding principle. The antibodies for detection are fluorescence dye (for example with fluorescein isothiocyanate (FITC)) labeled. If the cell carries the antigen the antibody is directed against on the cell surface (or inside the cell if an intracellular staining via cell permeabilization is performed), and it is thus fluorescently labeled via binding of the antibody to the antigen. The dye is excited with a laser that has a specific wavelength and then emits light of a specific wavelength, depending on the dye's structure. This emission can be detected by the flow cytometer. The emission of intracellular fluorescence proteins, like GFP or mCherry, can also be detected when the fluorescent protein expressing cell passes a laser with the specific excitation wavelength of the respective protein. Other features of a cell that can be detected by a laser are the "forward scatter" (FSC) and the "sideward scatter" (SSC). The FSC is a measure of the size of the cell, and the SSC is a measure of its granularity. Both features can help to distinguish different populations, different types of cells, and dead and living cells from each other in one tube. For direct flow cytometry analysis (GFP, mCherry), cells were treated with Trypsin/EDTA, washed with 1 ml FACS buffer (PBS + 2% FCS), and fixed with PBS + 2% PFA. For measuring of the binding of protein constructs to cells, they were treated as described in 4.2.3.11. At least 10,000 events (living cells) were measured per sample. Unstained cells were always used as a negative control.

4.2.3.11   Recombinant protein binding to cells

To determine if recombinant proteins generated from *E.coli* bind to cells, the cells from the required cell line were scraped from the bottom of the cell culture flask, counted, and separated into 500,000 cells per sample/FACS tube. Cells were washed with 2 ml FACS buffer (PBS + 2% FCS; centrifugated 3 minutes, 300*g). Subsequently, 10 µg of purified protein was added to each tube in 100 µl FACS buffer. For the detection of an inhibitory effect of GAGs on cell binding of the proteins, they were incubated with the respective GAG (500 µg/ml, again in 100 µl FACS buffer) for 30 minutes at 4°C and only then added to the cells. The cells were then incubated for 30 minutes at 4°C with the protein or the protein and the GAG. Subsequently, 2 ml of FACS buffer were added, the cells were centrifuged, and the supernatant was discarded. FACS buffer was then added a second time, this time only 1 ml was used prior to another centrifugation step. After discarding the supernatant, an anti-His tag antibody (mouse; in 50 µl FACS buffer) was added to the cells. A 30 minute incubation period at 4°C and washing with FACS buffer twice (first again with 2 ml, then 1 ml) followed.

The same incubation in the same volume was done with an anti-mouse IgG-FITC antibody following two identical washing steps. The cells were then fixed in 100 µl of PBS + 2% PFA, stored at 4°C in the dark, and flow cytometry (see 4.2.3.10) was completed on the same day. Cells that had not been incubated with protein/antibody before, or only with the two antibodies and not with one of the constructs were used as negative controls.

4.2.3.12   Fusion assay

To test compounds for their inhibitory effects on fusion of viral and endosomal membranes, a fusion assay was performed. Here, the structural rearrangements of the CHIKV envelope proteins were induced directly at the cell membrane by addition of an acidic fusion buffer to cells carrying CHIKV Env on their surface. The cellular membranes of adjacent cells fuse with each other and the cells form syncytia. These can be observed via a fluorescence microscope, because the CHIKV Env expressing cells also express GFP.

293T cells were seeded in 6-well plates and transfected with a plasmid containing a CHIKV Env expression cassette including an IRES eGFP. 48 hours later, they were exposed to fusion buffer (pH 5.2) for 5 minutes at 37°C in the presence or absence of the potential inhibitor. The fusion buffer then was replaced by fresh medium and an incubation of 3 hours at 37°C followed. The formation of syncytia was detected via a fluorescence microscope observing the eGFP distribution in the single cells or in the syncytia.

4.2.3.13   Mycoplasma tests

To test if cultured cells were contaminated with *Mycoplasma* bacteria (which could influence experimental results), the cells were seeded in 6-well plates. One day later, they were fixed with PBS + 2% PFA at 4°C for 15 minutes. In this fixation buffer, 4',6-diamidino-2-phenylindole (DAPI) had been added previously (1:5000). DAPI intercalates into the DNA double helix and can be excited by light exhibiting a wavelength of 358 nm (emission: 461 nm). It thus labels DNA and can be visualized via a fluorescence microscope. After the fixation/staining, the cells were washed two times with PBS and then stored in PBS at 4°C. If the cells were contaminated with *Mycoplasma*, labeled DNA fragments occur not only in the nucleus but also in the cytoplasm of the cell. This was detected via a fluorescence microscope.

4.2.3.14   Preparation of cell lysates

For the preparation of cell lysates, the cells were removed from the plastic surface by scraping or treatment with Trypsin/EDTA. Subsequently, they were washed once with PBS (centrifuged 3 min, 300*g; followed by an addition of PBS to the pellet, resuspension; and a second centrifugation) and the pellet was then resuspended in 100, 250, or 900 µl lysis buffer (for one well of a 12-well plate, of a 6-well plate, and a 10 cm dish, respectively). The lysate was incubated for 15 minutes at 4°C, then it was centrifuged at 13,000 rpm (in the small centrifuge for 1.5 and 2 ml tubes), 4°C, for 15 minutes. The supernatants were transferred to a new tube. 4x SDS sample buffer (plus β-mercaptoethanol) was added to reach the volume required for the amount of sample. It was then boiled at 95°C for 5 minutes. Subsequently, the lysates were frozen at -20°C or directly used for SDS-PAGE. The lysates without sample buffer that were not required were also frozen at -20°C. If cell supernatants were to be analyzed via SDS-PAGE/Western blot, they were first sterile filtered (0.45 µm) and subsequently 4x SDS sample buffer was added. Afterwards they were boiled and used or frozen as described above.

4.2.3.15   MTT assay

The MTT assay is used to measure cell viability and is based in the reduction of the yellow, water-soluble 3-(4,5-dimethylthiazol-2-yl)-2,5-diphenyltetrazolium bromide (MTT) to its purple, insoluble formazan. This is only done by living cells. 293T cells were seeded in 24-well plates, on the next day they were exposed to the tested compound in DMEM (500 µl, 2% FCS) at different concentrations, the highest concentration used was also the highest one used in inhibition experiments with the compound. Cells were incubated with the compound for 20 hours at 37°C. Then, the supernatant (with dead cells) was replaced by MTT medium (0.5 mg/ml MTT in 200 µl DMEM per well). An incubation for 4 hours at 37°C followed, afterwards the MTT medium was discarded and 400µl DMSO per well was added. After another 30 minutes at 37°C, the readout was done by a microplate reader (Tecan) and the Tecan XFluor™ software at 560 nm.

4.2.4 Virological methods

4.2.4.1 Modified vaccinia virus Ankara (MVA) methods
Generation of recombinant MVA

For generation of recombinant modified vaccinia virus Ankara (MVA), the strain MVAII new was used for transgene insertion. First, a recombination plasmid (pIII-lacZ2_A SecTag-CHIKV E2 D AB, originating from pIII-lacZ2_A) was cloned. It contained a poxviral promoter (pmH5), the transgene *sAB*[+] (including a eukaryotic secretion signal; formerly called E2 D AB), and the host-range gene *K1L*. This cassette was surrounded by specific sequences (flanks), which were also present 5' and 3' from the deletion III in MVA where the transgene should be cloned into. Via these homologous sequences, homologous recombination takes place (done on BHK-21 cells). The integration of the *K1L* host-range gene into the cassette present in the recombinant virus allows it to replicate on RK-13 cells. Thus, *K1L* allows only the recombinant virus to replicate, but not the wild-type virus without *K1L* and the transgene. After a few passages on RK-13 cells, there should only be recombinant virus left and wild-type virus should not be detectable anymore. The viral detection was completed via PCR. After the selection of recombinant viruses, the host-range gene is not needed anymore. *K1L* can now be deleted via homologous recombination of the repetitive sequences directly surrounding it in the expression cassette. For the deletion, the recombinant virus was serially passaged on BHK-21 cells. On these cells, *K1L* is not necessary for a successful replication. This deletion was again analyzed by PCR.

4.2.4.1.1 Transfection and infection

The initial step for the generation of recombinant MVA was done on the MVA permissive BHK-21 cell line. These cells were infected with the wild-type virus MVAII new in a 6-well plate (MOI 0.1) and 2 hours later transfected with the recombination plasmid pIII-lacZ2_A SecTag-CHIKV E2 D AB. The cells were scraped 48 hours after infection/transfection, transferred to a 1.5 ml reaction tube and freeze-thawed at -80°C 3 times. Then they were treated with an ultrasound 3 times for 1 minute (100%). To eliminate remaining wild-type virus, the viral mixture was now passaged on RK-13 cells.

4.2.4.1.2   Blind passage on RK-13 cells

Via the blind passage, the recombinant viruses are enriched and at the same time the wild-type virus is depleted. RK-13 cells were seeded in a 6-well plate and infected with 200 µl of the sample from 4.2.4.1.1. 72 hours later, the infected cells were scraped and treated as described in 4.2.4.1.1.

4.2.4.1.3   Passaging and selection on RK-13 cells

To enrich the recombinant virus, RK-13 cells that had previously been seeded in 12-well plates (75% confluency) were infected with 300 µl of sample from the blind passage (see 4.2.4.1.2). 10-fold dilutions from this initial amount were made in the following wells. Two to four days later (when the plaques were of sufficient size), single viral plaques were picked with a pipette and transferred into 50 µl of medium, treated with freezing-thawing cycles (see 4.2.4.1.1) and ultrasound, and subsequently passaged again using serial dilutions (starting with 20 µl from the 50 µl pick). After 3 to 4 passages, the passaged clones were checked for presence of the transgene and *K1L* via PCR. If the required genes were not present, further passages were performed until a positive clone occurred. Then, passages continued on BHK-21 cells to eliminate *K1L* (see 4.2.4.1).

4.2.4.1.4   Passaging and selection on BHK-21 cells

The passaging on BHK-21 cells (removal of *K1L*) was done analogous to that on RK-13 cells (see 4.2.4.1.3). The selection was finished when no *K1L* but still the transgene could be detected via PCR. Furthermore, expression of the protein sAB$^+$ was confirmed via SDS-PAGE/Western blot.

4.2.4.1.5   Analysis of the viral clones

To analyze whether the chosen clones contained the transgene *sAB$^+$* or *K1L*, the genomic DNA was isolated from cells infected with the respective clone with the DNeasy Blood & Tissue Kit (Qiagen). For the subsequent PCR, the primer pairs C7L for/rev (for *C7L* detection; needed for efficient late expression of sAB$^+$), Del III for/rev (to check if the expression cassette from the recombination plasmid is inserted into the MVA deletion III), K1L int-1/2 (for *K1L* detection), and Del III for/ChW35 int rev (transgene *sAB$^+$* detection) were used. The elongation time in every cycle (see 4.2.2.9) was 1 minute. To verify not only the

presence of the transgene, but also the expression of the respective protein, infected cells were lysed and subsequently checked for protein expression (alongside the cell supernatants) via SDS-PAGE/Western blot with an anti-c-myc antibody. When the transgene was present in the chosen clone and *K1L* was absent, and the respective transgene protein was expressed and secreted from infected cells, the respective clone (MVA-CHIKV-sAB[+]) was propagated to obtain viral amounts and titers that could be used for vaccination of mice.

4.2.4.1.6   Propagation of (recombinant) modified vaccinia virus Ankara (MVA)

The propagation and expansion of MVA-CHIKV-sAB[+] was done on BHK-21 cells. The RPMI medium used for the propagation contained only 2% FCS. The propagation was completed stepwise. Three T175 cell culture flasks (seeded before, confluency 75%) were infected with one single viral clone (MOI 0.2). This was done via shaking the flasks with the virus (in 5 ml cell culture medium) at room temperature for 1 hour. Then, 25 ml of cell culture medium were added and an incubation at 37°C in the incubator followed. After the flasks had been infected completely (2 to 4 days later), the cells of ten T175 cell culture flasks (seeded before, confluency 75%) were infected with the virus amount that had grown in these three flasks. In the next step, 60 new T175 flasks were infected. After the flasks had been fully infected, they were frozen at -80°C. After thawing, the cells that were still attached to the bottom of the flask were scraped from the plastic surface. The supernatant containing both cells and virus was then centrifuged in an ultracentrifuge (16,000 rpm, 90 minutes, 4°C). The supernatant was discarded and the pellet was respuspended in 30 ml TRIS (pH 9.0). The suspension was freeze-thawed at -80°C two times and subsequently treated with ultrasound via a sterile ultrasound needle (3 x 1 minute, 100%). To separate the cell debris from the viral particles, the solutions were centrifuged through a 36% sucrose cushion (13,500 rpm, 80 minutes, 4°C). The pellet was resuspended in 1.8 ml TRIS (pH 9.0) and frozen at -80°C. In the next step, the viral titer was determined (4.2.4.1.7).

4.2.4.1.7   Virus titration

To determine the viral titer of MVA (in infectious units IU/ml), confluent BHK-21 cells in 6-well plates were infected with serial 10-fold dilutions of MVA (2 wells per dilution) at 37°C. Two hours later, the virus dilutions were replaced by fresh medium. Another incubation period of 48 hours followed. The cells were then fixed with an ice-cold 1:1 blend of acetone/methanol for 5 minutes, dried and blocked by the addition of PBS containing 2% FCS (room

temperature (RT), 30 minutes). An anti-vaccinia virus antibody was added (in PBS/FCS, 1:2000) and cells were incubated for three hours on the shaker (RT). After two washing steps with PBS, the secondary antibody (anti-rabbit IgG-HRP) was added (1:2000) and incubated for 1 hour at RT, followed again by 2 washing steps. Subsequently, 0.5 ml per well of the HRP substrate TrueBlue were added to the cells. To stop the reaction, cells were washed with Reinstwasser and dried. In the wells where about 10 to 100 plaques were detected, those plaques were counted and the mean value of identical dilutions was calculated to determine the viral titer.

4.2.4.1.8   Viral growth analysis

To analyze the growth features of MVA, 6-well plates with different cell lines (BHK-21, HeLa, DF-1) were infected with an MOI of 0.5. The infection took place for 1 hour. The infection medium was subsequently replaced by fresh cell culture medium. The cells of one well were directly scraped for the 0 hours value. The same was done with one well after 8, 24, and 48 hours. The scraped cells were treated as in 4.2.4.1.1 and the viral titers were analyzed as described in 4.2.4.1.7 .

4.2.4.2   Chikungunya virus methods

4.2.4.2.1   Production of CHIKV-mCherry-490

To produce CHIKV-mCherry-490, the plasmid pCHIKV-mCherry-490 was first linearized with *Not*I and then *in vitro*-transcribed using the T7 Quick High Yield RNA Synthesis Kit (NEB) following the manufacturer's protocol. Lipofectamine 2000 (Invitrogen, see 4.2.3.6) was used for transfection of the resulting mRNA into BHK-21 in 6-well plates. The virus containing supernatants were harvested after 48 hours and directly used to infect fresh BHK-21 cells (6-well plates). The supernatants were collected after 24 hours, centrifuged for 10 min at 300*g (4°C) to remove cell debris, and pooled. They were stored at -80°C until the determination of the viral titer or usage.

4.2.4.2.2   Propagation of wild-type CHIKV

The propagation of CHIKV was performed on Vero cells. The infections were started in 6-well plates (always from the same virus stock; MOI 1), and the supernatants were then passaged to Vero cells seeded in T25 flasks once the majority of the cells revealed a cytopathic effect. This was continued with T75, T175, and then several T175 flasks until a sufficient volume of virus containing supernatant was produced. The supernatants were centrifuged as described in 4.2.4.2.1, pooled, and stored at -80°C until the purification of the virus.

4.2.4.2.3   Purification of wild-type CHIKV

CHIKV wild-type was purified by centrifugation through 2 ml of 30% sucrose for 2 hours at 28,000 rpm**.** The pellet was resuspended in a small volume (approx. 0.5 ml) PBS and stored at -80°C until the determination of the viral titer or usage.

4.2.4.2.4   Determination of viral titer (CHIKV-mCherry-490 and wild-type CHIKV)

For determination of the viral titer, Vero cells were seeded in 6-well plates one day before infection. They were infected (75% confluence) with 20 µl of virus, which was then serially 10-fold diluted on the cells. After 2 hours at 37°C, virus was washed away and an incubation at 37°C for 48 hours followed. Then, the supernatant was replaced by a crystal violet staining solution (0.1 g crystal violet, 20 ml ethanol, 80 ml ddH$_2$O) for 5 minutes (RT) and removed again. When the wells were dry, the titer was determined by counting the plaques.

4.2.4.2.5   CHIKV-mCherry binding/entry assay

The binding/entry assay was performed similar to the normal infection (see 4.2.4.2.4). In this assay, however, virus and potential inhibitor were first pre-incubated at 4°C (30 minutes). The mixture was then added to the cells and an incubation period for the same amount of time and at the same temperature (viral MOI 1) followed. Unbound virus was washed away and replaced by fresh cell culture medium. After an incubation of 6 hours (37°C), the mCherry signal of infected cells was detected via flow cytometry as described above.

4.2.5 Protein biochemistry methods

4.2.5.1 Quantification of the protein content

Protein quantification with the Pierce® BCA Protein Assay Kit (Fisher Scientific) was completed following the manufacturer's instructions. The detection was performed with a microplate reader (Tecan) and the Tecan XFluor™ software.

4.2.5.2 Sodium Dodecyl Sulfate Polyacrylamide Gel Electrophoresis (SDS-PAGE)

Via Sodium Dodecyl Sulfate Polyacrylamide Gel Electrophoresis (SDS-PAGE), proteins can be separated by their molecular mass. The proteins migrate through a polyacrylamide matrix. The gel contains 30% acrylamide and 0.8% bis acrylamide (Rotiphorese® Gel 30) and polymerizes in the presence of ammonium persulfate (APS) and tetramethylendiamine (TEMED). These chemicals serve as starters for the radical polymerization. The SDS associated with the proteins sheilds the intrinsic charge of the protein and denatures it. The SDS/protein complexes are thus uniformly negatively charged and migrate to the anode in an electric field. The cell lysates or supernatants containing SDS sample buffer (see 4.2.3.14) were loaded onto the gel. Once a voltage was induced, the protein mixture in every sample was first concentrated in one band in the stacking gel (5% acrylamide; due to the pH value and the ionic environment) and subsequently separated in the running gel (12.5% or 15% acrylamide) due to their different molecular masses. For SDS-PAGE, an electrophoresis chamber from BioRad was used according to the manufacturer's instructions. The gels ran at a voltage of 120 to 160 V and were stopped when the bromophenol blue dye from the sample buffer was about to migrate out of the gel. The recipe for the SDS-PAGE buffers and gels are shown in 4.1.10.1.1.

4.2.5.3 Coomassie staining

Coomassie dye interacts with the basic side chains of amino acids and can therefore be used to stain proteins separated by SDS-PAGE. The acidic, alcoholic coomassie staining solution fixes the proteins in the gel and the dye forms a complex with them. After an SDS-PAGE, the gel was incubated in the staining solution on the shaker for 40 minutes at RT. Subsequently, it was repeatedly incubated in clean destaining solution I for short periods (replacement of solution after about 2, 5, 10, 30, 60 minutes) and then overnight in the destaining solution II. The destaining procedure was repeated until the background staining of the gel had completely vanished and the protein bands were clearly visible. The gel was

washed with water Reinstwasser and a picture of it was taken using a GS-800 densitometer (BioRad).

4.2.5.4   Silver staining

For silver staining (the silver ions interact with negatively charged residues of a protein; for solution preparation see 4.1.10.1.1) of SDS-gels after a run, the gels were first incubated in fixation solution (50 ml/gel) for at least 30 minutes (if necessary overnight) at RT on a shaker. For one gel, a volume of 50 ml was used for every solution during the silver staining and the gels were incubated on the shaker at RT. After that, the gel was incubated for 20 minutes in conditioner solution. It was subsequently washed 3 times for 5 minutes with Reinstwasser. An incubation time of 20 minutes on the shaker in staining solution (in the dark) followed. Afterwards, the staining solution was discarded and developing solution was added. The reaction was stopped by the addition of 10 ml acetic acid per gel when the intensity of the protein bands was sufficient. Then the gel was washed with Reinstwasser and a picture of it was taken by a GS-800 densitometer (BioRad).

4.2.5.5   Western blot

The negatively charged proteins in an SDS-gel are transferred via Western blotting onto a Polyvinylidene fluoride (PVDF) membrane and fixed on it. Then it is possible to label the proteins specifically via incubation of the membrane with an antibody directed against the protein of choice. Subsequently, a secondary antibody (coupled to horseradish peroxidase, HRP) directed against the constant part of the primary antibody is added. The substrate of the HRP is then added, which induces the enhanced chemiluminescence (ECL) reaction. During this reaction, the oxidation of luminol, which emits light, is catalyzed. The light emission can be detected with an appropriate chemiluminescence detection system.

A semi-dry blot apparatus (BioRad) was used for Western blots following the manufacturer's instructions. Prior to blotting, the membrane was activated in methanol and then the blot itself was subsequently performed for 75 minutes using 100 mA per gel/membrane. After successful blotting, the free protein binding sites on the membrane were blocked using the blocking solution Roti-Block (at least 1 hour, RT, on the shaker) to reduce unspecific binding of antibodies in the following step. Then, the primary antibody was added. Incubation was done at 4°C overnight with constant rotating on a roller mixer. After washing 3 times (15 minutes) with TBS-T, incubation with the HRP-coupled secondary antibody for 1 hour at RT (constant rotating) was performed. Another washing (3 times) followed, then the HRP

substrate was pipetted onto the membrane and the light signal was detected by the Fusion FX-7 (Vilber).

4.2.5.6 Stripping of membranes

Stripping of membranes was performed if (an) additional protein(s) fixed on the PVDF membrane were detected along with the one that had already been visualized. For the membrane stripping, the already bound primary and secondary antibodies were washed away using the ReBlot Plus Mild Antibody Stripping Solution (from Millipore) according to the manufacturer's protocol. After the washing, the membrane was again blocked for 1 hour. Subsequently, the new primary antibody was added, following incubation with the secondary antibody and the detection as described in 4.2.5.5.

4.2.5.7 Recombinant protein purification from *E.coli*
4.2.5.7.1 Native purification of proteins via HPLC (Ni-NTA)

To purify recombinant proteins natively from *E.coli,* first the frozen bacteria pellets that contained the recombinant protein (see 4.2.1.3) were thawed. Subsequently, they were resuspended in 10 ml sample buffer, transferred to glass tubes and treated with an ultrasound needle (4 x 1 minute, 4 cycles, 20% power, pauses of 1 minute between the treatments) on ice. Via this treatment, the cell walls of the bacteria break and the recombinant proteins within the cells can diffuse into the sample buffer. All following steps were performed on ice or at 4°C. The lysates were centrifuged at 12,000 rpm (15 minutes) in 2 ml tubes to get rid of the cell debris. The supernatants were collected in 10 ml syringes and sterile filtered with 0.2 µm filters. By performing this step, small cell debris is also removed and during the HPLC performed later, there is no danger of clogging the device. The samples were filtered into 15 ml tubes and filled up to a total volume of 10 ml with sample buffer. Afterwards (always on the same day), the HPLC separation was performed using an ÄKTA Purifier 10 (GE Healthcare). The purification was done using Ni-NTA HisTrap FF Crude 1 ml columns (GE Healthcare). In principle, the imidazole side chain of the His-tag of the recombinant proteins interacts with the Ni^{2+}-columns and fixes the proteins onto the column. The sample buffer contained 1 mM imidazole to avoid unspecific binding of histidine-rich proteins. Higher concentrations of imidazole (300 mM) in the elution buffer then extruded the His-tagged proteins from the Ni^{2+} and led to their elution. The ÄKTA Purifier was used according to the manufacturer's instructions. The column was first equilibrated with 5 ml sample buffer. The sample was injected in a volume of 10 ml. Subsequently, the column was

washed with 7 ml of sample buffer. A gradient to 100% elution buffer over 6 ml followed. After 4 additional ml of 100% elution buffer were run through, the column was washed with 5 ml elution buffer. The eluted recombinant proteins were collected in 1 ml fractions and the flow rate was 1.5 ml/min. The described conditions were saved in the running program "nintanat ChW 22" (24.01.14) on the ÄKTA computer. The collected elution fractions were stored at 4°C and analyzed via SDS-PAGE (5 µl/fraction) and silver staining. The purest fractions (with a still satisfying yield of recombinant protein) were pooled and dialyzed using Slide-A-Lyzer Dialysis Cassettes (Thermo scientific), according to the manufacturer's instructions, to remove the imidazole in the elution buffer. 4 to 16 ml of the pooled fractions were used in 3 times 4.5 L PBS (2 times 2-3 hours, one time overnight, all at 4°C). After the dialysis, the samples were concentrated using Amicon centrifugal filter units (Millipore, cutoff 3 kDa) and their concentration was determined by SDS-PAGE and subsequent coomassie staining using a BSA concentration row for estimation of concentration. The proteins were quick-frozen with liquid N_2 (also always directly after usage in experiments) in 1.5 ml tubes and stored at -80°C. If used for experiments, they were thawed in a 37°C water bath. This protocol was performed for all recombinant proteins except A and E2.

4.2.5.7.2 Denaturing purification of proteins via HPLC (Ni-NTA)

Some of the proteins recombinantly expressed in *E.coli* were not soluble in the bacterial cytoplasm due to incorrect folding and were stored in inclusion bodies within the bacterium. These cannot be cracked via ultrasound alone. To obtain these proteins trapped within the inclusion bodies, one has to lyse them with denaturing buffers and subsequently follow a denaturing purification protocol. The frozen pellets of bacteria which had expressed the recombinant proteins (for this protocol A and E2) were resuspended in 10 ml sample/lysis buffer and then lysed for 10 minutes on ice. After the lysis, the protocol utilizing ultrasound was performed exactly as described in 4.2.5.7.1. At the ÄKTA HPLC step, however, this time 3 different buffers were used. The Ni-NTA columns were equilibrated with 7 ml equilibration buffer and the sample (in sample/lysate buffer) was injected in a total volume of 10 ml. After washing with 7 ml washing buffer, the buffer was switched to elution buffer (without a gradient) and elution with subsequent washing took place for 22 ml. The flow rate was again 1.5 ml/minute and all the conditions are saved in "Histrapautocomplden1Christophetr" (23.01.14) on the ÄKTA computer. After SDS-PAGE analysis as in 4.2.5.2, and in 4.2.5.4, the fractions containing sufficient amounts of recombinant protein were used for ion-exchange chromatography as described in chapter 4.2.5.7.3. The following steps were similar to that in 4.2.5.7.1. However, to get rid of the 6 M urea in the elution buffer (to reduce

precipitation of recombinant protein during refolding), the proteins were first dialyzed in PBS + 4 M urea, then an identical step with 2 M urea was performed (both 4.5 L, overnight and 2-3 hours, respectively). Only then the dialysis was done as described in 4.2.5.7.1 using PBS 3 times and performing an overnight incubation. After dialysis, the samples were centrifuged at 12,000 rpm (4°C, 15 minutes) to remove precipitated proteins. The supernatants were transferred to fresh 1.5 ml tubes and treated as described in 4.2.5.7.1.

4.2.5.7.3 Protein purification via ion-exchange chromatography

To obtain purer recombinant proteins, an ion-exchange chromatography was additionally done directly after affinity chromatography using Ni-NTA columns. During ion-exchange chromatography, proteins are separated by their isoelectric point. It is extremely unlikely that histidine-rich *E.coli* proteins that had been co-purified during the Ni-NTA purification share an identical isoelectric point with the wanted protein. Proteins A and E2 were checked for their isoelectric points using the internet tool described in 4.1.17. Both had a basic isoelectric point (8.8 and 8.2 for A and E2, respectively) and were thus dialyzed against an acidic binding buffer (pH 6.0) in order to have buffer conditions in which the proteins have a preferably high charge (acidic side chains still deprotonated and basic side chains protonated). This dialysis (10 ml sample, 4.5 L dialysis buffer, 4°C, overnight) was performed directly after elution and SDS-PAGE analysis of the His-tag chromatography, with all of the fractions containing the recombinant protein in sufficient amounts (see 4.2.5.7.2). The dialyzed samples were loaded onto a column containing acidic chemical groups (Mono S, GE healthcare) to allow binding of the rather positively charged proteins (more basic than acidic amino acids (isoelectric point basic), acidic buffer conditions). Elution (linear gradient) was done with a buffer containing extremely high amounts of NaCl (1 M) and thus the ions interrupt the binding of the proteins to the acidic column. The more basic (positively charged) a protein is, the tighter it binds to the column and the later (higher NaCl concentrations in the buffer) it is eluted. During performance of the purification protocol, the column was first equilibrated with 10 ml binding buffer and then the sample (in 10 ml) was loaded onto the column. A washing step (5 ml) followed. The gradient to 100% elution buffer spanned a volume of 12 ml. After completing the gradient, another 11 ml of elution buffer was flown through. The purification protocol (flow rate: 0.7 ml/minute) was saved under the name "cwmonos" (17.04.14). The elution fractions were collected in 1 ml, and stored at 4°C. Afterwards, dialysis was performed as described in 4.2.5.7.2.

4.2.5.8   Mass spectrometry analyses

The mass spectrometry analyses for confirmation of the identity of the recombinant proteins were performed by Andreas Reuter (Paul-Ehrlich-Institut, department 5/0).

4.2.6 Animal experiments

4.2.6.1 Animals

The animals used in these studies were all female Balb/c mice. They were purchased from Janvier (Saint Berthevin Cedex, France) and arrived at the Paul-Ehrlich-Institut animal facility at an age of 5 weeks. Experiments were started earliest 8 days after arrival. They were weighed weekly and kept in the animal facility following the FELASA guidelines (Federation of European Laboratory Animal Science Associations). The animals were labeled with an ear puncher. All mice experiments were performed according to the respective approved animal experiment request (Tierversuchsantrag). Mice were maintained by the staff of the animal facility.

4.2.6.2 Application techniques

4.2.6.2.1 Subcutaneous injection

Vaccines were subcutaneously injected into the neck region of the animals using a 26G needle (Braun) and a 1 ml syringe. The maximum total volume used was 200 µl per mouse. Proteins (100 µg per injection; in PBS) were mixed 1:1 with Alhydrogel 2% ("alum", InvivoGen), and MVA particles ($1*10^8$ pfu per injection) were applied in 10 mM TRIS (pH 9.0). The mice were anesthesized for the injections.

4.2.6.2.2 Intraperitoneal injection

Intraperitoneal injections were performed via the scruff method exposing the ventral side of the mouse. The animal was tilted down to about 30° and injection was done via a 25G needle (1 ml syringe; position during injection 30° tilted upwards relative to the animal) in the lower right quadrant of the animal's abdomen.

4.2.6.2.3 Intranasal infection

Intranasal infections with wild-type CHIKV were performed using a 100 µl pipette (Eppendorf) with 100 µl filter tips. Before infection, mice were anesthesized with a ketamine/xylazine mixture (mixed and provided by Roland Plesker of the Paul-Ehrlich-Institut animal facility 4/ZT). For applying this anesthetic, 10 µl/g body weight were injected intraperitoneally into the mice. When the mouse no longer showed reflexes, $1.0*10^6$ plaque-forming units (PFU)

CHIKV were pipetted onto the nose of the mouse in 30 µl PBS. They then inhaled the liquid and were kept under observation until their awakening.

4.2.6.3 Retro-orbital sinus blood collection

For blood collection, mice were anesthesized using isoflurane. A Pasteur pipette was used, and the collection was performed behind the eye at the medial canthus. When the sinus was punctured, the blood entered the pipette. The blood collection was finished after a sufficient volume was inside the pipette, then the pipette tip was withdrawn and gauze was used to stop bleeding. It was transferred to blood collection tubes. The mice were awake after about 1 minute.

4.2.6.4 Inhalation anesthesia

For short time anesthesia, isoflurane was used. By this method, mice lose consciousness, experience of pain, the ability for reflexes changes, and a damping of respiration occurs. In contrast to this, isoflurane lacks analgesic features.

The anesthesia was done using the narcotization apparatus Matrix (Midmark).

4.2.6.5 Euthanasia

Mice were sacrificed by the use of CO_2. After death, mice were decapitated with scissors and the blood exiting the torso was collected with a blood collection tube gold (BD). The disposal was performed by the staff of the animal facility.

4.2.6.6 Isolation of serum from blood samples

Sera were obtained from blood samples via blood collection tubes gold (BD). Centrifugation (RT, 5 minutes, 10,000 rcf) separated the sera from the cellular fractions of the blood according to the manufacturer's instructions. If viral RNA was to be isolated from the sera later, the sera were directly frozen at -80°C (and always kept on ice before freezing). If the sera were to be used for neutralization assays, they were first incubated at 56°C for 30 minutes (to inactivate the complement system) and then frozen.

4.2.6.7 Isolation of viral RNA from mouse sera

Viral RNA was isolated from mouse sera using the QIAamp Viral RNA Mini Kit (Qiagen) according to the manufacturer's protocol. The eluted RNA was stored at -80°C until used for RT-PCR.

4.2.6.8 RT-PCR with isolated viral RNA

The concentration of viral RNA isolated from mouse sera was determined using the RealStar® Chikungunya RT-PCR Kit 1.0 (altona Diagnostics GmbH) according to the manufacturer's instructions. A quantitative analysis was done with standard samples provided by the company. The readout was done by the Lightcycler® 480 instrument II (Roche) following the manufacturer's protocol.

4.2.7 Statistical analysis

The p-values were calculated using the paired two-tailed t test (confidence interval: 95%) for the AUC and NT_{50} values of the mouse sera (Figure 24; Figure 48), and the unpaired two-tailed t test (confidence interval: 95%) for all other experiments. Significance was indicated with * to ****, using the following intervals ("n. s." is "not significant"):

n. s. $P > 0.05$
* $P \leq 0.05$
** $P \leq 0.01$
*** $P \leq 0.001$
**** $P \leq 0.0001$

5. Results

5.1 Characterization of CHIKV Env pseudotyped vector particles

To have a system at hand that is suitable for focusing solely on the entry process of the Chikungunya virus (CHIKV), the usage of CHIKV envelope (Env) pseudotyped lentiviral vector particles (VPs) was established. VPs pseudotyped with different viral envelope proteins are a common tool used to study the entry mechanisms of the respective viruses (Cronin et al., 2005)). Furthermore, pseudotyped VPs often enable work under reduced safety conditions as compared to the wild-type virus (wt; e.g., for Chikungunya virus S2 instead of S3). For the production of pseudotyped VPs, 293T cells were transfected with two plasmids encoding the necessary genes for HIV-1 particle formation and genome reverse transcription/integration in transduced target cells. In addition, one plasmid containing a luciferase or green fluorescent protein (GFP) reporter gene, the HIV-1 packaging signal Ψ and the LTRs, and a plasmid carrying the genetic information for the respective envelope protein (CHIKV Env, Vesicular stomatitis virus glycoprotein (VSV-G), Gibbon ape leukemia virus transmembrane protein (GaLV TM), or Lymphocytic Choriomeningitis Virus envelope protein (LCMV Env)) were transfected. The supernatant of the transfected cells contained the produced vector particles and could be used for transduction of different cell lines.

To investigate whether the transfected VP producer cells effectively expressed the CHIKV envelope proteins, an SDS-PAGE/Western blot analysis using the lysates of 293T cells transfected with the four plasmids mentioned above was performed. Additionally, the supernatants expected to contain the CHIKV Env pseudotyped VPs were ultracentrifuged and also analyzed by Western blot. The CHIKV envelope protein E2 was detected in cell lysates and concentrated supernatants via an E2 specific antibody. Figure 18 A reveals that CHIKV Env protein E2, with an expected molecular mass of 56 kDa, was indeed expressed by the VP producer cells. Furthermore, E2 was effectively incorporated into the VPs, as it could be detected together with the HIV-1 structural protein p24 in the ultracentrifuged supernatant of the VP producing cells (Figure 18 B).

A)

B)
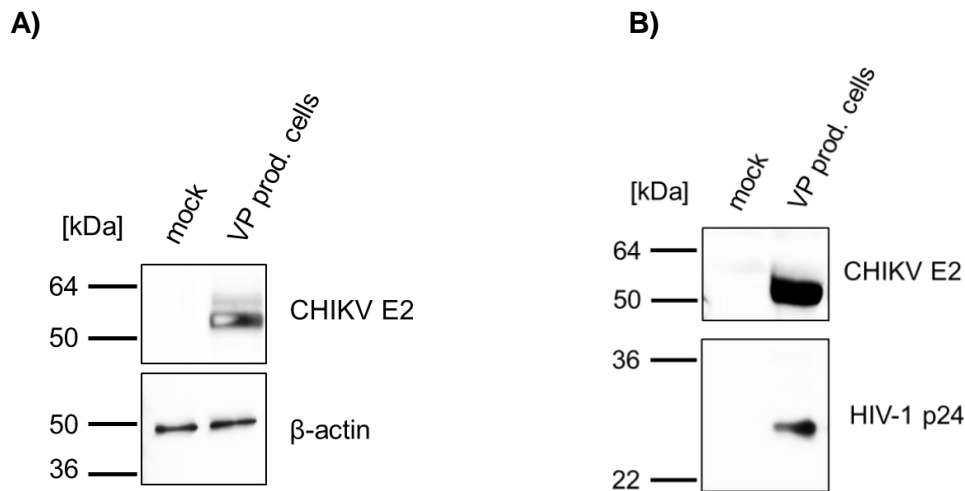
Figure 18: Validation of CHIKV E2 expression and VP formation in transfected 293T cells.
293T cells were seeded in 10 cm dishes and transfected with the plasmids pMDLg/pRRE, pRSVrev, pRRLsinCMV-GFPpre, and pIRES2-EGFP-CHIKV E3-E1. After 48 hours of incubation, cell lysates were prepared from the cells and the supernatants were ultracentrifuged. The pellet was resuspended in a small volume of PBS and an SDS-PAGE/Western blot was performed with cell lysates (A) and concentrated supernatants (B). For detection, primary antibodies specific for the respective protein and secondary antibodies (against IgG of the primary antibodies) coupled to HRP were used. β-actin and HIV-1 p24 were used as loading controls.

To assess whether the CHIKV Env pseudotyped VPs cell entry is dependent on acidic pH, which is the case for the wild-type virus, Huh7 cells were transduced in the presence of different amounts of chloroquine and analyzed by flow cytometry of the transduced GFP gene. Chloroquine is a chemical compound that prevents acidification of endosomes. As it can be seen in Figure 19 A, transduction with VSV-G pseudotyped VPs (as a positive control) was inhibited with increasing amounts of chloroquine in the medium. This was not the case for the negative control (GaLV TM pseudotyped VPs; Figure 19 B), but was observed again for the CHIKV Env pseudotyped VPs (Figure 19 C). Thus, the CHIKV Env pseudotyped VPs required an acidic endosomal pH for efficient cell entry and revealed similar properties to the CHIKV wild-type entry in that respect.

A)

B)

C)
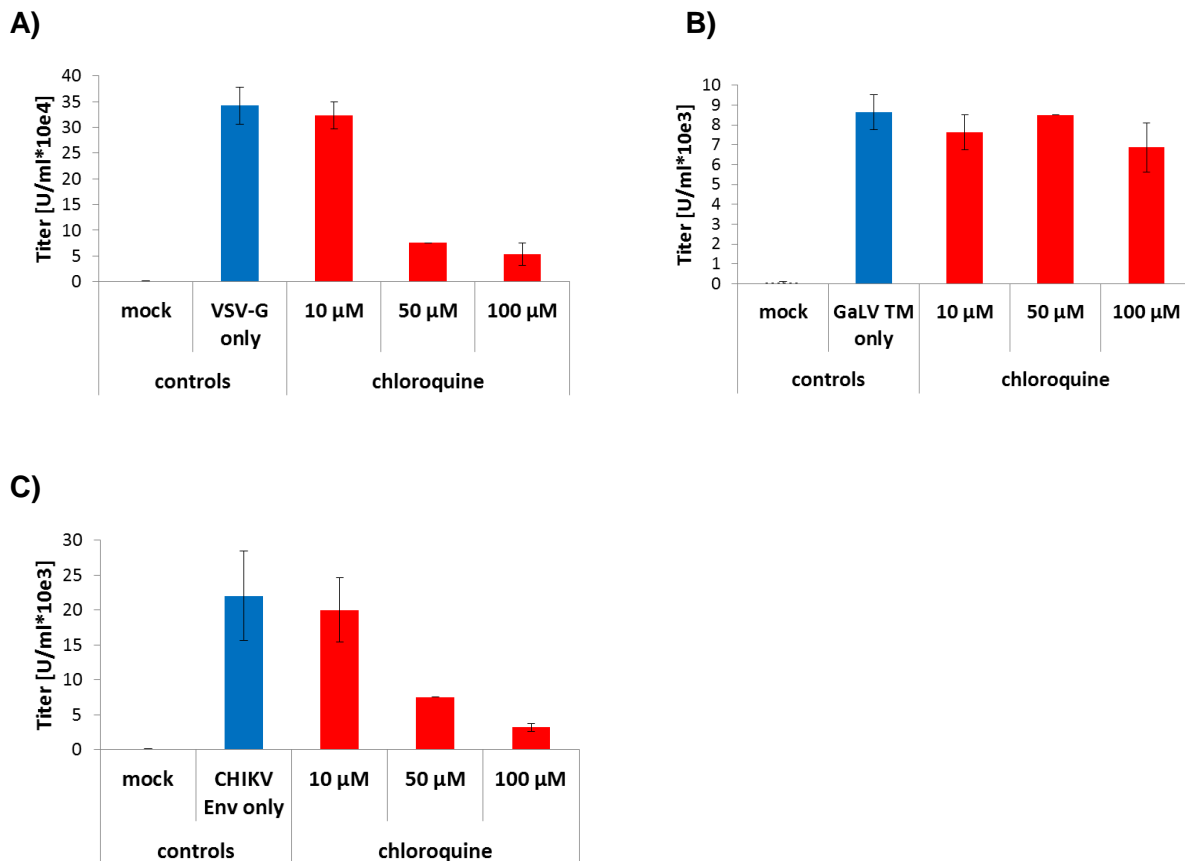
Figure 19: Transduction of CHIKV Env pseudotyped VPs in the presence of chloroquine.
Huh7 cells were transduced with CHIKV Env pseudotyped VPs carrying a *GFP* gene in the presence of the indicated amounts of chloroquine. The cells were analyzed to obtain the proportion of transduced GFP-positive cells 72 hours after transduction via flow cytometry. VSV-G (A) and GaLV TM (B) pseudotyped VPs served as controls for the CHIKV Env (C) pseudotyped VPs. The experiment was performed in three independent repeats.

Wild-type CHIKV infects a wide variety of epithelial and endothelial cells from different vertebrate species (and mosquitoes), but does not infect hematopoietic cells (e.g., B and T cells). To examine if the CHIKV Env pseudotyped VPs transduce the same cell spectrum as the wild-type CHIKV infects, different mammalian cell lines of epithelial, endothelial, and hematopoietic origin were incubated in the presence of pseudotyped VPs and analyzed three days later via flow cytometry for GFP-positive cells. Transduction of cells with VSV-G VPs served as a control. Figure 20 displays that all epithelial and endothelial cell lines were transducable by CHIKV Env pseudotyped VPs, which was not the case for the hematopoietic cell lines, where transduction rates were close to 0.0%. However, there were also major differences in the transduction rates among the endo-/epithelial cell lines. For example, Huh7 and A549 cells were highly transducable in comparison to VSV-G VPs. In contrast to that, HepG2 or Renca cells had much lower transduction rates. Thus, the CHIKV Env pseudotyped VPs resembled the wild-type virus regarding the spectrum of transducable and infectable cells. In general, titers of CHIKV Env were about 10-fold lower than VSV-G VPs.

All together it could be shown that the CHIKV envelope proteins are efficiently incorporated into VPs and have the same entry properties as the wild-type CHIKV regarding pH dependence and range of transducable/infectable cells. They were then used as the basis to study the CHIKV cell entry in detail.
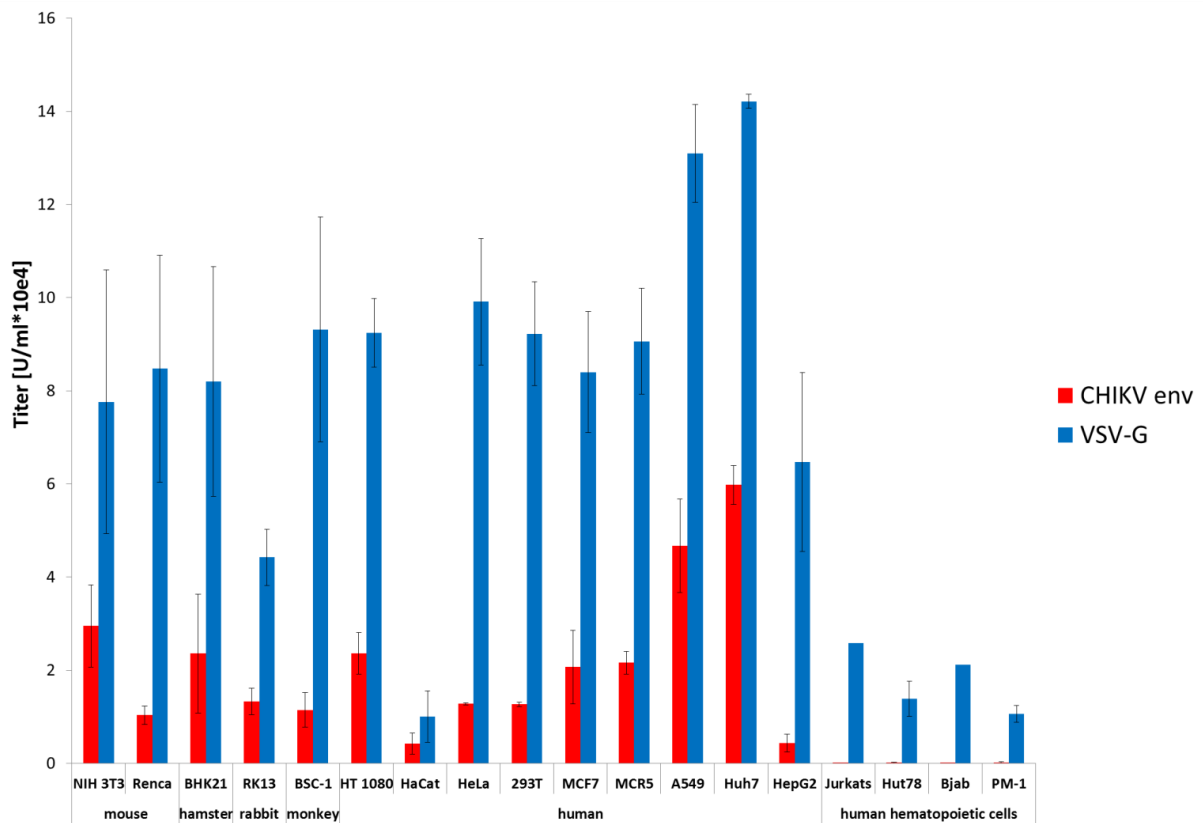
Figure 20: Transduction of different mammalian cell lines with CHIKV Env pseudotyped VPs.
Different cell lines of mammalian origin (human cells: hematopoietic and non-hematopoietic) were transduced with the same volume and batch of CHIKV Env pseudotyped VPs. The transduction rate (GFP positive cells) was measured 72 hours later via flow cytometry and the titers were calculated. VSV-G pseudotyped VPs were used as a control. The experiment was done in three independent replicates.

5.2   CHIKV vaccine development

5.2.1   Design and production of the constructs for protein vaccination

Many vaccination strategies have been studied in animal models for CHIKV (see 2.2.2.1). However, no one (current state of literature) so far has tried to determine the minimal requirements for an effective CHIKV vaccine including antigens of the E2 envelope protein, thus which parts of it are really necessary to induce an effective neutralizing immune response. E2 covers the whole surface of the viral particle and is therefore the main target for neutralizing antibodies during an infection in humans (see 2.2.2.1). The goal was to develop a minimal vaccine that contains only the absolutely necessary parts to be effective. For this purpose, seven artificially derived CHIKV E2 envelope proteins were created. They were all based on three basic parts:

One part was a linear epitope reported to be the binding site for most of the early neutralizing antibodies humans develop during a CHIKV infection (Kam et al., 2012b). Because it consists of only twelve N-terminal amino acids of E2, this epitope was connected five times in series to enhance immunogenicity. The single parts were linked by glycine-serine linkers (Figure 21 A). The construct was called L for "linear epitope".

A)

B)
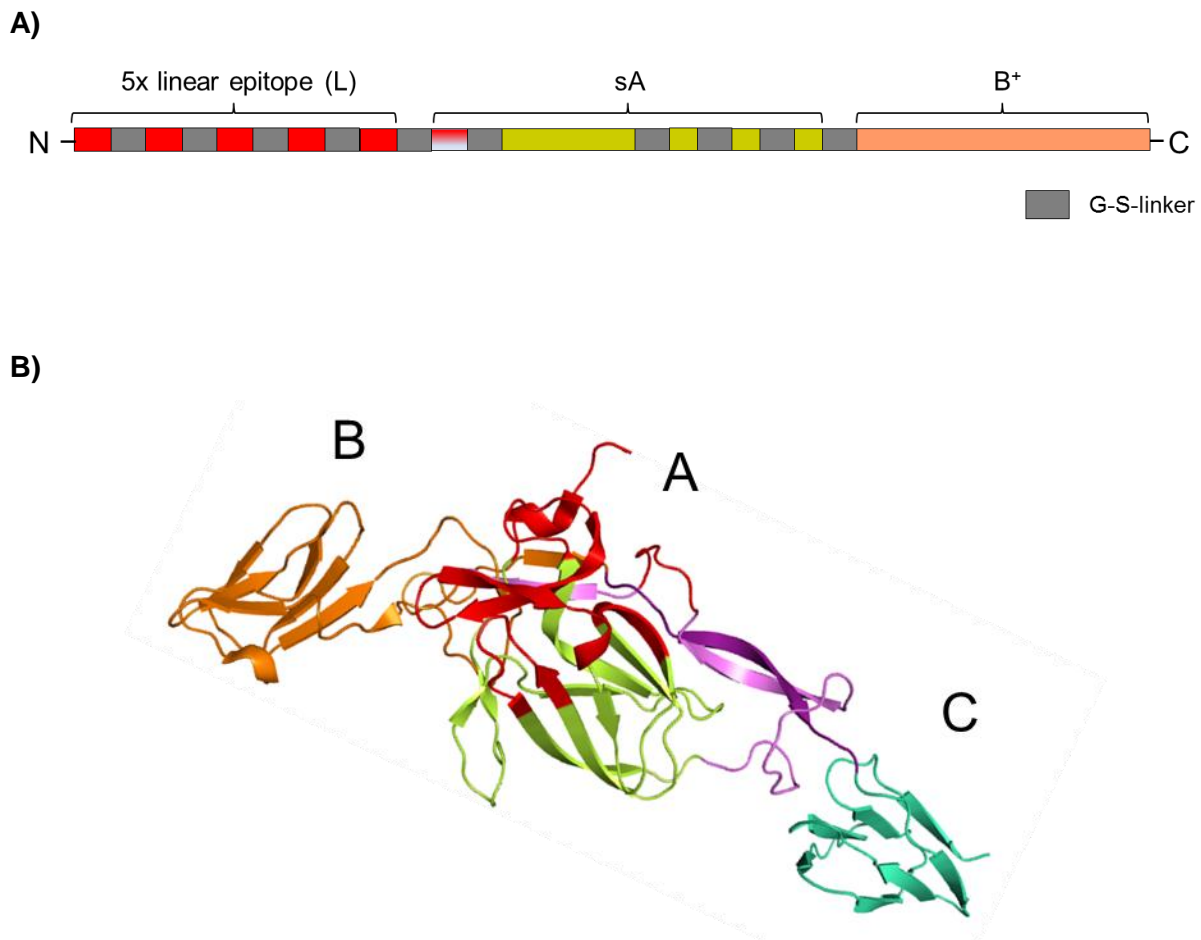
Figure 21: Representation of the CHIKV E2 regions chosen for vaccine design.
A) The linear epitope of E2 (amino acids 1-12, red) was linked via glycine-serine linkers (grey) and is present five times in the construct L. The construct surface exposed regions of domain **A** (red) contains five selected surface exposed regions of domain A (including one time construct L, red-white), and part of the β-ribbon connector, again linked by glycine-serine linkers (sA). For domain **B** plus another part of the β-ribbon connector (B[+], orange), the whole amino acid sequence was used for the vaccine. The construct LsAB[+], which contains all three constructs, is shown in this figure. B) The three-dimensional structure of CHIKV E2 with its three domains A, B, and C (A in yellow, β-ribbon connector (no domain) in violet, C in turquoise) is shown in ribbon style. The parts chosen for the vaccine constructs are labeled in red (sA, including L (amino acids 1-12)), and in orange (B[+]). Adapted from (Voss et al., 2010)

The second basic part was built up by selected surface exposed regions of E2 domain A and a part of the β-ribbon connector. The regions were selected on the basis of the 3D structure of the protein and known important antigenic regions from other Alphaviruses (Voss et al., 2010) (Figure 21 B). Again, the different regions were connected using glycine-serine linkers. The twelve N-terminal amino acids were also chosen to be part of this second part, this time only occurring once in the protein. The molecule was called sA for "**s**urface exposed regions of domain **A**" (Figure 21 A, B).

For the third part, the whole domain B and another part of the C-terminal from B followed by the β-ribbon connector was used. Because it was not only derived from domain B, but also from a part of the β-ribbon connector, it was named B$^+$ (see Figure 21 A, B). The amino acid sequences of all proteins are given in the appendix (see 10.2.1).

These three basic components were used as single molecules, but also combined in every combination that was possible, ending up with the seven constructs: LsAB$^+$ (see Figure 21 A), LsA, LB$^+$, sAB$^+$, sA, B$^+$, and L (see Figure 22). The corresponding genes were synthesized by GeneArt, sent in a vector, and cloned into the pET-15b vector to add an N-terminal polyhistidine-tag and for expression in the *E. coli* strain BL21-CodonPlus (DE3)-RIPL via the IPTG/lac operon system.
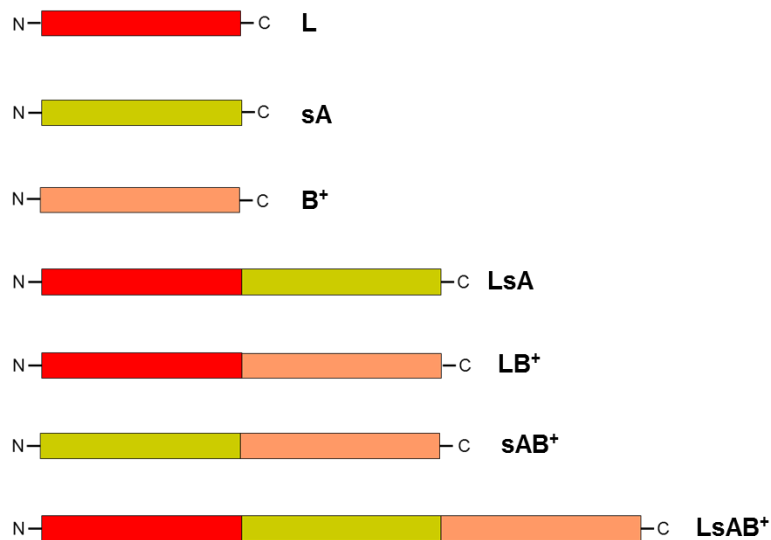
Figure 22: The seven different vaccine constructs in schematic representation.

The three constructs L (red), sA (yellow), and B$^+$ (orange) were used as single molecules for vaccinations and combined in every possible way to obtain the artificial CHIKV E2 derived proteins listed above.

The constructs L and sAB$^+$ were cloned from the GeneArt plasmid via *Nde*I and *Bam*HI (L was first modified as described in 4.1.9 and then directly cloned; for sAB$^+$ primers, see 4.1.8). The constructs sA, B$^+$, LB$^+$, LsA, and LsAB$^+$ were derived from the two synthesized genes via PCR and also cloned into pET-15b (already containing the L part for LB$^+$, LsA and LsAB$^+$) via *Nde*I and *Bam*HI. The sequence identities were verified by sequencing. The expressed proteins were purified from the *E. coli* pellets with Ni-NTA columns via ÄKTA HPLC under native conditions, dialyzed against PBS, and concentrated. The identity of the proteins was confirmed by mass spectrometry (data not shown). A coomassie-stained gel shows all the purified constructs (Figure 23). LsAB$^+$ should have an expected molecular mass of 30.7 kDa,

LsA of 20.7 kDa, LB$^+$ of 21.4 kDa, sAB$^+$ of 21.0 kDa, sA of 10.9 kDa, B$^+$ of 11.7 kDa, and L of 12.0 kDa, respectively. The gel revealed that all constructs (except sAB$^+$) ran at the expected size. An exception was the construct sAB$^+$, which should run at a height between Lsa and LB$^+$, and not slightly higher than LB$^+$. However, the molecular mass was also in this case roughly correct. The lower fat bands visible in the lane of LB$^+$ were identified by mass spectrometry as fragments of the purified protein (data not shown).

In summary all seven artificial CHIKV E2-derived proteins were expressed and could be purified successfully.
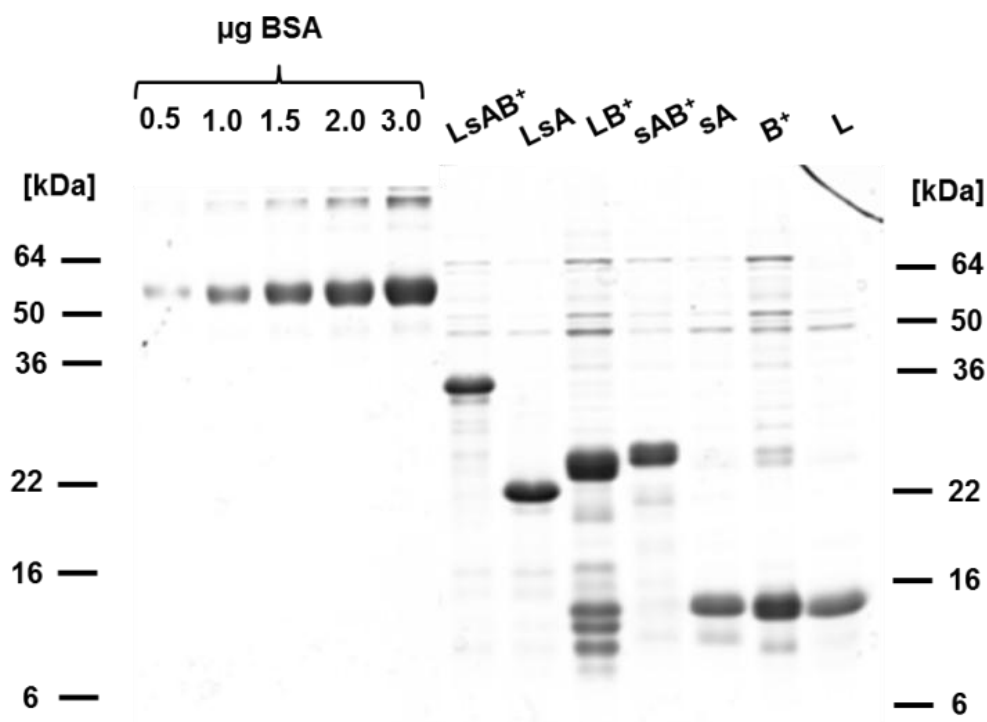
Figure 23: Expression and purification of the seven vaccine constructs.

The seven artificial E2 derived constructs were cloned into the pET-15b vector, expressed *in E.coli*, and purified natively via HPLC (Ni-NTA beads). Subsequently, they were dialyzed against PBS and concentrated. Afterwards, their concentration was adapted to about 1 µg/µl. Shown is an SDS-PAGE with subsequent coomassie staining of the purified proteins. A BSA concentration row was used for estimation of concentration (left side). The identity of the proteins was confirmed by mass spectrometry (data not shown).

5.2.2   Vaccination of mice and induction of neutralizing antibodies

To determine which of the designed protein constructs induces a neutralizing immune response *in vivo*, mice were vaccinated with the purified proteins. Three seven weeks old Balb/c mice (at the time of the first immunization) per construct were immunized subcutaneously into the neck with 100 µg of protein in PBS plus alum as an adjuvant (1:1 mixed with the protein) per mouse per immunization. Three control mice received only PBS plus alum. Each mouse was vaccinated three times: At time point 0, 3.5 weeks, and 7.5 weeks after the first immunization, respectively. Blood was collected before the first immunization, 3.5 weeks after the first immunization and 1 week after the second and third immunizations, respectively.

With the blood-derived mouse sera, a neutralization assay was performed to test if mice developed neutralizing antibodies upon vaccination with the different proteins. The assay was based on CHIKV Env pseudotyped VPs containing a lentiviral transfer gene coding for luciferase. The mouse sera were five times three-fold serially diluted (the final dilutions on the cells ranged from 1:60 to 1:4860) and mixed with the VPs. This mixture was added to 293T cells seeded the day before in a 384-well plate. VSV-G pseudotyped VPs were used as a control. The luciferase signal was detected after one day in a luminometer.

The measured relative light units, relative to the signal, obtained using VPs without serum added are displayed in Figure 48. When CHIKV Env VPs were used, the neutralizing activity (lower relative light unit values) was enhanced with a growing number of immunizations for the constructs LsAB$^+$, LsA, LB$^+$, sAB$^+$, and B$^+$ (Figure 48). In contrast, all curves generated from the sera of mice that received sA or L, and the VSV-G control VPs for all constructs, laid on one another, thus there was no significant difference between the signals (Figure 48). Figure 24 shows the final statistical evaluation of the curves from Figure 48. The areas under the curves (AUC), and the dilution at which the neutralization activity of the respective serum was 50% (NT$_{50}$), were determined using the program CombiStats$^{©}$. The AUC and the NT$_{50}$ values of the naïve sera (before the first immunization) were divided by the serum values after the third immunization. A value higher than one thus indicates neutralization activity of the respective serum. As observed in Figure 24 A, there were significant differences between the VSV-G control and the CHIKV Env VPs AUC values for the constructs LB$^+$, sAB$^+$ and B$^+$. The constructs LsAB$^+$ and LsA also induced some neutralizing antibodies in the mice. However, the differences between the VSV-G VPs controls were not significant. L and sA vaccinations did not result in neutralizing antibodies at all. Similar results were obtained from the NT$_{50}$ evaluation of the neutralization curves (Figure 24 B). Yet with this evaluation, only the values for sAB$^+$ and B$^+$ were significantly different from the controls. Sera obtained from mice that received the constructs LB$^+$, LsAB$^+$ and LsA showed some neutralizing activity, but

again without significant differences to the VSV-G controls. L and sA vaccinated mice showed no neutralizing activity in their sera.

In conclusion, B^+ was part of every construct that was able to induce a significant neutralizing antibody reaction. sAB^+ vaccination yielded the best neutralizing activities in both the AUC and the NT_{50} evaluation. In contrast to these results, no neutralization was observed for L and sA. One can conclude from this data that B^+ was necessary and sufficient to induce a neutralizing antibody activity in mice. The other basic vaccine components, L and sA, were not able to do so.

A)
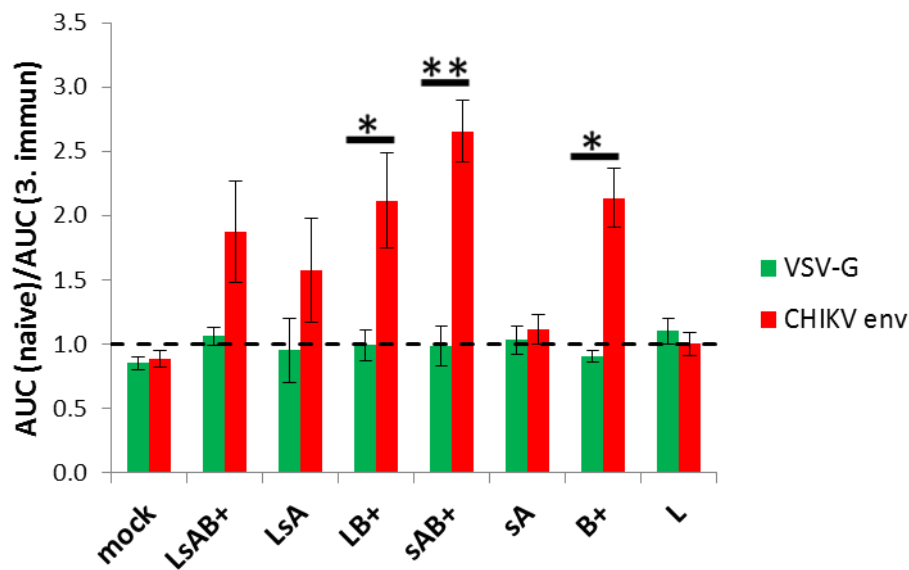
B)
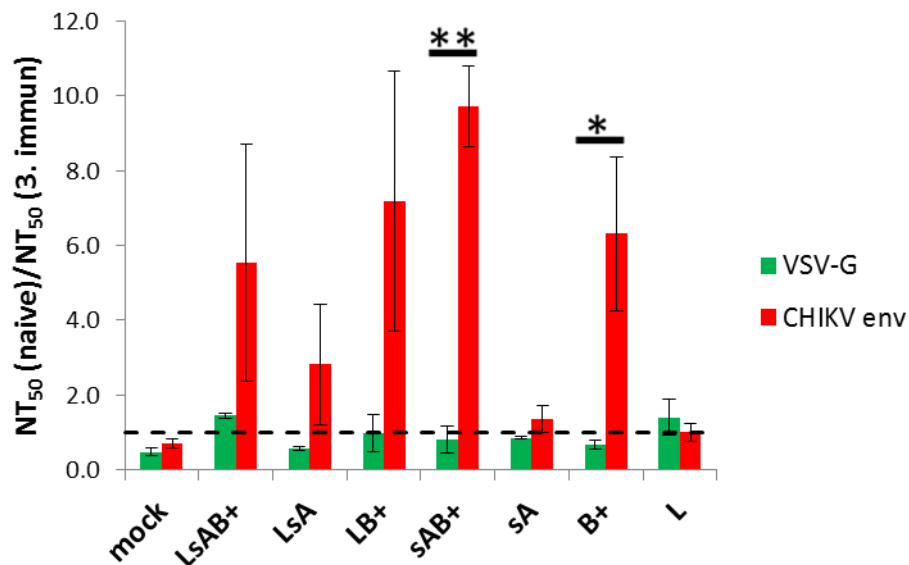
Figure 24: Neutralization assay with CHIKV Env VPs using mouse sera from vaccinated mice as potential inhibitors.

Mice (n=3 per construct) were vaccinated with the seven indicated constructs three times. Blood was collected directly before the first immunization, 3.5 weeks after the first immunization, and 1 week after the second and third immunizations, respectively. The sera were screened in a 384-well plate luciferase-based assay with CHIKV Env pseudotyped VPs for neutralizing activity. They were tested in five 3-fold serial dilutions, ranging from 1:60 to 1:4860. One day after transduction, the transduction rate was measured in a luminometer. The results are presented as area under the curve (A; AUC; curves of luciferase signals for different serum dilutions, see Figure 48) obtained from the curve of the naïve serum from a mouse divided by the AUC obtained from the curve of the serum from the same mouse after the third immunization, or as the NT_{50} values of the curves. * and ** indicate significant differences in AUC ratios of CHIKV Env VPs to those of VSV-G VPs. (B) Values higher than one reveal

neutralization (indicated by the dashed line). VSV-G pseudotyped VPs were used as controls. Shown are the results averaged for the AUC ratios of the mice receiving the same construct. The experiment was performed in three independent replicates. *, and ** indicate significant differences in NT_{50} ratios of CHIKV Env VPs to those of VSV-G VPs.

5.2.3   Humoral immune response in vaccinated mice

Considering the results of the luciferase screening (see 5.2.2), the next goal was to determine if the lack of inducing neutralizing antibodies by some constructs was due to a general lack of inducing antibodies at all.

All proteins used for vaccination were separated by SDS-PAGE and immobilized on a membrane. An irrelevant protein, which had not been used for vaccination, the human endogenous retrovirus K (HERV-K) UTPase (14.8 kDa in size), served as the negative control. After cutting the membranes into stripes, every mouse serum (the ones before immunization and the ones after the third immunization) was incubated with the corresponding protein used for vaccination on the membrane. An anti-His tag antibody served as a positive control.

The results are given in Figure 25. No specific signal was detected for any of the control or naïve mouse sera (Figure 25 A-H). Additionally, only weak or wrong-sized bands were detected regarding the irrelevant protein construct on the membranes, although the positive control antibody revealed binding at the expected size on these membranes (Figure 25 A-H). In contrast to that, all the sera obtained from the mice after the third immunizations except one (construct sA, mouse 3, see Figure 25 F) recognized a protein at the respective expected size (see 5.2.1). The signal was rather weak for some sera (LsAB⁺ mouse 3, LsA mouse 3, sAB⁺ mouse 3, sA mouse 1, L mice 2 and 3; see Figure 25 B, C, E, F and H, respectively). However, a prominent band was detected for all the other sera and at least one mouse per construct developed a high amount of specific protein binding antibodies upon immunization (Figure 25 B-H).

One can conclude from this data that a lack of induction of antibodies binding to the immunogen was not the reason for the poor neutralizing activity of some mouse sera.

A)

mock sera

(LsAB⁺ blotted)

mock sera

(HERV-K UTPase blotted)

B)

LsAB⁺ sera

(LsAB⁺ blotted)

LsAB⁺ sera

(HERV-K UTPase blotted)

C)

LsA sera

(LsA blotted)

LsA sera

(HERV-K UTPase blotted)

D)

LB$^+$ sera

(LB$^+$ blotted)

LB$^+$ sera
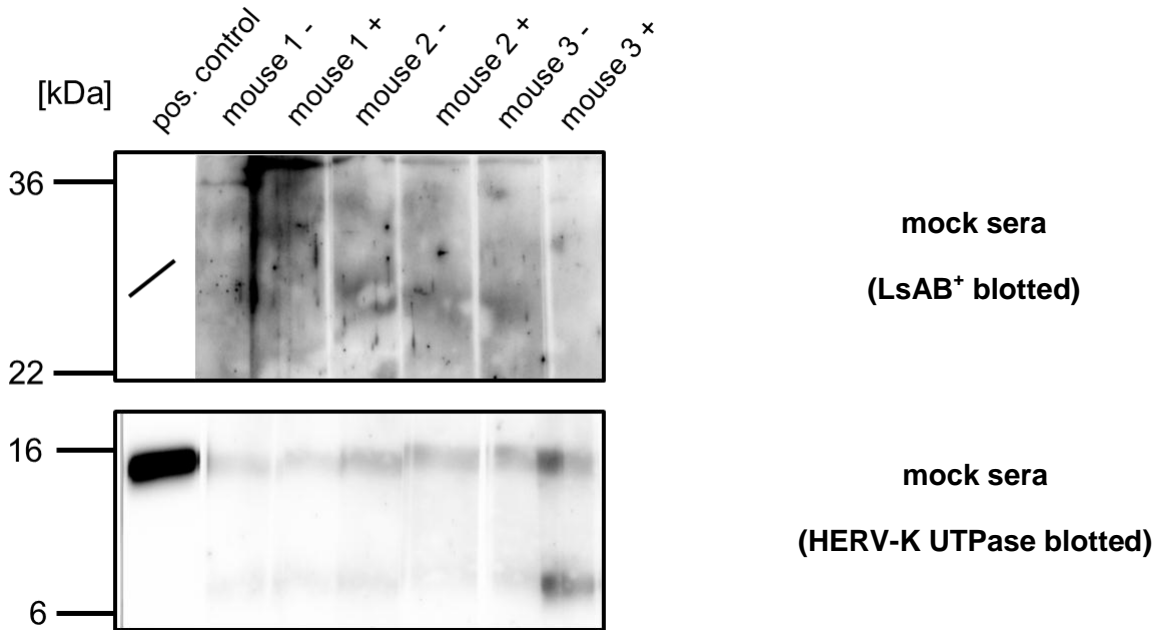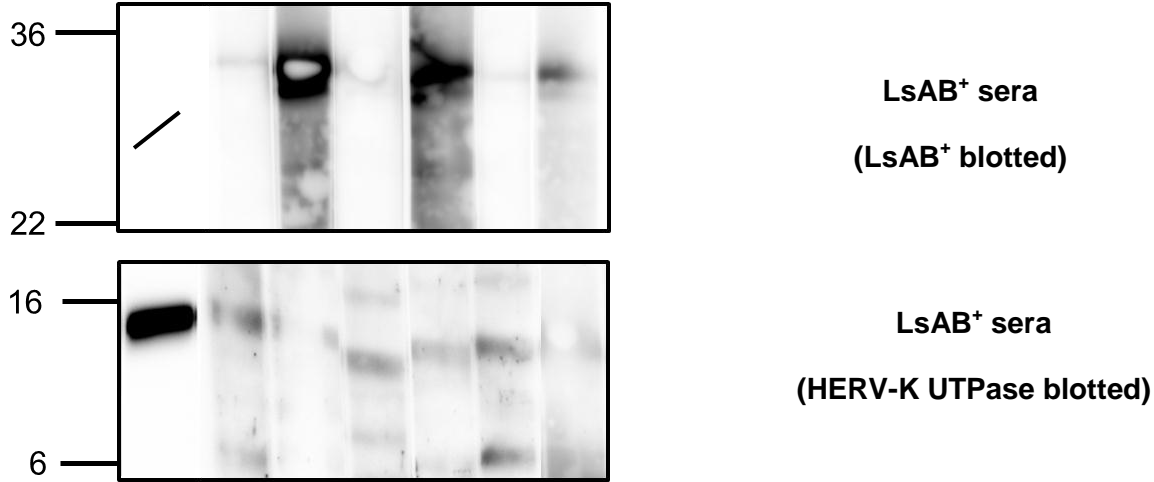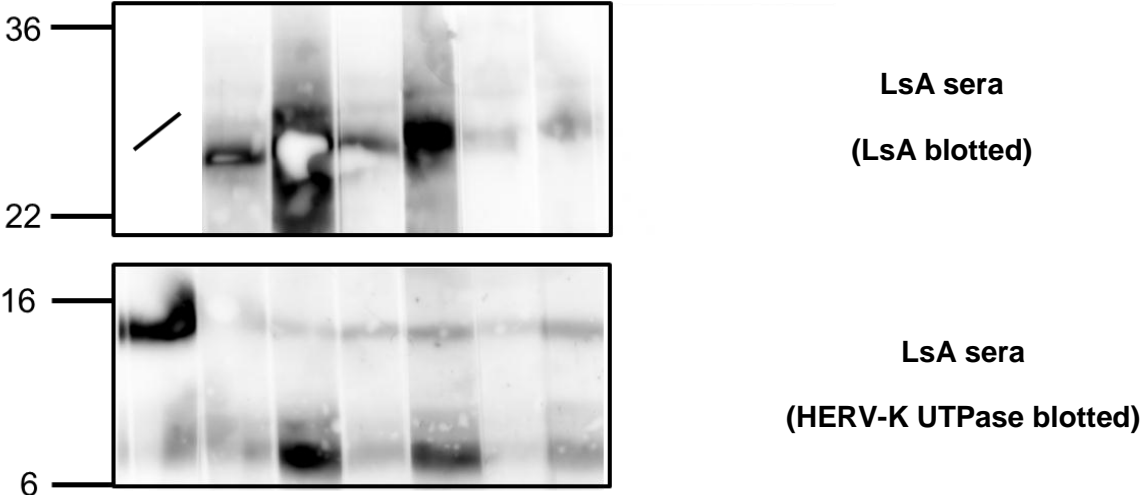
(HERV-K UTPase blotted)
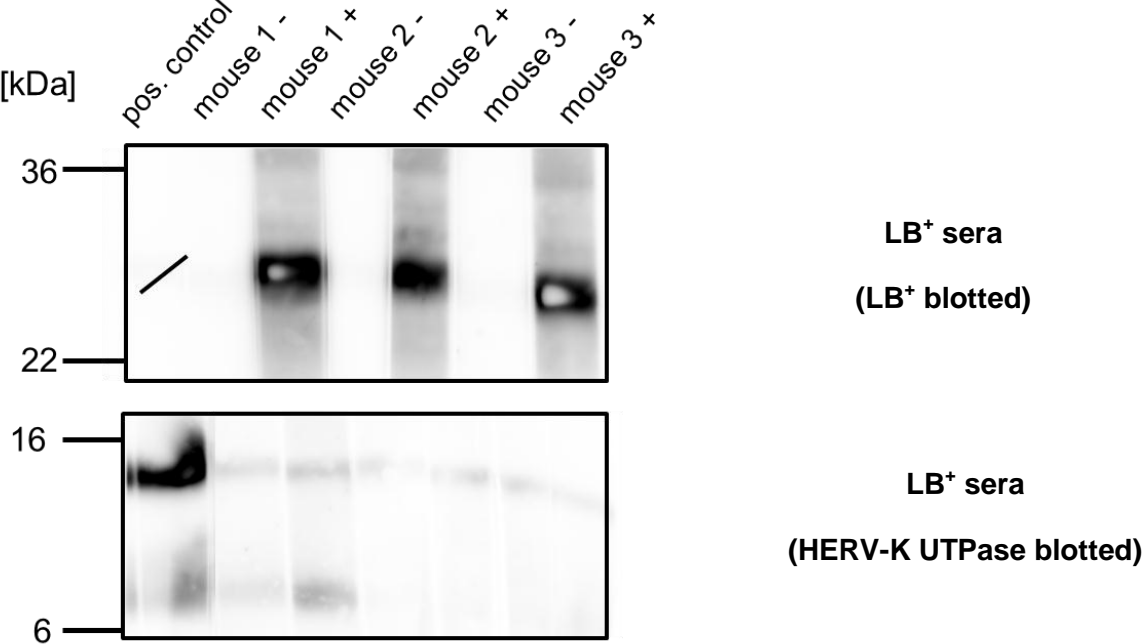
E)
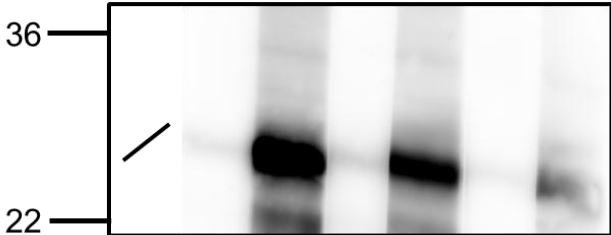
sAB⁺ sera

(sAB⁺ blotted)
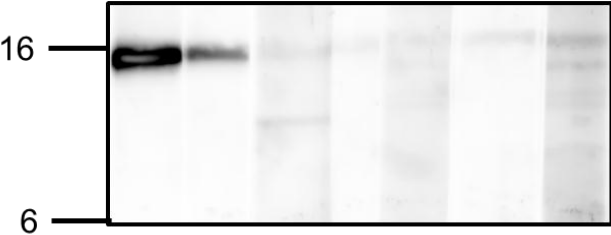
sAB⁺ sera

(HERV-K UTPase blotted)

F)
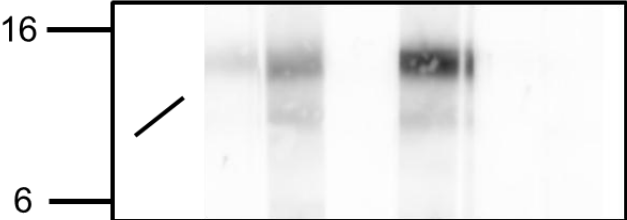
sA sera

(sA blotted)
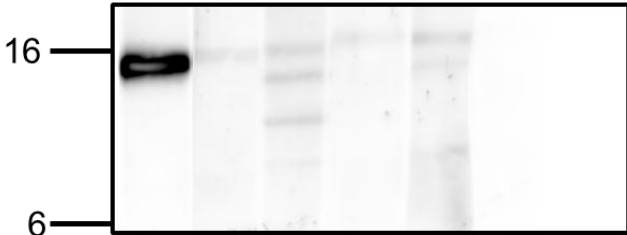
sA sera

(HERV-K UTPase blotted)

G)
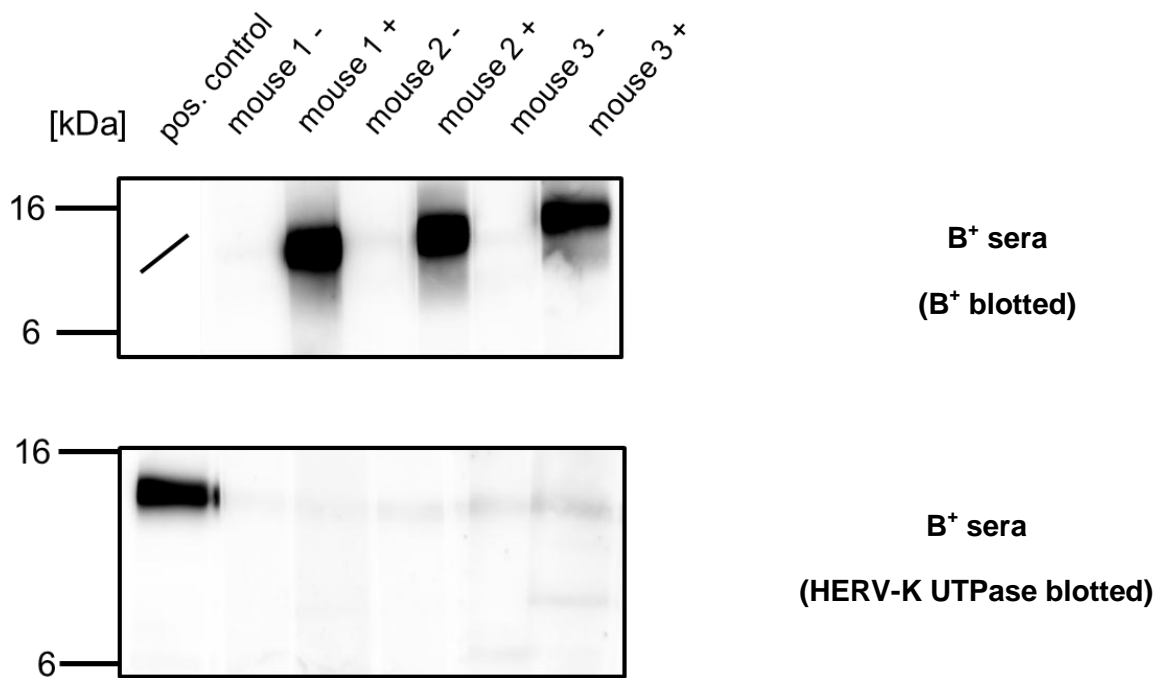
H)
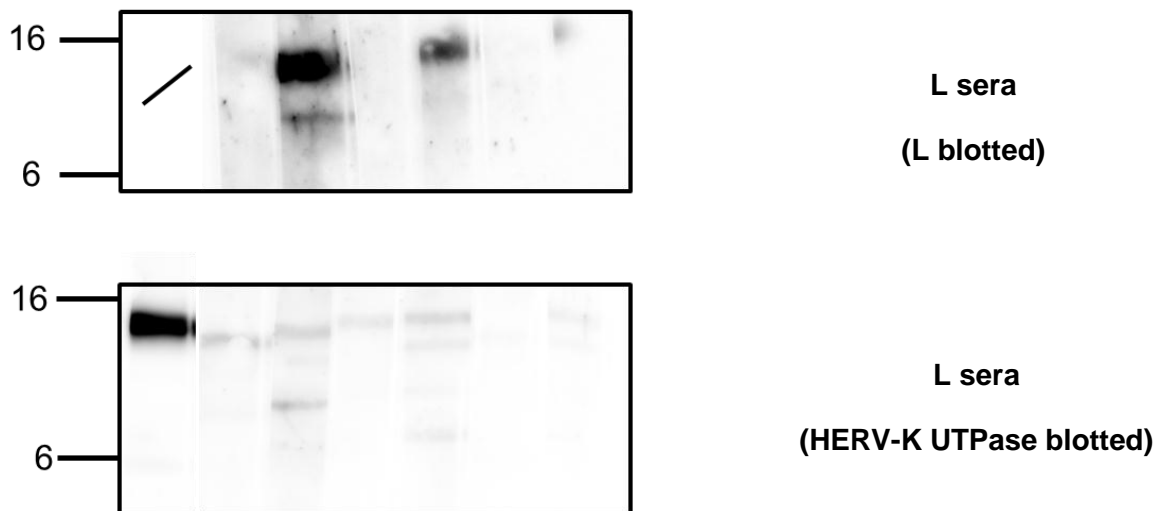
Figure 25: Binding of antibodies from sera of vaccinated mice to the proteins the mice had been vaccinated with.

The seven proteins LsAB$^+$ (A (with mock sera), B (with sera of mice vaccinated with LsAB$^+$)), LsA (C), LsB$^+$ (D), sAB$^+$ (E), sA (F), B$^+$ (G), and L (H) used for vaccination were separated by SDS-PAGE (0.1 µg purified protein/lane) and subsequently blotted onto a membrane (upper panel). The membrane was cut into 5 mm stripes and incubated with the sera (naïve (-) and after 3.immunizations (+), 1:100) obtained from the mice (n=3) that received the respective construct for vaccination. The sera from the mock mice were incubated with membrane stripes containing the protein LsAB$^+$. The irrelevant recombinant protein HERV-K UTPase in which the mice had not been vaccinated against before was used as a negative control (lower panel). One strip of every blot of the negative control was also incubated with an anti-His antibody as a loading control. An HRP-coupled anti-mouse antibody was used for detection.

5.2.4 Generation of a recombinant Modified Vaccinia virus Ankara (MVA) encoding the construct sAB⁺

To further improve the CHIKV vaccine, a Modified Vaccinia virus Ankara (MVA) containing the gene encoding the most successful protein in the protein vaccinations, sAB⁺, was developed. MVA is an orthopox virus strain, which was attenuated by serial passages on chicken embryo fibroblasts (see 2.2.2.2). MVA is not able to form infectious particles in primate cells anymore (Sutter and Moss, 1992). However, protein production is still possible. Any transgene of choice can be inserted into the deletions of the MVA genome under the control of a poxviral promoter. Human cells infected with this virus will, alongside with other viral proteins, express the transgene of choice but do not produce infectious particles. Thus, MVA is a useful "adjuvant" for a vaccination and has already been used as the basis of several vaccines in a number of clinical studies (Sutter and Staib, 2003).

To obtain a recombinant MVA encoding CHIKV E2 genes, first the sAB⁺ gene was cloned into the pSecTag2 B vector to add an N-terminal secretion signal, a C-terminal myc- and a polyhistidine-tag. Secretion of sAB⁺ by infected cells might improve immunogenicity of the protein. The synthesized gene (GeneArt) *sAB⁺* was cut out with *Sfi*I and *Apa*I and inserted into pSecTag2 B. Afterwards, it was cloned into the MVA expression plasmid pIII-pmH5 containing the strong early/late poxviral promoter pmH5. For this gene insertion, the plasmid's *Bam*HI site was blunted via T4-DNA polymerase. The *sAB⁺* gene was excised from the pSecTag2 B vector by *Nhe*I and *Pme*I and subsequently blunted as well. Ligation resulted in the MVA vector plasmid pIII-CHIKV-sAB⁺ (Figure 26).
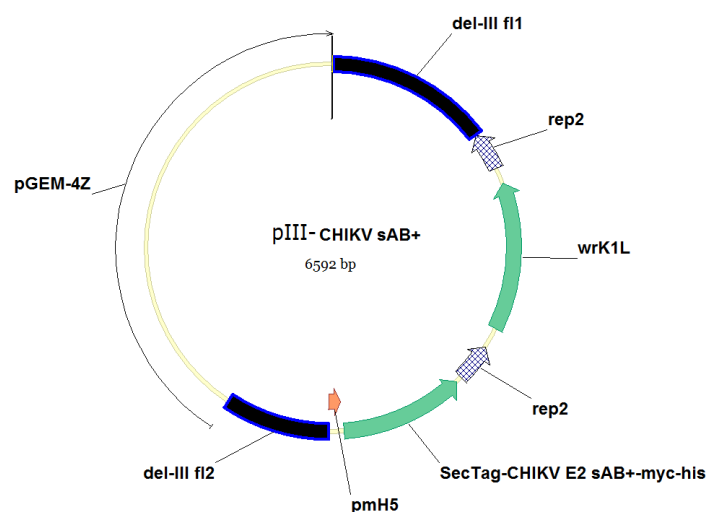
Figure 26: Schematic diagram of pIII-CHIKV-sAB⁺.
The plasmid pIII-CHIKV-sAB⁺ is shown in detail. The flanks 5' and 3' of the expression cassette with *sAB⁺* (under control of the pmH5 promoter) and *K1L* are named "del-III fl1" and "del-III fl2". The repetitive sequences surrounding *K1L* are called "rep2". The plasmid backbone is designated as pGEM-4Z.

To confirm correct expression and secretion of the construct under control of the pmH5 promoter, 293T cells were infected with wild-type MVA and in parallel transfected with pIII-CHIKV-sAB$^+$. The pmH5 promoter is only recognized by the MVA transcription machinery, which must be provided by infection with MVA in *trans*. The supernatants of the infected/transfected cells were collected and sterile filtered 24 hours post-infection. Cells were lysed and both supernatants and cell lysates were analyzed via SDS-PAGE/Western blot. Figure 27 shows that a signal could be detected at the expected protein size (24.1 kDa and 21.4 kDa with and without signal peptide, respectively) in the cell lysates. There was also a signal visible in the supernatants showing the correct molecular mass (21.4 kDa without signal peptide for secretion). However, the signal consisted of a double band, indicating that there was also sAB$^+$ with signal peptide in the supernatant. In the mock infected and only wild-type MVA infected cells, there were no bands detected. Thus, sAB$^+$ is expressed in and secreted from infected/transfected 293T cells under control of the pmH5 poxviral promoter.
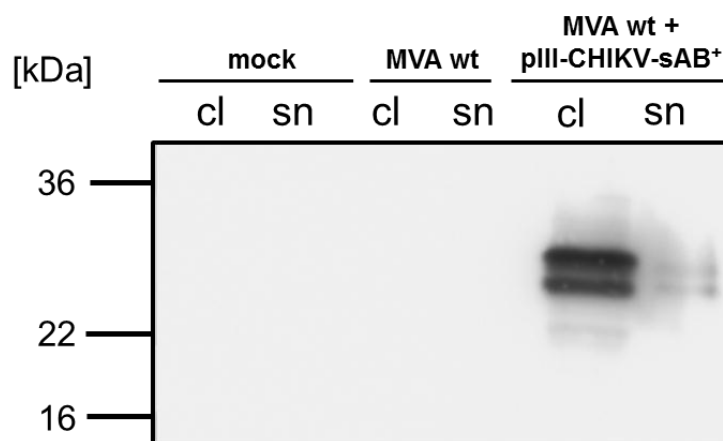
Figure 27: SDS-PAGE/Western blot of cells infected/transfected with pIII-CHIKV-sAB$^+$/MVA wt.
293T cells were seeded in a 6-well plate, infected with MVA wt (MOI 5) and one hour later transfected with 2 µg pIII-CHIKV-sAB$^+$. Cell lysates (cl) were prepared 24 hours later and the supernatants (sn) were additionally collected. Both were analyzed by SDS-PAGE with subsequent Western blot and detected using an anti-myc antibody as the primary antibody and an anti-mouse HRP conjugate as the secondary antibody followed by ECL detection. Mock infected and only MVA wt infected cells served as controls.

To integrate the *sAB$^+$* gene into the MVA genome, cells (this time BHK-21 cells) were infected/transfected at the same time with the above mentioned virus and plasmid. The plasmid contains the 5' and 3' ends from the transgene insertion region sequences that are homologous to the 5' and 3' regions that flank the respective deletion in the MVA genome (see Figure 26). Thus, via homologous recombination, the transgene (plus the host range

gene *K1L*, which is also included in the plasmid's expression cassette between the homologous flank regions) is inserted into the MVA genome during infection/transfection. To get rid of non-recombinant wild-type virus where the homologous recombination did not take place, the virus mixture was passaged on RK13 cells. MVA is only able to grow on this rabbit cell line if its genome contains *K1L*, which is therefore a selection marker for viruses that contain the transgene of choice, sAB⁺. After several plaque passages on RK13 cells of selected single clones, there was no wild-type MVA detectable anymore (detected by PCR, data not shown). After the selection procedure, the presence of *K1L* was not necessary anymore. The recombinant MVA-CHIKV-sAB⁺ was passaged on permissive BHK-21 cells several times (where it does not need *K1L*) to remove *K1L* from the genome. It is surrounded by repetitive sequences to facilitate its recombination out of the MVA genome upon release of the selection pressure on it.

The detailed characterization of the recombinant MVA-CHIKV-sAB⁺ is described in the following chapter.

5.2.5   Characterization of recombinant MVA-CHIKV-sAB⁺

The presence of *sAB*⁺ and the absence of *K1L* in the MVA genome were confirmed after a bulk production of the single clone-derived recombinant virus in BHK-21 cells and subsequent purification. PCR analysis was performed with genomic MVA DNA isolated from infected cells. Figure 28 A shows the results for primers surrounding the deletion used to integrate the transgene (del III) and for primers amplifying *C7L* (which is needed in the MVA genome for efficient late protein expression and found to be frequently deleted during virus passaging, see 4.2.4.1.5). It was observed for the deletion-PCR that there is a strong signal at about 800 bp for wild-type MVA infected cells, at about 3000 bp for the control plasmid pIII-CHIKV-sAB⁺, and at about 1700 bp for the MVA-CHIKV-sAB⁺ infected cells. The band for the wild-type virus is the lowest (800 bp), because here neither *K1L* nor *sAB*⁺ are present. In the plasmid pIII-CHIKV-sAB⁺, both *K1L* and *sAB*⁺ are included, which results in a band of 3000 bp. In MVA-CHIKV-sAB⁺, sAB⁺ should be present and *K1L* should not be, resulting, as observed, in a "medium" band of 1700 bp. These results exhibit the presence of *sAB*⁺ and the absence of *K1L* in the recombinant MVA-CHIKV-sAB⁺.

For the *C7L* PCR there was a signal at approx. 450 bp in both the wild-type virus infected cells and in the MVA-CHIKV-sAB⁺ samples, indicating the presence of this gene in wild-type virus and MVA-CHIKV-sAB⁺.

In Figure 28 B, which displays the results of the *K1L* and of the transgene, *sAB*$^+$, PCR, a prominent band *(K1L* PCR) can be seen in the lane with the control plasmid pIII-CHIKV-sAB$^+$. In all other lanes, there are weak identical bands and additional intensive primer signals below.

These detected signals indicate that *K1L* is only present in the plasmid control and nowhere else. The weak bands in the other samples are most likely due to DNA contamination, as the negative controls also show the same weak signal and the bands of unused primers illustrate non-efficient amplification due to small template amounts. Additionally, the signals from the deletion PCR (see Figure 28 A) indicate the absence of *K1L* in all samples but the plasmid control.

The PCR amplifying the transgene revealed a specific band only for the plasmid control and for the MVA-CHIKV-sAB$^+$ infected cells and thus showed the presence of *sAB*$^+$ in the plasmid control and in the recombinant MVA-CHIKV-sAB$^+$. The bands in the MVA-wt sample were unspecific because of their incorrect size. Summarizing the obtained data, one can conclude that the generated recombinant MVA-CHIKV-sAB$^+$ contained the poxviral *C7L* gene for efficient late expression, along with the transgene *sAB*$^+$ itself, and it is devoid of the selection marker *K1L*.

A)
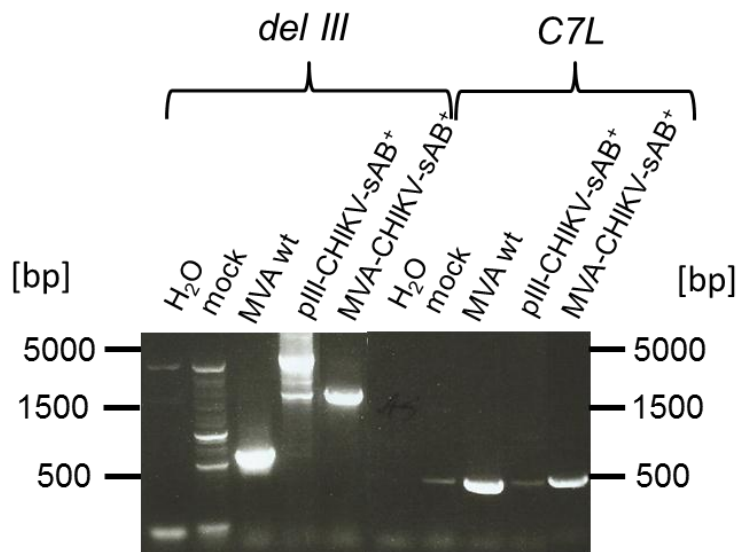
B)
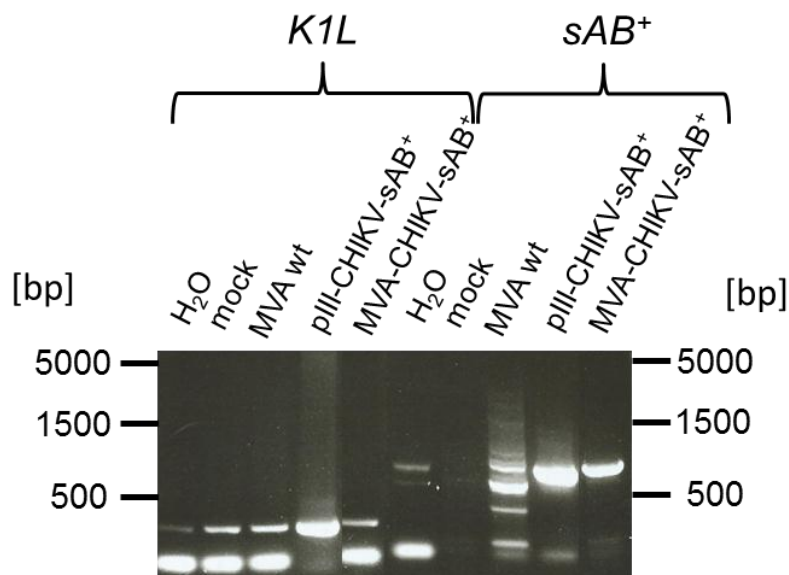
Figure 28: Validation of the correct genetic organization of MVA-CHIKV-sAB$^+$.
BHK-21 cells were seeded in 6-well plates, and infected with MVA-CHIKV-sAB$^+$ (MOI 0.1). 72 hours later, the genomic DNA of the cells was isolated. It was used as a template in a PCR with the appropriate primers for del III and C7L (A), and for K1L and the sAB$^+$ transgene (B). H$_2$O, the DNA of mock- and MVA wt-infected cells, respectively, and the plasmid DNA pIII-CHIKV-sAB$^+$ were used as controls. The PCR products were loaded onto an agarose gel, the DNA was stained, and the detection was carried out using UV light.

To confirm not only the presence of the sAB$^+$ gene in MVA-CHIKV-sAB$^+$ infected cells, but also expression and secretion of the respective protein, an SDS-PAGE/Western blot with cell lysates and supernatants from MVA-CHIKV-sAB$^+$ infected BHK-21 cells was performed. The samples from the infection/transfection of 293T cells (see Figure 27) were used as a positive control. A signal was visible in the cell lysate (Figure 29 A) and supernatant (Figure 29 B) of MVA-CHIKV-sAB$^+$ infected cells and it was identical to the lower band of the positive control (in cell lysates) and to the double band in the positive control (in supernatants), respectively. Thus, recombinant MVA-CHIKV-sAB$^+$ infected BHK-21 cells expressed and secreted the sAB$^+$ protein.
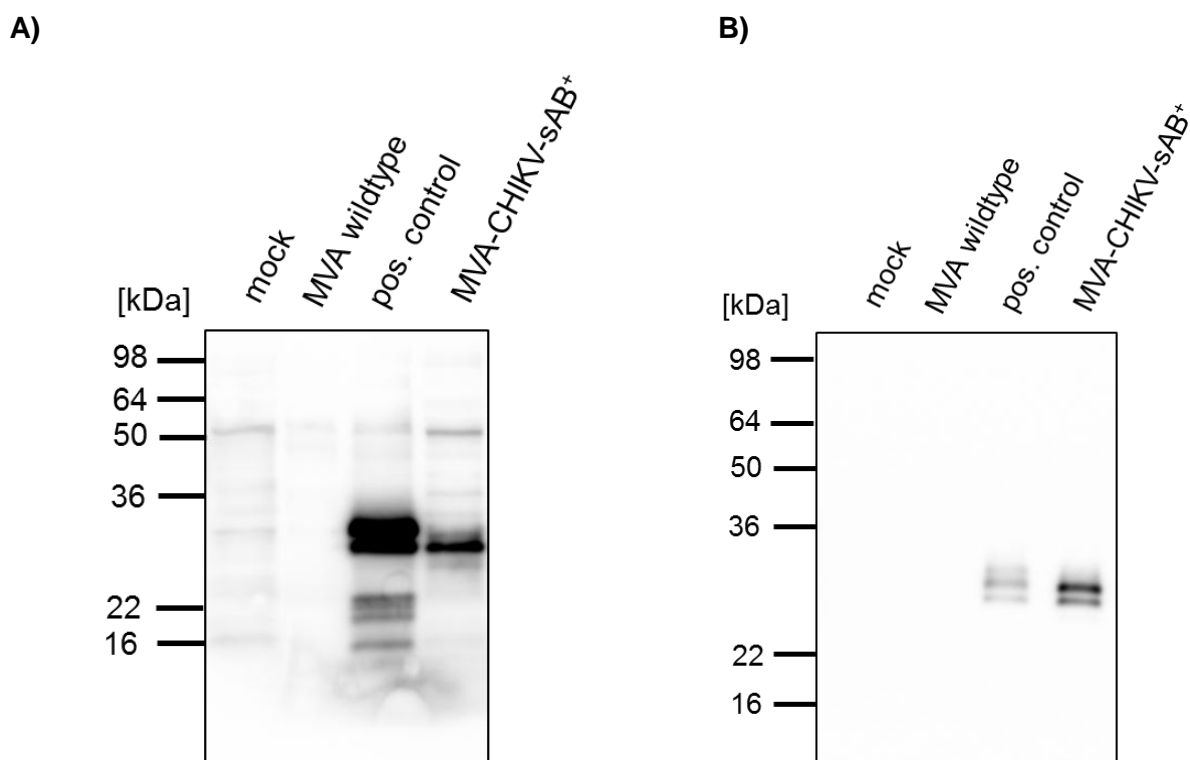
Figure 29: Presence of sAB$^+$ in the cell lysates and supernatants of MVA-CHIK-sAB$^+$ infected cells.
BHK-21 cells were seeded in 6-well plates and infected with MVA-CHIKV-sAB$^+$ (MOI 0.1). 72 hours later, cells were lysed (A) and the supernatants (B) were collected and used to perform an SDS-PAGE/Western blot. sAB$^+$ was detected via an anti-myc antibody and a secondary anti-mouse HRP antibody followed by ECL detection. MVA wt infected cells and the cells from the infection/transfection (Figure 27) were used as controls.

To rule out the possibility that the recombinant MVA had regained the ability to grow in primate and thus human cells via acquisition of the transgene, the growth kinetics of MVA-CHIKV-sAB$^+$ in DF-1 cells (chicken), in BHK-21 cells (hamster), and in HeLa cells (human) were observed. Figure 30 points out that the wild-type virus (Figure 30 A) was only to a very limited extent able to grow in human cells, but showed strong amplification in the DF-1 and

BHK-21 cell lines. The recombinant MVA-CHIKV-sAB$^+$ (Figure 30 B) showed comparable growth kinetics in these non-primate cell lines, but no replication in the human HeLa cell line. Hence, the insertion of the *sAB$^+$* gene into the MVA genome did not interfere with its attenuated phenotype.

A)
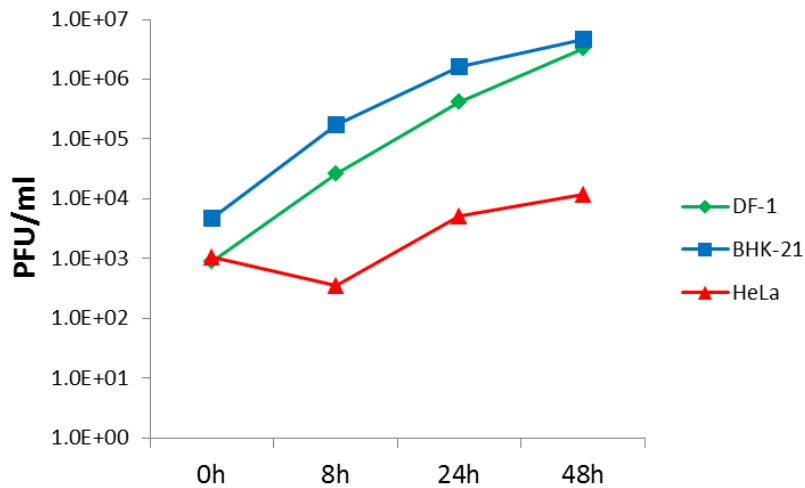
B)
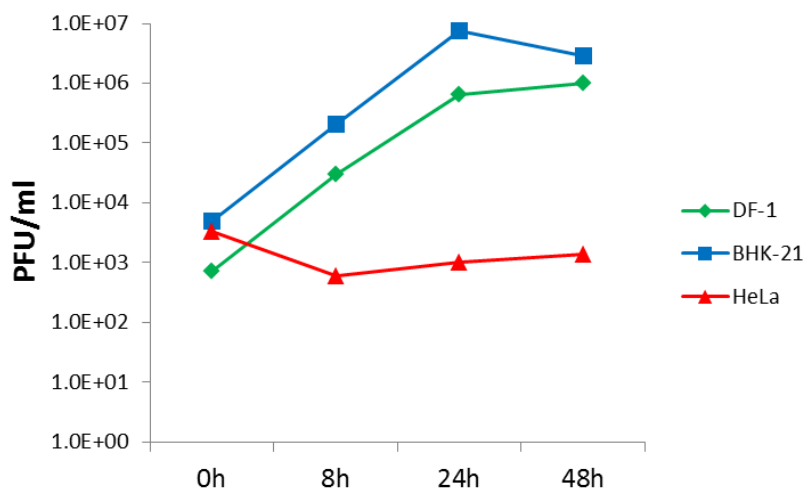
Figure 30: Growth analysis of MVA-CHIKV-sAB$^+$ in primate and non-primate cell lines.
DF-1 chicken, BHK-21 hamster, and HeLa human cells were seeded in 6-well plates and infected with MVA wt (A), or MVA-CHIKV-sAB$^+$ (B) with an MOI of 0.5. Viral titers were determined at the indicated time points.

For a conclusive confirmation that the CHIKV Env-derived protein sAB[+] is efficiently expressed in infected cells over the whole time course of infection, cell lysates from different time points post-infection were prepared. The sAB[+]-derived signal was enhanced with time (Figure 31). Even after a time frame as short as 8 hours post-infection, there was already a signal detectable. This indicates that sufficient sAB[+] is expressed shortly after infection and that production continues until at least 48 hours post-infection.

Thus, the characterization of MVA-CHIKV-sAB[+] revealed correct genetic organization, successful protein expression/secretion and no switches of growth characteristics in infected cells.
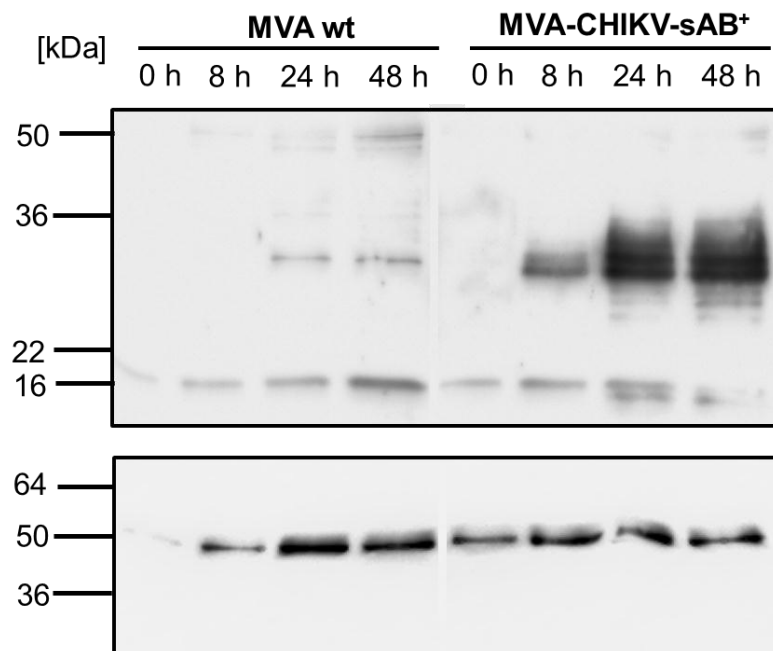
Figure 31: Kinetics of sAB[+] expression in MVA-CHIKV-sAB^{+} infected cells by Western blot analysis.
BHK-21 cells were seeded in 6-well plates and infected with MVA wt or MVA-CHIKV-sAB[+]. Cell lysates were prepared at the indicated time points post-infection. sAB[+] was detected via an anti-myc antibody and a secondary anti-mouse HRP antibody (upper panel) and ECL detection. After stripping, the membrane was incubated with an anti-β-actin and then again with an anti-mouse HRP antibody, as a loading control (lower panel).

5.2.6   Vaccination and infection of mice with MVA-CHIKV-sAB+ and/or the protein sAB+

To investigate if vaccination with the protein sAB+, the recombinant MVA-CHIKV-sAB+ or a combination of both leads to a better protection against wild-type CHIKV challenge, mice were vaccinated following the same schedule as in 5.2.2 (five mice per immunization variant, four per control group). This time however, an additional fourth vaccination was done two weeks after the third immunization. Two weeks after the fourth immunization (one week after blood was collected) mice were infected with wild-type CHIKV intranasally using $1*10^6$ pfu in 30µl PBS. On days 2 and 4 post-infection, blood was collected from the mice. The viral RNA was isolated from the blood-derived sera and a CHIKV specific RT-PCR was performed. The copy number of genomic CHIKV RNA in the sera of the different mice on day 2 post-infection is displayed in Figure 32. Protein sAB+ vaccinated mice showed an over 25-fold reduction of viral titers compared to the non-immunized control group. MVA-CHIKV-sAB+ vaccinated mice showed no reduction of viral titers compared to wild-type MVA infection. The difference compared to sAB+ vaccinated mice was significant. Mice that received the combination of protein and recombinant MVA revealed only a less than 2-fold reduction of CHIKV RNA in their sera. Control mice that had been infected with CHIKV seven weeks before, had no or nearly no detectable viral load. This difference was also significant compared to MVA wt infected mice. 4 days after infection, the viral titers of all mice decreased to levels close to 0 copies/µl (data not shown). Overall, low CHIKV titers could be detected in all sAB+ vaccinated mice. Consequently, vaccination of Balb/c mice with MVA-CHIKV-sAB+ did not result in a protective immune response against viral replication, but protein sAB+ immunization reduced viral titers in sera drastically. An immunization with MVA-CHIKV-sAB+ and a combination of recombinant MVA and protein in the following three immunizations only had minor protective effects.
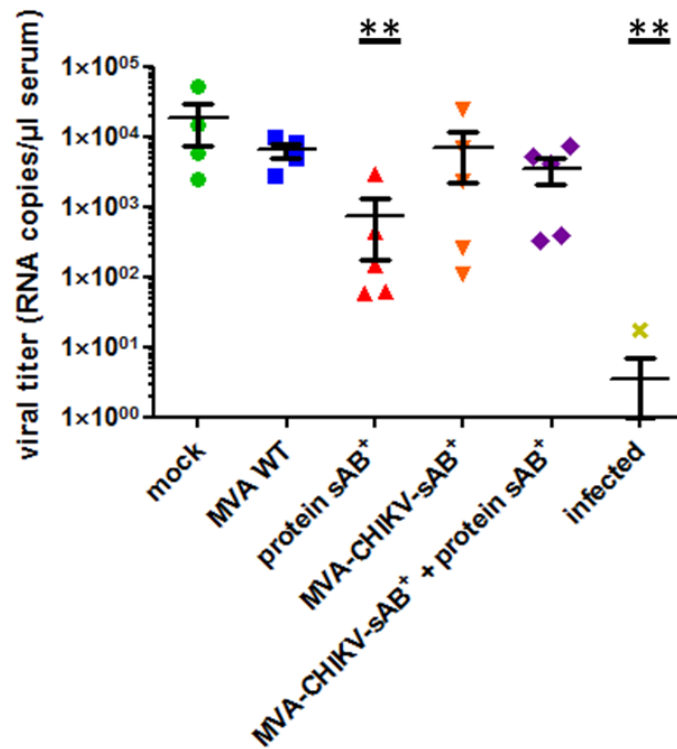
Figure 32: Viral titer determination in sera from CHIKV infected mice previously vaccinated with protein sAB+ and/or MVA-CHIKV-sAB+.

Seven-week old Balb/c mice were vaccinated with MVA wt ($1*10^8$ pfu per mouse per vaccination; n=4), protein sAB+ (100 µg; adjuvant "alum" 1:1, n=5), MVA-CHIKV-sAB+ ($1*10^8$ pfu; n=5), or a combination of both (first immunization with MVA-CHIKV-sAB+, for the further injections protein sAB+ was additionally used). Vaccinations were done at time point 0, and 3, 4, and 6 weeks after. For the mock mice (n=4) injections, only PBS was used. CHIKV challenge (10^6 pfu in 30 µl PBS per mouse, intranasally) were carried out 2 weeks after the last immunization. As a control, 5 mice that had already been infected with CHIKV 7 weeks prior to immunizations served as a control. Sera were collected on day 2 post-infection. Viral RNA was isolated from the sera and a CHIKV specific RT-PCR was carried out for detection of viral load in the sera. ** indicates significant differences in viral loads to MVA wt infected mice.

5.2.7 Humoral immune responses of MVA-CHIKV-sAB⁺ and/or protein sAB⁺ vaccinated mice

To determine the cause of the poor protective effect of MVA-CHIKV-sAB⁺, the production levels of anti-E2 antibodies in the sera of vaccinated mice was determined (collected one week after the fourth immunization, thus one week before infection). Lysates of CHIKV-infected BHK-21 cells were separated by SDS-PAGE and blotted onto a PVDF membrane. Lysates from mock infected and MVA wt infected cells were used as controls. The membranes (cut in strips) were incubated with the mouse sera of two randomly-selected mice from every vaccination variant. An anti-mouse IgG-HRP antibody and ECL were used for detection.

The results are given in Figure 33 A-B. All strips incubated with sera from mice, which received protein sAB⁺ and/or MVA-CHIKV-sAB⁺ or were CHIKV infected (an additional control), showed a double band (p62, the E2 precursor, and E2 itself) corresponding to the E2 positive control band (rabbit-derived peptide antibody against E2, the negative control was naïve serum from the same rabbit). This double band was more pronounced in sera of MVA-CHIKV-sAB⁺ vaccinated mice than protein vaccinated mice or in sera of infected mice. The respective naïve sera (and also all other naïve sera) did not reveal that signal. The same was true for the sera derived from MVA wt and non-immunized mice, respectively. All sera obtained from mice that received any MVA construct (recombinant or wild-type) produced a signal slightly above the p62/E2 double band.

Thus, all mice that were vaccinated with protein sAB⁺ and/or MVA-CHIKV-sAB⁺ developed CHIKV E2 binding antibodies upon immunization.

A)
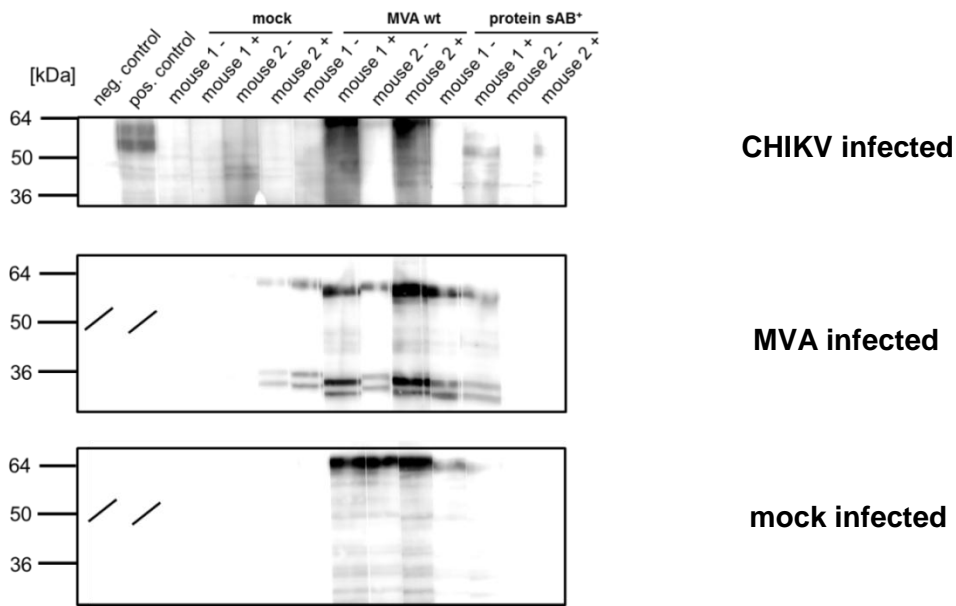
B)
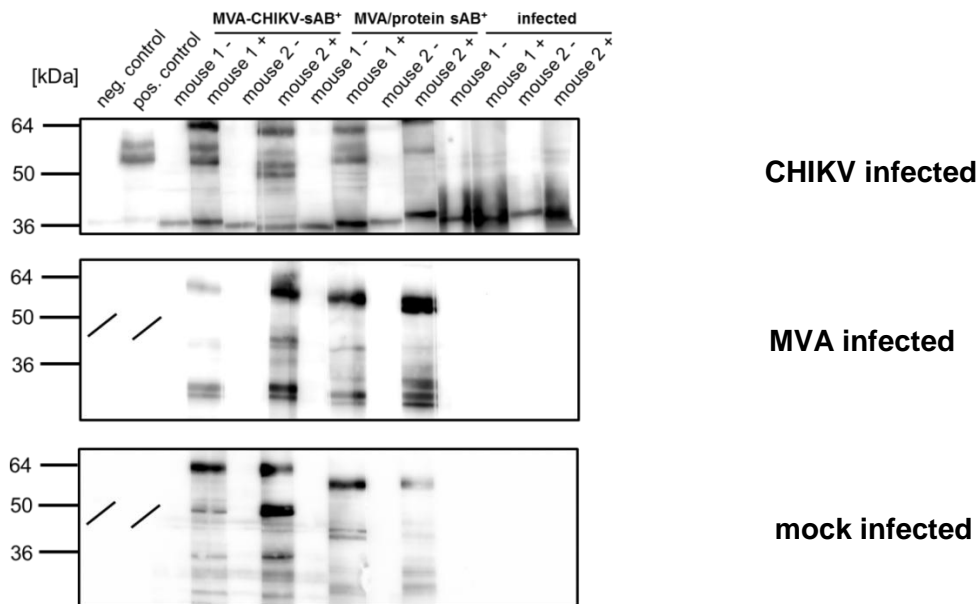
Figure 33: Binding of antibodies from sera of vaccinated mice to CHIKV E2.

A, B) BHK-21 cells were seeded in 10 cm dishes and infected with CHIKV (MOI 0.5; upper panel), MVA wt (MOI 1.0; middle panel), or mock (only PBS; lower panel). Cells were harvested 32 hours post-infection and cell lysates were prepared for SDS-PAGE. The lysates were separated by SDS-PAGE and blotted onto membranes. These membranes were cut into 5 mm stripes, which were incubated with the sera from two mice per vaccination variant (mice selected randomly; sera collected before the first and one week after the fourth immunization, and thus one week before infection, respectively; 1:100). Naïve serum and anti-CHIKV E2 serum from a rabbit was used as a positive control. Detection was carried out using an anti-mouse (for the mice sera), and an anti-rabbit HRP conjugate (for the rabbit control sera) and ECL detection.

5.3 Characterization of the Chikungunya virus entry process

5.3.1 Binding of the recombinant protein B^{+} to cells

In the earlier experiments, it was found that the protein B[+] (consisting of E2 domain B and a part of the C-terminal β-ribbon connector; see 5.2.1) plays an important role in the induction of neutralizing antibodies against CHIKV E2 (see Figure 24). Therefore, one could speculate that this part of E2 is an important component utilized in the binding of the virus to the unknown cellular receptor of CHIKV (see 2.1.5) or it is another structure necessary or beneficial for CHIKV cell attatchment and/or entry.

The protein B[+] was incubated at 4°C with cells that showed good transduction efficiencies (BHK-21 and Huh7 cells; see Figure 20) and with cells that revealed very low transduction efficiencies (Jurkat cells). Bound protein was detected via an anti His-tag antibody and an anti-mouse IgG-FITC antibody. The readout was completed by flow cytometry. In addition, the protein sA, which did not induce neutralizing anti-E2 antibodies upon vaccination (see Figure 24), was also used in this binding study.

The results in Figure 34 are expressed as fold-FITC mean relative to the control (cells incubated with anti His-tag and anti-mouse IgG-FITC antibody alone). The protein sA did not bind to any cell type used. The opposite was true for B[+], which bound to all cell types examined, including the poorly transducable Jurkat cells.
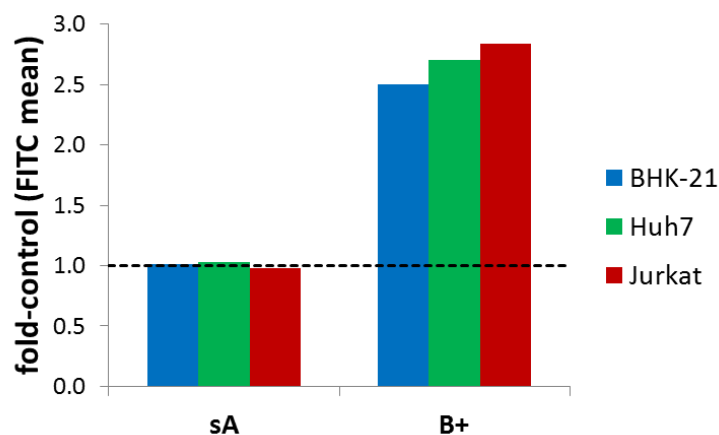
Figure 34: Binding of recombinant sA and B^{+} to cells.
BHK-21, Huh7, and Jurkat cells were incubated with 10 µg recombinant protein sA or B[+]. Binding was measured using an anti-His-tag antibody and an anti-mouse FITC conjugate. The readout was done by flow cytometry. The results are shown relative to the control (anti-His and anti-mouse FITC antibody alone). A value higher than one indicates binding and is labeled by the dashed line. The experiment was perfomed 4 times with slightly different conditions, one representative result is shown.

5.3.2 Cloning and production of recombinant extracellular E2 and of the E2 derived protein domains A, B, and C alone

To further analyze which domains of the E2 protein are involved in cell binding, domain A (including the β-ribbon connector; in contrast to the artificial protein used so far, sA), domain B (comparable to the thus far used extended construct B$^+$), and domain C genes were cloned into the bacterial expression vector pET-15b. The same was done for the whole extracellular part of the E2 protein, which served as a positive control. Cloning was completed by adding the restriction sites *Nde*I and *Bam*HI via primers in a PCR (template DNA: pIRES2-EGFP-CHIKV E3-E1), cutting the DNA products and the vector with these constructs, and subsequent ligation. For domain A, two fragments were derived via PCR. One fragment contained the domain A itself and the first part of the β-ribbon connector (C-terminal of domain A). The other fragment contained the second half of the connector, and the C-terminal of domain B. The fragments were cloned into the pET-15b vector by a triple ligation (via *Nde*I and *Bam*HI). The two fragments were linked via a shared *Sma*I restriction site (at the C-terminal part of fragment one and the N-terminal part of fragment two, respectively). By this procedure, E2 domain B was bypassed and replaced by the sequence G_4PG_5. The domains also contained an N-terminal polyhistidine-tag (see 5.2.1) for purification. The domains were expressed in *E. coli* as described in 4.2.1.3, and purified via ÄKTA HPLC (Ni-NTA columns) under native (B, C) and under denaturing (A, E2) conditions. For A and E2, ion-exchange chromatography was additionally subsequently performed to remove contaminants (i.e. bacterial proteins).

Figure 35 shows a coomassie stained SDS-PAGE separation of the purified proteins. Domain A has a molecular mass of 26.5 kDa, B of 8.5 kDa, C of 10.7 kDa, and E2 of 40.4 kDa. The purified proteins ran at the expected size, furthermore their identity was confirmed by mass spectrometry (data not shown). The lower bands visible in the lanes of A and E2 were identified by mass spectrometry as fragments of the purified protein (data not shown). Hence, the E2 domains A, B, C, and the extracellular part of E2 were successfully expressed and purified. Their exact amino acid sequences are given in 10.2.2.
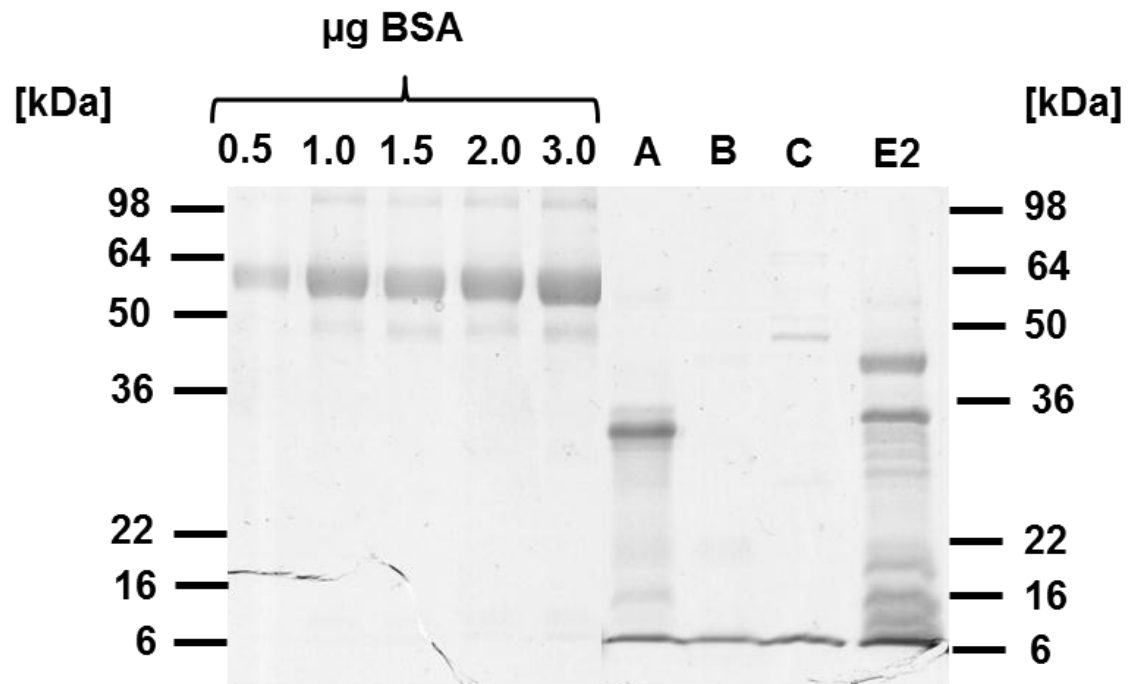
Figure 35: Cloning, expression, and purification of the CHIKV E2 domains A, B, C, and the whole extracellular part of E2.
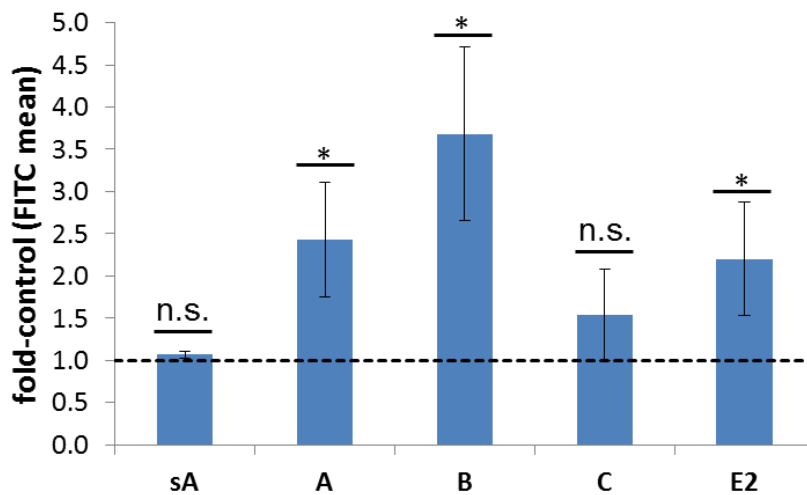
The CHIKV E2 domains A, B, C, and the whole extracellular part of E2 were cloned into the pET-15b vector, expressed in *E.coli*, and purified natively (B, C), and under denaturing conditions (A, E2) via HPLC (Ni-NTA beads). For A and E2, an ion-exchange chromatography was additionally performed after HPLC. Subsequently, they were dialyzed against PBS and concentrated. Shown is an SDS-PAGE with subsequent coomassie staining of the purified proteins. A BSA concentration row was used for estimation of concentration. The identity of the proteins was confirmed by mass spectrometry (data not shown).

5.3.3   Cell binding of recombinant proteins A, B, C, and E2

For testing if the E2 domains A, B, C, and/or the whole E2 protein bind to cells, the above mentioned cell binding experiment (see 5.3.1) was repeated with the new constructs. However, sA was again used as a negative control. The binding experiment was done with 293T, Jurkat, Huh7, and BHK-21 cells (for the latter two, data not shown). Again, the evaluation was the fold-FITC mean values of the sample in comparison to the FITC mean values of the control. Figure 36 A reveals that domains A, B, and the whole protein E2 showed a significant difference in the FITC signal compared to the control sample, indicating binding of these proteins to 293T cells. In contrast, there was no significant difference in cell binding detectable for the negative control, sA, and only minor binding of domain C. The same pattern could be confirmed for Jurkat cells (although on a lower binding level in general; Figure 36 B) and was also observed in the experiments using Huh7 and BHK-21 cells (data not shown).

Thus, domains A, B, and the entire E2 protein bound to all cell types examined, including the non-transducable Jurkat cell line. Domain C never bound to any of the cells tested.

A)

B)
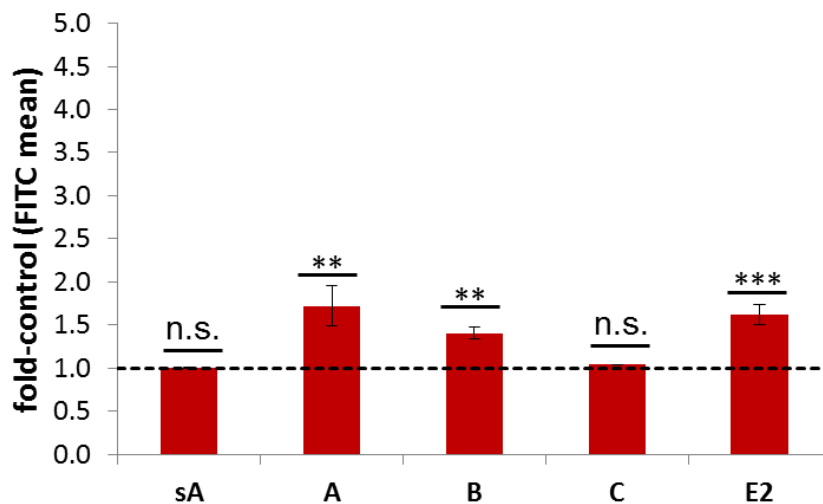
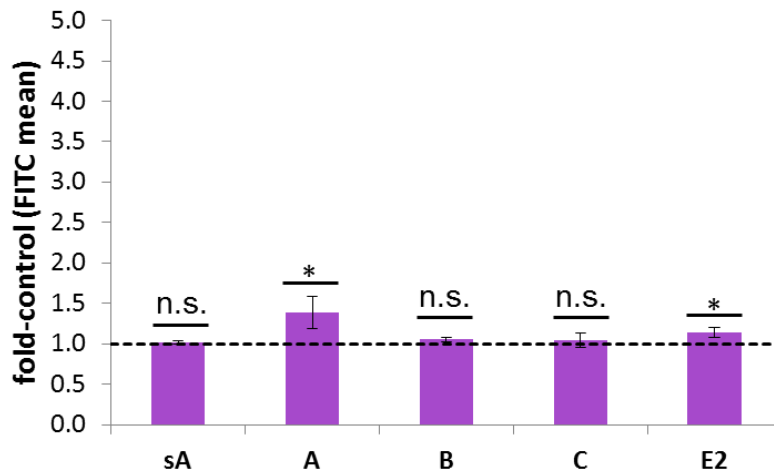**Figure 36: Binding of recombinant CHIKV E2 domains A, B, C, and the whole extracellular part of E2 to 293T and Jurkat cells.**

293T (A) and Jurkat (B) cells were incubated with 10 µg of the indicated recombinant proteins. Binding was measured using an anti-His-tag antibody and an anti-mouse FITC conjugate. The readout was done via flow cytometry. The results are shown relative to the control (anti-His and anti-mouse FITC antibody alone). A value higher than one indicates binding and is labeled by the dashed line. The experiment was done three times independently from one another. *, **, and *** indicate significant differences in fold-control to the recombinant protein-free controls. "n. s." means "not significant".

5.3.4 Binding of the recombinant proteins A, B, C, and the entire E2 protein to glycosaminoglycan-deficient pgsA-745 cells

The next goal was to determine which structures common to all cell surfaces proteins A and B (and whole E2) bind to.

Glycosaminoglycans (GAGs) are a structural component on the surface of all animal cells (see 2.1.5.4). They consist of long linear chains of disaccharide (30-60 per chain) units. These disaccharides are sulfated to different degrees and thus negatively charged. When covalently linked to a core protein, these GAGs are called proteoglycans. Depending on the carbohydrates that form the disaccharide units, there are different kinds of GAGs. The most important GAGs linked to core proteins on human cells are heparan sulfate (HS), chondroitin sulfate (CS), and dermatan sulfate (DS). GAGs are an essential component of the extracellular matrix and connective tissues in general, but they were also reported to act as receptors or attachment factors for different viruses (e. g., hepatitis C virus, herpes simplex virus, adeno-associated virus).

pgsA-745 cells are a CHO-K1 derived cell line that is, due to an enzymatic defect, not able to produce GAGs. To find out if GAGs play a crucial role for cell binding of domains A and B, the cell binding experiment (see 5.3.1, 5.3.3) was performed with pgsA-745 cells and the parental CHO-K1 cell line.

The results (Figure 37) exhibited that, for the parental CHO-K1 cell line, the binding pattern of the previous experiments was confirmed (Figure 37 A). However, conducting the experiment with pgsA-745 cells resulted in reduced, yet still significant, binding of domain A and no binding of domain B (Figure 37 B). The same as for domain A was true for the entire E2 protein. Accordingly, it was concluded that the binding of E2 domain A to cells is partly and the binding of domain B to cells is solely dependent on cell surface GAGs.

A)
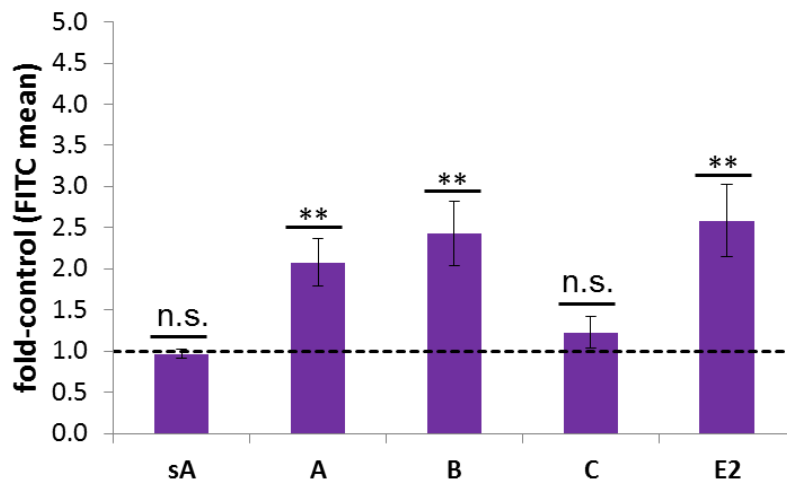
B)

Figure 37: Binding of recombinant CHIKV E2 domains A, B, C, and the whole extracellular part of E2 to CHO-K1 and pgsA-745 cells.

CHO-K1 (A) and pgsA-745 (B) cells were incubated with 10 µg of the indicated recombinant proteins. Binding was measured using an anti-His tag antibody and an anti-mouse FITC conjugate. The readout was done via flow cytometry. The results are shown relative to the control (anti-His and anti-mouse FITC antibody alone). A value higher than one indicates binding and is labeled by the dashed line. The experiment was performed three times independently from one another. *, and ** indicate significant differences in fold-control to the recombinant protein-free controls. "n. s." means "not significant".

5.3.5   Binding of A, B, and the whole E2 protein to cells in the presence of soluble GAGs

Next, it was to be discovered if the binding of A and B to cells containing GAGs on their surface could be inhibited by addition of soluble GAGs. The domains and different cell lines were again incubated at 4°C for binding. However, this time A, B, and the entire E2 protein were incubated in the presence of soluble GAGs beforehand. Then the cells were added to the mixture. Heparin (HP) was used as a control to ascertain the role of charge in the protein-cell binding. It is structurally derived from HS, but more heavily sulfated and thus has a higher negative charge density.

It is visible in Figure 38 A that binding of domain A to 293T cells was not reduced in the presence of any of the soluble GAGs, except in the presence of HP (about 2.5-fold). The opposite was true for B, where the presence of all GAGs (CS weaker than the others) reduced cell binding up to 3.0-fold. Again, HP showed the most effective inhibition. E2 revealed binding inhibition features that were in between those of domain A and B. Cell viability of 293T cells incubated with 500 µg/ml of the differenct GAGs (the maximum concentration used in all experiments of this work) was tested by an MTT assay. All GAGs were not or negligibly cytotoxic at that concentration (data not shown). A similar picture could be observed for CHO-K1 cells (Figure 38 B). Here, in contrast to 293T cells, HP did not play a more prominent role in inhibition compared to the other GAGs. A minor inhibition of domain A binding was detectable by HS and CS.

The same experiment was performed with pgsA-745 cells. Figure 38 C shows the results of protein binding in the presence of GAGs compared to the control without GAGs. Additionally, it was measured if the binding of domain C is influenced by GAGs. It could be observed that the binding of none of the proteins to pgsA-745 cells was inhibited or enhanced in the presence of soluble GAGs.

In summary: Binding of E2 domain A to 293T and CHO-K1 cells was not or only slightly inhibited by the addition of soluble GAGs. Only the strongly negatively charged HS derivate HP inhibited the domain A - 293T cell interaction. Contrarily, binding of domain B to both cell lines was massively decreased in the presence of HP, HS, CS, and DS. The addition of GAGs to the domains A, B, or C did not influence binding of these proteins to pgsA-745 cells.

A)

293T

B)

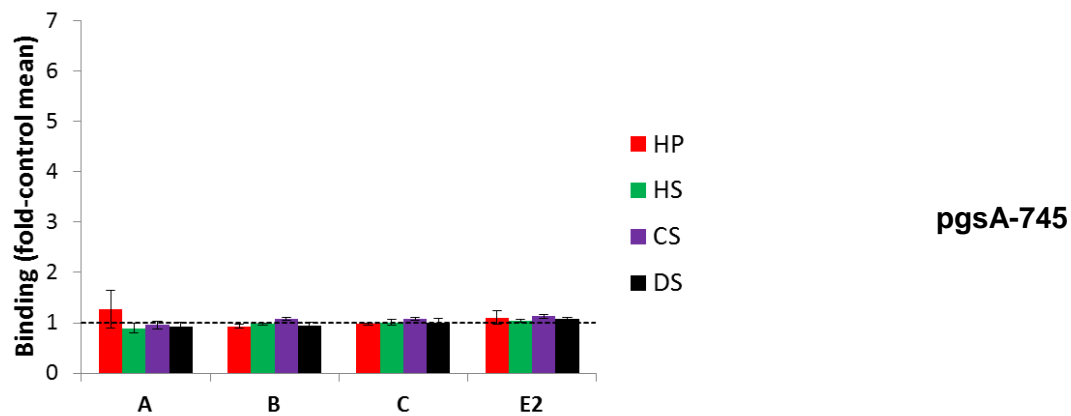

CHO-K1

C)
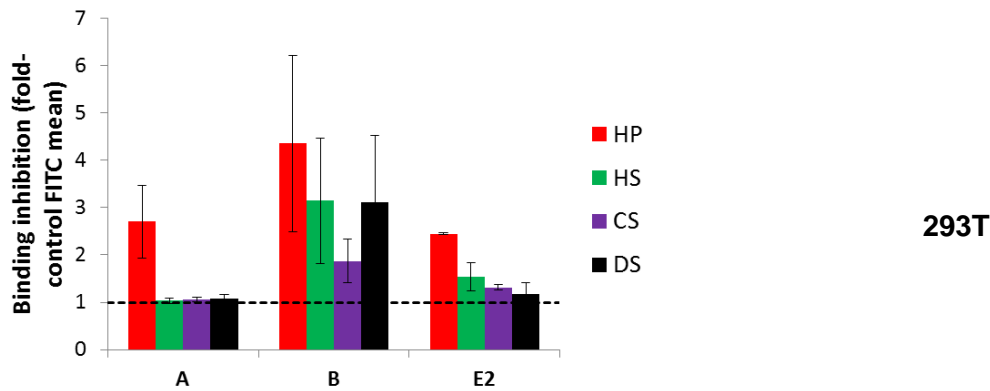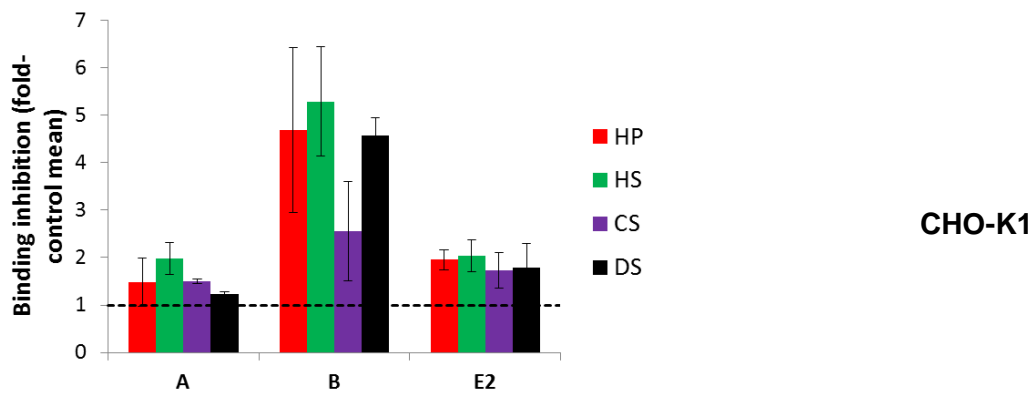
pgsA-745

Figure 38: Binding of recombinant CHIKV E2 protein domains A, B, C, and the entire extracellular part of E2 to 293T, CHO-K1, and pgsA-745 cells in the presence of soluble GAGs.

10 µg of the indicated recombinant proteins were incubated with the indicated soluble GAGs (500 µg/ml) for 30 minutes at 4°C. 293T (A), CHO-K1 (B), and pgsA-745 (C) cells were then incubated with this mixture. Binding was measured using an anti-His tag antibody and an anti-mouse FITC conjugate. The readout was done by flow cytometry. The results are shown relative to the control (incubation of cells with the respective construct alone, as in Figure 36 and Figure 37). A value higher than one indicates inhibition of binding (A, B), or enhanced binding (C) and is labeled by the dashed line. The experiment was done three times independently from one another.

5.3.6 Transduction of pgsA-745 cells with CHIKV envelope pseudotyped vector particles

Next, it was investigated whether the dependence on GAGs for cell binding, especially for E2 domain B, also plays a role on the level of viral entry. For this investigation, 293T cells, CHO-K1 cells, and the GAG-deficient CHO-K1 derived cell line pgsA-745 were transduced with CHIKV Env or VSV-G pseudotyped VPs.

The results displayed in Figure 39 show that CHIKV cell entry was about as efficient for 293T as for CHO-K1 cells. However, the transduction rate of pgsA-745 cells was significantly reduced by more than 50% in comparison to the parental cell line (relative to VSV-G).

Thus, cell entry of CHIKV into GAG deficient cells is strongly and significantly reduced in comparison to those which carry cell surface GAGs. However, cell entry is not reduced to zero, but to about 50 % of the control cell line.
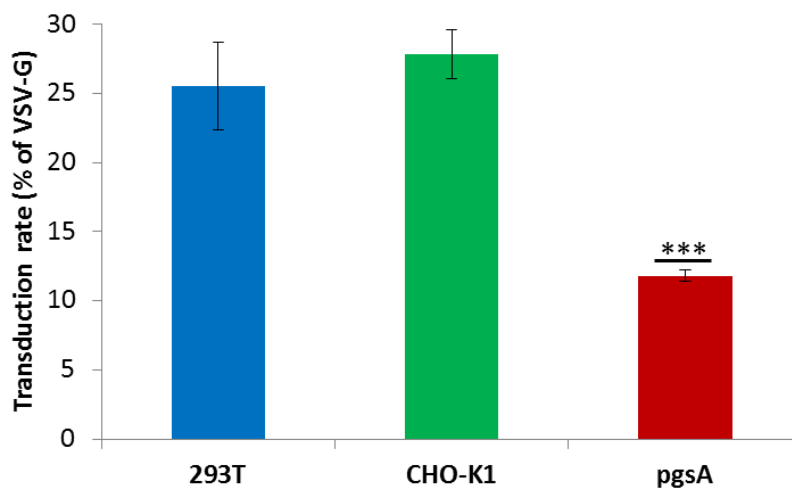
Figure 39: Transduction of the GAG-deficient pgsA-745 cells with CHIKV Env VPs.

293T, CHO-K1, and pgsA-745 cells were seeded in 24-well plates and transduced with *gfp* containing CHIKV Env pseudotyped VPs. The cells were analyzed by flow cytometry for GFP expression 48 hours post transduction. The proportion of GFP positive cells is given relative to that of the VSV-G control. The experiment was done three times independently from one another. *** indicates significant differences in transduction rates to CHO-K1 cells.

5.3.7 Transduction of cells with CHIKV envelope pseudotyped vector particles in the presence of soluble GAGs

CHIKV cell entry into GAG-deficient cells was reduced; accordingly it was then aimed to discover whether the presence of soluble GAGs inhibits the CHIKV Env VP entry into GAG containing cells or influences the entry into GAG-free cells. 293T, CHO-K1, and pgsA-745 cells were transduced with CHIKV Env containing VPs in the presence of different amounts of soluble GAGs. VSV-G and LCMV Env pseudotyped VPs, along with AAV-2 VPs, served as controls. An additional control for the soluble GAGs, besides HP, was used: Dextran sulfate (DX), which consists of long chains of highly sulfated glucose units. Hence, it has a similar charge compared to HP or the other GAGs, but the structural background is built up of totally different carbohydrates. The experiment was done in a 384-well plate format (see 5.2.2) with VPs containing the luciferase gene.

In the presence of increasing amounts of all soluble GAGs, VSV-G VP gene transfer to all cell types was enhanced (Figure 40 A i-iii). DX and HP especially, generally enhanced the luciferase signal. This effect was especially prominent on pgsA-745 cells (note the different scale of the y-axis). Here, VSV-G VP entry was enhanced up to 800% of the control in the presence of 500 µg/ml DX (Figure 40 A iii). The lowest enhancement (147%) at 500 µg/µl could be observed for CS on 293T cells. At concentrations below 500 µg/µl, no effect could be observed, and the values were mainly around 100% of the control.

In contrast to these results, adding increasing amounts of soluble GAGs to AAV-2 VPs resulted mostly in an inhibition of transduction (Figure 40 B i-iii). HS exhibited the weakest inhibition on all three tested cell lines. DX and HP reduced AAV-2 VP gene transfer most effectively on all three cell lines. Regarding HS, CS, and DS, the data were similar on 293T and CHO-K1 cells, but on pgsA-745 cells there was an enhancement of transduction at lower (HS) or higher (CS, DS) GAG concentrations (Figure 40 B iii). This enhancement was very prominent at the highest concentration of CS (nearly 500% of the control). At lower concentrations of CS and DS, transduction was inhibited, whereas the same was the case at higher concentrations of HS. However, DX and HP reduced viral entry, similar to what was observed on 293T and CHO-K1 cells.

Most of the LCMV Env VP transductions were not influenced by the addition of GAGs on any cell line (Figure 40 C i-iii). On 293T cells, it was only efficiently inhibited by DX and HP, CS and HS induced a change in transduction efficiency only at their highest concentration (500 µg/µl). On CHO-K1 and on pgsA-745 cells, only DX reduced the luciferase signal with increasing concentrations.

Transducing 293T and CHO-K1 cells with CHIKV Env VPs in the presence of GAGs resulted generally in reduced transduction efficiencies compared to the control without GAGs (Figure 40 D i-iii). Again, DX and HP were on both cell lines the most potent inhibitors. On 293T cells, the cell entry could be inhibited up to about 10-20 % of the control at a concentration of 500 µg/µl. On CHO-K1 cells, transduction was reduced to about 20-30% of the GAG-free control. Cell entry of CHIKV Env VPs into pgsA-745 cells was, on the contrary, enhanced by the addition of raising GAG concentrations to the medium. The highest enhancement values lied, at 500 µg/µl, between 121 (DX) and 177 (HP) % of the control. Noteworthy values lower than 100% (up to only 55%) were only observed for DX at concentrations lower than 500 µg/µl.

In conclusion, transduction of control VSV-G VPs in the presence of increasing amounts of GAGs (and DX) was enhanced in 293T, CHO-K1, and pgsA-745 cells. Contrary to this enhancement, AAV-2 VP entry into cells was inhibited in 293T and CHO-K1 cells by adding GAGs to the cell supernatant. In pgsA-745 cells, AAV-2 VP transduction was enhanced by using high amounts of CS and DS or low amounts of HS. DX and HP did not reveal that enhancement, but instead an inhibition phenotype. LCMV Env VP transduction was not inhibited or enhanced in CHO and pgsA-745 cells for all GAGs except the DX control. Only in 293T cells did some GAGs alter the luciferase signals. The CHIKV Env VPs revealed a similar picture as the AAV-2 VPs, whereby on 293T cells the GAG inhibition efficiency was slightly higher than on CHO-K1 cells, indicating that CHIKV Env directed VP entry is GAG dependent. Similar to the AAV-2 VPs, the entry into pgsA-745 cells was enhanced with increasing amounts of GAGs, in this case by all GAGs and DX.
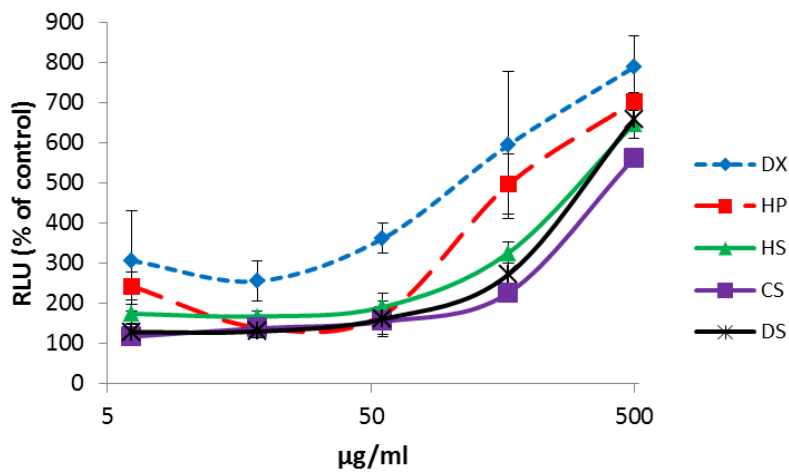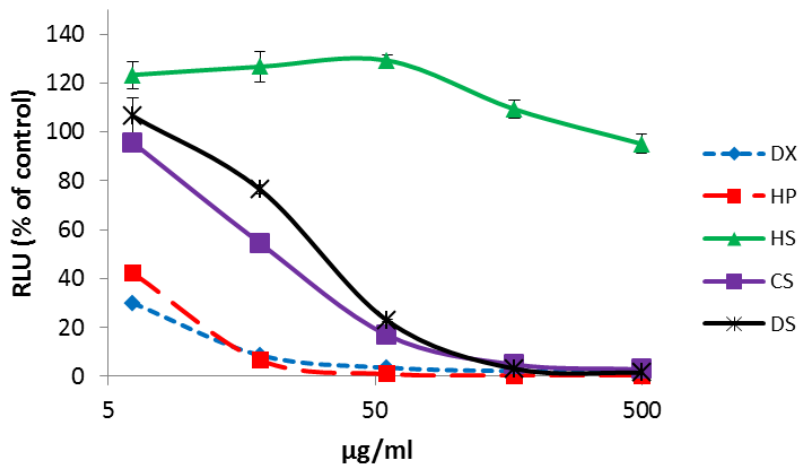
A) i
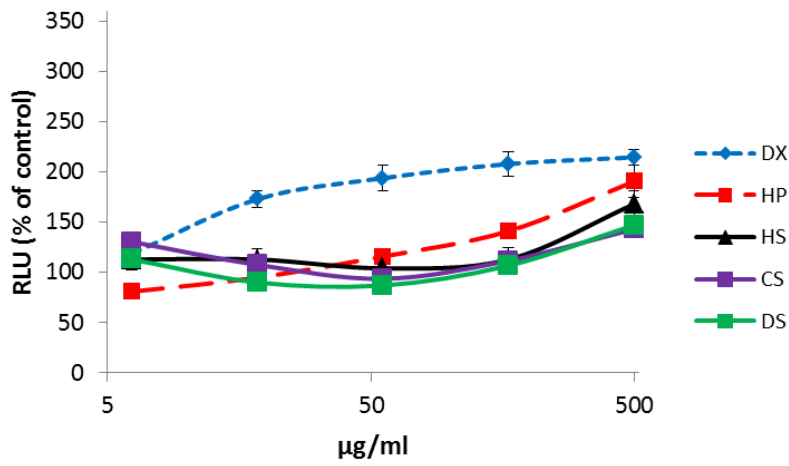
293T

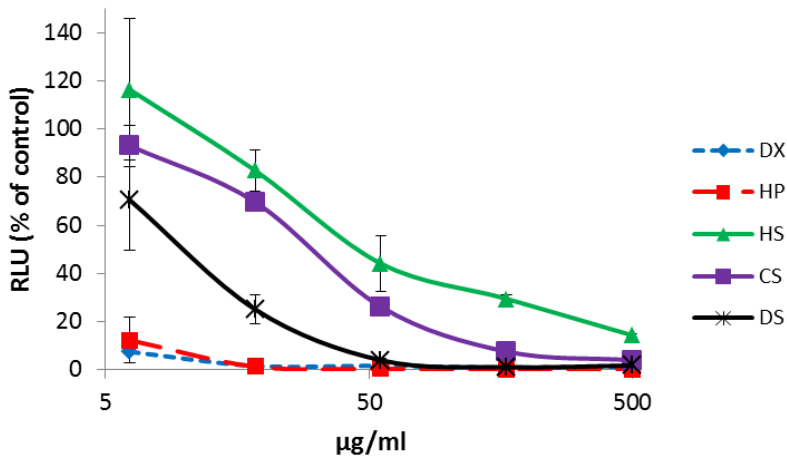VSV-G VPs

A) ii
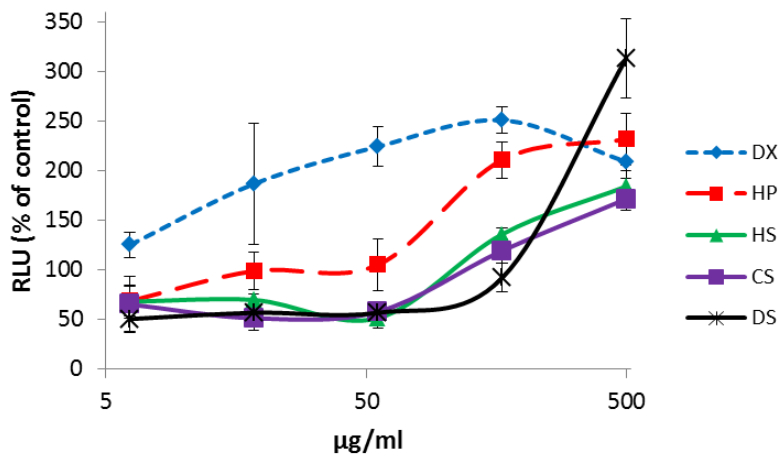
CHO-K1

VSV-G VPs

A) iii

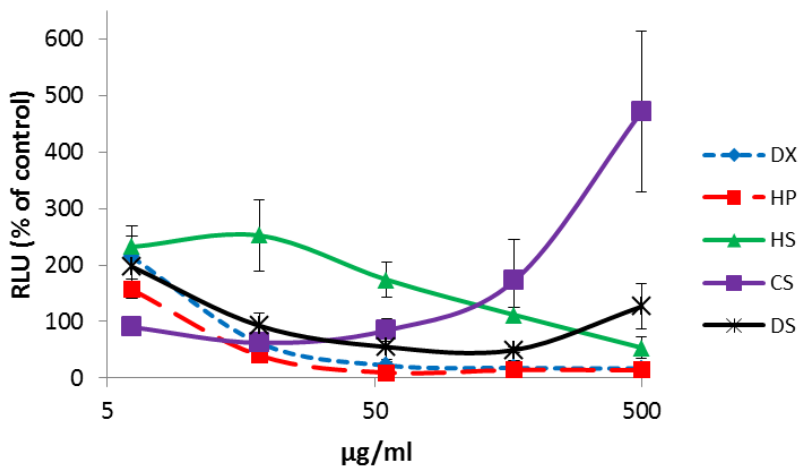pgsA-745

VSV-G VPs

B) i

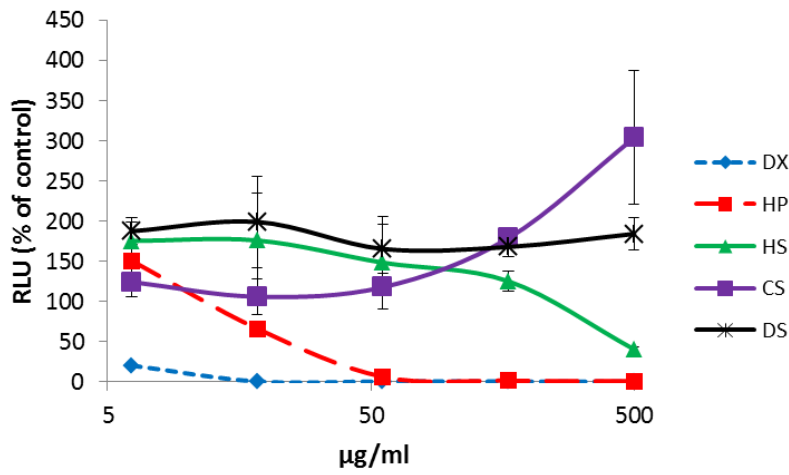293T

AAV-2 VPs

B) ii

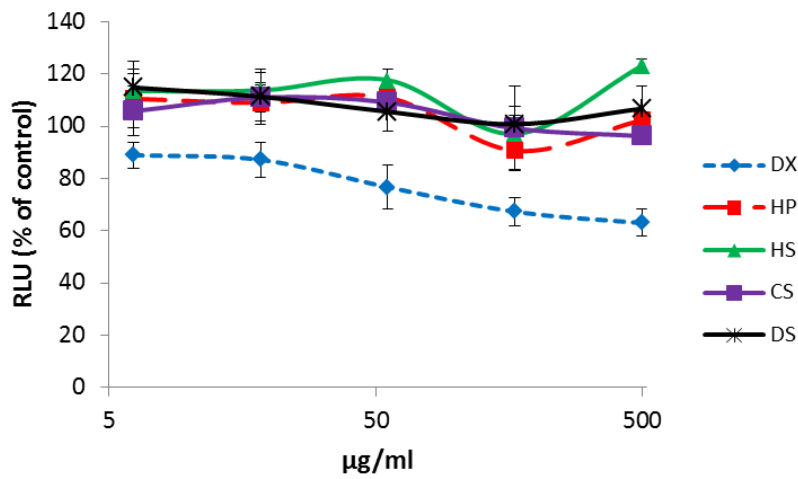CHO-K1

AAV-2 VPs
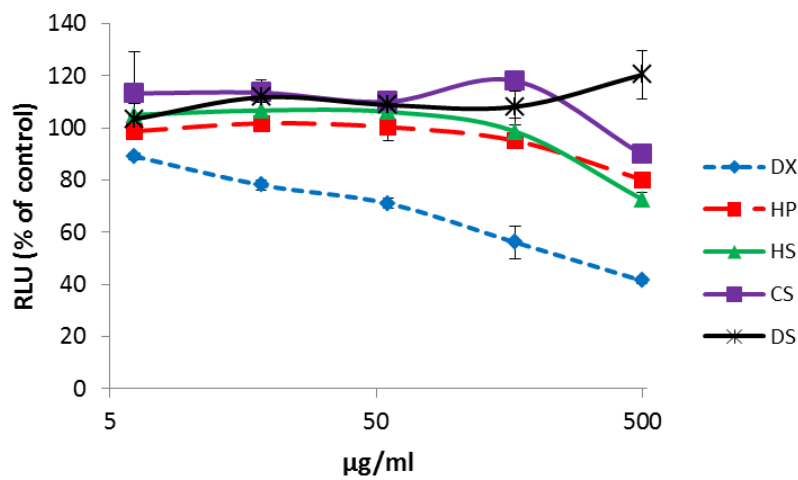
B) iii

pgsA-745

AAV-2 VPs

C) i
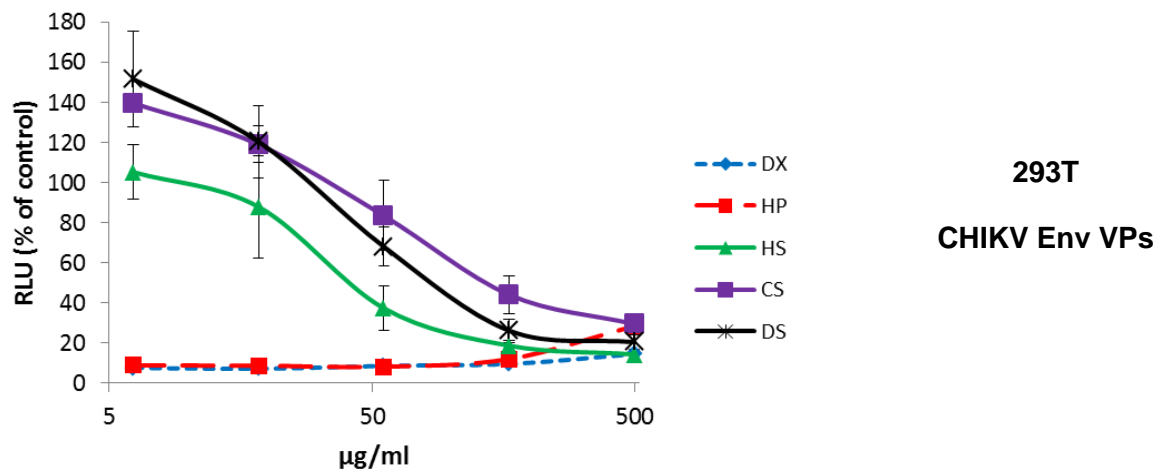

293T

LCMV Env VPs

C) ii
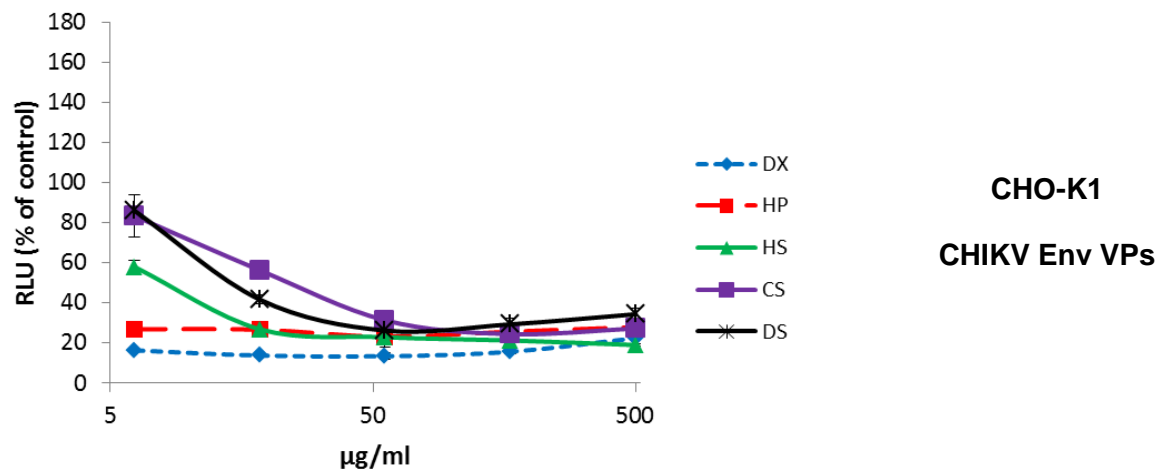

CHO-K1

LCMV Env VPs

C) iii

pgsA-745

LCMV Env VPs

D) i
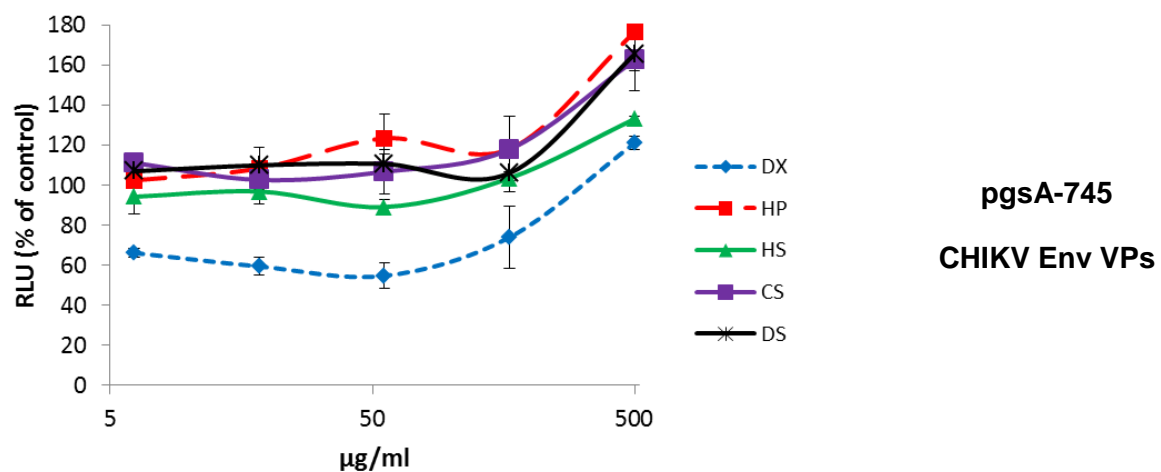

D) ii

D) iii

Figure 40: Transduction of cells with CHIKV Env VPs in the presence of soluble GAGs.

293T (A-D i), CHO-K1 (A-D ii), and pgsA-745 (A-D iii) cells were seeded in 384-well plates and transduced with a *luciferase* gene containing CHIKV Env pseudotyped VPs (D). VSV-G (A), AAV-2 (B), and LCMV Env (C) VPs

were used as controls. Before addition to the cells, the VPs were incubated with DX or one of the indicated GAGs for 30 minutes at 4°C (DX and GAGs in five 3-fold dilutions, ranging from 500.0 to 6.2 µg/µl). One day after transduction, the luciferase expression of the cells was detected by a luminometer. The results are shown relative to the DX/GAG-free control. Note the partially different scales of the y-axis in diagrams showing the results for the same viral envelope protein/VPs. The experiment was done two times in triplicates, showing one representative triplicate result.

5.3.8 GAG dependency of CHIKV infections

To confirm the relevance of the above experiments, dependency of CHIKV infections on cell surface GAGs was studied. For this, CHO-K1 and pgsA-745 cells were both infected with the recombinant CHIKV-mCherry-490 established by (Kümmerer et al., 2012) using an MOI of 1. This virus contains an mCherry gene within the nsP3 gene of CHIKV and has growth characteristics similar to the wild-type virus. Viral replication was determined at 6 and 24 hours post-infection by flow cytometry.

The infection rate 6 hours post-infection was 9.9-fold and significantly reduced in pgsA-745 cells compared to CHO-K1 cells (Figure 41). At 24 hours post-infection, the difference decreased to a 1.5-fold higher infection rate in CHO-K1 than in pgsA-745 cells, still this difference was significant.

Thus, not only was the cell entry of CHIKV VPs reduced, but also the replication of a mCherry containing CHIKV was reduced on pgsA-745 cells lacking cell surface GAGs, indicating that GAGs enhance virus entry, but are not essential for entry.
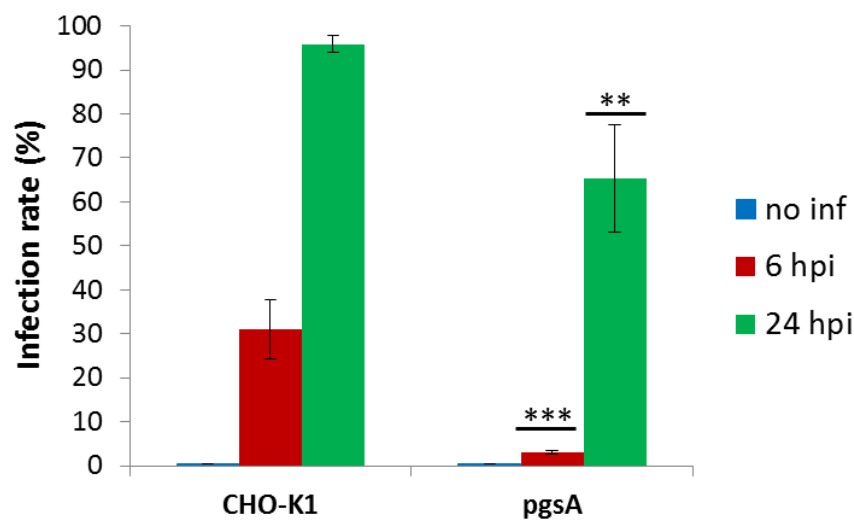

Figure 41: Infection of CHO-K1 and pgsA-745 cells with CHIKV-mCherry-490.
CHO-K1 and pgsA-745 cells were seeded in 24-well plates and infected with CHIKV-mCherry with an MOI of 1. The viral replication was determined 6 and 24 hours post-infection, respectively, by flow cytometry detecting mCherry. The experiment was done three times independently from one another. **, and *** indicate significant differences in infection rates to CHO-K1 cells after 6 and 24 hours, respectively.
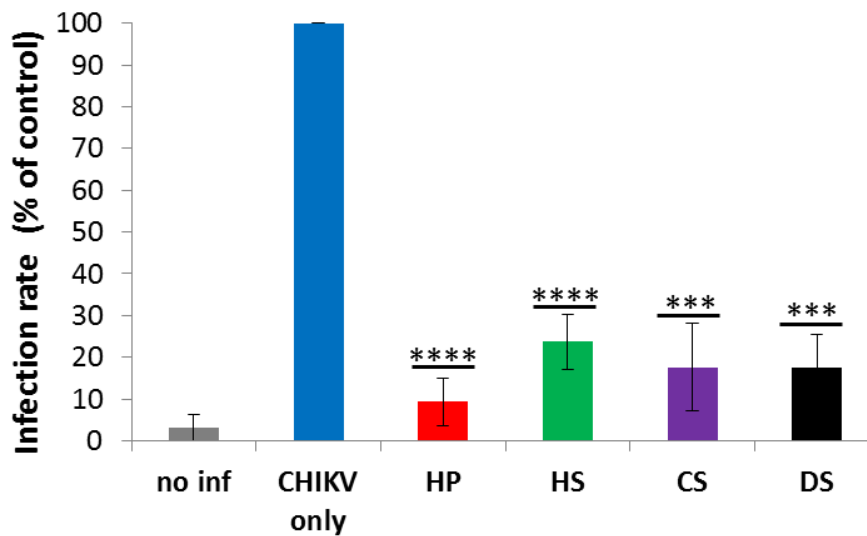
5.3.9   Infection of cells with CHIKV-mCherry in the presence of soluble GAGs

CHIKV replication in GAG-deficient cells was diminished. Accordingly, this raised the question whether the infection of cells is inhibited in the presence of soluble GAGs, as it is true for the transduction with CHIKV Env VPs. 293T cells were infected with CHIKV mCherry (MOI 1) in the presence of 500 µg/ml of the respective soluble GAG (but 500 U/ml HP). Six hours later, cells were analyzed by flow cytometry. Figure 42 A reveals that all GAGs reduced viral replication by at least 76.3% (HS). HP was most effective with a reduction to 90.7% of the GAG-free control. All GAG-dependent reductions were in comparison to the control infections significant.

To figure out if the inhibition of CHIKV replication by GAGs occurs at the attachment/entry step of the viral life cycle, the different GAGs were incubated together with the virus at 4°C to allow viral attachment to the cells but to avoid the subsequent endocytosis step. After 30 minutes, unbound virus and the GAGs were washed away and the cells were incubated for six hours at 37°C in fresh medium. Infection rates were measured via flow cytometry. Figure 42 B shows, similar to the previous experiment, a significant reduction of cell attachment/entry by 62.1 (HS) to 82.4% (HP).

In conclusion, replication of the recombinant CHIKV-mCherry-490 in 293T cells is significantly inhibited by the addition of soluble GAGs. The attachment and/or endocytosis is one critical step in the viral life cycle where this inhibition occurs.
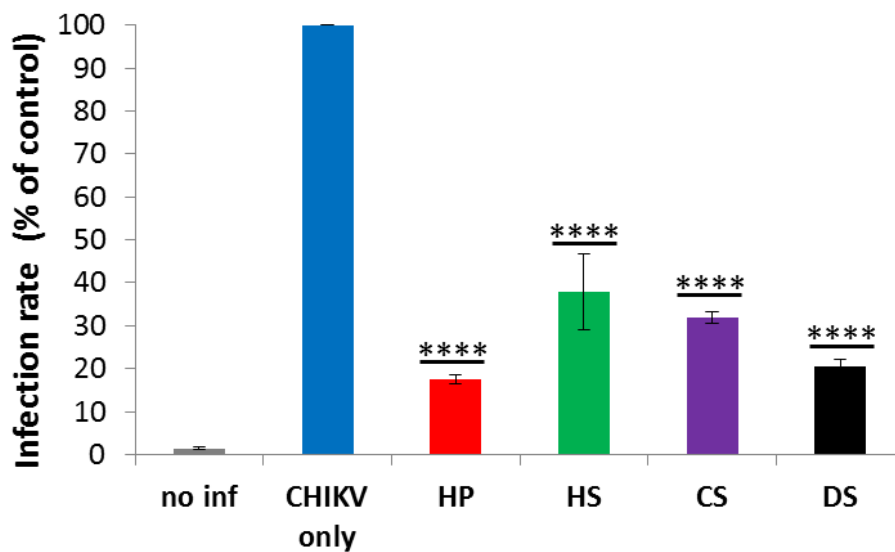
A)

B)

Figure 42: Infection and cell entry by CHIKV-mCherry-490 in the presence of soluble GAGs.

A) 293T cells were seeded in 24-well plates and 500 µg/ml of the indicated GAG was added. Afterwards, cells were infected with CHIKV-mCherry-490 using an MOI of 1. The viral replication was determined 6 hours post-infection by flow cytometry detecting mCherry. B) 500 µg/ml of the indicated GAG and CHIKV-mCherry-490 (MOI 1) were incubated together at 4°C for 30 minutes. After addition to 293T cells seeded previously, another incubation of 30 minutes at 4°C followed. Then, the unbound virus together with the respective GAG was washed away and fresh medium was added to the cells. The viral replication was determined 6 hours post-infection by flow cytometry detecting mCherry. The experiment was performed three times independently from one another. ***, and **** indicate significant differences in infection rates to the soluble GAG-free control cells.

5.4   Screening for CHIKV entry inhibitors

5.4.1   Infection of 293T cells with CHIKV-mCherry in the presence of epigallocatechin-3-gallate (EGCG)

Epigallocatechin-3-gallate (EGCG) is the major catechin found in green tea and was found to have anticancer and antiviral activities (see 2.2.1.2). Therefore, experiments with CHIKV were completed to investigate whether EGCG exhibits anti-CHIKV activity as well.

In the first experiment, 293T cells were infected with CHIKV-mCherry (MOI 1) in the presence of 10 µg/ml EGCG. Epicatechin (EC) is also a compound found in green tea but lacks the galloyl side chain of EGCG, which is thought to have a major role in the biological functions of EGCG (Nagle et al., 2006). It was used as a control. Flow cytometry was used for detection. As the results presented in

Figure 43 reveal, the infection rate was significantly lowered by over 50% in the presence of EGCG in comparison to the control (in the absence of EGCG). In contrast to this decrease, EC reduced viral infection only negligibly.
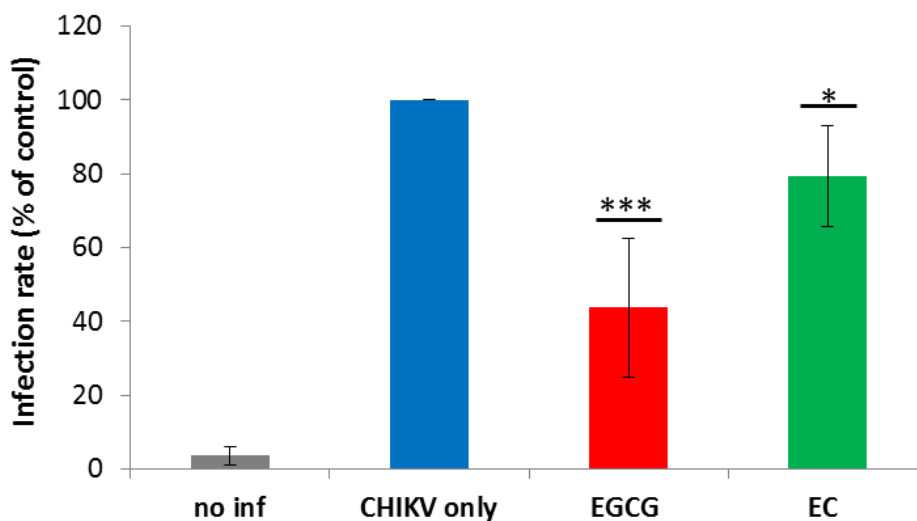

Figure 43: Infection by CHIKV-mCherry-490 in the presence of EC and EGCG.
293T cells were seeded in 24-well plates and 10 µg/ml EC or EGCG was added. Afterwards, cells were infected with CHIKV-mCherry-490 using an MOI of 1. The viral replication was determined 6 hours post-infection by flow cytometry detecting mCherry. The experiment was done five times independently from one another. *, and *** indicate significant differences in infection rates to the EGCG- and EC-free control cells.
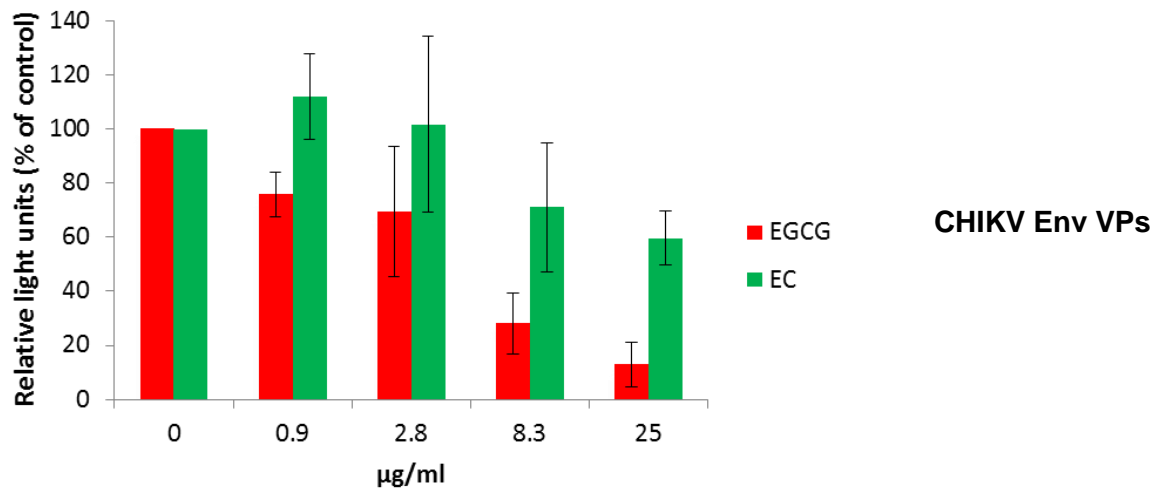
5.4.2   Transduction of CHIKV Env VPs in the presence of EGCG

To figure out if the anti-CHIKV effect of EGCG is based on the inhibition of viral entry, a 384-well plate luciferase assay was performed. 293T cells were transduced with CHIKV Env VPs in the presence of different amounts of EGCG. EC was used as a compound control, VSV-G pseudotyped VPs and AAV-2 VPs as transduction controls. VSV entry has been published to be inhibited by EGCG (Steinmann et al., 2013), and AAV-2 entry depends on cell surface GAGs binding, with which EGCG might interfere (O'Donnell et al., 2009).

Figure 44 A shows that CHIKV Env directed cell entry was more strongly inhibited by EGCG than by EC at all used concentrations. The inhibition effect was dose-dependent. Transduction with VSV-G VPs (Figure 44 B) was also more strongly inhibited by EGCG than by EC, although the difference was smaller than for CHIKV Env VPs. Additionally, the entry block by EGCG was more pronounced using CHIKV VPs in comparison to VSV-G VPs (IC_{50} EGCG with VSV-G VPs: 14.12 µg/ml; with CHIKV Env VPs: 6.54 µg/ml). An inhibition of AAV-2 VP entry by EC or EGCG (Figure 44 C) was only observed at the highest compound concentration of 25 µg/ml. The effects at lower concentrations were negligible. The corresponding IC_{50} values of EGCG and EC from A), B), and C) were in general lower for EGCG than for EC, and the experiments with CHIKV Env VPs revealed the lowest IC_{50} values (Figure 44 D). Cell viability of 293T cells incubated with 25 µg/ml EGCG or EC (the maximum concentration used in all experiments of this work) was tested by an MTT assay. Neither EGCG nor EC was cytotoxic at that concentration (data not shown).

Thus, EGCG inhibited significantly the entry of CHIKV into target cells. This was also true for EC, but to a lower extent. The EGCG effect was also less pronounced for VSV-G VPs and for AAV-2 VPs only existing at the highest concentration.
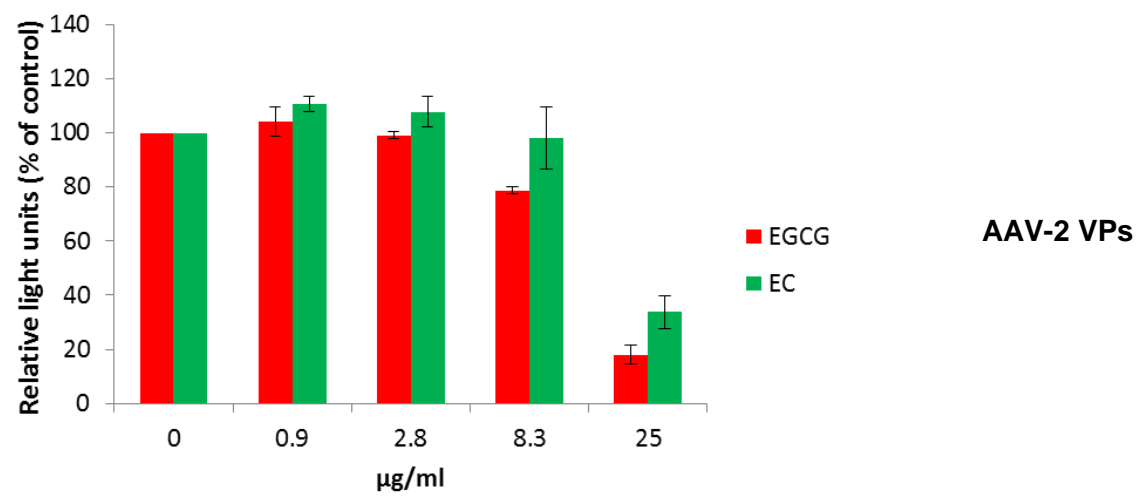
A)

B)
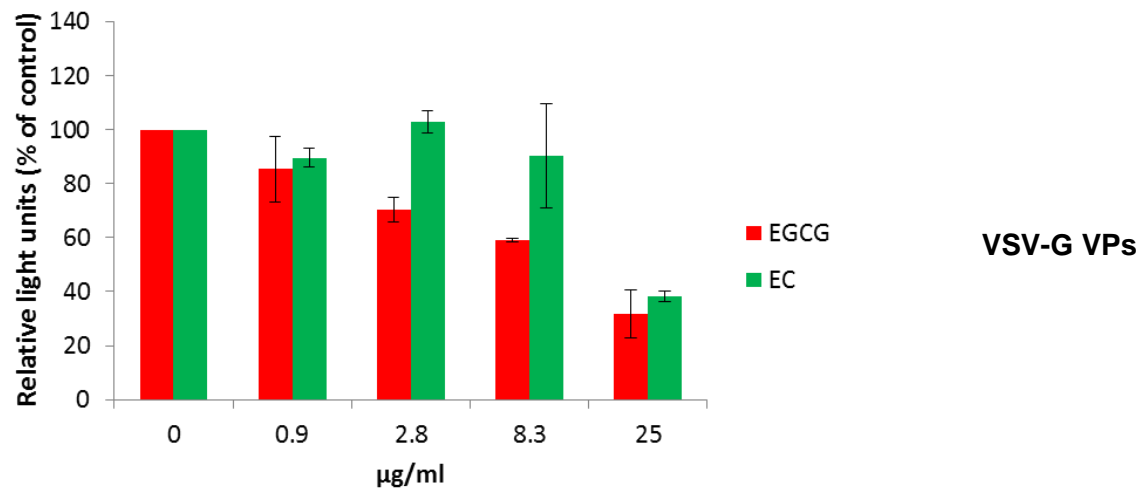
C)

D)

IC$_{50}$ [µg/ml]	CHIKV Env	VSV-G	AAV-2
EGCG	6.5	14.1	13.4
EC	8.6	21.7	18.5

Figure 44: Transduction of cells with CHIKV Env VPs in the presence of EC and EGCG.

293T cells were seeded in 384-well plates and transduced with a *luciferase* gene containing CHIKV Env pseudotyped VPs (A). VSV-G (B), and AAV-2 (C) VPs were used as controls. Before addition to the cells, the VPs were incubated with EC or EGCG for 30 minutes at 4°C (in four 3-fold dilutions, ranging from 25.0 to 0.9 µg/µl). One day after the transduction, the luciferase expression of the cells was detected by a luminometer. The results are shown relative to the EC/EGCG free control. The experiment was done two times in triplicates, above shows the representative results of one triplicate experiment. In D), the IC$_{50}$ values of EGCG and EC for the CHIKV Env, VSV-G, and AAV-2 VPs (A, B, C) are shown.

5.4.3   Cell attachment and entry of CHIKV-mCherry in the presence of EGCG

To assess if it is also the entry process of CHIKV that is inhibited by EGCG in wild-type CHIKV, 293T cells were incubated with a CHIKV-mCherry-490/EGCG mixture (MOI 1 and 10 µg/ml, respectively) for 30 minutes at 4°C to allow viral attachment, but not endocytosis. After this incubation period, unbound virus was washed away and replaced by fresh cell culture medium. An incubation at 37°C for six hours and the analysis via flow cytometry followed. Again, EC was used as a control. The results (Figure 45) show that CHIKV-mCherry attachment, endocytosis, and/or fusion was significantly inhibited by EGCG by more than 50%, again EC had only minor, but still significant, effects.

Focusing solely on the inhibitory effect of these compounds on the fusion process of CHIKV, cells were transfected with CHIKV Env expression vector (containing an IRES eGFP). After 48 hours, the conformational changes of the CHIKV envelope proteins upon acidification in the endosome were induced directly at the cell membrane by the addition of an acidic fusion buffer to the CHIKV Env expressing cells. The cells form syncytia if cell membrane fusion occurs, this was detected via GFP detection with a fluorescence microscope. The presence of EGCG during this fusion assay did not result in a noteworthy inhibition of fusion. Slight syncytia formation inhibition was only observed at very high EGCG concentrations of 100 µg/ml (data not shown).

These results show that EGCG inhibits CHIKV attachment and/or subsequent endocytosis, but not fusion of viral and endosomal membranes.
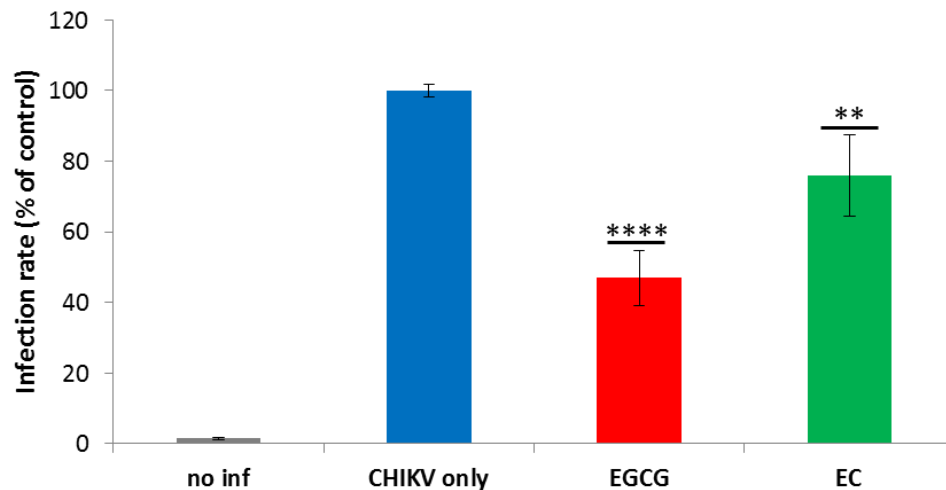
Figure 45: Cell entry by CHIKV-mCherry-490 in the presence of EC and EGCG.

10 µg/ml EC or EGCG and CHIKV-mCherry (MOI 1) were incubated together at 4°C for 30 minutes. After addition to 293T cells seeded previously, another incubation of 30 minutes at 4°C followed. Then, the unbound virus together with EC or EGCG was washed away and fresh medium was added to the cells. The viral replication was determined 6 hours post-infection by flow cytometry detecting mCherry. The experiment was performed four times independently from one another. **, and **** indicate significant differences in infection rates to the EGCG- and EC-free control cells.

5.4.4   Dependency of the inhibitory effect of EGCG on CHIKV-mCherry replication on the time point of addition

To test whether EGCG also has an inhibitory effect on the replication of CHIKV post entry, 293T cells were first incubated with CHIKV-mCherry (MOI 1) for 2 hours at 37°C. Only then was EGCG or EC added at a concentration of 10 µg/ml. An additional 4 hours later, the cells were fixed and analyzed via flow cytometry.

The late addition of EGCG to the cells (after the initial infection), caused the compound to lose all of its anti-CHIKV activity (Figure 46). The infection rate was not significantly influenced by neither EGCG nor EC. Therefore, the inhibitory effect of EGCG on CHIKV seems to be limited to the entry process of the virus.
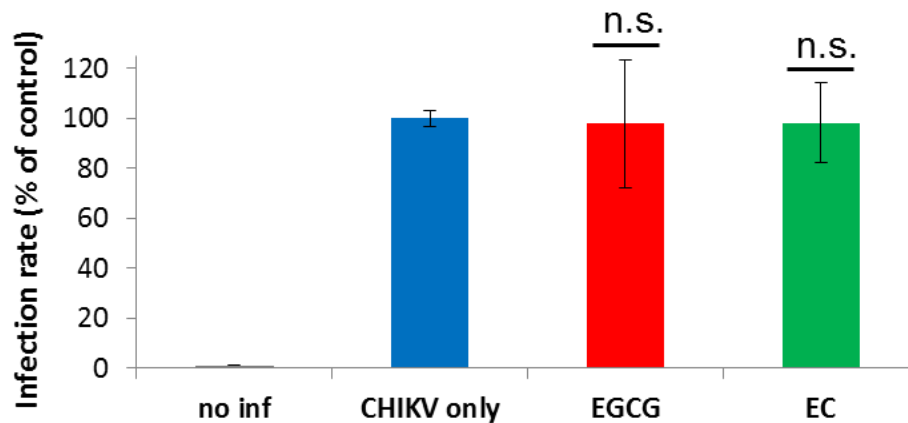
Figure 46: Addition of EC and EGCG 2 hours post-infection to CHIKV mCherry.
293T cells were seeded in 24-well plates and infected with CHIKV-mCherry using an MOI of 1. After 2 hours at 37°C, 10 µg/ml EC or EGCG was added. The viral replication was determined 4 hours later by flow cytometry detecting mCherry. The experiment was done six times independently from one another. "n. s." means "no significant" differences in infection rates to the EGCG- and EC-free control cells.

5.4.5   Effects of EGCG on the CHIKV replication bypassing the CHIKV entry

The lack of CHIKV post entry inhibition by EGCG was further confirmed by a different experimental approach. 293T cells were transfected with *in vitro*-transcribed viral mRNA (CHIKV-mCherry-490), and 2 hours later the transfection mix of lipofectamine/RNA was discarded and 10 µg/ml EGCG or EC were added. After 16 hours of incubation at 37°C, the infection rate was not altered by the addition of the green tea compounds (Figure 47) in comparison to the control without any catechin.

Bypassing the viral entry by direct transfection of the viral RNA thus eliminated the anti-CHIKV effect of EGCG, similar to its late addition during the viral infection cycle (see Figure 46).
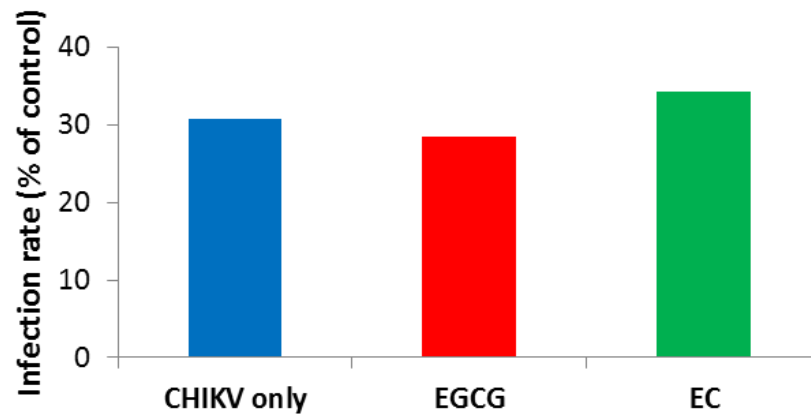
Figure 47: EC and EGCG inhibitory effects when bypassing the cell entry of CHIKV-mCherry.

293T cells were seeded in 24-well plates and transfected with CHIKV-mCherry-490 *in vitro* transcribed viral mRNA. Two hours later, this mixture was replaced by fresh medium containing 10 µg/ml EC or EGCG. The viral replication was determined 16 hours later by flow cytometry detecting mCherry.

6. Discussion

The Chikungunya virus (CHIKV) has, especially since 2004, spread to formerly CHIKV-free regions of the world and caused several epidemics with very high infection rates of about 30%. These epidemics have caused major problems in the public health system and high economic costs due to manpower reduction, especially because of the recurrent arthritic symptoms that last for months or even years. Additionally, because of the more attentive surveillance and higher numbers of infection (millions of infections worldwide since 2004), several severe cases of encephalitis or hepatitis have been observed. The virus is expected to continue to spread to more temperate regions of the world in the next years and decades. A major prerequisite for this spread is the adaption of one virus lineage to a much more efficient transmission by *Aedes albopictus* (*A. albopictus*). This adaption is based on only a single mutation in a viral envelope protein (E1 A226V) and increases the risk of continued CHIKV spread, because this mosquito, in contrast to the usual main vector *Aedes aegypti* (*A. aegypti*), also occurs in temperate world regions. *A. albopictus* is also expected to further spread in the next years and decades, especially due to globalization and climate change.

Before 2004, the research on CHIKV was neglected. Only after the La Réunion epidemic (La Réunion is a French territory) in 2006, did attention and research increase substantially. However, many parts of the viral life cycle, including the entry process, are still not characterized in detail. Furthermore, there is still no licensed vaccine or specific treatment against CHIKV infection.

The focus of this work was to better understand and characterize the CHIKV entry process. This work may lead to the discovery of novel antiviral strategies and new therapeutic approaches and opportunities. Additionally, novel CHIKV entry inhibitors and vaccination strategies were tested. These may be the basis for a future CHIKV treatment and vaccine development.

6.1   Characterization of CHIKV Env pseudotyped vector particles

Pseudotyped vector particles (VPs) are a useful tool to study specifically the entry process of a virus in detail and under reduced safety conditions (Schambach et al., 2013; King and Daly, 2014). By pseudotyping VPs with the envelope protein (Env) of an enveloped virus, the entry properties of this virus are obtained. VPs based on lentiviral structural proteins are thus frequently used. Since the main topic of this work was the characterization of the CHIKV entry process, first lentiviral VPs were pseudotpyed with the CHIKV Env proteins.

The characterization of these CHIKV Env pseudotyped VPs revealed production of CHIKV Env in the transfected producer cells (Figure 18 A). Furthermore, analysis of the ultracentrifuged pellets of producer cells also resulted in the detection of CHIKV Env (Figure 18 B). CHIKV Env could be detected alongside p24, a major structural component of lentiviral VPs. Thus, the CHIKV Env and p24 proteins both could simultaneously be pelleted by ultracentrifugation. This data indicates an efficient incorporation of these proteins into the produced VP, which is a prerequisite for successful transduction of target cells.

Transduction of Huh7 cells in the presence of chloroquine with VPs led to, in the case of CHIKV Env pseudotyping, decreased transduction rates with increasing amounts of chloroquine (Figure 19). Pseudotyping of VPs with vesicular stomatitis virus glycoprotein (VSV-G) revealed the same results, and pseudotyping with Gibbon ape leukemia virus transmembrane protein (GaLV TM) rendered VP entry insensitive to chloroquine treatment. Chloroqine is an organic small molecule that neutralizes the acidic pH in endosomes (Farias, Kleber Juvenal Silva et al., 2014). VSV cell entry was found to be pH dependent (Johannsdottir et al., 2009), whereas GaLV is not (Weiss and Tailor, 1995). The cell entry of CHIKV again is dependent on an acidic pH in endosomes (Sourisseau et al., 2007). Thus, CHIKV Env is not only efficiently incorporated in lentiviral VPs, but it additionally shares a key feature of the entry with the wild-type (wt) virus.

Another key feature of viral cell entry is its cell tropism, which is due to the presence or absence of several virus-specific molecules or structures on the cell surface, and other molecules involved in the internalization of the virus. Many different cell lines were transduced with CHIKV Env VPs and compared to transduction rates of VSV-G VPs to match lentiviral VP effects on transduction (Figure 20). All endothelial and epithelial cell lines were transduced, and Huh7 and A549 cells showed especially high transduction rates relative to the VSV-G control. In contrast, HepG2 cells showed very low transduction rates. All so far mentioned cell lines were of human origin. However, cells also derived from mice, hamsters, rabbits, or monkeys could be transduced by CHIKV env VPs. A different picture was observed with the human hematopoietic cell lines (Jurkat, Hut78, BJAB, and PM-1 cells).

Jurkat, Hut78, and PM-1 cells are T cell lineage derived, whereas BJAB cells are B cell derived. Here, no transduction was observed. CHIKV wild-type virus exhibits a very similar cellular tropism. Cell lines like HeLa, HEK 293T, or MRC5 show high infection rates, whereas peripheral blood mononuclear cells (PBMCs) or Jurkat cells are not infectable (Sourisseau et al., 2007). The only hematopoietic cells with a low infection rate by wild-type CHIKV were monocyte-derived macrophages. However, such cells were not tested for CHIKV entry in this study. The molecular basis for the lack of infection of these cells by CHIKV is not known. Comparable results regarding the overall cell tropism were also observed in another study using CHIKV Env pseudotyped VPs (Salvador et al., 2009). Interestingly, A549 lung cells are highly transducable by CHIKV Env pseudotypes in this work and the mentioned study, while infection with wild-type virus is strongly reduced in comparison to HeLa or HEK 293T cells (Sourisseau et al., 2007). Thus, in these cells, obviously CHIKV replication is inhibited at a post-entry step. The efficient VP entry into cells of different mammalian origin resembles the wild-type virus properties, which infects a variety of vertebrate species in the wilderness (Vourc'h et al., 2014).

Summarized, the produced CHIKV Env VPs efficiently incorporate CHIKV Env, their entry is characterized by a pH sensitivity (which is a hallmark of wild-type CHIKV entry), and the cellular tropism is comparable to that of CHIKV Env VPs produced in another study and to the entry range of wild-type CHIKV. The CHIKV env VPs produced in this study thus resemble the key entry properties of wild-type CHIKV and could therefore be used for the following in-depth characterization of the CHIKV entry process, and allow testing of the efficacy of novel CHIKV entry inhibitors and vaccines.

6.2 CHIKV vaccine development

6.2.1 Design, expression, purification, and characterization of protein vaccines; vaccination of mice

A variety of different vaccination approaches against CHIKV have been tested in mice and nonhuman primates (Weaver et al., 2012). These approaches have been based on DNA, proteins, virus-like particles, recombinant heterologous viral vectors, or attenuated wild-type virus. However, only one vaccine candidate has completed the clinical phase I recently (Chang et al., 2014). The further testing and development of a CHIKV vaccine that had already finished phase II was stopped due to safety reasons (Edelman et al., 2000; Schwartz and Albert, 2010). The vast majority of the so far tested vaccines include the E2 protein as a viral antigen (Weaver et al., 2012). It is thought to bind to a cellular receptor, and the majority of alphaviral neutralizing antibodies bind to epitopes within E2 (Voss et al., 2010; Kam et al., 2012b). However, the parts of E2 that are important for a viral envelope-based CHIKV vaccine, and the ones that are negligible, have so far not been defined. The longitudinal analysis of possible linear epitopes within E2 revealed that most early neutralizing antibodies in CHIKV infected humans are directed against one single linear epitope of the E2 protein (Kam et al., 2012b). The same is true for infected nonhuman primates (Kam et al., 2014) and mice (Lum et al., 2013). Furthermore, the early appearance of these antibodies during an infection were associated with long-term clinical protection of these patients (Kam et al., 2012c). Not surprisingly, this linear epitope is very prominently exposed on the surface of CHIKV particles (Figure 21 B). Based on these findings, several artificial E2-based protein vaccines were designed, expressed in, and purified from *E.coli* in this work. The potential vaccines contained either five repeats of the mentioned linear epitope (L), other surface exposed regions of E2 domain A (called sA; including the linear epitope once) linked by glycine-serine linkers, the E2 domain B plus a part of the β-ribbon connector (B[+]), or a combination of these three mentioned modules (Figure 21, Figure 22). These combinations resulted in seven artificial proteins called LsAB[+], LsA, LB[+], sAB[+], sA, B[+], and L. The selection of E2-derived peptides included in the vaccines was based on the location of previously reported neutralizing antibody binding sites within E2, on E2 regions important for cell binding of related alphaviruses, and on the 3D structure of CHIKV E2 (Voss et al., 2010). The successful expression, purification (via His-tag/Ni-NTA), and concentration of all E2-derived vaccine candidates was verified by a Coomassie-stained SDS-PAGE of the proteins (Figure 23). All proteins (except sAB[+]) ran at the expected size and could be purified under native conditions. The slight size deviation of sAB[+] is probably due to co- or post-translational modifications. These should however not modify the majority of the construct's antigenic determinants and thus not alter the effectiveness of the vaccine. The observed minor

contaminations in the gel were not expected to interfere with the efficiency of the E2-derived vaccines, as immune responses against contaminations in a vaccine should not decrease the immune response against the main part of the specific antigens. By mass spectrometry, the only prominent additional bands in the lane of construct LB$^+$ were identified as degradation products of LB$^+$. Thus, these protein fragments should also contribute to the immune response against LB$^+$.

Mice were vaccinated with the recombinant proteins and the sera obtained after the third immunization were screened for the presence of CHIKV neutralizing antibodies. For efficient screening, a high-throughput CHIKV neutralization assay in a 384-well format was developed. It was based on CHIKV-Env pseudotyped lentiviral vectors containing a luciferase gene. This assay was superior over previously published approaches for CHIKV neutralization assay (Gläsker et al., 2013; Kishishita et al., 2013), because of less effort for the production of the luciferase particles, less pipetting work, and/or less time for consumption/incubation periods and overall duration. Additional to these advantages, the 384-well format allows the analysis of many mouse sera in parallel and in several dilutions to obtain quickly a high number of solid data. It is furthermore easily adaptable to the screening of CHIKV entry inhibitors of any substance class. This functional assay can thus be exploited for CHIKV vaccine development or virus entry characterization studies.

The analysis of the sera derived from the protein vaccinated mice revealed significant differences in the inhibition of control VSV-G pseudotyped VPs compared to CHIKV-VPs for the proteins LB$^+$, sAB$^+$, and B$^+$. It was calculated as the difference of the areas under the curves (AUCs) of the neutralization assay (Figure 24 A, Figure 48). When the antibody dilutions, at which the neutralization activity was 50% (NT$_{50}$ values), were compared to the values obtained for VSV-G VPs, results were significantly different for sAB$^+$ and B$^+$ (Figure 24 B, Figure 48). In contrast to these results, the constructs sA or L alone were not able to induce a neutralizing immune response against CHIKV VPs in the vaccinated mice. This result is surprising regarding the fact that three vaccinations of mice with the linear immuno-dominant peptide alone were reported to result in reduced footpad swelling of mice upon CHIKV wild-type challenge (Kam et al., 2012b). However, in this experiment, the peptide was mixed with the strong Freund's adjuvant for vaccination. In this work here, the much milder adjuvant alhydrogel (aluminium hydroxide, "alum") was used. Freund's adjuvant elicits a much stronger antibody response than alum, but is, due to severe side effects such as skin lesions, only used for animal experiments (Alving et al., 2014). In contrast to this adjuvant, alum exhibits usually no or mild side effects, and has already been used as an adjuvant in human vaccines. Thus, in this study, alum was used to resemble vaccination conditions that are more relevant for later use in humans. The species difference between humans and mice

should not contribute to the failure of a neutralizing immune response in mice vaccinated with L, because this antigen was also found to be an important epitope for antibodies in infected mice (Lum et al., 2013). However, in the mentioned studies, only linear epitopes were analyzed and also weak binding of antibodies to these might be detected by the very sensitive ELISA. The majority of selected antibodies might essentially recognize structural epitopes but would also be able to bind linear parts within their structural epitope. This would lead to an overestimation of the proportion of antibodies directed against linear epitopes. Thinking about these possibilities from the vaccine development side, a vaccination solely with the linear epitope might not be sufficient to induce high amounts of neutralizing antibodies due to the lack of a structural epitope within the linear epitope.

The induction of neutralizing antibodies with antigens of domain A (sA) could also not be reached. This result again suggests that structural epitopes are necessary in a potential CHIKV vaccine. Another possibility is that the antigens chosen for sA were not accessible to neutralizing antibodies. However, this possibility is unlikely given the data from CHIKV and other alphaviruses regarding the chosen antigens. A weak induction of neutralizing antibodies upon vaccination with peptides/proteins composed of CHIKV E2 antigens might occur, as shown for the linear epitope mixed with Freund's adjuvant (Kam et al., 2012b) and the construct LsA vaccination in this study (Figure 24), which induced an anti CHIKV immune response shown by Western blot. However, this effect was not significant in this work and was, in general, most probably too weak to be the basis for a CHIKV vaccine in humans.

In contrast to this data, the protein B^+ was part of all vaccines that induced CHIKV neutralizing antibodies. Presumably, the B^+ vaccine was composed of structural and linear epitopes, as it was not composed of artificially linked possible linear epitopes/antigens (like L and sA), but consisted of the whole CHIKV E2 domain B plus a part of the C-terminal β-ribbon. Both regions within E2 contain several antigens for many neutralizing antibodies in other alphaviruses (Voss et al., 2010). Domain B and the acid sensitive region (ASR) within the β-ribbon connector are the first delocalized regions of E2 upon exposure to an acidic pH (Li et al., 2010). Otherwise, domain B might also play a role in binding the cellular receptor of CHIKV (Voss et al., 2010). It would thus require further experiments to ascertain if the neutralizing antibodies directed against parts of B^+ mainly inhibit CHIKV cell binding or E2-E1 heterodimer dissociation in the acidic endosome. The fact that the construct sAB^+ elicits more neutralizing antibodies than B^+ alone might be due to a stabilization of the structure of B^+ by sA, by prolonging the protein's half-life, by elevating immunogenicity due to a larger protein size, and/or by a small additional contribution of sA to the neutralizing capacity (some additional antigens) of induced neutralizing antibodies. The insignificant neutralization of

LsAB[+] immunized mice sera (except the presence of B[+]) might be due to a negative effect of L on the protein's immunogenic properties, by mechanisms opposite of those above.

As depicted in Figure 25, a lack of antibody induction in general was not the reason for the non-existent neutralizing activity of sera obtained from mice vaccinated with LsAB[+], LsA, or L. Only vaccination with sA led to a rather weak antibody production, all other protein constructs induced high amounts of binding antibodies in at least one mouse. Thus, not the lack of binding antibodies, but a lack of neutralizing antibodies was the underlying reason for the observed poor neutralization activity of the mentioned sera. This data again supports the hypothesis that structural epitopes are needed in an efficient CHIKV vaccine.

Altogether, B[+] was necessary and sufficient to induce a neutralizing CHIKV antibody response in mice. sAB[+] induced the most effective responses and was thus used as the essential part for a recombinant Modified Vaccinia virus Ankara (MVA) vaccine.

6.2.2   Generation and characterization of recombinant MVA-CHIKV-sAB[+]

MVA is a highly attenuated virus strain that was used for vaccination of smallpox without inducing remarkable side effects (Stickl, 1974). Furthermore, any transgene of choice can be introduced into the MVA genome (Sutter et al., 1994). MVA infected cells will then, along with the other viral proteins, express high amounts of the protein encoded by the transgene. However, MVA has lost the ability to produce infectious particles in human cells. It is thus a suitable expression platform for any protein vaccine and serves as an "adjuvant" for the essential antigen (Volz and Sutter, 2013). MVA has also been tested in many clinical studies (Sutter and Staib, 2003). Therefore, a recombinant MVA with a transgene encoding the protein that yielded the best neutralization results after vaccination, sAB[+], was created in this work. To enhance its humoral immunogenicity, an N-terminal secretion signal was added.

After successful creation of MVA-CHIKV-sAB[+], the characterization on the genetic level (Figure 28) revealed that the constructed recombinant MVA contained the transgene, but no longer contained the selection marker *K1L* (Figure 26). The observed weak bands of K1L were due to sample contamination (most probably with plasmid DNA). This result is confirmed by the height of the other PCR bands. Furthermore, an in-depth analysis on the protein expression level (Figure 27, Figure 29, Figure 31) revealed efficient long-time expression and secretion of sAB[+] from infected cells. A growth analysis (Figure 30) showed that the insertion of the transgene did not change the host range of MVA, as it was able to grow in human cells.

Summarizing, a stable recombinant MVA-CHIKV-sAB[+] single clone could be isolated, and revealed the desired genetic and expression properties. The vaccination experiments with this isolate are discussed in the next chapter.

6.2.3 Vaccination of mice with MVA-CHIKV-sAB[+] and/or protein sAB[+] with subsequent CHIKV challenge infection

To detect a possible protective effect of MVA-CHIKV-sAB[+] and/or protein sAB[+] vaccination *in vivo*, mice were vaccinated with one of the mentioned vaccines, or a combination of both. Afterwards, they were challenged with wild-type CHIKV and the viral titers in the sera were detected via RT PCR. As visible in Figure 32, viral titers in protein sAB[+] vaccinated mice and in control mice that had already been infected with CHIKV seven weeks before were significantly reduced in comparison to control MVA wild-type vaccinated mice. In contrast to that result, vaccination with MVA-CHIKV-sAB[+] alone or in combination with protein sAB[+] reduced only the titers of 2 out of 5 mice markedly for both immunization approaches. Surprisingly, MVA-sAB[+] vaccination did not reduce viral titers significantly. Other CHIKV vaccination studies with recombinant MVA as an expression platform inserted the whole gene encoding the structural polyprotein C-E3-E2-6K-E1, or the genes for E3-E2 (García-Arriaza et al., 2014; van den Doel et al., 2014; Weger-Lucarelli et al., 2014) into the MVA genome. The vaccination of mice with these recombinant MVA variants resulted in full protection of mice from viremia. However, these studies are difficult to compare with the experiments in this work, because different mouse strains (AG129, C57BL/6 instead of Balb/c), different doses of MVA and infection (about 10-fold lower amount of recombinant MVA, but 100 to 10,000-fold lower amount of CHIKV), and different routes of vaccination and infection (intramuscular, intradermal, or intraperitoneal instead of subcutaneous immunizations; subcutaneous hind foot, or intraperitoneal instead of intranasal infection route) were used. The relatively high number of $1*10^6$ pfu for infection in this study was used to get stable CHIKV titers in the non-immunized control mice. It was 10-fold higher than an intranasal CHIKV infection in another publication (Kumar et al., 2012), because by using $1*10^6$ pfu, the infections were not reproducible (data not shown). The route of infection with direct virus exposure to the mucosae and the relatively high infection dose especially might have led to a lack of significant CHIKV titer reduction in the MVA-CHIKV-sAB[+] vaccinated mice and to a still detectable, however significantly reduced, viral load in protein sAB[+] vaccinated mice.   Another difference to the other studies is that, in CHIKV-sAB^{+} infected cells, the vaccination protein was secreted. All vaccinated mice developed E2 binding antibodies (Figure 33), but they obviously did not have enough neutralization capacity to

reduce viral titers markedly upon infection. Interestingly, another MVA-based CHIKV vaccine also induced CHIKV binding, but not neutralizing antibodies (Weger-Lucarelli et al., 2014). These results indicate a minor role for antibodies in the protective effect of this MVA vaccination. However, a high titer of neutralizing antibodies might be necessary to neutralize incoming virus directly at the mucosal site of infection and thereby to avoid viremia. In two of the other CHIKV MVA studies (García-Arriaza et al., 2014; Weger-Lucarelli et al., 2014), the viral titers in blood were determined via plaque assay, which is a much less sensitive method than the RT PCR detection method used in this work. With a plaque assay, one can detect only replication-competent virus, whereas an RT PCR measures the amount of total viral RNA copies, not distinguishing if these are associated with replication-competent viruses or not. This additional difference in the experimental setting might also contribute to the higher viral titers of vaccinated animals observed in this work. However, reflecting the results of this study, the protein sAB$^+$ is a more promising candidate for a future CHIKV vaccine than MVA-CHIKV-sAB$^+$. Boost immunizations with a mixture of MVA- and protein-based vaccines following an initial vaccination with the recombinant MVA also did not significantly reduce viral titers, indicating that the protein vaccine must be used from the beginning of vaccination to reduce viral titers markedly.

Nonetheless, it was for the first time shown that a small, rationally designed, and artificial protein, which only contains fragments of E2, can reduce viral titers significantly using a mild and clinically tested adjuvant such as alum. These results underscore the potential of E2 domain B and the β-ribbon alone to be the basis for a vaccine that protects from CHIKV replication. Additionally, it confirms their role of being a main target for neutralizing antibodies against alphaviruses (Voss et al., 2010). A protein vaccine like sAB$^+$ is much easier and cheaper to produce than the VLPs tested as a CHIKV vaccine in a clinical study (Chang et al., 2014). Using an optimized vaccination protocol and an appropriate effective adjuvant, sAB$^+$ might be a rationally reduced, safe, and easy-to-produce CHIKV vaccine. Additionally, this work's results indicate that, for other viral vaccines, small protein antigens containing all or most of the relevant and important antigens might be sufficient to develop safe and cheap vaccines. This possibility is especially of importance for developing nations, where CHIKV currently mainly circulates.

6.3   Characterization and inhibition of the Chikungunya virus entry process

6.3.1   Binding of CHIKV E2 to cells

The key role of the E2 domain B in the induction of CHIKV neutralizing antibodies might be due to its putative function in binding to cells, possibly to the unknown cellular receptor. To test if the protein B^+ binds to cells, binding of B^+ or sA to cells of different origin was tested. Indeed, B^+ bound to BHK-21, Huh7, and Jurkat cells, whereas the protein sA did not (Figure 34).

It has been speculated that domain A binds to the cellular receptor of CHIKV, but evidence for that is still lacking (Li et al., 2010; Voss et al., 2010; Porta et al., 2014). To further elucidate the roles of domains A (including the β-ribbon connector), B (lacking the β-ribbon connector in comparison to B^+), and C in CHIKV cell binding, all domains were cloned into a bacterial expression vector, expressed in *E.coli*, and purified via His-tag. The analysis by SDS-PAGE/Coomassie staining revealed a successful expression and the generation of pure CHIKV E2 protein domains and whole extracellular E2 protein as a control (Figure 35). The visible additional bands, especially in the E2 lane, were solely identified as fragments of the respective purified protein. This was a solid starting point for further binding experiments.

Binding experiments with proteins A, B, C, and E2 revealed a significant binding of A, B, and E2 (but not C) to HEK 293T and Jurkat cells (Figure 36). Notably, binding to Jurkat cells was reduced in comparison to binding to 293T cells. Domains A and B (but again not C) bound also to CHO-K1, but domain B not to pgsA-745 cells (Figure 37). Binding of domain A to pgsA-745 cells was also markedly, but not totally, reduced and still significant. For the extracellular part of E2, the same binding pattern as domain A alone was observed. The pgsA-745 cells are a CHO-K1 derived cell line, which lacks all glycosaminoglycans (GAGs) on its surface. GAGs are long, linear chains of sulfated, and thus negatively charged, disaccharide units that are covalently linked to membrane-associated core proteins (Gandhi and Mancera, 2008). They are collectively called proteoglycans (PGs). PGs play an important role in cell signaling (Bishop et al., 2007) and are also exploited by different viruses to promote cell entry (Liu and Thorp, 2002; Kamhi et al., 2013) (see 2.1.5.4).

Binding of domain B to PG-containing cells in the presence of different soluble GAGs was also highly reduced (Figure 38 A, B). For domain A, only heparin (HP) led to a marked decrease in 293T binding, whereas heparan sulfate (HS), chondroitin sulfate (CS), and dermatan sulfate (DS) did not interfere with cell binding (Figure 38 A). HP is a more strongly sulfated, and thus a more negatively charged derivate of HS, that does not occur naturally at

the cell surface or linked to a core protein. Binding of domain A to CHO-K1 cells was only moderately decreased by all soluble GAGs (Figure 38 B). The binding of A, B, C, or E2 to the GAG cell surface-deficient pgsA-745 cells was not altered in a positive or negative way by the presence of soluble GAGs (Figure 38 C). Thus, recombinant E2 domain B binds PGs and facilitates cell binding via PGs, because a lack of cell surface PGs and competition with soluble GAGs both decreased, but did not totally diminish, E2 domain A cell binding.

Performing the appropriate experiments with CHIKV Env pseudotyped VPs yielded similar results. Transduction of pgsA-745 cells is significantly reduced by over 50% in comparison to transduction of the parental CHO-K1 cell line and to 293T cells (Figure 39). If cells were transduced in the presence of soluble GAGs with CHIKV Env VPs using the established 384-well luciferase neutralization assay, the luciferase signal was reduced with increasing GAG amounts on 293T and CHO-K1 cells, HP and dextran sulfate (DX) were especially very effective (Figure 40 D i-ii). Dextran sulfate is also, like the GAGs, a sulfated and thus negatively charged carbohydrate polymer, but its backbone consists solely of glucose monomers. Notably, the transduction rates could not be reduced to less than 10% of the GAG-free control. On pgsA-745 cells, the presence of GAGs did not decrease, but rather enhance transduction with CHIKV VPs (Figure 40 D iii). DX had the weakest enhancing activity. The VSV-G control VPs' transduction efficiencies were enhanced on all cell types by all GAGs and by DX (Figure 40 A i-iii). The adeno-associated virus isolate 2 (AAV-2) control VPs yielded a similar picture as CHIKV Env VPs, but the enhancement of transduction on pgsA-745 cells was only observed for CS and DS (Figure 40 B i-iii). Lymphocytic Choriomeningitis Virus envelope protein (LCMV Env) pseudotyped VP transduction was not influenced by the presence of any soluble GAG or DX on CHO-K1 and pgsA-745 cells, and only on 293T cells were some effects visible (Figure 40 C i-iii). Further experiments revealed that the replication of wild-type CHIKV was also reduced significantly in pgsA-745 cells in comparison to CHO-K1 cells (6 hours post infection). However, this effect was less pronounced 24 hours post infection, yet still significant (Figure 41). Additionally, CHIKV wild-type replication in 293T cells was significantly reduced in the presence of soluble GAGs (Figure 42 A). It was shown in subsequent experiments that this reduced replication is due to significantly reduced cell binding and/or internalization of CHIKV (Figure 42 B).

The described findings reveal a novel and very interesting role for cell surface GAGs during CHIKV infection. So far, the role of GAGs in CHIKV replication has only been studied during viral attenuation. Point mutations within the E2 domain A (e.g., E79K or G82R) have been found in attenuated vaccine strains, which were cell culture adapted and GAG-dependent, but showed reduced *in vivo* replication (Ashbrook et al., 2014; Gardner et al., 2014; Silva et

al., 2014). Additionally, it was published that for some CHIKV strains cell surface GAGs promote replication, but that the replication is not inhibited by the presence of soluble GAGs (Silva et al., 2014). Additionally, one CHIKV strain was published to not be influenced by the presence or absence of PGs at all (Gardner et al., 2012). Interestingly, however, GAG utilization was observed to enhance neurovirulence in the related alphavirus eastern equine encephalitis virus (EEEV) (Gardner et al., 2011). It must be mentioned that the viral titers for CHIKV replication in the absence of PG, or the lack of inhibition by soluble GAGs, in the above mentioned studies were measured 48 (Gardner et al., 2012) and 18 (Silva et al., 2014) hours post-infection. However, the observed effects in this work were most prominent at 6 hours post-infection. At 24 hours post-infection, viral titers in CHO-K1 cells and pgsA-745 cells were more comparable, which is in accordance with the mentioned published data (Figure 41).

This data supports a scenario in which cell surface GAGs are not absolutely necessary for CHIKV replication, but undoubtedly they promote viral replication. This hypothesis is supported by the fact that transduction with CHIKV pseudotyped VPs is significantly reduced, but not totally diminished, in pgsA-745 cells (Figure 39). The same is true for the inhibition of transduction by soluble GAGs, which are able to reduce transduction of PG-containing cells, but only by a maximal 90% (Figure 40). The other studies thus measured viral titers at time points that were too late, when the GAG-dependency was no longer detectable. The lack of GAG-dependency at a later time point during infection can be explained by possible direct cell-to-cell transmission, as it was observed for CHIKV (Lee et al., 2011) in cell culture, or could just be due to kinetic reasons (for example, the majority of cells are already infected 18 hours post-infection and the viral titer is already on a plateau, regardless of whether the cell entry is less efficient or not). In cell culture, the virus is obviously able to compensate the lack of binding to cell surface GAGs with time, but this might not be true for the *in vivo* situation. *In vivo*, the virus is confronted with much more complicated tissue barriers, lower local concentrations of virus, and the immune system. The data from this study further strongly proposes that the promotion of viral replication occurs at the entry point of the viral life cycle. This conclusion could be demonstrated with both CHIKV Env pseudotyped VPs and wild-type CHIKV (Figure 39; Figure 40 D i,ii; Figure 42 B). These observations make sense, as GAGs are, as mentioned, found on the cell surface of all animal cells (Bishop et al., 2007).

Another noteworthy fact is that all soluble GAGs and DX even enhance the transduction rates of CHIKV Env VPs on pgsA-745 cells (Figure 40 D iii). Thus, they compensate for the lack of GAGs on the cell surface of this cell line. The soluble GAGs are most probably solely

present in the cell supernatant and not associated with the cell membrane. The arguments for this presumption are i) that the strongly negatively charged and hydrophilic GAGs are not expected to bind to the likewise negatively charged and rather hydrophobic membrane, and ii) that soluble GAGs did not enable the recombinant E2 domains A and especially B to bind to the cell membrane (Figure 38 C). The responsible molecular event/interaction for transduction enhancement consequently has to take place in the cell supernatant before cell attachment. Furthermore, this transduction enhancement is not due to an unspecific enhancement of lentiviral VP transduction in general, as lentiviral VPs pseudotyped with LCMV Env did not reveal an enhanced transduction by the treatment with GAGs on CHO-K1 and pgsA-745 cells (Figure 40 C ii,iii). On 293T cells, the effects were also diverse (Figure 40 C i). The inhibition of CHIKV Env VP transduction on 293T and CHO-K1 cells (Figure 40 D i, ii) is most efficient using HP (also for infection with wild-type virus; Figure 42) and DX. Enhancement on pgsA-745 cells is most efficiently done again by HP, and also mediated by DX, which features a totally different carbohydrate backbone in comparison to the GAGs (Figure 40 D iii). These facts highlight that negative charge is an important factor for the observed effects of GAGs on CHIKV entry. Nonetheless, the carbohydrate structure of the GAG backbone obviously also plays a role, as DX is the weakest enhancer of transduction on pgsA-745 cells (and HP, as mentioned, the strongest). AAV-2 entry is also most efficiently inhibited by HP and DX (Figure 40 B i,ii), although HS is an important cellular attachment factor for AAV-2 (Summerford and Samulski, 1998). The enhancement effect for AAV-2 on pgsA-745 cells is interestingly only visible for CS and DS, and only at higher GAG concentrations (Figure 40 B iii). Summarizing these results, one can conclude that the observed inhibition and enhancement impacts of GAGs on CHIKV Env VP transduction are specific effects.

The mechanism behind the observed enhancement of transduction efficiencies by soluble GAGs could be a pre-activation of the CHIKV envelope proteins through binding to the soluble GAGs. This binding might induce conformational changes within the envelope proteins that render them to bind more effectively to structures on the cell surface, which then would promote viral uptake. Such an activation of the virus was also described for the human papillomavirus type 16 (HPV-16) in the presence of HP, which allowed HPV-16 infection in the absence of cell surface PGs (Cerqueira et al., 2013). Cell surface HS is an important attachment factor for HPV-16 (Raff et al., 2013). For AAV-2 particles, slight structural rearrangements on the cell surface were also described upon HP binding (O'Donnell et al., 2009), which might explain the observed enhanced transduction by the addition of CS and DS (Figure 40 B iii) Furthermore, it was proposed that initial structural rearrangements on the alphavirus surface occur directly after binding to the cell surface

(Vaney et al., 2013), based on the observation that transitional epitopes of the Sindbis virus (SINV) became accessible to antibodies upon cell binding (Flynn et al., 1990; Meyer and Johnston, 1993). This activation of a CHIKV Env molecule, resulting in binding to an unknown cell surface structure, might then lead to an allosteric transmission of the activation signal through the whole viral particle (Wu et al., 2007; Vaney et al., 2013). Additionally, findings that SINV membrane fusion occurred directly at the plasma membrane at neutral pH (Kononchik et al., 2011), and that the E2-E1 heterodimer only dissociates fully after insertion of the E1 fusion loop into the host cell membrane (Cao and Zhang, 2013), challenge the state-of-the-art alphavirus cell entry model and suggest a more complex and possibly heterogeneous entry scenario(s). Based on the mentioned publications, it is tempting to speculate that binding to GAGs induces an allosteric structural rearrangement of CHIKV envelope proteins, which primes them for the subsequent binding to another cell surface molecule. Binding to this second molecule is only possible after activation by GAGs. On the other hand, there must be at least one other cell entry pathway, as CHIKV entry into GAG-deficient cells is still possible (Figure 39, Figure 41), and soluble GAGs or DX cannot fully block CHIKV cell entry (Figure 40 D, Figure 42). This additional pathway(s) consequently includes different cell surface receptors and is totally independent of cell surface GAGs. For 293T and CHO-K1 cell entry, CHIKV would, following this hypothesis, use both (or more) pathways, and on pgsA-745 cells, the GAG-dependent pathway is blocked, which leads to a decreased replication rate in these cells. However, the virus can compensate for this blocked entry pathway by using the alternative pathway(s) and receptor(s). The kinetic disadvantage in cell infection on pgsA-745 cells is due to the alternative(s) and the absence of any other anatomic or immunological hurdles, at least in cell culture, is compensated with time (Figure 41). Through the addition of soluble GAGs, the lack of cell surface GAGs is artificially compensated for and the required structural rearrangements occur in the supernatant instead of at the cell surface (which is the case for 293T and CHO-K1 cells). This enables the CHIKV Env proteins to bind to the proposed second molecule involved in GAG-dependent entry, which broadens the opportunities for the virus to infect pgsA-745 cells and consequently leads to the observed enhanced transduction rates.

The results obtained from binding studies of E2 domains suggest that domain A cell binding is promoted by cell surface GAGs, as A binding to CHO-K1 cells is stronger than binding to pgsA-745 cells (Figure 37). However, significant binding to GAG-deficient cells by domain A occurs and is not or only moderately inhibited by the addition of soluble GAGs (expect HP on 293T cells) using 293T or CHO-K1 cells (Figure 38). Hence, domain A binds to another additional molecule(s) on the cell surface, possibly the cellular receptor(s) of CHIKV. In contrast, domain B binding is literally absent on pgsA-745 cells and inhibited on CHO-K1 and

293T cells by the addition of soluble GAGs. This implies that domain B solely binds to GAGs. Domain C, on the other hand, does not bind to any cell type (Figure 36, Figure 37). These findings are in line with the crystal structure of the E2-E1 heterodimer and the whole alphavirus trimer (Li et al., 2010; Voss et al., 2010), where domain C is located close to the viral membrane, hidden and not directly accessible on the viral surface. In contrast, domain A and especially domain B are prominently exposed on the viral membrane and it was speculated that mainly domain A interacts with the cellular receptor (Li et al., 2010; Voss et al., 2010; Porta et al., 2014), which is in line with the findings in this work. Looking closely at the data, the degree of inhibition of domains A/B binding by HP is comparable to that of the other GAGs (except for domain A on 293T cells, Figure 38 A). This again suggests that negative charge is not the only feature of GAGs that makes them bind to CHIKV E2. The cell binding data with the recombinant protein domains support the hypothesis that at least two cell entry pathways for CHIKV exist. One is GAG-dependent, the other is not.

During the GAG-dependent pathway, the prominently exposed domain B binds to cell surface GAGs. This induces a conformational change of the CHIKV Env molecules, which might allosterically spread to the other CHIKV Env molecules on the particle's surface (Vaney et al., 2013). The conformational change is promoted by the GAG's negative charge and the structure of the carbohydrate backbone. A neutral pH might be sufficient, but the negative charge could also promote the conformational change by creating an acidic microenvironment in the vicinity of the CHIKV envelope proteins. This activation enables the envelope molecules to bind to a second molecule on the cell surface via domain A. Following this binding, the virus is taken up by receptor-mediated endocytosis and the further pH induced conformational changes occur.

In the GAG-independent pathway, the virus directly binds via domain A to a second cellular receptor of CHIKV, which again promotes the endosomic uptake. Further alternative pathways may exist.

The proposed entry pathways must be mediated by different binding sites on the E2 protein, because the second pathway is not inhibited in the presence of soluble GAGs on 293T and CHO-K1 cells. Furthermore, there is entry enhancement on GAG-deficient pgsA-745 cells. This means that by the addition of soluble GAGs, a new door is opened, while the first door still remains opened.

PGs on the cell surface thus are not totally required, but they are part of one strategy CHIKV employs in order to enter cells. They might be comparable with T cell immunoglobulin and mucin (TIM) membrane proteins that promote, although are not absolutely required, the cell

entry of a number of viruses, including CHIKV (Moller-Tank et al., 2014). Additionally, direct cell-to-cell transmission of CHIKV particles might play a role *in vivo* and is another option to infect cells, as proposed in cell culture (Lee et al., 2011). The fact that CHIKV is able to infect a wide range of, and evolutionary only distantly related, species, and infect, within one organism, many different cell types and organs (Schwartz and Albert, 2010), makes the scenario in which the virus can utilize the ubiquitously expressed GAGs (Bishop et al., 2007) for entry plausible, but the virus additionally exploits other opportunities and receptors to get into the host cell.

The published data about enhanced GAG-dependency mediated by mutations in domain A (Ashbrook et al., 2014; Gardner et al., 2014; Silva et al., 2014) provide evidence that extremely cell culture adapted GAG-binding and dependency attenuates viral replication *in vivo*. The results of this work provide evidence that GAG binding in principle promotes viral fitness and is mainly mediated by cell binding via domain B. In summary, the virus possibly has to find a balance between too weak and too strong GAG-binding to efficiently replicate *in vivo*.

However, one has to take into account that the proposed activation of CHIKV particles by GAGs prior to receptor binding is based on results with pseudotyped VPs and not with wild-type virus. The CHIKV Env proteins are, as shown in this work, expressed and incorporated into VPs. Additionally, the entry properties of the pseudotypes resemble those of the wild-type virus by testing different conditions. However, it cannot be stated that the detailed molecular structure and the entry mechanisms of the CHIKV Env VPs are exactly the same as for the wild-type virus, especially when keeping in mind the stringent and complex structure of the CHIKV shell and surface. Furthermore, it cannot be excluded that the purified recombinant single domains A, B, C, and the whole E2 proteins might exhibit a different folding pattern, and thus binding properties, than when they are integrated into the E2-E1 heterodimer. The proteins were produced by prokaryotes and folding was not promoted by interactions within the E2-E1 heterodimer. Hence, further experiments are needed to further support the proposed scenarios for CHIKV entry. Nonetheless, in summary, the obtained results give a consistent picture and support the proposed model. It is worthwhile to further check this model and to clarify the role and detailed mechanisms of GAG-mediated CHIKV cell entry, especially regarding its *in vivo* relevance. GAG mimetica might thus be promising broad-spectrum antiviral candidates for treatment of CHIKV infections and other pathogens (Mathias et al., 2013; Zoppe et al., 2014).

6.3.2   CHIKV entry inhibition by Epigallocatechin-3-gallate (EGCG)

EGCG is a catechin and the major component of green tea. It is believed to have various biological, including antiviral, activities, acting mainly at the cell entry step of the viral life cycle (Colpitts and Schang, 2014). Its galloyl side chain, which is missing in another catechin in green tea, epicatechin (EC), is believed to be responsible for its biological activities (Nagle et al., 2006). For these reasons, a possible anti CHIKV effect of EGCG was evaluated in this work.

Infection of cells in the presence of EGCG was significantly inhibited (Figure 43). This was also the case for EC, however to lesser extent (Figure 43). Using pseudotyped VPs, which only resemble the CHIKV entry process, the same inhibition as GAGs was observed by EGCG, and EC induced inhibition was weaker (Figure 44 A, D). VSV-G VP entry into target cells was also inhibited by EGCG and only slightly inhibited for EC (Figure 44 B, D). However, the overall inhibition was weaker than for CHIKV Env VPs, and the difference between EGCG and EC regarding the degree of inhibition was less pronounced. A possible general effect of EGCG on transduction with lentiviral VPs would influence both pseudotypes to the same degree, suggesting a specific anti-CHIKV effect of EGCG. Moreover, VSV entry inhibition by EGCG was published recently (Colpitts and Schang, 2014), which supports these findings and a specific anti-CHIKV effect of EGCG. AAV-2 entry was inhibited by EGCG and EC only at very high concentrations (Figure 44 C, D).
EGCG also inhibited wild-type virus at the cell entry step significantly, and EC again showed a less prominent, but still significant, inhibition of infection (Figure 45). The anti-CHIKV effect disappeared if EGCG was added to the cells 2 hours post-infection (Figure 46). Additionally, when bypassing the cell entry step by direct transfection of CHIKV genomic RNA into cells, EGCG or EC did not influence CHIKV replication (Figure 47).
This data strongly indicates that EGCG inhibits CHIKV replication at the entry step of the viral life cycle. Effects of EC treatment were only moderate in comparison to EGCG, indicating that the galloyl side chain of EGCG plays a major role in the anti-CHIKV activity.

The CHIKV entry might be inhibited at the attachment or the fusion step. If CHIKV Env expressing cells are exposed to a low pH, they are able to fuse with neighboring untreated cells and form syncytia with them. When lowering of the pH took place in the presence of EGCG, the formed syncytia were not lesser in degree (data not shown). An inhibition of syncytia formation, yet not significant, was observed only at very high EGCG concentrations of 100 µg/ml. The CHIKV Env spikes on the cell surface could already interact with attachment molecules of neighboring cells prior to the addition of EGCG, making it difficult for

EGCG to compete with these preexisting complexes. This proposed mechanism is most probably the reason that EGCG could not inhibit syncytia formation significantly, and makes it very unlikely that it interferes with viral fusion. Instead, the cell attachment of CHIKV is the step that is very likely inhibited by EGCG.

It has been previously published that EGCG inhibits viral attachment through competition with sialic acid or HP on the cell surface (Colpitts and Schang, 2014). This result could explain the broad antiviral effect of EGCG, taking into account that many viruses use these cell surface structures to promote their entry (see 2.1.5.4). Additionally, it is also a reasonable mode of action for the inhibition of CHIKV, which was shown in this work to exploit cell surface GAGs as an attachment factor (see 6.3.1). The EGCG inhibitory effect on viral replication was published previously to be in the range of about 12 µM (IC_{50}) (Steinmann et al., 2013), which is in line with the IC_{50} values observed in the CHIKV Env VP experiments of this work (6.5 µg/ml).

The oral consumption of EGCG, through drinking green tea, most probably is not sufficient to obtain the required EGCG concentrations into the relevant tissues. However, application of EGCG via a transdermal gel has been tested in mice. Upon application, it was found in the dermis and epidermis (Lambert et al., 2006). Furthermore, polyphenon E is an approved topical treatment against genital and anal warts, which contains a mixture of green tea catechins (Steinmann et al., 2013). Thus, topical EGCG application might be an option to treat mosquito bites, in order to inhibit a potential initial CHIKV replication at the site of the bite. Additionally, EGCG could serve as a lead compound for development of a small compound with higher efficacy that could be an efficient drug for the treatment of CHIKF.

7. Outlook

In this work, it could be shown that vaccination with a small artificial Chikungunya virus (CHIKV) E2-derived protein, sAB$^+$, could reduce viral titers significantly in mice. The results furthermore suggest that structural epitopes of E2 are superior over linear epitopes to induce neutralizing antibodies, because vaccination with a protein containing short antigens of domain A (sA) linked by glycine-serine linkers did not lead to a neutralizing immune response, whereas the whole domain B plus a part of the β-ribbon connector (B$^+$) did. However, this result has not been shown in a direct comparison so far. To further elucidate the role of structural versus linear epitopes, one could vaccinate mice with the protein sA in comparison to the whole domain A, and a construct with only the surface-exposed regions of domain B linked by glycine-serine linkers (sB) versus the whole domain B. Subsequently, the induction of neutralizing antibodies should be detected. These experiments would provide clear and directly comparable data to determine if structural epitopes are needed, and are always superior over linear epitopes, for vaccination against CHIKV. At the same time, a direct comparison of vaccination with domain A versus domain B could be performed to have an additional small protein as a potential vaccine at hand. Furthermore, the tested protein vaccine sAB$^+$ could be further improved by testing different adjuvants, routes of vaccination, mouse models, and routes of infection challenge.

A high-throughput CHIKV luciferase-based neutralization assay was developed in this work to detect the CHIKV entry inhibition potential of mouse sera, antibodies, and Epigallocatechin-3-gallate (EGCG). Further potential inhibitors of CHIKV entry derived from any source could be tested by this assay quickly, easily, in several dilutions and in high numbers, and then checked for their potential as antivirals in additional experiments, as it was done for EGCG.

An important role of cell surface glycosaminoglycans (GAGs) for CHIKV cell entry was uncovered in this work. However, the molecular details of this mode of interaction are still missing. One could, for example, remove the sulfates from cell surface GAGs and detect how infection rates with CHIKV or transduction rates with CHIKV envelope (Env) pseudotyped vector particles (VPs) change. Furthermore, differences in the GAG pattern of different cell lines could be measured via mass spectrometry (MS) and related to CHIKV transduction data of these cell lines. Circular dichroism (CD) spectra of the purified recombinant E2 domains A, B, C, and whole extracellular E2 could be made to confirm their correct and native folding. Incubation of the domains with cells, subsequent precipitation and MS analysis would reveal the molecular binding partners of these domains on the cell surface.

8. Summary

The Chikungunya virus (CHIKV) is a mosquito-transmitted alphavirus that causes high fever, rash, and recurrent arthritis in humans. The majority of symptoms disappear after about one week. However, arthritis can last for months or even years (in about 30% of cases), which makes people unable to work during this period. The virus is endemic in Sub-Saharan Africa, the Indian Ocean islands, India, and Southeast Asia. It has additionally caused several large outbreaks in the last few years, affecting millions of people. The mortality rate is very low (0.1%), but the infection rates are high (sometimes 30%) and the number of asymptomatic cases is rare (about 15%). The first CHIKV outbreak in a country with a moderate climate was detected in Italy in 2007. Furthermore, the virus has spread to the Caribbean in late 2013. Due to climate change, globalization, and vector switching, the virus will most likely continue to cause new worldwide outbreaks. Additionally, more temperate regions of the world like Europe or the USA, which have recently reported their first cases, will likely become targets. Alarmingly, there is no specific treatment or vaccination against CHIKV available so far.

The cell entry process of CHIKV is also not understood in detail, and was thusly the focus of study for this project. The E2 envelope protein is responsible for cell attachment and entry. It consists of the domain C, located close to the viral membrane, domain A, in the center of the protein, and domain B, at the distal end, prominently exposed on the viral surface.

In this work, the important role of cell surface glycosaminoglycans (GAGs) for CHIKV cell attachment was uncovered. GAGs consist of long linear chains of heavily sulfated disaccharide units and can be covalently linked to membrane associated proteins. They play an important role in different cell signaling pathways. So far, solely cell culture passage has revealed an increased GAG-dependency of CHIKV due to mutations in E2 domain A, which was associated with virus attenuation *in vivo*. However, in this work it could be shown that cell surface GAGs promote CHIKV entry using non-cell culture adapted CHIKV envelope (Env) proteins. Transduction and infection of cell surface GAG-deficient pgsA-745 cells with CHIKV Env pseudotyped vector particles (VPs) and with wild-type CHIKV revealed decreased transduction and replication rates. Furthermore, cell entry and transduction rates of GAG-containing cells were also dose-dependently decreased in the presence of soluble GAGs. In contrast, transduction of pgsA-745 cells with CHIKV Env pseudotyped VPs was enhanced by the addition of soluble GAGs. This data suggests a mechanism by which GAGs activate CHIKV particles for subsequent binding to a cellular receptor. However, at least one GAG-independent entry pathway might exist, as CHIKV entry could not be totally inhibited by

soluble GAGs and entry into pgsA-745 was, albeit at a lower rate, still possible. Further binding experiments using recombinant CHIKV E2 domains A, B, and C suggest that domain B is responsible for the GAG binding, domain A possibly for receptor binding, and domain C is not involved in cell binding. These results are in line with the geometry of CHIKV Env on the viral surface. They altogether reveal that GAG binding promotes viral cell entry and that the E2 domain B plays a central role for this mechanism.

As no vaccine against CHIKV has been approved so far, another goal of this project was to test new vaccination approaches. It has been published that a single linear epitope of E2 is the target of the majority of early neutralizing antibodies against CHIKV in patients. Artificial E2-derived proteins were created, expressed in *E.coli*, and successfully purified. They consisted of 5 repeats of the mentioned linear epitope (L), the surface exposed regions of domain A linked by glycine-serine linkers (sA), the whole domain B plus a part of the β-ribbon connector (B[+]), or a combination of these 3 modules. Vaccination experiments revealed that B[+] was necessary and sufficient to induce a neutralizing immune response in mice, with the protein sAB[+] yielding the best results. sAB[+], as a protein vaccine, efficiently and significantly reduced viral titers in mice upon CHIKV challenge, which was not the case for recombinant Modified Vaccinia virus Ankara (MVA; MVA-CHIKV-sAB[+]), as a vaccine platform expressing the same protein. These experiments show that a small rationally designed CHIKV Env derived protein might, after optimization of some vaccination parameters, be sufficient as a safe, easy-to-produce, and cheap CHIKV vaccine.

Epigallocatechin-3-gallate (EGCG) is a catechin found in green tea and was, in this work, found to inhibit the CHIKV life cycle at the entry state in *in vitro* experiments using CHIKV Env VPs and wild-type virus. EGCG was recently published to inhibit attachment of several viruses to cell surface GAGs, which is in line with the role for GAGs in CHIKV entry revealed in this work. EGCG might serve as a lead compound for the development of a small molecule treatment against CHIKV.

9. References

Agarwal, A., Dash, P.K., Singh, A.K., Sharma, S., Gopalan, N., Rao, Putcha Venkata Lakshmana, Parida, M.M., and Reiter, P. (2014). Evidence of Experimental Vertical Transmission of Emerging Novel ECSA Genotype of Chikungunya Virus in Aedes aegypti. PLoS Negl Trop Dis *8*, e2990.

Agarwal, S., Nikolai, B., Yamaguchi, T., Lech, P., and Somia, N.V. (2006). Construction and use of retroviral vectors encoding the toxic gene barnase. Mol. Ther. *14*, 555-563.

Aggarwal, M., Tapas, S., Preeti, Siwach, A., Kumar, P., Kuhn, R.J., and Tomar, S. (2012). Crystal structure of aura virus capsid protease and its complex with dioxane: new insights into capsid-glycoprotein molecular contacts. PLoS ONE *7*, e51288.

Akahata, W., Yang, Z.-Y., Andersen, H., Sun, S., Holdaway, H.A., Kong, W.-P., Lewis, M.G., Higgs, S., Rossmann, M.G., and Rao, S., et al. (2010). A virus-like particle vaccine for epidemic Chikungunya virus protects nonhuman primates against infection. Nat. Med. *16*, 334-338.

Alving, C.R., Matyas, G.R., Torres, O., Jalah, R., and Beck, Z. (2014). Adjuvants for vaccines to drugs of abuse and addiction. Vaccine *32*, 5382-5389.

Andersson, H., Barth, B.U., Ekström, M., and Garoff, H. (1997). Oligomerization-dependent folding of the membrane fusion protein of Semliki Forest virus. Journal of Virology *71*, 9654-9663.

Antoine, G., Scheiflinger, F., Dorner, F., and Falkner, F.G. (1998). The Complete Genomic Sequence of the Modified Vaccinia Ankara Strain: Comparison with Other Orthopoxviruses. Virology *244*, 365-396.

Arias-Goeta, C., Mousson, L., Rougeon, F., and Failloux, A.-B. (2013). Dissemination and transmission of the E1-226V variant of chikungunya virus in Aedes albopictus are controlled at the midgut barrier level. PLoS ONE *8*, e57548.

Arnaud, F., Caporale, M., Varela, M., Biek, R., Chessa, B., Alberti, A., Golder, M., Mura, M., Zhang, Y.-P., and Yu, L., et al. (2007). A paradigm for virus-host coevolution: sequential counter-adaptations between endogenous and exogenous retroviruses. PLoS Pathog. *3*, e170.

Ashbrook, A.W., Burrack, K.S., Silva, L.A., Montgomery, S.A., Heise, M.T., Morrison, T.E., and Dermody, T.S. (2014). Residue 82 of the Chikungunya Virus E2 Attachment Protein Modulates Viral Dissemination and Arthritis in Mice. J. Virol.

Bernard, E., Solignat, M., Gay, B., Chazal, N., Higgs, S., Devaux, C., and Briant, L. (2010). Endocytosis of chikungunya virus into mammalian cells: role of clathrin and early endosomal compartments. PLoS ONE *5*, e11479.

Bishop, J.R., Schuksz, M., and Esko, J.D. (2007). Heparan sulphate proteoglycans fine-tune mammalian physiology. Nature *446*, 1030-1037.

Bouraï, M., Lucas-Hourani, M., Gad, H.H., Drosten, C., Jacob, Y., Tafforeau, L., Cassonnet, P., Jones, L.M., Judith, D., and Couderc, T., et al. (2012). Mapping of Chikungunya virus interactions with host proteins identified nsP2 as a highly connected viral component. J. Virol. *86*, 3121-3134.

Bourjot, M., Delang, L., van Nguyen, H., Neyts, J., Guéritte, F., Leyssen, P., and Litaudon, M. (2012). Prostratin and 12-O-tetradecanoylphorbol 13-acetate are potent and selective inhibitors of Chikungunya virus replication. J. Nat. Prod. *75*, 2183-2187.

Brandler, S., Ruffié, C., Combredet, C., Brault, J.-B., Najburg, V., Prevost, M.-C., Habel, A., Tauber, E., Desprès, P., and Tangy, F. (2013). A recombinant measles vaccine expressing chikungunya virus-like particles is strongly immunogenic and protects mice from lethal challenge with chikungunya virus. Vaccine *31*, 3718-3725.

Broukamp, P., Petrussevska, R.T., Breitkreutz, D., Hornung, J., Markham, A., and Fusenig, N.E. (1988). Normal keratinization in a spontaneously immortalized aneuploid human keratinocyte cell line. The Journal of Cell Biology *106*, 761-771.

Calland, N., Albecka, A., Belouzard, S., Wychowski, C., Duverlie, G., Descamps, V., Hober, D., Dubuisson, J., Rouillé, Y., and Séron, K. (2012). (-)-Epigallocatechin-3-gallate is a new inhibitor of hepatitis C virus entry. Hepatology *55*, 720-729.

Caminade, C., Medlock, J.M., Ducheyne, E., McIntyre, K.M., Leach, S., Baylis, M., and Morse, A.P. (2012). Suitability of European climate for the Asian tiger mosquito Aedes albopictus: recent trends and future scenarios. J R Soc Interface *9*, 2708-2717.

Cao, S., and Zhang, W. (2013). Characterization of an early-stage fusion intermediate of Sindbis virus using cryoelectron microscopy. Proc. Natl. Acad. Sci. U.S.A. *110*, 13362-13367.

Carey, D.E. (1971). Chikungunya and Dengue: A case of mistaken identity? Journal of the History of Medicine *26*, 243-262.

Cauchemez, S., Ledrans, M., Poletto, C., Quenel, P., Valk, H. de, Colizza, V., and Boelle, P.Y. (2014). Local and regional spread of chikungunya fever in the Americas. Euro Surveillance *19*, 1-9.

Cerqueira, C., Liu, Y., Kühling, L., Chai, W., Hafezi, W., van Kuppevelt, Toin H, Kühn, J.E., Feizi, T., and Schelhaas, M. (2013). Heparin increases the infectivity of Human Papillomavirus type 16 independent of cell surface proteoglycans and induces L1 epitope exposure. Cell. Microbiol. *15*, 1818-1836.

Chang, L.-J., Dowd, K.A., Mendoza, F.H., Saunders, J.G., Sitar, S., Plummer, S.H., Yamshchikov, G., Sarwar, U.N., Hu, Z., and Enama, M.E., et al. (2014). Safety and tolerability of chikungunya virus-like particle vaccine in healthy adults: a phase 1 dose-escalation trial. The Lancet.

Chen, C., Qiu, H., Gong, J., Liu, Q., Xiao, H., Chen, X.-W., Sun, B.-L., and Yang, R.-G. (2012). (-)-Epigallocatechin-3-gallate inhibits the replication cycle of hepatitis C virus. Arch. Virol. *157*, 1301-1312.

Chen, R., Wang, E., Tsetsarkin, K.A., and Weaver, S.C. (2013). Chikungunya virus 3' untranslated region: adaptation to mosquitoes and a population bottleneck as major evolutionary forces. PLoS Pathog. *9*, e1003591.

Chen, W., Foo, S.-S., Rulli, N.E., Taylor, A., Sheng, K.-C., Herrero, L.J., Herring, B.L., Lidbury, B.A., Li, R.W., and Walsh, N.C., et al. (2014). Arthritogenic alphaviral infection perturbs osteoblast function and triggers pathologic bone loss. Proc. Natl. Acad. Sci. U.S.A. *111*, 6040-6045.

Chernomordik, L.V., and Kozlov, M.M. (2008). Mechanics of membrane fusion. Nat. Struct. Mol. Biol. *15*, 675-683.

Chu, H., Das, S.C., Fuchs, J.F., Suresh, M., Weaver, S.C., Stinchcomb, D.T., Partidos, C.D., and Osorio, J.E. (2013). Deciphering the protective role of adaptive immunity to CHIKV/IRES a novel candidate vaccine against Chikungunya in the A129 mouse model. Vaccine *31*, 3353-3360.

Ciesek, S., Hahn, T. von, Colpitts, C.C., Schang, L.M., Friesland, M., Steinmann, J., Manns, M.P., Ott, M., Wedemeyer, H., and Meuleman, P., et al. (2011). The green tea polyphenol, epigallocatechin-3-gallate, inhibits hepatitis C virus entry. Hepatology *54*, 1947-1955.

Colpitts, C.C., and Schang, L.M. (2014). A small molecule inhibits virion attachment to heparan sulfate- or sialic acid-containing glycans. J. Virol. *88*, 7806-7817.

Cronin, J., Zhang, X.-Y., and Reiser, J. (2005). Altering the tropism of lentiviral vectors through pseudotyping. Curr Gene Ther. *5*, 387-398.

Dull, T., Zufferey, R., Kelly, M., Mandel, Kelly R. J., Nguyen, M., Trono, D., and Naldini, L. (1998). A third-generation lentivirus vector with a conditional packaging system. Journal of Virology *72*, 8463-8471.

Edelman, R., Tacket, C.O., Wasserman, S.S., Bodison, S.A., Perry, J.G., and Mangiafico, J.A. (2000). Phase II safety and immunogenicity study of a live chikungunya virus vaccine TSI-GSD-218. American Journal of Tropical Medicine and Hygiene *62*.

Farias, Kleber Juvenal Silva, Machado, Paula Renata Lima, de Almeida Junior, Renato Ferreira, de Aquino, Ana Alice, and da Fonseca, Benedito Antônio Lopes (2014). Chloroquine interferes with dengue-2 virus replication in U937 cells. Microbiol. Immunol. *58*, 318-326.

Fassina, G., Buffa, A., Benelli, R., Varnier, O.E., Noonan, D.M., and Albini, A. (2002). Polyphenolic antioxidant (-)-epigallocatechin-3-gallate from green tea as a candidate anti-HIV agent. Aids *16*, 939-941.

Fenner, F. (1988). Smallpox and its eradication (Geneva: World health organization).

Firth, A.E., Chung, B.Y., Fleeton, M.N., and Atkins, J.F. (2008). Discovery of frameshifting in Alphavirus 6K resolves a 20-year enigma. Virol. J. *5*, 108.

Fischer, M., and Staples, J.E. (2014). Chikungunya virus spreads in the Americas - Caribbean and South America, 2013-14. Morbidity and Mortality Weekly Report *63*, 500-501.

Flynn, D.C., Meyer, W.J., Mackenzie Jr, J M, and Johnston, R.E. (1990). A conformational change in Sindbis virus glycoproteins E1 and E2 is detected at the plasma membrane as a consequence of early virus-cell interaction. J. Virol. *64*, 3643-3653.

Fongsaran, C., Jirakanwisal, K., Kuadkitkan, A., Wikan, N., Wintachai, P., Thepparit, C., Ubol, S., Phaonakrop, N., Roytrakul, S., and Smith, D.R. (2014). Involvement of ATP synthase β subunit in chikungunya virus entry into insect cells. Arch. Virol.

Fric, J., Bertin-Maghit, S., Wang, C.-I., Nardin, A., and Warter, L. (2013). Use of human monoclonal antibodies to treat Chikungunya virus infection. J. Infect. Dis. *207*, 319-322.

Gallian, P., Lamballerie, X. de, Salez, N., Piorkowski, G., Richard, P., Paturel, L., Djoudi, R., Leparc-Goffart, I., Tiberghien, P., and Chiaroni, J. (2014). Prospective detection of chikungunya virus in blood donors, Caribbean 2014. Blood *123*, 3679-3681.

Gandhi, N.S., and Mancera, R.L. (2008). The structure of glycosaminoglycans and their interactions with proteins. Chem Biol Drug Des *72*, 455-482.

García-Arriaza, J., Cepeda, V., Hallengärd, D., Sorzano, Carlos Óscar S, Kümmerer, B.M., Liljeström, P., and Esteban, M. (2014). A novel poxvirus-based vaccine, MVA-CHIKV, is highly immunogenic and protects mice against chikungunya infection. J. Virol. *88*, 3527-3547.

Gardner, C.L., Burke, C.W., Higgs, S.T., Klimstra, W.B., and Ryman, K.D. (2012). Interferon-alpha/beta deficiency greatly exacerbates arthritogenic disease in mice infected with wild-type chikungunya virus but not with the cell culture-adapted live-attenuated 181/25 vaccine candidate. Virology *425*, 103-112.

Gardner, C.L., Ebel, G.D., Ryman, K.D., and Klimstra, W.B. (2011). Heparan sulfate binding by natural eastern equine encephalitis viruses promotes neurovirulence. Proc. Natl. Acad. Sci. U.S.A. *108*, 16026-16031.

Gardner, C.L., Hritz, J., Sun, C., Vanlandingham, D.L., Song, T.Y., Ghedin, E., Higgs, S., Klimstra, W.B., and Ryman, K.D. (2014). Deliberate attenuation of chikungunya virus by adaptation to heparan sulfate-dependent infectivity: a model for rational arboviral vaccine design. PLoS Negl Trop Dis *8*, e2719.

Gérardin, P., Sampériz, S., Ramful, D., Boumahni, B., Bintner, M., Alessandri, J.-L., Carbonnier, M., Tiran-Rajaoefera, I., Beullier, G., and Boya, I., et al. (2014). Neurocognitive outcome of children exposed to perinatal mother-to-child Chikungunya virus infection: the CHIMERE cohort study on Reunion Island. PLoS Negl Trop Dis *8*, e2996.

Gläsker, S., Lulla, A., Lulla, V., Couderc, T., Drexler, J.F., Liljeström, P., Lecuit, M., Drosten, C., Merits, A., and Kümmerer, B.M. (2013). Virus replicon particle based Chikungunya virus neutralization assay using Gaussia luciferase as readout. Virol. J. *10*, 235.

Goh, Lucas Y H, Hobson-Peters, J., Prow, N.A., Gardner, J., Bielefeldt-Ohmann, H., Pyke, A.T., Suhrbier, A., and Hall, R.A. (2013). Neutralizing monoclonal antibodies to the E2 protein of chikungunya virus protects against disease in a mouse model. Clin. Immunol. *149*, 487-497.

Grandadam, M., Caro, V., Plumet, S., Thiberge, J.M., Souarès, Y., Failloux, A.-B., Tolou, H.J., Budelot, M., Cosserat, D., and Leparc-Goffart, I., et al. (2011). Chikungunya virus, southeastern France. Emerging Infect. Dis. *17*, 910-913.

Greene, I.P., Wang, E., Deardorff, E.R., Milleron, R., Domingo, E., and Weaver, S.C. (2005). Effect of alternating passage on adaptation of sindbis virus to vertebrate and invertebrate cells. J. Virol. *79*, 14253-14260.

Hallengärd, D., Kakoulidou, M., Lulla, A., Kümmerer, B.M., Johansson, D.X., Mutso, M., Lulla, V., Fazakerley, J.K., Roques, P., and Le Grand, R., et al. (2014). Novel attenuated Chikungunya vaccine candidates elicit protective immunity in C57BL/6 mice. J. Virol. *88*, 2858-2866.

Hawman, D.W., Stoermer, K.A., Montgomery, S.A., Pal, P., Oko, L., Diamond, M.S., and Morrison, T.E. (2013). Chronic joint disease caused by persistent Chikungunya virus infection is controlled by the adaptive immune response. J. Virol. *87*, 13878-13888.

Hoarau, J.-J., Gay, F., Pellé, O., Samri, A., Jaffar-Bandjee, M.-C., Gasque, P., and Autran, B. (2013). Identical Strength of the T Cell Responses against E2, nsP1 and Capsid CHIKV Proteins in Recovered and Chronic Patients after the Epidemics of 2005-2006 in La Reunion Island. PLoS ONE *8*, 1-9.

Hochstein-Mintzel, V., Hanichen, T., Huber, H.C., and Stickl, H. (1975). [An attenuated strain of vaccinia virus (MVA). Successful intramuscular immunization against vaccinia and variola (author's transl)]. Zentralbl. Bakteriol. Orig. A *230*.

Johannsdottir, H.K., Mancini, R., Kartenbeck, J., Amato, L., and Helenius, A. (2009). Host cell factors and functions involved in vesicular stomatitis virus entry. J. Virol. *83*, 440-453.

Jose, J., Przybyla, L., Edwards, T.J., Perera, R., Burgner, J.W., and Kuhn, R.J. (2012). Interactions of the cytoplasmic domain of Sindbis virus E2 with nucleocapsid cores promote alphavirus budding. J. Virol. *86*, 2585-2599.

Jose, J., Snyder, J.E., and Kuhn, R.J. (2009). A structural and functional perspective of alphavirus replication and assembly. Future Microbiol *4*, 837-856.

Kam, Y.-W., Lee, Wendy W L, Simarmata, D., Harjanto, S., Teng, T.-S., Tolou, H., Chow, A., Lin, Raymond T P, Leo, Y.-S., and Rénia, L., et al. (2012a). Longitudinal analysis of the human antibody response to Chikungunya virus infection: implications for serodiagnosis and vaccine development. J. Virol. *86*, 13005-13015.

Kam, Y.-W., Lee, Wendy W L, Simarmata, D., Le Grand, R., Tolou, H., Merits, A., Roques, P., and Ng, Lisa F P (2014). Unique epitopes recognized by antibodies induced in Chikungunya virus-infected non-human primates: implications for the study of immunopathology and vaccine development. PLoS ONE *9*, e95647.

Kam, Y.-W., Lum, F.-M., Teo, T.-H., Lee, Wendy W L, Simarmata, D., Harjanto, S., Chua, C.-L., Chan, Y.-F., Wee, J.-K., and Chow, A., et al. (2012b). Early neutralizing IgG response to Chikungunya virus in infected patients targets a dominant linear epitope on the E2 glycoprotein. EMBO Mol Med *4*, 330-343.

Kam, Y.-W., Simarmata, D., Chow, A., Her, Z., Teng, T.-S., Ong, Edward K S, Rénia, L., Leo, Y.-S., and Ng, Lisa F P (2012c). Early appearance of neutralizing immunoglobulin G3 antibodies is associated with chikungunya virus clearance and long-term clinical protection. J. Infect. Dis. *205*, 1147-1154.

Kamhi, E., Joo, E.J., Dordick, J.S., and Linhardt, R.J. (2013). Glycosaminoglycans in infectious disease. Biol Rev Camb Philos Soc *88*, 928-943.

Kaur, P., and Chu, Justin Jang Hann (2013). Chikungunya virus: an update on antiviral development and challenges. Drug Discov. Today *18*, 969-983.

Kielian, M. (2010). An alphavirus puzzle solved. Nature *468*, 645-646.

Kielian, M., Chanel-Vos, C., and Liao, M. (2010). Alphavirus Entry and Membrane Fusion. Viruses *2*, 796-825.

Kielian, M., and Rey, F.A. (2006). Virus membrane-fusion proteins: more than one way to make a hairpin. Nat. Rev. Microbiol. *4*, 67-76.

Kim, M., Kim, S.-Y., Lee, H.W., Shin, J.S., Kim, P., Jung, Y.-S., Jeong, H.-S., Hyun, J.-K., and Lee, C.-K. (2013). Inhibition of influenza virus internalization by (-)-epigallocatechin-3-gallate. Antiviral Res. *100*, 460-472.

King, B., and Daly, J. (2014). Pseudotypes: your flexible friends. Future Microbiology *9*, 135-137.

Kishishita, N., Takeda, N., Anuegoonpipat, A., and Anantapreecha, S. (2013). Development of a pseudotyped-lentiviral-vector-based neutralization assay for chikungunya virus infection. J. Clin. Microbiol. *51*, 1389-1395.

Kononchik, J.P., Hernandez, R., and Brown, D.T. (2011). An alternative pathway for alphavirus entry. Virol. J. *8*, 304.

Kumar, M., Sudeep, A.B., and Arankalle, V.A. (2012). Evaluation of recombinant E2 protein-based and whole-virus inactivated candidate vaccines against chikungunya virus. Vaccine *30*, 6142-6149.

Kümmerer, B.M., Grywna, K., Gläsker, S., Wieseler, J., and Drosten, C. (2012). Construction of an infectious Chikungunya virus cDNA clone and stable insertion of mCherry reporter genes at two different sites. J. Gen. Virol. *93*, 1991-1995.

Labadie, K., Larcher, T., Joubert, C., Mannioui, A., Delache, B., Brochard, P., Guigand, L., Dubreil, L., Lebon, P., and Verrier, B., et al. (2010). Chikungunya disease in nonhuman primates involves long-term viral persistence in macrophages. J. Clin. Invest. *120*, 894-906.

Lambert, J.D., Kim, D.H., Zheng, R., and Yang, C.S. (2006). Transdermal delivery of (-)-epigallocatechin-3-gallate, a green tea polyphenol, in mice. J. Pharm. Pharmacol. *58*, 599-604.

Lee, C.Y., Kam, Y.-W., Fric, J., Malleret, B., Koh, Esther G L, Prakash, C., Huang, W., Lee, Wendy W L, Lin, C., and Lin, Raymond T P, et al. (2011). Chikungunya virus neutralization antigens and direct cell-to-cell transmission are revealed by human antibody-escape mutants. PLoS Pathog. *7*, e1002390.

Leparc-Goffart, I., Nougairede, A., Cassadou, S., Prat, C., and Lamballerie, X. de (2014). Chikungunya in the Americas. The Lancet *383*, 514.

Li, L., Jose, J., Xiang, Y., Kuhn, R.J., and Rossmann, M.G. (2010). Structural changes of envelope proteins during alphavirus fusion. Nature *468*, 705-708.

Lim, P.J., and Chu, Justin Jang Hann (2014). A polarized cell model for Chikungunya virus infection: entry and egress of virus occurs at the apical domain of polarized cells. PLoS Negl Trop Dis *8*, e2661.

Liu, J., and Thorp, S.C. (2002). Cell surface heparan sulfate and its roles in assisting viral infections. Med Res Rev *22*, 1-25.

Lobigs, M., Hongxing, Z., and Garoff, H. (1990). Function of Semliki Forest virus E3 peptide in virus assembly: replacement of E3 with an artifical signal peptide abolishes spike heterodimerization and surface expression of E1. Journal of Virology *64*, 4346-4355.

Lum, F.-M., Teo, T.-H., Lee, Wendy W L, Kam, Y.-W., Rénia, L., and Ng, Lisa F P (2013). An essential role of antibodies in the control of Chikungunya virus infection. J. Immunol. *190*, 6295-6302.

Martinez, M.G., Snapp, E.-L., Perumal, G.S., Macaluso, F.P., and Kielian, M. (2014). Imaging the alphavirus exit pathway. J. Virol. *88*, 6922-6933.

Mathias, D.K., Pastrana-Mena, R., Ranucci, E., Tao, D., Ferruti, P., Ortega, C., Staples, G.O., Zaia, J., Takashima, E., and Tsuboi, T., et al. (2013). A small molecule glycosaminoglycan mimetic blocks Plasmodium invasion of the mosquito midgut. PLoS Pathog. *9*, e1003757.

Merten, C.A., Stitz, J., Braun, G., Poeschla, E.M., Cichutek, K., and Buchholz, C.J. (2005). Directed evolution of retrovirus envelope protein cytoplasmic tails guided by functional incorporation into lentivirus particles. J. Virol. *79*, 834-840.

Messaoudi, I., Vomaske, J., Totonchy, T., Kreklywich, C.N., Haberthur, K., Springgay, L., Brien, J.D., Diamond, M.S., Defilippis, V.R., and Streblow, D.N. (2013). Chikungunya virus infection results in higher and persistent viral replication in aged rhesus macaques due to defects in anti-viral immunity. PLoS Negl Trop Dis *7*, e2343.

Meyer, H., Sutter, G., and Mayr, A. (1991). Mapping of deletions in the genome of the highly attenuated vaccinia virus MVA and their influence on virulence. Journal of General Virology *72*, 1031-1038.

Meyer, W.J., and Johnston, R.E. (1993). Structural rearrangement of infecting Sindbis virions at the cell surface: mapping of newly accessible epitopes. J. Virol. *67*, 5117-5125.

Moller-Tank, S., Albritton, L.M., Rennert, P.D., and Maury, W. (2014). Characterizing Functional Domains for TIM-Mediated Enveloped Virus Entry. J. Virol. *88*, 6702-6713.

Mullis, K., Faloona, F., Scharf, S., Saiki, R., Horn, G., and Erlich, H. (1992). Specific enzymatic amplification of DNA in vitro: the polymerase chain reaction. 1986. Biotechnology *24*, 17-27.

Münch, R.C., Janicki, H., Völker, I., Rasbach, A., Hallek, M., Büning, H., and Buchholz, C.J. (2013). Displaying high-affinity ligands on adeno-associated viral vectors enables tumor cell-specific and safe gene transfer. Mol. Ther. *21*, 109-118.

Muthumani, K., Lankaraman, K.M., Laddy, D.J., Sundaram, S.G., Chung, C.W., Sako, E., Wu, L., Khan, A., Sardesai, N., and Kim, J.J., et al. (2008). Immunogenicity of novel consensus-based DNA vaccines against Chikungunya virus. Vaccine *26*, 5128-5134.

Nagle, D.G., Ferreira, D., and Zhou, Y.-D. (2006). Epigallocatechin-3-gallate (EGCG): chemical and biomedical perspectives. Phytochemistry *67*, 1849-1855.

O'Donnell, J., Taylor, K.A., and Chapman, M.S. (2009). Adeno-associated virus-2 and its primary cellular receptor--Cryo-EM structure of a heparin complex. Virology *385*, 434-443.

Olagnier, D., Scholte, Florine E M, Chiang, C., Albulescu, I.C., Nichols, C., He, Z., Lin, R., Snijder, E.J., van Hemert, Martijn J, and Hiscott, J. (2014). Inhibition of dengue and chikungunya virus infections by RIG-I-mediated type I interferon-independent stimulation of the innate antiviral response. J. Virol. *88*, 4180-4194.

PAHO and WHO (2014). Number of Reported Cases of Chikungunya Fever in the Americas, by Country or Territory 2013-2014 (to week noted); Epidemiological Week / EW 38 (Updated 19 September 2014).
http://www.paho.org/hq/index.php?option=com_topics&view=article&id=343&Itemid=40931.

Pal, P., Dowd, K.A., Brien, J.D., Edeling, M.A., Gorlatov, S., Johnson, S., Lee, I., Akahata, W., Nabel, G.J., and Richter, Mareike K S, et al. (2013). Development of a highly protective combination monoclonal antibody therapy against Chikungunya virus. PLoS Pathog. *9*, e1003312.

Panning, M., Charrel, R.N., Donoso Mantke, O., Mantke, O.D., Landt, O., Niedrig, M., and Drosten, C. (2009). Coordinated implementation of chikungunya virus reverse transcription-PCR. Emerging Infect. Dis. *15*, 469-471.

Parashar, D., Paingankar, M.S., Kumar, S., Gokhale, M.D., Sudeep, A.B., Shinde, S.B., and Arankalle, V.A. (2013). Administration of E2 and NS1 siRNAs inhibit chikungunya virus replication in vitro and protects mice infected with the virus. PLoS Negl Trop Dis *7*, e2405.

Pialoux, G., Gaüzère, B.-A., Jauréguiberry, S., and Strobel, M. (2007). Chikungunya, an epidemic arbovirosis. The Lancet Infectious Diseases *7*, 319-327.

Plante, K., Wang, E., Partidos, C.D., Weger, J., Gorchakov, R., Tsetsarkin, K., Borland, E.M., Powers, A.M., Seymour, R., and Stinchcomb, D.T., et al. (2011). Novel chikungunya vaccine candidate with an IRES-based attenuation and host range alteration mechanism. PLoS Pathog. *7*, e1002142.

Poo, Y.S., Nakaya, H., Gardner, J., Larcher, T., Schroder, W.A., Le, T.T., Major, L.D., and Suhrbier, A. (2014). CCR2 Deficiency Promotes Exacerbated Chronic Erosive Neutrophil-Dominated Chikungunya Virus Arthritis. J. Virol. *88*, 6862-6872.

Porta, J., Jose, J., Roehrig, J.T., Blair, C.D., Kuhn, R.J., and Rossmann, M.G. (2014). Locking and blocking the viral landscape of an alphavirus with neutralizing antibodies. J. Virol. *88*, 9616-9623.

Powers, A.M., Brault, A.C., Tesh, R.B., and Weaver, S.C. (2000). Re-emergence of chikungunya and o'nyong-nyong viruses: evidence for distinct geographical lineages and distant evolutionary relationships. Journal of General Virology *81*, 471-479.

Raff, A.B., Woodham, A.W., Raff, L.M., Skeate, J.G., Yan, L., Da Silva, Diane M, Schelhaas, M., and Kast, W.M. (2013). The evolving field of human papillomavirus receptor research: a review of binding and entry. J. Virol. *87*, 6062-6072.

Raman, R., Sasisekharan, V., and Sasisekharan, R. (2005). Structural insights into biological roles of protein-glycosaminoglycan interactions. Chem. Biol. *12*, 267-277.

Rana, J., Rajasekharan, S., Gulati, S., Dudha, N., Gupta, A., Chaudhary, V.K., and Gupta, S. (2014). Network mapping among the functional domains of Chikungunya virus nonstructural proteins. Proteins.

Rashad, A.A., and Keller, P.A. (2013). Structure based design towards the identification of novel binding sites and inhibitors for the chikungunya virus envelope proteins. J. Mol. Graph. Model. *44*, 241-252.

Rashad, A.A., Mahalingam, S., and Keller, P.A. (2014). Chikungunya virus: emerging targets and new opportunities for medicinal chemistry. J. Med. Chem. *57*, 1147-1166.

Rezza, G., Nicoletti, L., Angelini, R., Romi, R., Finarelli, A.C., Panning, M., Cordioli, P., Fortuna, C., Boros, S., and Magurano, F., et al. (2007). Infection with chikungunya virus in Italy: an outbreak in a temperate region. The Lancet *370*, 1840-1846.

Rose, P.P., Hanna, S.L., Spiridigliozzi, A., Wannissorn, N., Beiting, D.P., Ross, S.R., Hardy, R.W., Bambina, S.A., Heise, M.T., and Cherry, S. (2011). Natural resistance-associated macrophage protein is a cellular receptor for sindbis virus in both insect and mammalian hosts. Cell Host Microbe *10*, 97-104.

Roy, C.J., Adams, A.P., Wang, E., Plante, K., Gorchakov, R., Seymour, R.L., Vinet-Oliphant, H., and Weaver, S.C. (2014). Chikungunya vaccine candidate is highly attenuated and protects nonhuman primates against telemetrically monitored disease following a single dose. J. Infect. Dis. *209*, 1891-1899.

Salvador, B., Zhou, Y., Michault, A., Muench, M.O., and Simmons, G. (2009). Characterization of Chikungunya pseudotyped viruses: Identification of refractory cell lines and demonstration of cellular tropism differences mediated by mutations in E1 glycoprotein. Virology *393*, 33-41.

Sánchez-San Martín, C., Sosa, H., and Kielian, M. (2008). A stable prefusion intermediate of the alphavirus fusion protein reveals critical features of class II membrane fusion. Cell Host Microbe *4*, 600-608.

Schambach, A., Zychlinski, D., Ehrnstroem, B., and Baum, C. (2013). Biosafety features of lentiviral vectors. Hum. Gene Ther. *24*, 132-142.

Schuffenecker, I., Iteman, I., Michault, A., Murri, S., Frangeul, L., Vaney, M.-C., Lavenir, R., Pardigon, N., Reynes, J.-M., and Pettinelli, F., et al. (2006). Genome microevolution of chikungunya viruses causing the Indian Ocean outbreak. PLoS Med. *3*, e263.

Schwartz, O., and Albert, M.L. (2010). Biology and pathogenesis of chikungunya virus. Nat. Rev. Microbiol. *8*, 491-500.

Selvarajah, S., Sexton, N.R., Kahle, K.M., Fong, R.H., Mattia, K.-A., Gardner, J., Lu, K., Liss, N.M., Salvador, B., and Tucker, D.F., et al. (2013). A neutralizing monoclonal antibody targeting the acid-sensitive region in chikungunya virus E2 protects from disease. PLoS Negl Trop Dis *7*, e2423.

Shin, G., Yost, S.A., Miller, M.T., Elrod, E.J., Grakoui, A., and Marcotrigiano, J. (2012). Structural and functional insights into alphavirus polyprotein processing and pathogenesis. Proc. Natl. Acad. Sci. U.S.A. *109*, 16534-16539.

Silva, L.A., Khomandiak, S., Ashbrook, A.W., Weller, R., Heise, M.T., Morrison, T.E., and Dermody, T.S. (2014). A single-amino-acid polymorphism in Chikungunya virus E2 glycoprotein influences glycosaminoglycan utilization. J. Virol. *88*, 2385-2397.

Snyder, A.J., and Mukhopadhyay, S. (2012). The alphavirus E3 glycoprotein functions in a clade-specific manner. J. Virol. *86*, 13609-13620.

Snyder, J.E., Kulcsar, K.A., Schultz, Kimberly L W, Riley, C.P., Neary, J.T., Marr, S., Jose, J., Griffin, D.E., and Kuhn, R.J. (2013). Functional characterization of the alphavirus TF protein. J. Virol. *87*, 8511-8523.

Solignat, M., Gay, B., Higgs, S., Briant, L., and Devaux, C. (2009). Replication cycle of chikungunya: a re-emerging arbovirus. Virology *393*, 183-197.

Soneoka, Y., Cannon, P.M., Ramsdale, E.E., Griffiths, J.C., Romano, G., Kingsman, S.M., and Kingsman, A.J. (1995). A transient three-plasmid expression system for the production of high titer retroviral vectors. Nucl Acids Res *23*, 628-633.

Sourisseau, M., Schilte, C., Casartelli, N., Troillet, C., Guivel-Benhassine, F., Rudnicka, D., Sol-Foulon, N., Le Roux, K., Prévost, M.-C., and Fsihi, H., et al. (2007). Characterization of Reemerging Chikungunya Virus. PLoS Pathog. *3*, 804-817.

Staib, C., Drexler, I., and Sutter, G. (2004). Construction and isolation of recombinant MVA. Methods Mol Biol *269*, 77-99.

Stapleford, K.A., Coffey, L.L., Lay, S., Bordería, A.V., Duong, V., Isakov, O., Rozen-Gagnon, K., Arias-Goeta, C., Blanc, H., and Beaucourt, S., et al. (2014). Emergence and transmission of arbovirus evolutionary intermediates with epidemic potential. Cell Host Microbe *15*, 706-716.

Steinmann, J., Buer, J., Pietschmann, T., and Steinmann, E. (2013). Anti-infective properties of epigallocatechin-3-gallate (EGCG), a component of green tea. Br. J. Pharmacol. *168*, 1059-1073.

Stickl, H. (1974). [MVA vaccination against smallpox: clinical tests with an attenuated live vaccinia virus strain (MVA) (author's transl)]. Dtsch. Med. Wochenschr. *99*, 2386-2392.

Strauss, J.H., and Strauss, E.G. (1994). The alphaviruses: gene expression, replication, and evolution. Microbiology and Molecular Biology Reviews *58*, 491-562.

Summerford, C., and Samulski, R.J. (1998). Membrane-associated heparan sulfate proteoglycan is a receptor for adeno-associated virus type 2 virions. J. Virol. *72*, 1438-1445.

Sutter, G., and Moss, B. (1992). Nonreplicating vaccinia vector efficiently expresses recombinant genes. Proc. Natl. Acad. Sci. U.S.A. *89*, 10847-10851.

Sutter, G., Ramsey-Ewing, A., Rosales, R., and Moss, B. (1994). Stable expression of the vaccinia virus K1L gene in rabbit cells complements the host range defect of vaccinia virus mutant. J. Virol. *68*, 4109-4116.

Sutter, G., and Staib, C. (2003). Vaccinia Vectors as Candidate Vaccines: The Development of Modified Vaccinia Virus Ankara for Antigen Delivery. CDTID *3*, 263-271.

Tang, B.L. (2012). The cell biology of Chikungunya virus infection. Cell. Microbiol. *14*, 1354-1363.

Tang, J., Jose, J., Chipman, P., Zhang, W., Kuhn, R.J., and Baker, T.S. (2011). Molecular links between the E2 envelope glycoprotein and nucleocapsid core in Sindbis virus. J. Mol. Biol. *414*, 442-459.

Teo, T.-H., Lum, F.-M., Claser, C., Lulla, V., Lulla, A., Merits, A., Rénia, L., and Ng, Lisa F P (2013). A pathogenic role for CD4+ T cells during Chikungunya virus infection in mice. J. Immunol. *190*, 259-269.

Thiberville, S.-D., Boisson, V., Gaudart, J., Simon, F., Flahault, A., and Lamballerie, X. de (2013). Chikungunya fever: a clinical and virological investigation of outpatients on Reunion Island, South-West Indian Ocean. PLoS Negl Trop Dis *7*, e2004.

Tretyakova, I., Hearn, J., Wang, E., Weaver, S., and Pushko, P. (2014). DNA vaccine initiates replication of live attenuated chikungunya virus in vitro and elicits protective immune response in mice. J. Infect. Dis. *209*, 1882-1890.

Tsetsarkin, K.A., Chen, R., Leal, G., Forrester, N., Higgs, S., Huang, J., and Weaver, S.C. (2011). Chikungunya virus emergence is constrained in Asia by lineage-specific adaptive landscapes. Proc. Natl. Acad. Sci. U.S.A. *108*, 7872-7877.

Tsetsarkin, K.A., Chen, R., Yun, R., Rossi, S.L., Plante, K.S., Guerbois, M., Forrester, N., Perng, G.C., Sreekumar, E., and Leal, G., et al. (2014). Multi-peaked adaptive landscape for chikungunya virus evolution predicts continued fitness optimization in Aedes albopictus mosquitoes. Nat Commun *5*, 4084.

Tsetsarkin, K.A., McGee, C.E., Volk, S.M., Vanlandingham, D.L., Weaver, S.C., and Higgs, S. (2009). Epistatic roles of E2 glycoprotein mutations in adaption of chikungunya virus to Aedes albopictus and Ae. aegypti mosquitoes. PLoS ONE *4*, e6835.

Tsetsarkin, K.A., Vanlandingham, D.L., McGee, C.E., and Higgs, S. (2007). A single mutation in chikungunya virus affects vector specificity and epidemic potential. PLoS Pathog. *3*, e201.

Uchime, O., Fields, W., and Kielian, M. (2013). The role of E3 in pH protection during alphavirus assembly and exit. J. Virol. *87*, 10255-10262.

van den Doel, Petra, Volz, A., Roose, J.M., Sewbalaksing, V.D., Pijlman, G.P., van Middelkoop, I., Duiverman, V., van de Wetering, Eva, Sutter, G., and Osterhaus, Albert D M E, et al. (2014). Recombinant Modified Vaccinia Virus Ankara Expressing Glycoprotein E2 of Chikungunya Virus Protects AG129 Mice against Lethal Challenge. PLoS Negl Trop Dis *8*, e3101.

Vaney, M.-C., Duquerroy, S., and Rey, F.A. (2013). Alphavirus structure: activation for entry at the target cell surface. Curr Opin Virol *3*, 151-158.

Vazeille, M., Moutailler, S., Coudrier, D., Rousseaux, C., Khun, H., Huerre, M., Thiria, J., Dehecq, J.-S., Fontenille, D., and Schuffenecker, I., et al. (2007). Two Chikungunya isolates from the outbreak of La Reunion (Indian Ocean) exhibit different patterns of infection in the mosquito, Aedes albopictus. PLoS ONE *2*, e1168.

Volk, S.M., Chen, R., Tsetsarkin, K.A., Adams, A.P., Garcia, T.I., Sall, A.A., Nasar, F., Schuh, A.J., Holmes, E.C., and Higgs, S., et al. (2010). Genome-scale phylogenetic analyses of chikungunya virus reveal independent emergences of recent epidemics and various evolutionary rates. J. Virol. *84*, 6497-6504.

Volz, A., and Sutter, G. (2013). Protective efficacy of Modified Vaccinia virus Ankara in preclinical studies. Vaccine *31*, 4235-4240.

Voss, J.E., Vaney, M.-C., Duquerroy, S., Vonrhein, C., Girard-Blanc, C., Crublet, E., Thompson, A., Bricogne, G., and Rey, F.A. (2010). Glycoprotein organization of Chikungunya virus particles revealed by X-ray crystallography. Nature *468*, 709-712.

Vourc'h, G., Halos, L., Desvars, A., Boué, F., Pascal, M., Lecollinet, S., Zientara, S., Duval, T., Nzonza, A., and Brémont, M. (2014). Chikungunya antibodies detected in non-human primates and rats in three Indian Ocean islands after the 2006 ChikV outbreak. Vet. Res. *45*, 52.

Wang, D., Suhrbier, A., Penn-Nicholson, A., Woraratanadharm, J., Gardner, J., Luo, M., Le, T.T., Anraku, I., Sakalian, M., and Einfeld, D., et al. (2011a). A complex adenovirus vaccine against chikungunya virus provides complete protection against viraemia and arthritis. Vaccine *29*, 2803-2809.

Wang, E., Kim, D.Y., Weaver, S.C., and Frolov, I. (2011b). Chimeric Chikungunya viruses are nonpathogenic in highly sensitive mouse models but efficiently induce a protective immune response. J. Virol. *85*, 9249-9252.

Weaver, S.C. (2014). Arrival of chikungunya virus in the new world: prospects for spread and impact on public health. PLoS Negl Trop Dis *8*, e2921.

Weaver, S.C., Osorio, J.E., Livengood, J.A., Chen, R., and Stinchcomb, D.T. (2012). Chikungunya virus and prospects for a vaccine. Expert Rev Vaccines *11*, 1087-1101.

Weger-Lucarelli, J., Chu, H., Aliota, M.T., Partidos, C.D., and Osorio, J.E. (2014). A novel MVA vectored Chikungunya virus vaccine elicits protective immunity in mice. PLoS Negl Trop Dis *8*, e2970.

Weiss, R.A., and Tailor, C.S. (1995). Retrovirus receptors. Cell *82*, 531-533.

Williamson, M.P., McCormick, T.G., Nance, C.L., and Shearer, W.T. (2006). Epigallocatechin gallate, the main polyphenol in green tea, binds to the T-cell receptor, CD4: Potential for HIV-1 therapy. J. Allergy Clin. Immunol. *118*, 1369-1374.

Wintachai, P., Wikan, N., Kuadkitkan, A., Jaimipuk, T., Ubol, S., Pulmanausahakul, R., Auewarakul, P., Kasinrerk, W., Weng, W.-Y., and Panyasrivanit, M., et al. (2012). Identification of prohibitin as a Chikungunya virus receptor protein. J. Med. Virol. *84*, 1757-1770.

Wu, S.-R., Haag, L., Hammar, L., Wu, B., Garoff, H., Xing, L., Murata, K., and Cheng, R.H. (2007). The dynamic envelope of a fusion class II virus. Prefusion stages of semliki forest virus revealed by electron cryomicroscopy. J. Biol. Chem. *282*, 6752-6762.

Yamaguchi, K., Honda, M., Ikigai, H., Hara, Y., and Shimamura, T. (2002). Inhibitory effects of (-)-epigallocatechin gallate on the life cycle of human immunodeficiency virus type 1 (HIV-1). Antiviral Research *53*, 19-34.

Zoppe, J.O., Ruottinen, V., Ruotsalainen, J., Rönkkö, S., Johansson, L.-S., Hinkkanen, A., Järvinen, K., and Seppälä, J. (2014). Synthesis of cellulose nanocrystals carrying tyrosine sulfate mimetic ligands and inhibition of alphavirus infection. Biomacromolecules *15*, 1534-1542.

10.   Appendix

10.1 Appendix figure
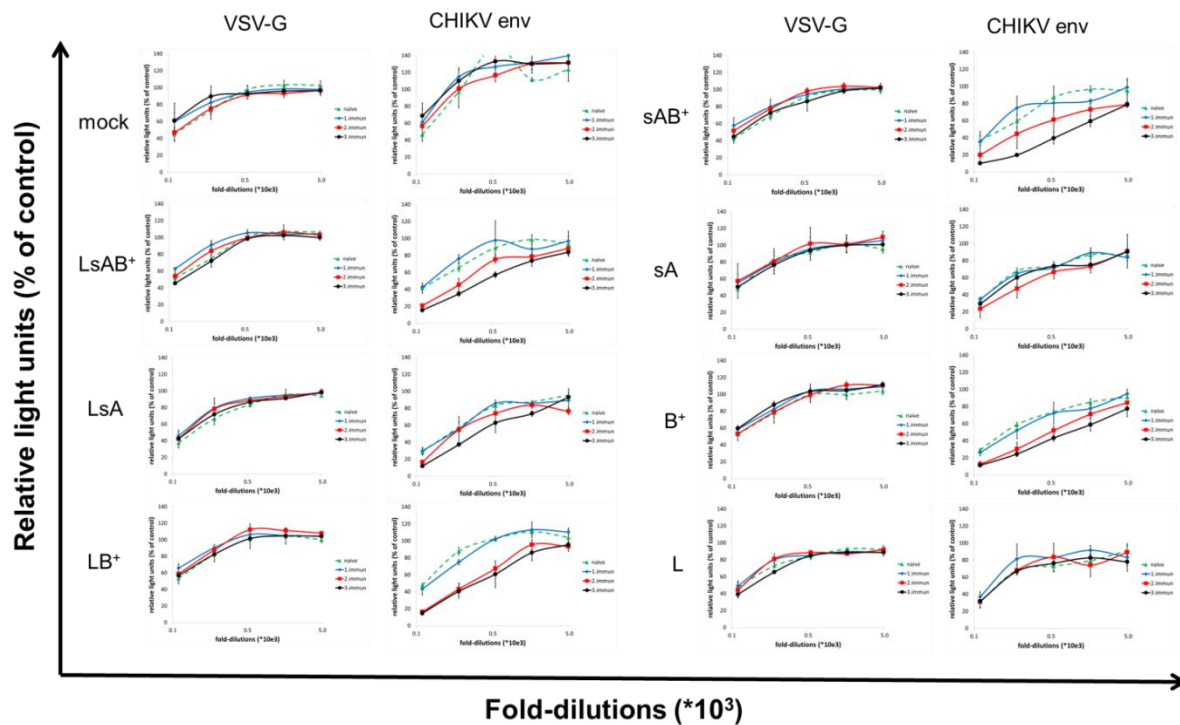
Figure 48: Neutralization assay with CHIKV Env VPs using mouse sera from vaccinated mice as potential inhibitors.

Mice (n=3 per construct) were vaccinated with the seven indicated constructs three times. Blood was collected directly before the first immunization, 3.5 weeks after the first immunization, and 1 week after the second and third immunization, respectively. The sera were screened in a 384-well plate luciferase-based assay with CHIKV Env pseudotyped VPs for neutralizing activity. They were tested in five 3-fold serial dilutions, ranging from 1:60 to 1:4860. One day after transduction, the transduction rate was measured by a luminometer. The results are presented as relative light units relative to the serum free control. VSV-G pseudotyped VPs were used as a control. Shown are the results summarized for the mice receiving the same protein. A further statistical analysis is shown in Figure 24.

10.2 Amino acid sequences of used recombinant proteins

CHIKV E2-derived

Linker regions

Other sequences (plasmid vector-derived (e. g., His-tag), secretion signal, etc.)

10.2.1 CHIKV E2-derived (strain LR2006) proteins for immunizations

LsAB+ (30.7 kDa)

MGSSHHHHHHSSGLVPRGSHMSTKDNFNVYKATGGGGSGGGGSTKDNFNVYKATGGGG
SGGGGSTKDNFNVYKATGGGGSGGGGSTKDNFNVYKATGGGGSGGGGSTKDNFNVYKA
TGGGGSGGGVDSTKDNFNVYKATGGGSGGGIKTDDSHDWTKLRYMDNHMPADAERAGG
GGGGSGTGTMGHGSGGGGGGFTDSRKISHGGSGGGGQSTAATTGGGGSGFEGPPDTP
DRTLMSQQSGNVKITVNGQTVRYKCNCGGSNEGQTTTDKVINNCKVDQCHAAVTNHKKW
QYNSPLVPRNAELGDRKGKIH

LsA (20.7 kDa)

MGSSHHHHHHSSGLVPRGSHMSTKDNFNVYKATGGGGSGGGGSTKDNFNVYKATGGGG
SGGGGSTKDNFNVYKATGGGGSGGGGSTKDNFNVYKATGGGGSGGGGSTKDNFNVYKA
TGGGGSGGGVDSTKDNFNVYKATGGGSGGGIKTDDSHDWTKLRYMDNHMPADAERAGG
GGGGSGTGTMGHGSGGGGGGFTDSRKISHGGSGGGGQSTAATT

LsB+ (21.4 kDa)

MGSSHHHHHHSSGLVPRGSHMSTKDNFNVYKATGGGGSGGGGSTKDNFNVYKATGGGG
SGGGGSTKDNFNVYKATGGGGSGGGGSTKDNFNVYKATGGGGSGGGGSTKDNFNVYKA
TGGGGSGGGVDPPDTPDRTLMSQQSGNVKITVNGQTVRYKCNCGGSNEGQTTTDKVINN
CKVDQCHAAVTNHKKWQYNSPLVPRNAELGDRKGKIH

sAB+ (21.0 kDa)

MGSSHHHHHHSSGLVPRGSHMSTKDNFNVYKATGGGSGGGIKTDDSHDWTKLRYMDNH
MPADAERAGGGGGGSGTGTMGHGSGGGGGGFTDSRKISHGGSGGGGQSTAATTGGGG
SGFEGPPDTPDRTLMSQQSGNVKITVNGQTVRYKCNCGGSNEGQTTTDKVINNCKVDQCH
AAVTNHKKWQYNSPLVPRNAELGDRKGKIH

sA (10.9 kDa)

MGSSHHHHHHSSGLVPRGSHMSTKDNFNVYKATGGGSGGGIKTDDSHDWTKLRYMDNH
MPADAERAGGGGGGGSGTGTMGHGSGGGGGGFTDSRKISHGGSGGGGGQSTAATT

B⁺ (11.7 kDa)

MGSSHHHHHHSSGLVPRGSHMPPDTPDRTLMSQQSGNVKITVNGQTVRYKCNCGGSNEG
QTTTDKVINNCKVDQCHAAVTNHKKWQYNSPLVPRNAELGDRKGKIH

L (12.0 kDa)

MGSSHHHHHHSSGLVPRGSHMSTKDNFNVYKATGGGGSGGGGSTKDNFNVYKATGGGG
SGGGGSTKDNFNVYKATGGGGSGGGGSTKDNFNVYKATGGGGSGGGGSTKDNFNVYKA
TGGGGSGGGVD

Control for SDS-PAGE/Western blot: Human endogenous retrovirus K (HERV-K) UTPase (14.8 kDa)

MTPTVPSVSGNKPVTTIQQLSPATSSSAAVDLCTIQAVSLLPGEPPQKIPTGVYGPLPEGTV
GLILGRSSLNLKGVQIHTSVVDSDYKGEIQLVISSSIPWSASPGDRSAQLLLLPYIKGEDPNSS
SVDKLAAALEHHHHHH

sAB⁺ in MVA-CHIKV-sAB⁺ (including secretion signal, 24.1 kDa)

METDTLLLWVLLLWVPGSTGDAAQPASTKDNFNVYKATGGGSGGGIKTDDSHDWTKLRYM
DNHMPADAERAGGGGGGGSGTGTMGHGSGGGGGGFTDSRKISHGGSGGGGGQSTAATTG
GGGSGFEGPPDTPDRTLMSQQSGNVKITVNGQTVRYKCNCGGSNEGQTTTDKVINNCKVD
QCHAAVTNHKKWQYNSPLVPRNAELGDRKGKIHGPEQKLISEEDLNSAVDHHHHHH

10.2.2 CHIKV E2 extracellular domains (strain S27) for cell binding experiments

E2 domain A (26.5 kDa, including β-ribbon connector, domain B bypassed)

MGSSHHHHHHSSGLVPRGSHMSTKDNFNVYKATRPYLAHCPDCGEGHSCHSPVALERIRN
EATDGTLKIQVSLQIGIGTDDSHDWTKLRYMDNHIPADAGRAGLFVRTSAPCTITGTMGHFIL
ARCPKGETLTVGFTDSRKISHSCTHPFHHDPPVIGREKFHSRPQHGKELPCSTYVQSNAAT
AEEIEVHMPGGGGPGGGGGNHKKWQYNSPLVPRNAELGDRKGKIHIPFPLANVTCMVPK

E2 domain B (8.5 kDa)

MGSSHHHHHHSSGLVPRGSHMPDTPDRTLLSQQSGNVKITVNSQTARYKCNCGGSNEGLI
TTDKVINNCKVDQCHAAVT

E2 domain C (10.7 kDa)

MGSSHHHHHHSSGLVPRGSHMARNPTVTYGKNQVIMLLYPDHPTLLSYRSMGEEPNYQEE
WVTHKKEVVLTVPTEGLEVTWGNNEPYKYWPQ

E2 whole extracellular part (40.4 kDa)

MGSSHHHHHHSSGLVPRGSHMSTKDNFNVYKATRPYLAHCPDCGEGHSCHSPVALERIRN
EATDGTLKIQVSLQIGIGTDDSHDWTKLRYMDNHIPADAGRAGLFVRTSAPCTITGTMGHFIL
ARCPKGETLTVGFTDSRKISHSCTHPFHHDPPVIGREKFHSRPQHGKELPCSTYVQSNAAT
AEEIEVHMPPDTPDRTLLSQQSGNVKITVNSQTARYKCNCGGSNEGLITTDKVINNCKVDQC
HAAVTNHKKWQYNSPLVPRNAELGDRKGKIHIPFPLANVTCMVPKARNPTVTYGKNQVIML
LYPDHPTLLSYRSMGEEPNYQEEWVTHKKEVVLTVPTEGLEVTWGNNEPYKYWPQ

10.3 One-letter-code amino acids and different abbreviations

Abbreviation	meaning
A	Alanine
R	Arginine
N	Asparagine
D	Aspartic acid
C	Cysteine
E	Glutamic acid
Q	Glutamine
G	Glycine
H	Histidine
I	Isoleucine
L	Leucine
K	Lysine
M	Methionine
F	Phenylalanine
P	Proline
S	Serine
T	Threonine
W	Tryptophan
Y	Tyrosine
V	Valine

Abbreviation	meaning
°C	Degree Celsius
A	Adenine
A.	*Aedes* spp.
AAV-2	Adeno-associated virus isolate 2
AUC	Area under the curve
bp	Base pairs
C	Cytosine
CHIKF	Chikungunya fever
CHIKV	Chikungunya virus
CS	Chondroitin sulfate
DMEM	Dulbecco's modified Eagle Medium
DNA	Deoxyribonucleic acid
DS	Dermatan sulfate
DX	Dextran sulfate
E.coli	*Escherichia coli*
EC	Epicatechin
ECSA	East-central-south African lineage
EGCG	Epigallocatechin-3-gallate
ELISA	Enzyme Linked Immunosorbent Assay
Env	Viral Envelope protein
FACS	Fluorescence-activated cell sorting
FCS	Fetal calf serum
Fig.	Figure
FSC	Forward scatter
G	Guanosine
GAG	Glycosaminoglycan
GaLV Env delta R TM	Gibbon ape leukemia virus transmembrane protein
GFP	Green fluorescent protein
HP	Heparin
HPLC	High-pressure liquid chromatography

IC_{50}	Inhibitor concentration, which results in 50% inhibition of detected signal
HS	Heparan sulfate
Ig	Immunoglobulin
IOL	Indian Ocean lineage
IRES	Internal ribosomal entry site
IU/ml	International Unit per milliliter
kDa	Kilodalton
LCMV	Lymphocytic Choriomeningitis Virus
mg	Milligram
min	Minutes
ml	Milliliter
MVA	Modified Vaccinia virus Ankara
n. s.	Not significant
NT_{50}	serum dilution, which results in 50% reduction of infectivity
PCR	Polymerase chain reaction
PFA	Paraformaldehyde
PG	Proteoglycan
RT	Room temperature
SSC	Sideward scatter
T	Thymidine
VP	Vector particle
VSV-G	Vesicular stomatitis virus Glycoprotein
µg	Microgram
µl	Microliter

10.4 List of figures

11.   Publications

Weber C *et al.*: A neutralization assay for chikungunya virus infections in a multiplex format. Journal of Virological Methods. 2014 Jun;201:7-12. doi: 10.1016/j.jviromet.2014.02.001

Another two manuscripts submitted, on:

- Identification of important antigens for vaccine development (sAB$^+$)

- Discovery of a novel inhibitor of CHIKV cell binding (EGCG)

One further manuscript in preparation, on:

Revealing the role of individual domains of the CHIKV envelope protein (E2 A, B) for cell entry and identification of certain cell surface molecules (GAGs) promoting viral entry

12.   Conferences

Conferences with own oral presentation:

- Three times Summer School of the graduate school (in August 2011, 2012 and 2013 in Löwenstein, Germany)
- Three times Winter School of the graduate school (in March 2012, 2013 and 2014 in Frankfurt am Main, Germany)
- PEI Retreat (in January 2013 in Löwenstein, Germany)
- PEI Retreat (in January 2014 in Heidelberg, Germany)

Conferences with own poster presentation:

- PEI Retreat (in January 2012 in Löwenstein, Germany)
- 22nd Annual Meeting of the Society for Virology (March 2012 in Essen, Germany)
- National Symposium on Zoonoses Research (October 2012 in Berlin, Germany)
- First international Chikungunya conference (October 2013 on Langkawi, Malaysia)
- Junior Scientist Zoonoses Meeting (June 2014 in Hannover, Germany)

13. Danksagungen

14. Lebenslauf

Persönliche Daten

Name: Christopher Weber

Geburtsdatum: 24.08.1984

Geburtsort: Mainz

E-Mail: chris-weber84@gmx.de

Akademische Ausbildung

06/2011 bis 10/2014	Stipendiat am Graduiertenkolleg-1172. Promotionsarbeit am Paul-Ehrlich-Institut in Langen zur Erlangung des Doktorgrades der Naturwissenschaften bei Prof. Dr. Barbara Schnierle und Prof. Dr. Rolf Marschalek mit dem Thema: „Characterization of the Chikungunya virus entry process and the development of novel antiviral strategies"
05/2010 bis 02/2011	Diplomarbeit am Institut für Molekulare Virologie der Universitätsklinik Ulm bei Prof. Dr. Frank Kirchhoff mit dem Thema: „Primate lentiviral Nef proteins modulate infected cells, but do not directly affect bystander cells"
10/2005 bis 02/2011	Diplomstudium der Biologie an der Universität Ulm Abschluss: Diplombiologe; Note 1,0

Schulische Ausbildung

08/1995 bis 03/2004	Herzog-Johann-Gymnasium, Simmern Abschluss: Abitur (Allgemeine Hochschulreife); Note 2,1
08/1991 bis 07/1995	Grundschule Rheinböllen